UNIVERSIDADE DE SÃO PAULO

FACULDADE DE MEDICINA DE RIBEIRÃO PRETO
DEPARTAMENTO DE BIOQUÍMICA E IMUNOLOGIA

STEFAN ALEXANDER BRÜCK

Changes in microbiotic enzyme activity on soil organic matter decomposition, on an altitudinal gradient of the volcano Iliniza Ecuador, as a model for climate change impacts on carbon storage in Andean peatlands

Ribeirão Preto – São Paulo
2023

UNIVERSIDADE DE SÃO PAULO

FACULDADE DE MEDICINA DE RIBEIRÃO PRETO
DEPARTAMENTO DE BIOQUÍMICA E IMUNOLOGIA

STEFAN ALEXANDER BRÜCK

Changes in microbiotic enzyme activity on soil organic matter decomposition, on an altitudinal gradient of the volcano Iliniza Ecuador, as a model for climate change impacts on carbon storage in Andean peatlands

Versão original

Tese apresentada ao Programa de Pós-Graduação em Bioquímica da Faculdade de Medicina de Ribeirão Preto da Universidade de São Paulo, como parte das exigências para a obtenção do título de Doutor em Ciências.
Área de concentração: Bioquímica

Orientadora: Profa. Dra. Maria de Lourdes T. M. Polizeli

Ribeirão Preto – São Paulo
2023

Catalogação da Publicação
Serviço de Documentação
Faculdade de Medicina de Ribeirão Preto – Universidade de São Paulo

FICHA CATALOGRÁFICA

Brück, Stefan Alexander

Changes of microbiotic enzyme activity on soil organic matter decomposition, on an altitudinal gradient of the volcano Iliniza Ecuador, as a model for climate change impacts on carbon storage in Andean peatlands, 184 p. Ribeirão Preto, 2023.

184 .: il.; 30 cm

Tese de Doutorado, apresentada à Faculdade de Medicina de Ribeirão Preto/USP – Área de concentração: Bioquímica.

Orientadora: Polizeli, Maria de Lourdes Teixeira de Moraes

1. Páramo 2. solo 3. enzimas 4. Fungos filamentosos psicrofílicos 5. Composição da microbiota

BRÜCK, S. A. **Changes of microbiotic enzyme activity on soil organic matter decomposition, on an altitudinal gradient of the volcano Iliniza Ecuador, as a model for climate change, impacts on carbon storage in Andean peatlands**. 2023. 184 p. Tese (Doutorado em Ciências – área de concentração Bioquímica) - Faculdade de Medicina de Ribeirão Preto, Universidade de São Paulo, Ribeirão Preto - SP, 2023.

Aprovado em: ___/___/_____

BANCA EXAMINADORA

Prof. Dr. _____ Instituição: _____

Julgamento:_____ Assinatura: _____

Prof. Dr. _____ Instituição: _____

Julgamento:_____ Assinatura: _____

Prof. Dr. _____ Instituição: _____

Julgamento:_____ Assinatura: _____

Prof. Dr. _____ Instituição: _____

Julgamento:_____ Assinatura: _____

APOIO E SUPORTE FINANCEIRO

O presente trabalho foi realizado com apoio do(a):

1) Bolsa da Universidade Central do Equador, Faculdade de Medicina em convênio com a Faculdade de Medicina de Ribeirão Preto

2) Programa de Doutorado-sanduíche no Exterior (PDSE) - CAPES - Processo: 88881.186934/2018-01;

3) Fundação de Amparo à Pesquisa do Estado de São Paulo – FAPESP - Processos: 2018/07522-6;

4) Fundação de Apoio ao Ensino, Pesquisa e Assistência – FAEPA (FMRP/USP);

5) Faculdade de Medicina de Ribeirão Preto – FMRP/USP;

6) Faculdade de Filosofia, Ciências e Letras de Ribeirão Preto – FFCLRP/USP.

DEDICATION

I dedicate this work to my three families. The one from Koblenz, which is where my roots are and always will be, the one from Aachen, although neither blood nor law defines us as such, our bonds could not be stronger; and the one in Quito, which represents my wings to create an always-changing future and has made my whole life become an adventure.

I love you all.

ACKNOWLEDGEMENTS

Acknowledgment

First of all, I want to thank my wife for taking me on this adventure in Brazil and accompanying me through the ups and downs, and my son, who also managed to make me smile at my most stressful hour with his unbreakable childish optimism.

To Dr. Maria de Lourdes Polizeli for her dedication, experience, patience, and her strict guidance when pressure is required to meet goals, and her understanding and loving care like a mother when things went wrong without own fault.

To Paul Gamboa, Pablo Lodoño, Ulrich Stahl and Vicky Cabrera at the Faculty of Chemical Engineering and Rommy Terán and Monserrat Naranjo from the Faculty of Chemistry as well as Mauricio at the Faculty of Agronomy. This work would not have been possible without their technical and laboratory support.

To Paulina Guarderas and Byron Medina, companions in suffering and important moral support, as well as Francisco Alvarez, Camila Acosta, and Raj Lakshminarayan for their advice.

To all the laboratory team in Ribeirão Preto for their help and kind reception, specifically Alex Contato, Thiago Pasín, Mariana Cereia, and Tássio Brito.

To the research management team for their support, specifically Maria Mercedes Gavilanez, Bertha Estrella, Eulalia Hurtado and the financial team.

To Maria Belen Mena and Dr. Donadi for taking me to the Ph.D. program, even though I was a weird creature, and to Sophia, Vivi ,and Edison for their support in Brazil.

To the students who helped with the field and laboratory work logistics, specifically Camilo Rosero, Paola Buitrón, Kevin Toapanta, Wendy Pacheco, Sandy Arguello, and Liliana Rojas.

To Eduardo and Rosita. Without their loving care for my child, this work would have been impossible.

To all the thousands of people who accompanied me for more than 4 years and whom I have surely forgotten to mention.

Thank you very much!

RESUMO

BRÜCK, Stefan Alexander. **Mudanças nas atividades enzimáticas da microbiótica na decomposição da matéria orgânica do solo, em um gradiente altitudinal do vulcão Iliniza Equador, como modelo para os impactos das mudanças climáticas no armazenamento de carbono em turfeiras andinas** 2023. 184 p. Tese (Doutorado em Bioquímica) - Faculdade de Medicina de Ribeirão Preto, Universidade de São Paulo, Ribeirão Preto - SP, 2020.

O Paramo andino reúne ambientes distintos descritos como ecossistemas montanhosos neotropicais situados entre a linha das árvores e a zona rochosa da Cordilheira dos Andes de 2.900 a 5.000 m. Possui a maior taxa média de diversificação entre todos os hotspots de biodiversidade da Terra. Seu papel como sumidouro de carbono e sua incrível capacidade de retenção de água desempenham papéis críticos na interação com os ecossistemas de encostas andinas. O Capítulo 1 analisa como a baixa degradação da matéria orgânica leva ao acúmulo maciço de depósitos de carbono como turfa. Esse sumidouro de carbono pode se transformar em uma fonte de carbono no futuro devido às mudanças climáticas, apoiado por evidências de pesquisa das turfeiras do hemisfério norte. O capítulo 2 trata do isolamento de fungos filamentosos de habitats remotos com condições climáticas extremas, descobrindo várias enzimas com propriedades atraentes, úteis em aplicações industriais. Dentre estes, enzimas adaptadas ao frio de fungos com comportamento psicrotrófico são agentes valiosos em processos industriais visando a redução de energia. Das oito cepas isoladas do solo do páramo equatoriano, três foram selecionadas para posterior experimentação e identificadas como Cladosporium michoacanense, Cladosporium sp. (complexo cladosporioides) e Didymella sp. A secreção de sete enzimas, endoglucanase, exoglicanase, β-D-glucosidase, endo-1,4-β-xilanase, β-D-xilosidase, fosfatases ácida e alcalina, foram analisadas sob agitação e condições estáticas otimizadas para o período de crescimento e temperatura de incubação. As cepas de Cladosporium sob agitação e incubação por 72 h mostraram ativação substancial para endoglucanase até 4563 mU/mL e xilanase até 3036 mU/mL. Didymella sp. mostrou a ativação mais robusta a 8 °C, indicando um perfil interessante para aplicações em processos de biorremediação e tratamento de águas residuais em climas frios. O Capítulo 3 descreve a atividade variável da sulfatase (Sulf), fosfatase (Phos), n-acetil-glucosaminidase (N-Ac), celobiohidrolase (Cellobio), β-glicosidase (β-Glu) e peroxidase (POX) em uma altitude escala de 3600-4200 m, nas estações chuvosa e seca a 10 e 30 cm de profundidade de amostragem, relacionado às características físicas e químicas do solo. Modelos lineares de efeito fixo foram estabelecidos para analisar esses fatores ambientais para determinar padrões distintos de decomposição em solos páramo. Os dados sugerem uma forte tendência de diminuição das atividades enzimáticas em altitudes mais elevadas e na estação seca até duas vezes mais forte ativação para Sulf, Phos, Cellobio e β-Glu. Especialmente a altitude mais baixa mostrou atividade N-Ac, β-Glu e POX muito mais forte. A profundidade de amostragem revelou diferenças significativas para todas as hidrolases, exceto Cellobio, mas teve efeitos menores nos resultados do modelo. Ademais, os componentes orgânicos do solo, em vez dos físicos ou metálicos, explicam as variações da atividade enzimática. Embora os teores de fenóis tenham coincidido principalmente com o teor de carbono orgânico do solo, não houve relação direta entre hidrolases, atividade da POX e substâncias fenólicas. O resultado sugere que pequenas mudanças ambientais com o aquecimento global podem causar mudanças importantes nas atividades enzimáticas, levando ao aumento da decomposição da matéria orgânica na fronteira entre a região do páramo e os ecossistemas em declive. No capítulo 4 assumimos que a baixa atividade de decomposição está diretamente ligada à sua composição microbiana, que ainda

não foi estudada em detalhes no solo páramo. As sequências 16S- para archaea e bactéria e ITS- para fungos foram amplificadas para análise em 4 altitudes distintas marcando zonas de vegetação nas estações seca e chuvosa. As amostras foram recolhidas em triplicado e agrupadas. Dados taxonômicos de riqueza e abundância revelaram que as comunidades bacterianas variam mais com a estação do que com efeitos altitudinais. Os filos mais abundantes foram Acidobacteriota, Actinobacteriota e Bacteriodota. Proteobacteriota, descrito como o principal filo do solo, mostrou apenas pouca abundância. Os fungos, por outro lado, apresentaram maior variação na diversidade para efeitos altitudinais e sazonais. Ascomycota, Basidiomycota e Mortierellomycota foram os mais abundantes. Em comparação com a atividade enzimática do capítulo 3, o padrão global da diversidade fúngica poderia explicar melhor as diferenças observadas na decomposição da matéria orgânica. A distribuição das classes de fungos indica padrões únicos para o ambiente páramo, o que convida a uma investigação mais aprofundada.

Palavras-chave: Paramo, solo enzimas, fungos filamentosos psicrofílicos, composição da microbiota

ABSTRACT

BRÜCK, Stefan Alexander. **Changes in microbiotic enzyme activity on soil organic matter decomposition, on an altitudinal gradient of the volcano Iliniza Ecuador, as a model for climate change impacts on carbon storage in Andean peatlands.** 2023. 184 p. Thesis (Doctorade in Biochemistry) – Faculty of Medicine Ribeirão Preto, University of São Paulo, Ribeirão Preto - SP, 2022.

The Andean Paramo unites distinct environments characterized as neotropical mountain ecosystems lying at high elevations between the tree line and the rocky zone of the Andean Mountain chain from 2900 up to 5000 m. It bears the highest average diversification rate among all biodiversity hotspots on earth. Its role as a carbon sink and its astonishing water retention capacity play critical roles in the interaction with Andean downslope ecosystems. Chapter 1 reviews how low organic matter degradation leads to the massive accumulation of peat-like carbon deposits and how this carbon sink might turn into a carbon source in the future due to climatic change, supported by research evidence of northern hemisphere peatlands. Chapter 2 treats the isolation of filamentous fungal strains from remote habitats with extreme climatic conditions in the paramo, discovering several enzymes with attractive properties, useful in various industrial applications. Among these, cold-adapted enzymes from fungi with psychrotrophic behavior are valuable agents in industrial processes aiming to reduce energy. Out of eight strains isolated from the soil of the paramo highlands of Ecuador, three were selected for further experimentation and identified as Cladosporium michoacanense, Cladosporium sp. (cladosporioides complex), and Didymella sp. The secretion of seven enzymes, endoglucanase, exoglycanase, β-D-glucosidase, endo-1,4-β-xylanase, β-D-xylosidase, acid, and alkaline phosphatases, were analyzed under agitation and static conditions optimized for the growth period and incubation temperature. Cladosporium strains under agitation and incubation for 72 h mostly showed substantial activation for endoglucanase up to 4563 mU/mL and xylanase up to 3036 mU/mL. Meanwhile, other enzymatic levels varied depending on growth and temperature. Didymella sp. showed the most robust activation at 8 °C, indicating an interesting profile for applications in bioremediation and wastewater treatment processes in cold climates. Chapter 3 describes the changing activity of sulfatase (Sulf), phosphatase (Phos), n-acetyl-glucosaminidase (N-Ac), cellobiohydrolase (Cellobio), β-glucosidase (β-Glu), and peroxidase (POX) on an altitudinal scale from 3600-4200 m, in rainy and dry seasons at 10 and 30 cm sampling depth, related to physical and chemical soil characteristics, like metals and organic elements. Linear fixed-effect models were established to analyze these environmental factors to determine distinct decomposition patterns within paramo soils. The data suggests a strong tendency toward decreasing enzyme activities at higher altitudes and in the dry season up to two-fold stronger activation for Sulf, Phos, Cellobio, and β-Glu. Especially the lowest altitude showed considerably stronger N-Ac, β-Glu, and POX activity. Sampling depth revealed significant differences for all hydrolases but Cellobio, but it had minor effects on model outcomes. Further organic rather than physical or metal components of the soil explain the enzyme activity variations. Although the levels of phenols coincided mostly with the soil organic carbon content, there was no direct relation between hydrolases, POX activity, and phenolic substances. The outcome suggests that slight environmental changes with global warming might cause important changes in enzyme activities leading to increased organic matter decomposition at the borderline between the paramo region and downslope ecosystems. In chapter 4 we assumed that low decomposing activity is directly linked to its microbial composition, which has not yet been studied in detail in paramo soil. 16S- for archaea and

bacteria and ITS-sequences for fungi were amplified for analysis on 4 distinct altitudes marking vegetational zones in the dry and rainy seasons. Samples were taken in triplicate and pooled. Taxonomical data of richness and abundance revealed that bacterial communities variate stronger with the season than with altitudinal effects. The most abundant phyla were Acidobacteriota, Actinobacteriota and Bacteriodota. Proteobacteriota, commonly described as the leading soil phylum, only showed little abundance. Fungi, on the other hand, showed greater variation in diversity for altitudinal and seasonal effects. Ascomycota, Basidiomycota, and Mortierellomycota were most abundant. In comparison to enzyme activity of chapter 3, the global pattern of fungal diversity could explain to a greater extent the observed differences in the decomposition of organic matter. The distribution of fungal classes indicates unique patterns for the paramo environment, which invites further investigation.

Keywords: Paramo, soil, enzyme, psychrophilic filamentous fungi, microbiota composition

LIST OF FIGURES

LIST OF TABLES

LIST OF ABBREVIATIONS

16S: ribosomal RNA gene (bacteria and archaea barcode region)

β-Glu: β-glucosidase enzyme

ASV: Amplicon Sequence Variant

BLAST: Basic local alignment search tool

Cellobio: Cellobiohydrolase enzyme

CUE: Carbon use efficiency

EC: Enzyme commission number

EDTA: Ethylendiaminetetraacetate

g: grams

g: Gravity

g/L: Grams per liter

ITS: internal transcribed spacer region (fungal barcode region)

kDa: Kilodaltons

M: Molar

min: Minimum

max: Maximum

mL: Milliliters

mg: Milligram

mg/mL: Milligram per milliliter

N-Ac: N-Acetyl-glucosaminidase

ng: Nanogram

OTU: Operational Taxonomical Unit

SD: Standard deviation

SEM: Standard error of the mean

pH: hydrogen potential

PCA: Principal Component Analysis

PCoA: Principal Coordinate Analysis

Phos: Phosphatase enzyme

Sulf: Sulfatase enzyme

POX: Phenol peroxidase enzyme

rpm: rounds per minute

µg: Micrograms

µL: Microliters

µmol: Micromole

µmol/mL: Micromole per milliliter

TABLE OF CONTENTS

Chapter 1

The Ecuadorian Paramo in danger: What we know and what might be learned from northern peatlands

This chapter is based on the review article of the same name

Abstract: The Andean Paramo unites a series of distinct ecosystems all together characterized as neotropical mountain ecosystems lying at high elevations between the tree line and the rocky zone of the Andean Mountain chain from 2900 up to 5000 m, dependent on its longitudinal location. The term Paramo (Latin Paramus, meaning “The highest”) was historically defined as an uncultivated mountain wasteland characterized by the absence of trees and harsh climatic conditions, whichpays little credit to its ecological, hydrological, climatic, and socio-cultural importance. The Andean Paramo region bears the highest average diversification rate among all biodiversity hotspots on earth. But most of all, its role as a carbon sink and its astonishing water retention capacity play critical roles in the interaction with Andean downslope ecosystems revealed by an increasing research interest in the area. The interplay between microorganism composition, enzyme activity, and soil characteristics play a crucial role in the formation of peat responsible for these characteristics. Nevertheless, still little is known about the unique ecosystem and its different forms of appearance due to the low research activity in South America. It is seriously threatened to disappear before we discover all of its secrets. Human intervention due to the upslope shift of agricultural activity, cattle farming, hunting, and wildfires have devastated large amounts ofits landscapes. However, the biggest threat, global climate change, is still in its early phase of manifestation. In this context, the present review summarizes important paramo characteristics andtakes advantage of previous studies performed in the northern hemisphere peatlands, which present similar features and have been studied intensively due to their critical role in global climate change for more than two decades.

Keywords: Paramo, ecosystem services, carbon fixation, water retention

1.1 Geography and soil composition

The Andean Paramo stretches along Southern America from southern Venezuela (8°N) to northern Peru (11°S) following the Andean Mountains. These are divided into three distinct chains, namely theOccidental Andean chain, the Central Andean chain, and the Oriental Andean chain, separated by tectonic depressions, which give rise to its heterogeneous topology with large inter-Andean valleysand highland plateaus in sharp contrast to steep slopes of active stratovolcanos [1,2]. This causes geographic isolation of distinct patches of paramo with unique environments but similar climatic conditions. From a geographical point of view, its uprise was a relatively recent event. Although most of the mountain uplift happened in the middle Miocene, 15- 20 million years ago, the development of paramo ecosystems falls within the latest uplift only about2,7 million years ago as it largely depends on the extreme altitudes [3,4]. The central Andean chain reaches from Venezuela to southern Colombia, which is why in Ecuador, there

are only the oriental and the occidental Andean chain distinguishable [5]. Nevertheless, Ecuador has the highest percentage of paramo compared to the total surface area on earth, reaching almost 7% of the national territory [6] (Figure 1.1 A). Within this area, there are 11 distinct ecosystems [7](Figure 1.1 B).

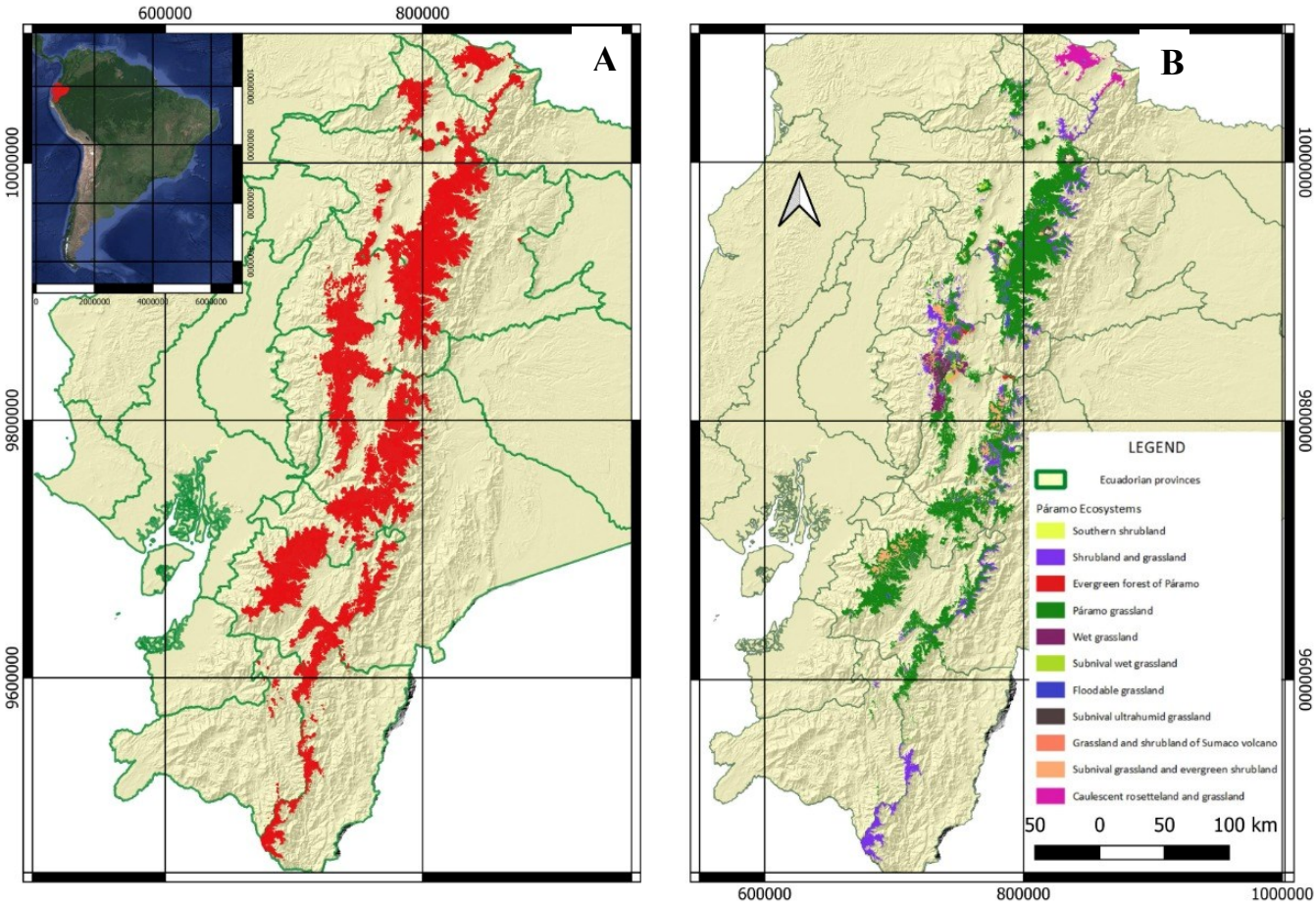

Figure 1.1 The distribution of Paramo in Ecuador
A) Extension of Paramo (red area) within Ecuadorian Territory B) Distribution of 11 different Paramo regions.

Paramos on the eastern chain of the Andes, mainly close to the Amazonian basin, tend to be more humid than those on the western Andean chain. Furthermore, they can be categorized into those belonging to the Northern Paramo characterized by a higher and more recent volcanic activity represented by remaining extensive ash depositions and the southern region with a higher presence of older weathered morphic bedrock of ancient volcanic origin leading to distinct soil types [5,8]. In northern Ecuador, most paramo soil types belong to molic or histic Andosols characterized by their dark brown or black color and their high content in organic

carbon leading to the formation of organometallic complexes with iron and aluminium released through worn volcanic parent material [9,10]. Southern Ecuador soils tend to be older, although not necessarily more developed. The predominant soil type is Inceptisol of ancient volcanic origin [11].

Although there is a general geographical distinction between paramo types, it is also very common to find several distinct types of paramo within one geographically isolated region (Figure 1.2) due to changes in topology, water access, erosion, and exposure to the wind. Most importantly, many paramos, especially in Northern Ecuador, are separated into subparamo, at the borderline between the high Andean Forest and Paramo, shrub-paramo, grass-paramo, and superparamo are differentiated only by the rising altitude within the same paramo stretch [12].

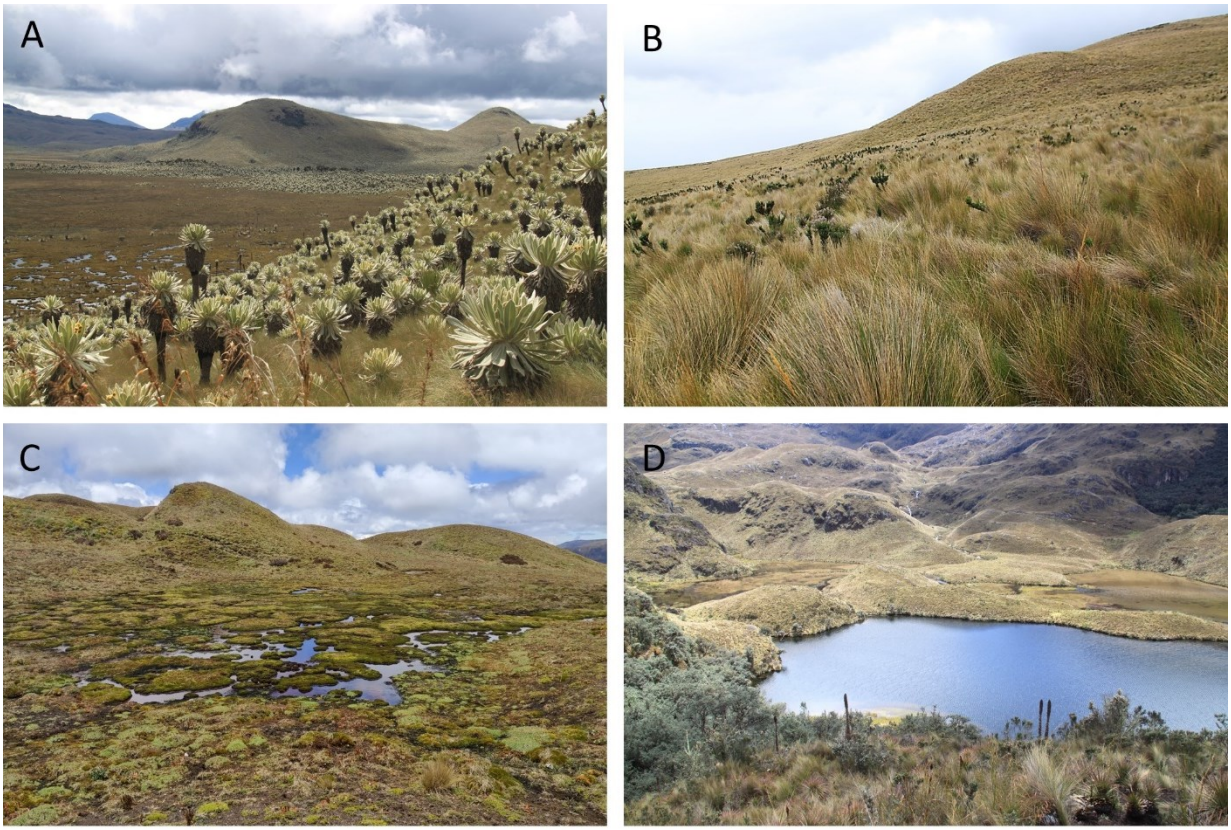

Figure 1.2 Types of Paramo
A) Paramo de Frailejones, Carchi province, Reserva El Angel; B) Grass Paramo, Napo province, Reserva Antisana; C) Herbal humid Paramo, Pichincha province, Reserva Papallacta; D) Herbal and Shrub sublevel Paramo, Azuay province, Parque Nacional Cajas (Fotos taken by the author)

1.2 Climate and Hydrology

The temperature in paramos shows a strong fluctuation between day and night, like those observed in desertic environments. Intense radiation paired with black soil, low vegetation, and the absence of shadow in most parts lead to surprisingly high temperatures considering the

altitude atwhich paramo is found [13]. On the other hand, the lack of vegetation also causes a low capacity to hold warmth within the environment during the night, leading to cold night temperatures. Furthermore, constant precipitation and fog in many paramo regions can add to the cooling effect. In conclusion, this can lead to temperature fluctuations of 20°C within a single day [14]. Even though temperatures close to the freezing point are common, temperatures below the freezing point are usually very scarce, which is influenced by water retention. Water serves as a heat reservoir heating during the daytime and slowly liberating this heat throughout the night.

Although rainfall intensity in the paramo is usually relatively low, the frequency of those events is high, mainly due to the orographic effect [15]. Additionally, from afternoonto early morning, much of the paramo is coated with mist and fog of low-hanging clouds covering the vegetation with dew [16,17]. Moreover, the water usage by the ecosystem is very low given that most plants present very low evapotranspiration due to adaptations against the extreme radiation at high elevations close to the equator and water lossthrough strong winds. In addition, many of those plants developed protecting hairs that facilitate the condensation of water on their surface [18].

The combination of the proximity of most paramos to the equator line and the extreme altitude of these ecosystems causes radiation to pass through an extremely narrow atmospheric layer [19]. It is believed that together with wind and cold temperatures, this radiation hinders the expansion of tree species within the given environment and leads to a series of morphological adaptations of plant species [13].

Another critical aspect of the paramo's climate is the abundant presence of strong winds. Its location at the borderlines of Andean slopes and the formation of wind channels of the High Andean valleys within the Andean mountain chains form anabatic flows [20], which are further intensified due to the lack of natural windshields such as trees. Furthermore, it is believed that the formation of new forests within the paramo area is difficult due to the strength of winds [13] which is observable by the presence of high Andean forests at the lee sides of mountains.

The impermeable rocky ground of the Andean mountains itself has minimal capacity to hold water on its own, lacking deep groundwater flows, and global warming threatens glaciers as natural water resources [20]. Therefore, soil formed by the paramo vegetation and microbiota interaction plays a crucial role in retaining vast quantities of water [21] due to its low apparent density and the presence of large pores [22]. The paramo does not only store the water, but its

soil structure can filter water and slowly and steadily distribute it into streams and rivers towards downslope ecosystems such as the emblematic mountainous cloud forests on both sides of the Andean slopes and the tropical Chocó rainforest on the western and the Amazonian basin on the eastern side of the Andes [9,23]. It is difficult to predict how future water scarcity might influence these ecosystems, and more studies are needed for estimation, but the effect is likely to be dramatic [24]. What is already becoming visible is that big cities are using these water supplies for a considerable population (Bogotá and Quito, for example) which makes them totally dependent on the ecosystem services of the paramo region [21].

1.3 Carbon fixation

The soil characteristics mentioned above and water retention capacities are a direct result of an astonishing carbon fixation capacity leading to high levels of soil organic carbon (SOC)(Figure 1.3). Although photosynthetic net fixation of CO_2 is not as high as in typical tropical downslope ecosystems, as can be seen by the slow growth rates of typical paramo vegetation, plants have developed adaptations to utilize the intense radiation for their benefit [18]. Still, more importantly, the degradation of accumulating organic matter is very slow. The combination of low temperatures at high elevations, little oxygen availability due to high water table depths, and harsh living conditions for soil microbiota have led to the deposition of huge layers of peat-like carbon-rich matter reaching more than six meters depth at northern Ecuadorian paramos [17].

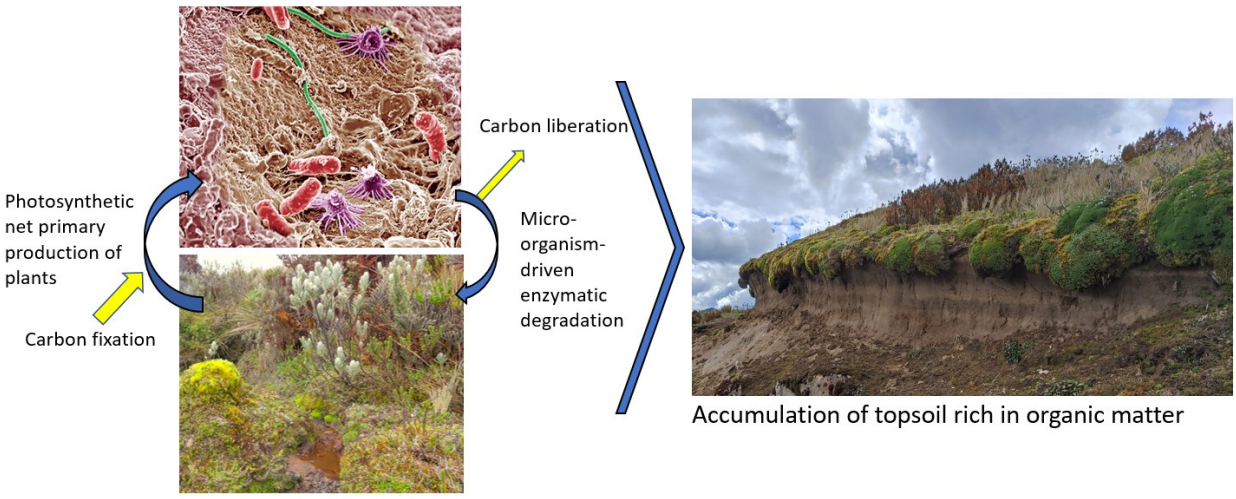

Figure 1.3 Accumulation of organic matter in paramo soil

Elaborated by the author (Photos taken from the Antisana Paramo Ecuador and scanning electron microscopy from Alice Dohnalkova, Pacific Northwest National Laboratory)[25]

The net fixation capacity of some paramo regions is even superior to those of tropical rainforests in the Amazonian basin, accumulating up to 134 g $m_{2^{-1}}$ $year^{-1}$ and qualifying them as some of the world's most carbon-dense peatlands [26]. Organic matter degradation is directly dependent on soil microbiota composition and its capacity to secrete degrading enzymes (Figure 1.3).

Little research emphasis has been made on determining soil microbiota diversity and enzyme activities, as well as greenhouse gas emission rates as a consequence of degradation but increasing microbiota diversity and enzyme activity are likely to be expected with climate change [17], to which extent largely depends on vegetational shifts due to the direct interplay with microorganisms and soil characteristics [27].

An essential aspect that remains to be studied is the interplay between the two most important ecosystem services, water retention, and carbon fixation. Retained water replaces oxygen within the poriferous ground causing long-term anoxic conditions similar to those observed in bogs and fens [28]. Although hydrolases, which are the dominant degrading enzymes, are not oxygen dependent, they are inhibited mainly by phenolic substances abundant in plant wall material. Phenolic substances are degraded by phenol oxidases which depend on oxygen intake, an effect known as the “Enzyme Latch Theory” discovered by Freeman and colleagues [29]. Again the effect has been studied for Northern Peatlands [30,31] but remains undiscovered in paramo wetlands although scientific data points towards similar behavior [32].

1.4 Species diversity and endemism

The Andean Paramo region is identified as one of the world’s most important biodiversity hotspots. It holds the highest average diversification rate among all ecosystems on the planet [3]. An estimated 60% of paramo plant species are endemic to this unique habitat [8,9], although this number is still in discussion, and the real endemism could be even higher, considering that genetic studies about plant diversity in the paramo are still scarce and purely morphological studies are known to underestimate this number [23].

Its unique landscapes were formed due to the elevation of the Andean Mountain peaks. In Pleistocene, where maximum glacial extensions were formed, the first paramos could also be found at lower elevations allowing for connectivity among them in a unique Andean belt [4].

This greatly facilitated the distribution of plant, animal, and fungi species. When temperatures rose and the glaciers retreated, the paramo also shifted upslope, causing the isolation of paramo ecosystems due to the loss of connectivity. It is believed that this event strongly supported recent and rapid allopatric speciation and subsequent adaptive radiation. This led to an astonishing level of endemism in an evolutionary short period of less than two million years [4,33].

Although, at first sight, the paramo looks homogenous due to the lack of forests, its topology gives rise to different microhabitats. Meanwhile, on steep slopes, especially those found at the flanks of stratovolcanos, where erosion removes organic matter, rocky soils are covered with pillows of lichens and mosses of great diversity [34]. This stands in sharp contrast to slightly inclined terrain and plains where the formation of bogs and fens accumulate deep layers of peat [26]. Therefore, local diversification within a landscape, which appears to be a single landscape like islands of different species can be found [23].

The endemism frequency in Ecuadorian Paramo also leads to remarkable diversity of soil microorganisms with potentially interesting enzymatic capacities. Some isolated fungi have great enzymatic potential even under cold climatic conditions demonstrating how little is known about the biotechnological potential within these unique environments [35].

1.4.1 Flora

The aspect of the paramo region is marked mainly by the presence of plants belonging to the families Asteraceae and Poaceae [12]. The plant genera differ depending on the type of paramo. Abundant are species from *Azorella, Werneria,* and *Plantago,* which can build thick pillowlike elevations, as well as *Calamagrostis*, *Stipa,* and *Festuca.* Typical shrub species are *Valeriana, Chuquiraga, Arcytophyllum, Pernettya,* and *Brachoyotum* [8] with dispersed remnants of dwarfed trees like *Polilepis.* Astonishing is also the abundance of Bryophytes represented dominantly by the families Dicranaceae and Lejeuneaceae as well as Dryopteridaceae (ferns) [36]. Especially in rocky zones and the superparamo, there is a notable diversity of lichens [34]. Remarkable species are *Espeletia pycnophylla* (frailejones) and *Stipa ichu* (paja brava), which gave name to specific types of paramo due to their dominant appearance in the landscape [18].

1.4.2 Fauna

The paramo extensions form habitats for big and medium mammals such as the Andean or spectacled bear (*Tremarctus ornatus*), the puma (*puma concolor)*, the Andean Tapir (*Tapirus pinchaque*), the white-tailed deer (*Odocoileus virginianus ustus*) and the Paramo wolf (*Lycalopex culpaeus reissii*) as well as emblematic birds of prey such as the Condor Andino (*Vultur gryphus*), the black-chested eagle (*Geranoaetus melanoleucus*), and the Caracara Curiquinge (*Phalcoboenus carunculatus*). Reptiles are very rare in the paramo, but the abundance of water bear habitats for amphibian species like *Eleutherodactylus whymperi* [8].

These emblematic animals, together with the unique landscape, make the paramos popular destinations for tourism which can support conservation with earnings but can also lead to furtherdestruction of the paramo landscape, as can be observed in the Cotopaxi paramo.

1.5 Human intervention

1.5.1 Cultivation and Cattle farming

Climate change has caused a continuous elevation of cultivatable areas within the paramo region.

The rise of the agricultural frontier has been visible since the first descriptions of agricultural activity by Alexander van Humboldt [37] until today, and since climate change effects are expected to be exponential, it is most probable that changes will become more dramatic within the future [38] (Figure 1.4).

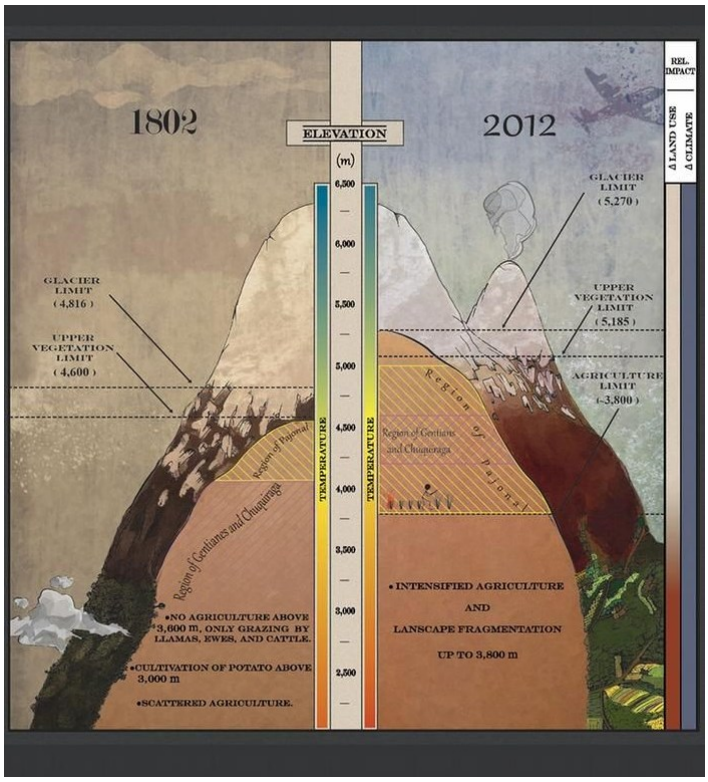

Figure 1.4 Vegetational upslope shifts in the volcano Chimborazo comparing a drawing of Alexander from Humboldt (1802) with the present situation (2012). The upslope shift of vegetational zones and especially agriculturally exploited areas is clearly noticeable. Picture taken from Morueta-Holme et al. (2015) [37]

It appears illogical that the paramo region with its carbon-rich black soil and its particular capacity to retain phosphates, is considered a barely fertile region which is due to its extreme climatic conditions, not suitable for every type of crop and the fact that the impaired microbial decomposition of organic matter does not release many nutrients up to the point where they become assimilable by plant roots [39]. It is therefore not surprising that paramo soil is transported to lower elevations and sold as the most fertile substrate for agriculture. Unfortunately, this leads to the destruction of whole peat bogs [40].

Many paramo landscapes are illegally transformed into pastureland, and it is common to release cattle at the borderlands of even protected areas to pasture. Trampling of cattle causes the compaction of soil which leads to the loss of water retention capacity and the change of vegetation towards a few resistant species. Selective grazing of native plant species further diminishes the biodiversity of affected areas with an important impact on the microbiota composition [39,41].

1.5.2 Burning

Although many adverse effects of burning paramo vegetation are widely recognized as harmful by the local population, in terms of the destruction of biodiversity as well as the exposure of the soil toerosion and the elimination of useful microorganisms, burning of paramo is still common practice. It represents the easiest way to transform paramo into pastureland, "clean up" terrain previous to theseeding of crops, deforestation, and the fastest way for illegal appropriation and colonization of abandoned terrain [8].

Human burning activity and the more frequent appearance of wildfires can represent a serious threat to the paramo. Furthermore, the continuous loss of water retention capacity in combination with global warming and its associated increase in extreme climate events [21] could lead to droughts and, therefore, the increased occurrence of spontaneous wildfires, as has been shown in northern peatlands [42,43]. Burning not only threatens the biodiversity of local areas but also causes a dramatic increase in released CO_2, which adds to the greenhouse effect. Within a concise period, vast amounts of carbon that have been accumulated over decades, fixed from the atmosphere, can be released [44].

1.6 Lessons to learn from northern hemisphere peatlands

Despite its continuously underestimated importance, tropical paramo ecosystems are barely studied. Although considerable efforts have been made to recollect information about this uniquehabitat [6,8], internationally published data is still very scarce.

Furthermore, most studies treat the observed biodiversity of flora and fauna and certain aspects about ecological characteristics meanwhile, studies such as paramo microbiome analyses or details about decomposition processes within its soils are scarce [45].

On the other hand, the northern hemisphere peatlands have gained a said reputation within the scientific community due to their important role in the massive liberation of greenhouse gases with climate change [38]. Therefore, this formerly rather inconspicuous environment attracted great scientific interest, and many studies have been performed to gain insight into environmental mechanisms, especially concerning carbon storage. Historically northern hemisphere peatlands have attracted greater research interest than tropical peatlands, although these are estimated to hold 18-23% of global peat carbon stocks [17]. The present review, therefore, aims to compare those distant habitats to understand whether certain insights gained

for northern hemisphere peatlands might help us understand what might be expected for mountain peatlands in South America. Given similarities and differences, the idea is not to directly project outcomes from the intensively studied northern peatlands to the less studied paramo, but rather an analysis of what might be expected in future research and to create hypothesis that remain to be tested.

1.6.1 Similarity and Differences

Although there are undoubtedly important differences between both types of peatlands which is a logical outcome of the extremely high endemism rate of Andean paramo regions as we previously discussed, as well as extreme differences in geographical localizations on earth with all their geological, topological, and climatic implications, there is still a significant number of astonishing similarities to be observed. First, both ecosystems are marked by their extreme capacity to retain water [21,46] as a direct consequence of their remarkable carbon storage capacity commonly visible by the several meters thick peat deposits in extended areas [26,47], leading to hardly developed soil horizons. Moreover, although species differ, predominant plant families are very similar in both areas. Both are dominated by Asteraceae y Poaceae plant species and present an unusual richness in bryophytes (especially *Sphagnum* spec.), lichens, ferns, and especially in colder regions, upslope or up-north, respectively,the gradual replacement of tree species by small shrubs [36]. Climatic conditions are similar in vast areas considering that temperature gradients towards the polar regions are similar to those observed towards the glaciers in mountain peatlands. Nevertheless, freezing events are obviously more frequent up north than close to the equator. On the other hand, radiation intensity tends to be far more intense in Andean paramo regions [19]. Both regions usually present a high frequency of rain and strong winds. These harsh conditions generally led to several comparable physiological adaptationsof plants and animals [8,47].

1.6.2 What we could learn

Northern hemisphere peatlands have been studied intensively for many decades due to their proximity to, or ubication within countries with high degrees of research funding and scientific production on the one hand and more recently in the last two decades due to its central role as a carbon sink in the context of global climate change as the most significant terrestrial

carbon stock worldwide [48]. Taking this last aspect alone it is worth asking whether mountain peatlands might show similar behavior in the future as they are just as capable as northern peatlands to fix and store carbon [26].

Higher temperatures favor microbiota diversification as well as its abundance, especially in colderpeatlands on a higher latitudinal level or at higher altitudes. This also changes the enzyme secretionbehavior of the microorganism community favoring degrading microorganism taxa [49,50]. Enzymes are known to be greatly influenced by rising temperatures leading mostly to increased catalytic rates [51].

Moreover, increasing temperatures generally increase levels of evapotranspiration of soil and plants, leading to increased desiccation of topsoil [52]. Furthermore, climate change is causing avisible increase in extreme climatic conditions where extreme rainfalls and floods follow prolonged and hotter droughts [38,48]. Taken together, these events are expected to increase soil aeration in peatlands with the subsequent decline in water table depth. Waterlogging is necessary to impede organic matter degradation, and several studies in different peatland sites in Canada and Europe have shown an increase in CO_2 and CH_4 release due to increased soil respiration [53], an increase in enzymatic degradation activities [31,51] and related loss of peat biomass as a consequence [54]. Furthermore, prolonged draughts can damage leaves, negatively influencing net photosynthetic production [48,52].

Particularly interesting is the loss of the “Enzyme latch” effect. As Peroxides become increasingly active upon oxygen availability, phenolic substance breakdown increases, leading to impaired inhibition of hydrolases and increased organic matter decomposition [28–30].

South American peatlands are considerably less studied, but the available information points towards similar behavior in terms of greenhouse gas release [55], enzyme activity on altitudinal gradients [32,56], the interplay of vegetation, soil type, and climatic conditions greatly impact soil microorganisms and, therefore, degradation processes and their vulnerability to climate change. Although temperature obviously plays a crucial role in the alteration of degradational processes within peatlands [28], it is important to mention that it should always be taken into account under the current vegetational conditions, as these play a key role in the microbiome interaction [57,58]. This is also the drawback of comparability between different types of peatlands, as vegetation and its associated microbiota might change significantly. Studies in northern peatlands have shown that even small temperature changes can have a

significant impact on vegetation shift models [48] which means they can affect each other mutually.

More research effort is needed to define the active role of the ecuadorian paramo in future climate change scenarios as well as determine the danger it faces to decrease due to the upcoming extreme climatic conditions. Research outcomes from former studies can help to adjust conservation policies and actions to mitigate global warming which are urgently needed.

1.7 Chapter References

1. Buytaert W, Célleri R, Bièvre BD, Cisneros F. HIDROLOGÍA DEL PÁRAMO ANDINO: PROPIEDADES IMPORTANCIA Y VULNERABILIDAD. 2008;27.

2. León S, Monsalve G, Bustamante C. How Much Did the Colombian Andes Rise by the Collision of the Caribbean Oceanic Plateau? Geophys Res Lett. 2021 Apr 1;48.

3. Luebert F, Muller LAH. Effects of mountain formation and uplift on biological diversity. Front Genet [Internet]. 2015 [cited 2022 Jun 13];6. Available from: https://www.frontiersin.org/article/10.3389/fgene.2015.00054

4. Madriñán S, Cortés A, Richardson J. Páramo is the world's fastest evolving and coolest biodiversity hotspot. Front Genet [Internet]. 2013 [cited 2022 Jun 13];4. Available from: https://www.frontiersin.org/article/10.3389/fgene.2013.00192

5. Hall ML, Mothes PA, Samaniego P, Militzer A, Beate B, Ramón P, et al. Antisana volcano: A representative andesitic volcano of the eastern cordillera of Ecuador: Petrography, chemistry, tephra and glacial stratigraphy. J South Am Earth Sci. 2017 Jan;73:50–64.

6. Chuncho G. Páramos del Ecuador, importancia y afectaciones: Una revisión. 2019 Dec 1;9:71–83.

7. Jiménez-Rivillas C, García JJ, Quijano-Abril MA, Daza JM, Morrone JJ. A new biogeographical regionalisation of the Páramo biogeographic province. Aust Syst Bot. 2018;31(4):296.

8. Hofstede R, Segarra P, Mena Vasconez P. Los paramos del mundo. Ecuador: Global Peatland Initiative; 2003.

9. Buytaert W, Cuesta-Camacho F, Tobon C. Potential impacts of climate change on the environmental services of humid tropical alpine regions. Glob Ecol Biogeogr. 2011 Jan;20(1):19–33.

10. Food and Agriculture Organization of the United Nations, editor. World reference base for soil resources. Rome: Food and Agriculture Organization of the United Nations; 1998. 88 p. (World soil resources reports).

11. Podwojewski P, Poulenard J. Los suelos de los paramos del Ecuador. 2000 Jan 1;

12. Sklenář P, Balslev H. Superpáramo plant species diversity and phytogeography in Ecuador. Flora - Morphol Distrib Funct Ecol Plants. 2005 Sep 6;200(5):416–33.

13. Bader MY, van Geloof I, Rietkerk M. High solar radiation hinders tree regeneration above the alpine treeline in northern Ecuador. Plant Ecol. 2007 Jul 1;191(1):33–45.

14. Buytaert W, Wyseure G, Bièvre BD, Deckers J. The effect of land-use changes on the hydrological behaviour of Histic Andosols in south Ecuador. Hydrol Process. 2005;19(20):3985–97.

15. Crespo P, Célleri R, Buytaert W, Ochoa B, Cárdenas I, Iñiguez V, et al. Impactos del cambio de uso de la tierra sobre la hidrología de los páramos húmedos andinos. CONDESAN. 2014;288–304.

16. Aparecido LMT, Teodoro GS, Mosquera G, Brum M, Barros F de V, Pompeu PV, et al. Ecohydrological drivers of Neotropical vegetation in montane ecosystems. Ecohydrology. 2018 Apr;11(3):e1932.

17. Hribljan JA, Suarez E, Bourgeau-Chavez L, Endres S, Lilleskov EA, Chimbolema S, et al. Multidate, multisensor remote sensing reveals high density of carbon-rich mountain peatlands in the páramo of Ecuador. Glob Change Biol. 2017 Dec 1;23(12):5412–25.

18. Valencia JB, Mesa J, León JG, Madriñán S, Cortés AJ. Climate Vulnerability Assessment of the Espeletia Complex on Páramo Sky Islands in the Northern Andes. Front Ecol Evol [Internet]. 2020 [cited 2022 Jun 13];8. Available from: https://www.frontiersin.org/article/10.3389/fevo.2020.565708

19. Pérez M, Chávez E, Echeverría M, Córdova R, Recalde C. Assessment of natural background radiation in one of the highest regions of Ecuador. Radiat Phys Chem. 2018 May 1;146:73–6.

20. Masiokas MH, Luckman BH, Vuille M, Villalba R, Poveda G. Editorial: Observed and Predicted Changes in Climate in the Andes Cordillera. Front Environ Sci [Internet]. 2020 [cited 2022 Jul 22];8. Available from: https://www.frontiersin.org/articles/10.3389/fenvs.2020.591996

21. Correa A, Ochoa-Tocachi BF, Birkel C, Ochoa-Sánchez A, Zogheib C, Tovar C, et al. A concerted research effort to advance the hydrological understanding of tropical páramos. Hydrol Process. 2020;34(24):4609–27.

22. Buytaert W, Deckers J, Wyseure G. Regional variability of volcanic ash soils in south Ecuador: The relation with parent material, climate and land use. CATENA. 2007 Jul 15;70(2):143–54.

23. Särkinen T, Pennington RT, Lavin M, Simon MF, Hughes CE. Evolutionary islands in the Andes: persistence and isolation explain high endemism in Andean dry tropical forests. J Biogeogr. 2012;39(5):884–900.

24. Viviroli D, Archer DR, Buytaert W, Fowler HJ, Greenwood GB, Hamlet AF, et al. Climate change and mountain water resources: overview and recommendations for research, management and policy. Hydrol Earth Syst Sci. 2011 Feb 4;15(2):471–504.

25. Soil Microbes [Internet]. EurekAlert! [cited 2023 Jan 16]. Available from: https://www.eurekalert.org/multimedia/879790

26. Hribljan JA, Suarez E, Heckman KA, Lilleskov EA, Chimner RA. Peatland carbon stocks and accumulation rates in the Ecuadorian paramo. Wetl Ecol Manag. 2016 Apr;24(2):113–27.

27. Bahram M, Netherway T, Hildebrand F, Pritsch K, Drenkhan R, Loit K, et al. Plant nutrient-acquisition strategies drive topsoil microbiome structure and function. New Phytol. 2020 Aug;227(4):1189–99.

28. Pinsonneault AJ, Moore TR, Roulet NT. Temperature the dominant control on the enzyme-latch across a range of temperate peatland types. Soil Biol Biochem. 2016 Jun;97:121–30.

29. Freeman C, Ostle NJ, Fenner N, Kang H. A regulatory role for phenol oxidase during decomposition in peatlands. Soil Biol Biochem. 2004 Oct;36(10):1663–7.

30. Brouns K, Verhoeven JTA, Hefting MM. Short period of oxygenation releases latch on peat decomposition. Sci Total Environ. 2014 May;481:61–8.

31. Romanowicz KJ, Kane ES, Potvin LR, Daniels AL, Kolka RK, Lilleskov EA. Understanding drivers of peatland extracellular enzyme activity in the PEATcosm experiment: mixed evidence for enzymic latch hypothesis. Plant Soil. 2015 Dec;397(1–2):371–86.

32. Brück S, Toapanta K, Buitrón P, Pachecho W, Rios-Quituizaca PB, Polizeli M de LT. Potential Impacts of Seasonal and Altitudinal Changes on Enzymatic Peat Decomposition in

the High Andean Paramo Region of Ecuador [Internet]. Rochester, NY; 2022 [cited 2023 Jan 16]. Available from: https://papers.ssrn.com/abstract=4132989

33. Monasterio M, Sarmiento L. Adaptive radiation of Espeletia in the cold andean tropics. Trends Ecol Evol. 1991 Dec 1;6(12):387–91.

34. González Rentería Y, Aragón G, Burgaz A, Prieto M. Records of terricolous lichens from páramos of southern Ecuador. Mycotaxon. 2017 Apr 27;132:153–75.

35. Brück SA, Contato AG, Gamboa-Trujillo P, de Oliveira TB, Cereia M, de Moraes Polizeli M de LT. Prospection of Psychrotrophic Filamentous Fungi Isolated from the High Andean Paramo Region of Northern Ecuador: Enzymatic Activity and Molecular Identification. Microorganisms. 2022 Feb;10(2):282.

36. Benítez Á, Gradstein SR, Cevallos P, Medina J, Aguirre N. Terrestrial bryophyte communities in relation to climatic and topographic factors in a paramo of southern Ecuador. Caldasia. 2019 Dec;41(2):370–9.

37. Morueta-Holme N, Engemann K, Sandoval-Acuña P, Jonas JD, Segnitz RM, Svenning JC. Strong upslope shifts in Chimborazo's vegetation over two centuries since Humboldt. Proc Natl Acad Sci. 2015 Oct 13;112(41):12741–5.

38. IPCC. IPCC international panel on climate change - report 2014 [Internet]. 2014 [cited 2022 Jan 10]. Available from: https://archive.ipcc.ch/pdf/assessment-report/ar5/syr/AR5_SYR_FINAL_SPM_es.pdf

39. Alvarez-Yela AC, Alvarez-Silva MC, Restrepo S, Husserl J, Zambrano MM, Danies G, et al. Influence of agricultural activities in the structure and metabolic functionality of paramo soil samples in Colombia studied using a metagenomics analysis in dynamic state. Ecol Model. 2017 May 10;351:63–76.

40. Hofstede R. El impacto de las actividades humanas sobre el paramo. 2002;24.

41. Avellaneda-Torres LM, León Sicard TE, Torres Rojas E. Impact of potato cultivation and cattle farming on physicochemical parameters and enzymatic activities of Neotropical high Andean Páramo ecosystem soils. Sci Total Environ. 2018 Aug;631–632:1600–10.

42. Turetsky MR, Donahue WF, Benscoter BW. Experimental drying intensifies burning and carbon losses in a northern peatland. Nat Commun. 2011 Nov 1;2:514.

43. Turetsky MR, Amiro BD, Bosch E, Bhatti JS. Historical burn area in western Canadian peatlands and its relationship to fire weather indices. Glob Biogeochem Cycles [Internet]. 2004 [cited 2022 Jul 4];18(4). Available from: https://onlinelibrary.wiley.com/doi/abs/10.1029/2004GB002222

44. Hofstede RGM. The effects of grazing and burning on soil and plant nutrient concentrations in Colombian páramo grasslands. Plant Soil. 1995 Jun 1;173(1):111–32.

45. Avellaneda-Torres LM, Melgarejo LM, Narváez-Cuenca CE, Sánchez J. Enzymatic activities of potato crop soils subjected to conventional management and grassland soils. J Soil Sci Plant Nutr. 2013;(ahead):0–0.

46. Waddington JM, Quinton WL, Price JS, Lafleur PM. Advances in Canadian Peatland Hydrology, 2003-2007. Can Water Resour J Rev Can Ressour Hydr. 2009 Jan 1;34(2):139–48.

47. Warner BG, Asada T. Biological diversity of peatlands in Canada. Aquat Sci. 2006 Oct 1;68(3):240–53.

48. Heijmans MMPD, van der Knaap YAM, Holmgren M, Limpens J. Persistent versus transient tree encroachment of temperate peat bogs: effects of climate warming and drought events. Glob Change Biol. 2013 Jul;19(7):2240–50.

49. Elliott DR, Caporn SJM, Nwaishi F, Nilsson RH, Sen R. Bacterial and fungal communities in a degraded ombrotrophic peatland undergoing natural and managed re-vegetation. PloS One. 2015;10(5):e0124726.

50. Siles JA, Cajthaml T, Filipova A, Minerbi S, Margesin R. Altitudinal, seasonal and interannual shifts in microbial communities and chemical composition of soil organic matter in Alpine forest soils. Soil Biol Biochem. 2017 Sep;112:1–13.

51. Burns RG, DeForest JL, Marxsen J, Sinsabaugh RL, Stromberger ME, Wallenstein MD, et al. Soil enzymes in a changing environment: Current knowledge and future directions. Soil Biol Biochem. 2013 Mar;58:216–34.

52. Feller U. Drought stress and carbon assimilation in a warming climate: Reversible and irreversible impacts. J Plant Physiol. 2016 Sep 20;203:69–79.

53. Estop-Aragonés C, Zając K, Blodau C. Effects of extreme experimental drought and rewetting on CO2 and CH4 exchange in mesocosms of 14 European peatlands with different nitrogen and sulfur deposition. Glob Change Biol. 2016 Jun;22(6):2285–300.

54. Fenner N, Freeman C. Drought-induced carbon loss in peatlands. Nat Geosci. 2011 Dec;4(12):895–900.

55. Veber G, Kull A, Villa JA, Maddison M, Paal J, Oja T, et al. Greenhouse gas emissions in natural and managed peatlands of America: Case studies along a latitudinal gradient. Ecol Eng. 2018 Apr 15;114:34–45.

56. Nottingham AT, Turner BL, Whitaker J, Ostle N, Bardgett RD, McNamara NP, et al. Temperature sensitivity of soil enzymes along an elevation gradient in the Peruvian Andes. Biogeochemistry. 2016 Feb;127(2–3):217–30.

57. Nottingham AT, Fierer N, Turner BL, Whitaker J, Ostle NJ, McNamara NP, et al. Microbes follow Humboldt: temperature drives plant and soil microbial diversity patterns from the Amazon to the Andes. Ecology. 2018 Nov;99(11):2455–66.

58. Ward SE, Orwin KH, Ostle NJ, Briones JI, Thomson BC, Griffiths RI, et al. Vegetation exerts a greater control on litter decomposition than climate warming in peatlands. Ecology. 2015 Jan;96(1):113–23.

Chapter 2

Prospection of Psychrotrophic Filamentous Fungi Isolated from the High Andean Paramo Region of Northern Ecuador: Enzymatic Activity and Molecular Identification

This chapter is based on the accepted article with the same name published on January 2022 in the journal Microorganisms

Abstract: The isolation of filamentous fungal strains from remote habitats with extreme climatic conditions has led to the discovery of a series of enzymes with attractive properties that can be useful in various industrial applications. Among these, cold-adapted enzymes from fungi with psychrotrophic lifestyles are valuable agents in industrial processes aiming toward energy reduction. Out of eight strains isolated from soil of the paramo highlands of Ecuador, three were selected for further experimentation and identified as *Cladosporium michoacanense*, *Cladosporium* sp. (cladosporioides complex), and *Didymella* sp., the latter being reported for the first time in this area. The secretion of seven enzymes, namely, endoglucanase, exoglycanase, β-D-glucosidase, endo-1,4-β-xylanase, β-D-xylosidase, acid, and alkaline phosphatases, were analyzed under agitation and static conditions optimized for the growth period and incubation temperature. *Cladosporium* strains under agitation, as well as incubation for 72 h, mostly showed substantial activation for endoglucanase reaching up to 4563 mU/mL and xylanase up to 3036 mU/mL. Meanwhile, other enzymatic levels varied enormously depending on growth and temperature. *Didymella* sp. showed the most robust activation at 8 °C for endoglucanase, β-D-glucosidase, and xylanase, indicating an interesting profile for applications such as bioremediation and wastewater treatment processes under cold climatic conditions.

Keywords: psychrotrophic fungi; High Andean Paramo; cold-adapted enzymes; bioprospecting

2.1 Introduction

2.1.1 The Paramo as a habitat for cold-adapted fungi

The High Andean mountain region is marked by the neotropical grassland paramo, covering mountainsides from 3500 up to 5000 m of altitude in Ecuador [1]. As mentioned in Chapter 1 it is considered a hotspot of biodiversity mainly due to the fact of its high degree of endemic species adapted to extreme environmental conditions [2] such as intense radiation close to the equator line [3], nighttime temperatures close to the freezing point, and low availability of nutrients [4]. Fungi growing under these conditions tend to develop a psychrophilic or psychrotrophic profile, developing at 0 °C with optimum growth conditions of ≤15 and 15–20 °C, respectively [5,6]. This restricted ecological group has been found in terrestrial and marine environments from Polar Regions, deep water and marine sediments of the oceans, and high mountains [7–9].

The Paramo Region of South America is a vastly unexplored area in terms of soil-derived microorganisms. Geospatial separation by Andean mountain chains creates a series of unique habitats, forcing microbes to adapt to a variety of given conditions, increasing the biological diversity with unique species within different paramo regions [10]. Most surveys of soil-borne fungi were conducted in the Colombian Paramo Region and predominantly with an agricultural background [11–13]. Information about fungi composition in Ecuadorian paramo soils is very scarce [14], and screenings for active enzymatic fungi with possible industrial applications have not been performed yet.

2.1.2 Cold adapted enzymes

Fungi isolated from the paramo can secrete cold-adapted enzymes [15], which are interesting in industrial procedures requiring low temperatures and employing energy to cool down the process. Nowadays, cold-active enzymes are mostly used in meat tenderization, food processing, flavoring, baking, brewing, cheese production, and animal feed [16,17]. They require low activation energies while showing during the meantime the highest activities, at low temperatures, of up to a 10-fold increase compared to mesophilic homologues [18], allowing for energy reduction [19]. This might become increasingly important due to the tendency towards neutral carbon dioxide balances in times of global warming [20].

2.1.3 Enzymes of the cellulolytic and xylanolytic system

The majority of organic matter in decomposition of topsoil consists of plant derived debris [21]. The lysis of plant cell walls is therefore a fundamental step in the multitude of degradation steps by soil derived microbiota. Once broken down, the subsequent degradational steps can accelerate considerably.

The cell wall of plants consists of about 90% polysaccharides and 10% proteins. The main component is cellulose, an unbranched homopolymer made of D-Glucose linked by β-1-4 glycosidic bonds (Figure 2.1 A). 36 cellulose chains together interact with hydrogen bonds to form a crystalline structure called microfibril, which is difficult to hydrolyze. The second most important component belongs to the heterogenous family of hemicellulose, defined by the ability to be extracted by alkaline solutions. Apart from glucose, these polysaccharides

synthesized out of other hexoses such as D-galactose, D-mannose D-fucose and pentoses like D-xylose and L-arabinose mostly connected via β-1-4 but also β-1-6 and β-1-2 glycosidic bonds (Figure 2.1 B) The composition largely depends on the plant species synthesizing it but one most prominent type of hemicellulose found abundantly in hardwood and grass species belongs to the polysaccharide xylan, formed by a backbone of β-1-4 linked xylose {Citation}subunits (Figure 2.1 C)[22,23]

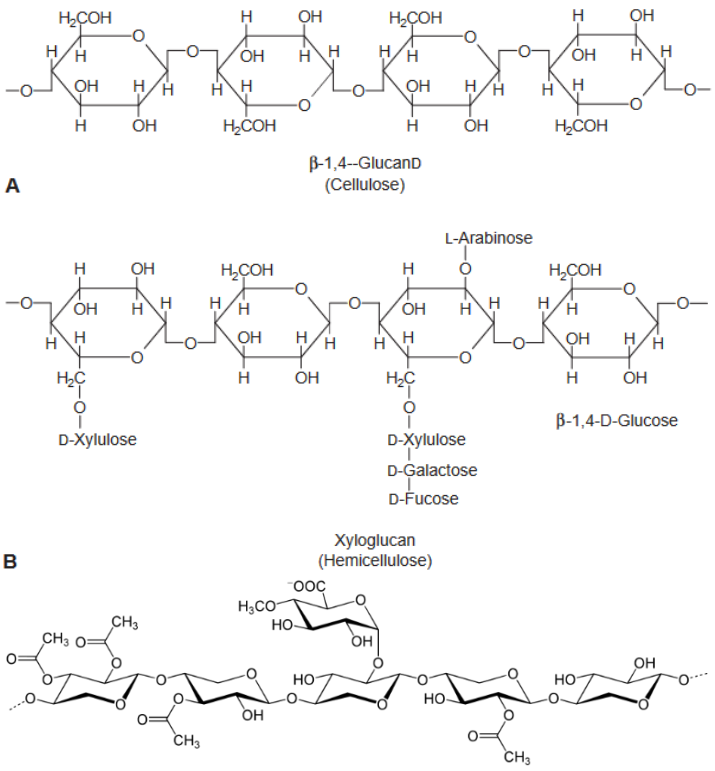

Figure 2.1 Polysaccharides
Chemical structure of **A** cellulose an important representative of hemicellulose called xyloglucan **B** and xylan **C** (Figures adapted from Heldt [24]

Several different enzymes are involved in the breakdown of plant cell wall components. The present study aimes at some of the most important members of the cellulolytic system (endoglucanases, exoglucanases, and β-glucosidase), for efficient cellulose cleavage and of the xylanolytic system (mainly endoxylanase and β-xylosidase) for xylan breakdown to the level of reducing sugars. Table 2.1 summarizes important facts about the analyzed enzymes to clarify their role in organic matter decomposition.

Table 2.1 Enzyme characteristics

Enzyme name	Substrate	Cleavage product	experimental substrate	EC nomenclature
Endoglucanase	cellulose	Cellulose oligomers	carboxymethyl cellulose (CMC)	EC 3.2.1.6
Exoglucanase	cellulose	cellobiose	*p*-nitrophenol-β-D-cellobiose	EC 3.2.1.4
β-glucosidase	cellulose and cellobiose	D-Glucose	*p*-nitrophenol-β-D-glucopyranoside	EC 3.2.1.21
Endoxylanase	xylan polymers	Xylan oligomers	beechwood xylan	EC 3.2.1.8
β-xylosidase	xylan oligomers	D-Xylose	*p*-nitrophenol-β-D-xylopyranoside	EC 3.2.1.37

They are widely applied to biotechnological processes in areas such as the food industry, production of fuels, detergents, and biopulping [23,25–27]. Especially interesting for these cold-adapted enzymes are the treatment of wastewater and environmental bioremediation in countries with shallow temperatures due to the necessity of stable in situ applications without the need for heating [28,29].

2.1.4 Phosphatases

Phosphatases catalyze the hydrolysis of phospho-ester bonds [30]. They play a crucial role in the release of phosphate groups form organic matter, which can subsequently be available for the uptake by plant roots. The action of phosphatases therefore plays an important role in the fertility of each soil type as phosphate is a growth limiting factor in natural soils [31].

The term includes a large family of enzymes further divided into phoshpo-monoesterases (EC 3.1.3), phospho-diesterases (EC 3.1.4) enzymes which use anhydrides with phosphoryl-groups as substrate (EC 3.6.1) and those which can act on phosphorus-nitrogen bonds (EC 3.9) [32]. Another important classification for phosphor-monoesterases is by the ph-

level they are most active, dividing them into acid (3.1.3.2) and alkaline (EC 3.1.3.1) phosphatases [30].

Due to their capacity to express phosphatases Fungi gain increasing importance as biofertilizers to improve crop yield. Given the broad range of climatic zones where crops are planted, biofertilizers must be equally adapted to these conditions including cold regions with generally lower productivity [6]. Cold adapted phosphatases can hydrolyze organic phosphate sources, which become assimilable by plant roots, improving their economic and ecologic growth, eliminating the need for chemical fertilizers [9,33].

This might be important for instance for the paramo region where nutrient availability is low although soil organic matter content is high.

2.1.5 Objective of the study

The present study, aimed to investigate filamentous fungi from paramo soil and optimize incubation conditions for optimal enzyme activity yield to analyze whether their extreme living conditions led to adapted enzymes of the carbon and phosphate cycle with possible interesting applications in the industry comparable to reported enzyme activities for mesophilic fungi. Unfortunately, soil-associated fungi of this region are poorly described and have never been analyzed for their enzymatic hydrolyzation capacities to the best of our knowledge.

2.2 Materials and Methods

2.2.1 Sample Collection and Preparation

Two sampling sites were established, each at two different altitudes within the grassland paramo (4000 m asl) and at the frontier between grassland paramo and superparamo (4150 m asl), lying on a lineal transect towards the peak of the volcano Northern Iliniza to guarantee similar climatic conditions and soil characteristics (Figure 2.2). Each sampling site was carefully selected for level ground, open vegetation in a good conservation state, and the absence of animal signs or human interference. Georeferencing with a GPS (Garmin, Olathe, KS, USA) was applied at each sampling site (Table S1). Then, 10 cm of topsoil was removed together with vegetation, and three soil samples were taken with sterile instruments, giving 12 samples.

Data dataloggers (HOBO, Lakeville, MN, USA) were established at different altitudes to collect temperature data (APPX 2.1). Soil samples were analyzed by the Ecuadorian National Institute for Agricultural Research (INIAP) for organic matter (OM), total nitrogen (Nt), phosphorus, potassium, calcium magnesium (Olsen modified), and sulfur (calcium phosphate standard protocols) (APPX 2.2). Conductivity was measured with water-saturated paste which is defined as the maximum amount of water retainable by the soil-sample without free-water accumulation and pH in a soil-to-water ratio of 1:2.5 (50 grams of soil mixed with 125 ml water under agitation).

Soil samples were diluted with sterile water at dilutions of 0.1 g in 10, 100, and 1000 mL with three replicates each, and 50 µL of each dilution were distributed with a sterilized spreading rod on 10 cm Petri dish containing 12 mL of potato dextrose agar (PDA) (Sigma–Aldrich, Saint Louis, MO, USA) with streptomycin at 1 mg/mL (GM, London, UK). Then, Petri dishes were incubated for 48 h at 20 °C. After incubation, eight samples of clearly isolated and visibly round-shaped fungal colonies were picked with sterile toothpicks and transferred to a fresh PDA petri dish for cultivation.

For the growth assay, each fungus was picked with a sterile toothpick and inoculated at the center of a PDA Petri dish. Then dishes were incubated at 4, 30, and 40 °C, respectively, for a total of 35 days. Growth was measured weekly in cm growth-diameter of the halo through the inoculation point.

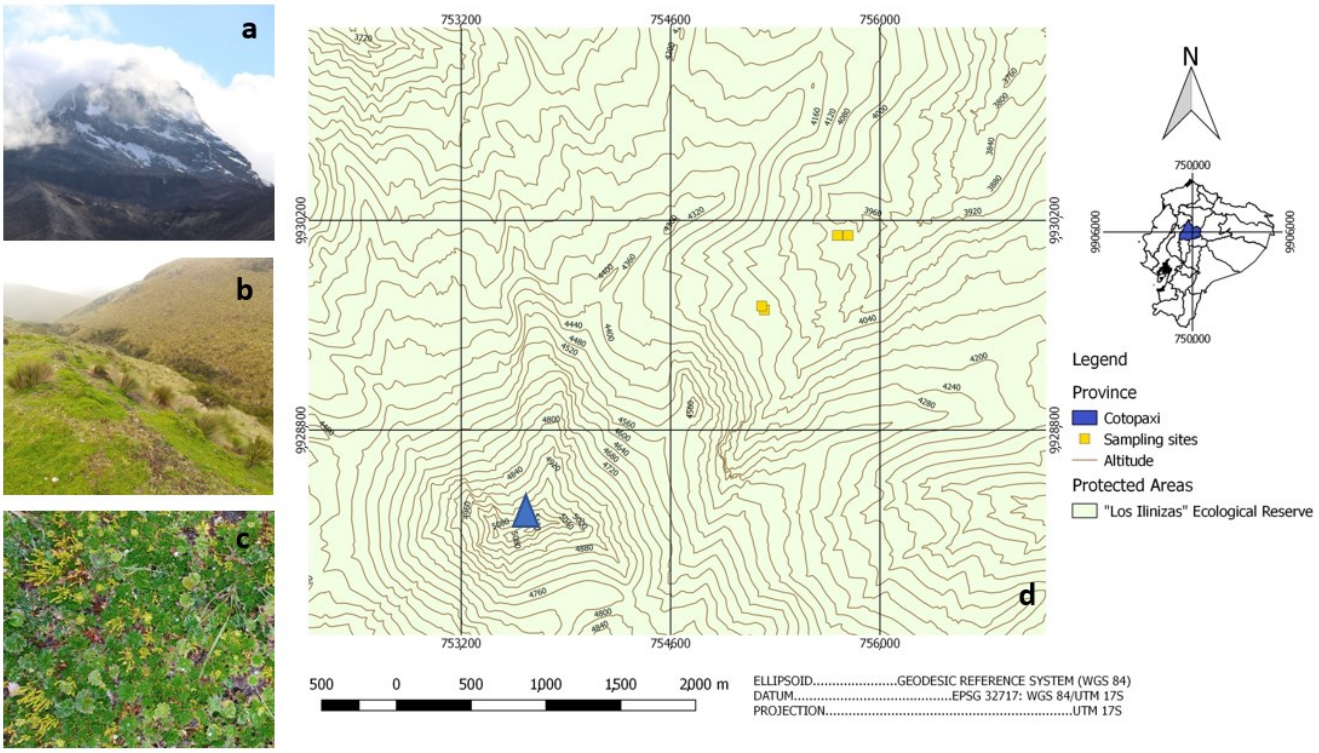

Figure 2.2 Sampling sites
Vision of the Iliniza north volcano (**a**); typical Andean grass paramo landscape (**b**); typical conserved paramo vegetation (**c**); the georeferenced linear transect of sampling towards the volcano peak (blue triangular) at the bottom left (**d**) (Source: **a**–**c** Author 2020; (**d**) modified from [34]).

2.2.2 Fungal Strain Identification

2.2.2.1 DNA Extraction

To obtain genomic DNA of three fungal strains, the mycelia were macerated with a mortar and pestle in TES lysis buffer (Tris 100 mM; EDTA 10 mM; 2% SDS). First, lysed tissue was incubated at 65 °C for 15 min. Then, 140 µL of 5 M NaCl were added, and the mixture was incubated on ice for 30 min. Afterward, 600 µL of chloroform/isoamyl alcohol (24:1) were added and centrifuged at 10,000× *g* for 10 min at 4 °C. The supernatant was isolated and mixed with 50 µL sodium acetate 3 M (pH 5.2) and 300 µL isopropanol. After the second centrifugation under the same conditions, the supernatant was discarded, and the mixture was washed twice with 600 µL of 70% ethanol following centrifugation steps. After discarding the final supernatant, the resulting pellet was diluted in 50 µL TE buffer (Tris 10 mM; EDTA 1 mM) and 5 µL RNAse (10 mg/mL).

2.2.2.2 Polymerase Chain Reaction

Genomic DNA was used to amplify the fungal ITS region (ITS1-5.8S-ITS2) applying the primer pairs ITS4 and ITS5 [35]. For amplification reactions, a PCR Master Mix Kit was used (Promega, Madison, WI, USA), following the manufacturer's instructions. To visualize the amplification, product electrophoresis was performed on a 1% agarose gel stained with Nancy dye (Sigma–Aldrich, Saint Louis, MO, USA). Next, the amplification products were purified using the Wizard® SV Gel kit and PCR Clean-Up System (Promega) following the kit's instructions. Finally, the PCR product was quantified on a NanoDrop® (Thermo Scientific, Waltham, MA, USA).

2.2.2.3 DNA Sequencing

Sequencing reactions were performed with the BigDye® Terminator Cycle Sequencing Kit (Life Technologies, Carlsbad, CA, USA) following the manufacturer's instructions and analyzed with ABI 3500 XL sequencer system (Life Technologies). Resulting forward and reverse sequences were quality checked and merged into a consensus sequence with BioEdit v.7.0.5.3 [36]. The BLASTn tool of the public NCBI-GenBank (www.ncbi.nlm.nih.gov) and the Trichokey database (http://isth.info/) were used to compare contigs with homologous sequences (both accessed on 12 April 2019). After a second, quality control sequences were aligned with homologous sequences from culture collections applying the ClustalW tool [37]. Then, the sequences were subjected to phylogenetic analysis. The phylogeny was assembled using the neighbor-joining method, calculating the evolutionary distance using the 2-parameter Kimura model, and are expressed as the units of the number of base substitutions per site. The rate variation among sites was modeled with a gamma distribution (shape parameter = 1). The analysis involved 58 nucleotide sequences. All positions containing gaps and missing data were eliminated. There was a total of 430 positions in the final data set. Tree support was calculated with bootstrap analysis with 1000 pseudo-replications, and the tree was inferred using MEGA v.7.0 [38].

2.2.3 Preparation of Crude Enzyme Extract

Isolated fungi were pre-cultured at 20 °C on inclined agar PDA medium in test tubes until sporulation. Concentrations of 10^6–10^7 spores per mL were established in sterile water using a Neubauer chamber for counting. These spores were then used to inoculate 50 mL of

sterile Adam's medium (pH = 6) with 1% wheat bran in 125 mL Erlenmeyer flasks (APPX 2.3) Triplicates were incubated at 20 °C under static and shaking conditions (120 rpm), respectively, for 120 h harvesting each 24 h. Each crude extract sample from flasks was filtered over Whatman paper using a vacuum pump and applied on the same day for enzyme assays.

2.2.4 Enzyme Activity Assay

2.2.4.1 Enzyme Determination with Natural Substrates

To measure enzyme activity, the crude enzyme extract was mixed with respective water-diluted substrates to obtain activity over time according to the Miller method [39]. Reducing sugars were quantified using 3,5-dinitrosalicylic acid (DNS) combined with 0.5% carboxymethylcellulose (CMC) (endoglucanase measurement) (Sigma–Aldrich®) and 0.5% xylan beechwood (endoxylanase measurement) in the following relation: 25 µL substrate, 10 µL buffer sodium acetate 50 mM pH 5.0, and 15 µL crude extract. Mixes were incubated in a thermocycler (Eppendorf®, Hamburg, Germany) for 20 min at 30 °C . In the assay to determine optimal incubation temperatures, a range was established from 4 to 32 °C. Then, 50 µL DNS was added to interrupt enzyme activity, and sample-absorbance was measured at 540 nm on a spectrophotometer (Shimadzu, Kyoto, Japan) compared to glucose and xylose standard curves (0–1 mg/mL). Blancs were established adding enzyme extract after incubation, directly interrupting the reaction with DNS. The results were expressed as milliunits per mL (mU/mL), defined as the enzyme quantity that releases one µmol of reducing sugars per minute per mL (APPX 2.4).

2.2.4.2 Enzyme Determination with Synthetic Substrates

To measure enzyme activity, the crude enzyme extract was mixed with respective water-diluted substrates to obtain activity over time. The amount of released *p*-nitrophenol as a result of enzyme cleavage was measured for the following substrates: *p*-nitrophenol-β-D-glycopyranoside (β-D-glucosidase measurement), *p*-nitrophenol-β-D-xylanopyranoside (β-D-xylosidase measurement), and *p*-nitrophenol-β-D-cellobiose (exoglucanase measurement) (all substrates obtained from Sigma—Aldrich®) used in the following relation: 25 µL substrate, 10 µL sodium acetate buffer 50 mM pH 5.0, and 15 µL crude extract [40].

For the measurement of phosphatases with *p*-nitrophenyl phosphate (acid and alkaline phosphatase), the assay mix was prepared accordingly using 10 µL crude extract, 40 µL substrate, and 100 µL buffer, where acid phosphatase was measured with acetate buffer 100 mM, pH 4.5 and alkaline phosphatase with Tris-HCl 100 mM, pH 8.0 (modified according to [41]). Mixes were incubated in a thermocycler (Eppendorf®) for 20 min at 30 °C. In the assay to determine optimal incubation temperatures, a range was established from 4 to 32 °C in steps of 4 °C. Then, 50 µL (100 µL for phosphatases) of 0.2 M Na_2CO_3 solution was added to interrupt enzyme activity and sample-absorbance was measured at 410 nm compared to a *p*-nitrophenol–standard curve (0–1 mg/mL) [42]. Blancs were established by adding enzyme extract after incubation, directly interrupting the reaction with Na_2CO_3 solution. The results are expressed as milliunits per mL (mU/mL), defined as the enzyme quantity that releases one µmol of *p*-nitrophenol per minute per mL.

2.2.5 Statistical Analysis

Measured enzyme activity is expressed as the mean ± standard deviation using Microsoft EXCEL. The Shapiro–Wilk test was used to prove the normal distribution of data and the Levene's test for homoscedasticity. To test for statistical difference between incubation types (i.e., agitation and static), averages of the maximum enzyme activities were compared using the *t*-test for independent variables or Mann–Whitney U test, respectively. To analyze maximum yields among the three studied fungi, one-way ANOVA or Kruskal–Wallis test were applied following Sidak–Bonferroni or Dunn post-hoc tests (APPX 2.5). All statistical analyses were performed using licensed STATA 16.0.

2.3 Results and Discussion

2.3.1 Sample Site Conditions and Soil Characteristics

This sampling sites in the Iliniza National Reserve were chosen due to the fact of their proximity to glacial areas of stratified volcanos in the High Andean region. At a 4000 m altitude, the vegetation zone of conserved paramo highlands is grassland, mainly characterized by herbaceous plants such as sphagnum mosses, tussock grass, and rosette plants (Figure 2.2b and c). At 4150 m asl, the zone of the superparamo builds the frontier between the last zone of

abundant vegetation and the beginning of the rocky glacial zone with only sporadic vegetation. Close to the equator, the radiation at this altitude is very high, causing drastic daily temperature changes between day and nighttime with an average temperature of 9.6 °C (Table 2.2). Due to the volcanic ash deposition and slow decomposition, the slightly acidic soil (pH 5.87–6.15) has mainly a sandy–loam texture with 7.7–9% organic matter, which is very high, as expected for Andisols [43].

Table 2.2 Sampling site characteristics

Sampling site	Coordinates	Altitude	Temperature (Ø)	Predominant vegetation	N° of isolates
1	Sº 78,701786; Wº 0,631899	3986	9.966	Poaceae, Asteraceae, Verbenaceae, Rosaceae	2
2	Sº 78,702426; Wº 0,631899	3998			1
3	Sº 78,706805; Wº 0,636392	4145	9.552	Poaceae, Apiaceae, Rosaceae	3
4	Sº 78,706972; Wº 0,63616	4149			2

The stabilization of large organic particles also accounts for its vast water retention capacity [44], which, together with the related oxygen availability, directly interferes with the development of microorganisms and the solubilization of phosphorus [45]. The formation of humic acids in the breakdown of organic matter allows for the formation of metal–humus complexes retaining chelated ions like calcium [46] and magnesium [47], which might explain their abundance in analyzed soils and further account for the observed high levels of conductivity [48]. On the other hand, under the environmental conditions of the paramo region, organic matter breakdown is slow. It might negatively interfere with nutrient availability due to the microbial activity as indicated by the observed low phosphorus, sulfur [49], and nitrogen levels (Table 2.3) [50–52].

Table 2.3 Soil characteristics at sampling sites.

Sample Site	Soil Type	Soil Texture	pH	COND (µS/cm²)	Nt %	OM %	P (ppm)	S (ppm)	K (meq/100 g)	Ca (meq/100 g)	Mg (meq/100 g)
1	Andisol	sandy–loam, loamy	6.15	21.5	0.31	8.8	9.01	8.4	0.54	9.78	1.71
2			6.78	21.3	0.36	9.7	14	9.3	0.48	9.76	1.28
3	Andisol	sandy–loam	5.93	15.51	0.25	7.7	6.04	4.7	0.42	7.49	1.01
4			5.87	20.8	0.27	9	12	4.1	0.37	4.87	0.73

COND = conductivity, Nt = total nitrogen, and OM = organic matter.

2.3.2 Screening for Cultivable Fungi

The first screening for cultivable fungal strains from soil samples showed relatively few growing colonies clearly separated from each other, allowing for easy isolation of distinct strains. Out of 12 soil samples, eight colonies were chosen for the study. These strains were further screened for their capacity to grow at different temperature conditions. Generally, all strains showed better growth at 4 °C than 30 °C, indicating their adaptation to cold environments (Figure 2.3 Temperature dependent growth). At 40 °C, no development could be detected. The results showed a potentially psychrophilic profile for the best growing behavior of strain 3.3 at 4 °C given that it was not able to grow at 30 °C and psychrotrophic profiles for the strains 1.1 and 3.1 at 30 °C [5], which were chosen for further experimentation (Figure 2.4).

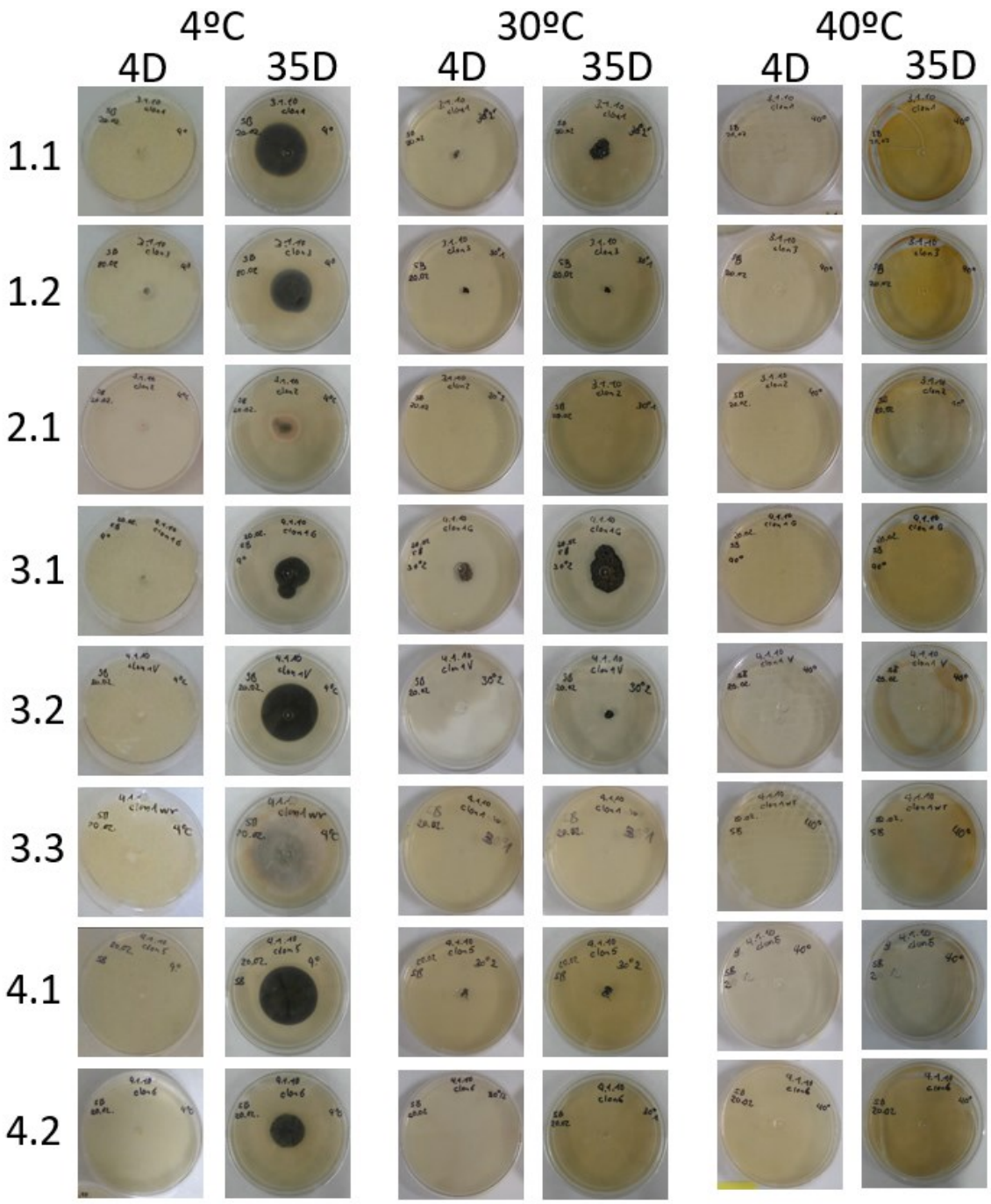

Figure 2.3 Temperature dependent growth
Growth of 8 different isolated fungal strains from 4 different sampling sites after 4 and 35 days (D) at different temperatures.

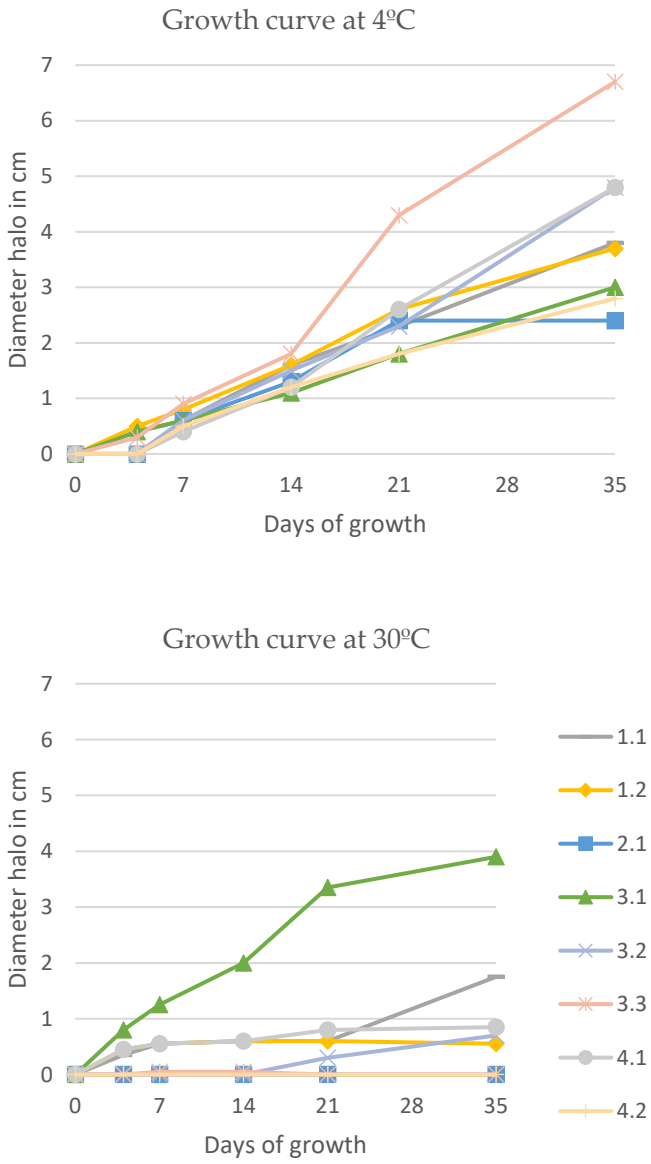

Figure 2.4 Temperature dependent growth curves
Growth curves of isolated fungal strains at 4ºC and 30ºC.

2.3.3 Identification of Fungi

Phylogenetic analysis of the ITS region revealed that all three fungi were ascomycetes with strains 1.1 and 3.1 belonging to the genus *Cladosporium: C. michoacanense* and *Cladosporium* sp. 3.1 (*C. Cladosporioides* species complex), respectively, and 3.3 to the genus *Didymella* (Figure 2.5). Since the ITS region is not sufficient for species delimitation in some of these groups, other secondary barcodes would be needed for more accurate identification. The genus *Cladosporium* is a highly heterogeneous group with cosmopolitan distribution and strong capability of adaptation [53] with species formerly isolated from arctic soils [8,27] and

marine sponges [54]. A third strain belonged to the genus *Didymella* which has mainly been studied due to the existence of pathological strains and plant–host interaction [55] but so far to a lesser extent due to the fact of its resistance to extreme conditions and, therefore, its arising enzymatic capacities [56]. Both *Cladosporium* and *Didymella* strains have formerly been reported in soil isolates from Himalaya mountain environments [57,58]. Still, only *Cladosporium* has formerly been described for Andean regions [12,14], and the present study is the first registry of the genus *Didymella* in the paramo ecosystem.

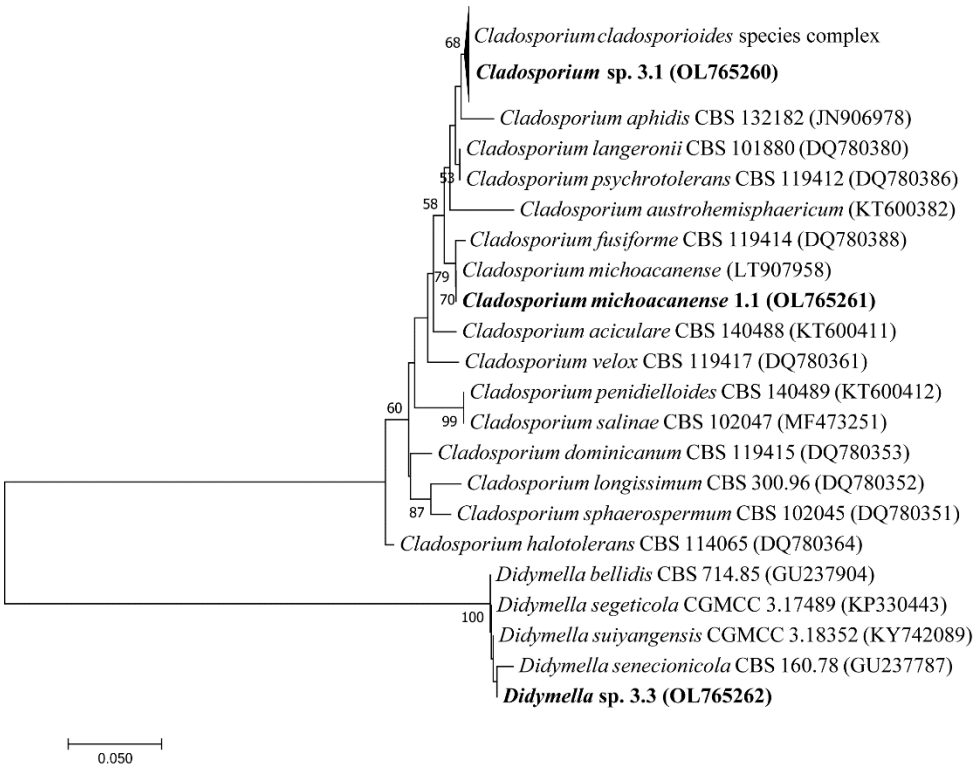

Figure 2.5 Phylogenetic analysis of filamentous fungi
isolated from paramo soil samples (bold) and the closest related species.

Images taken of the growth behavior in culture dishes of PDA indicate a dark brown colorization of mycelia, which possibly shows intense melanin pigmentation as a protective adaptation to the strong radiation in their natural habitat as formerly described [59,60] (Figure 2.6 d–f). Furthermore, differential growth behavior was detected under static and agitation conditions (Figure 2.6 g–i). Especially, the *Cladosporium* strains tended to grow better under agitation, developing a darker aspect apparently due to the stronger sporulation [61]. Meanwhile, its impact on *Didymella* was less evident.

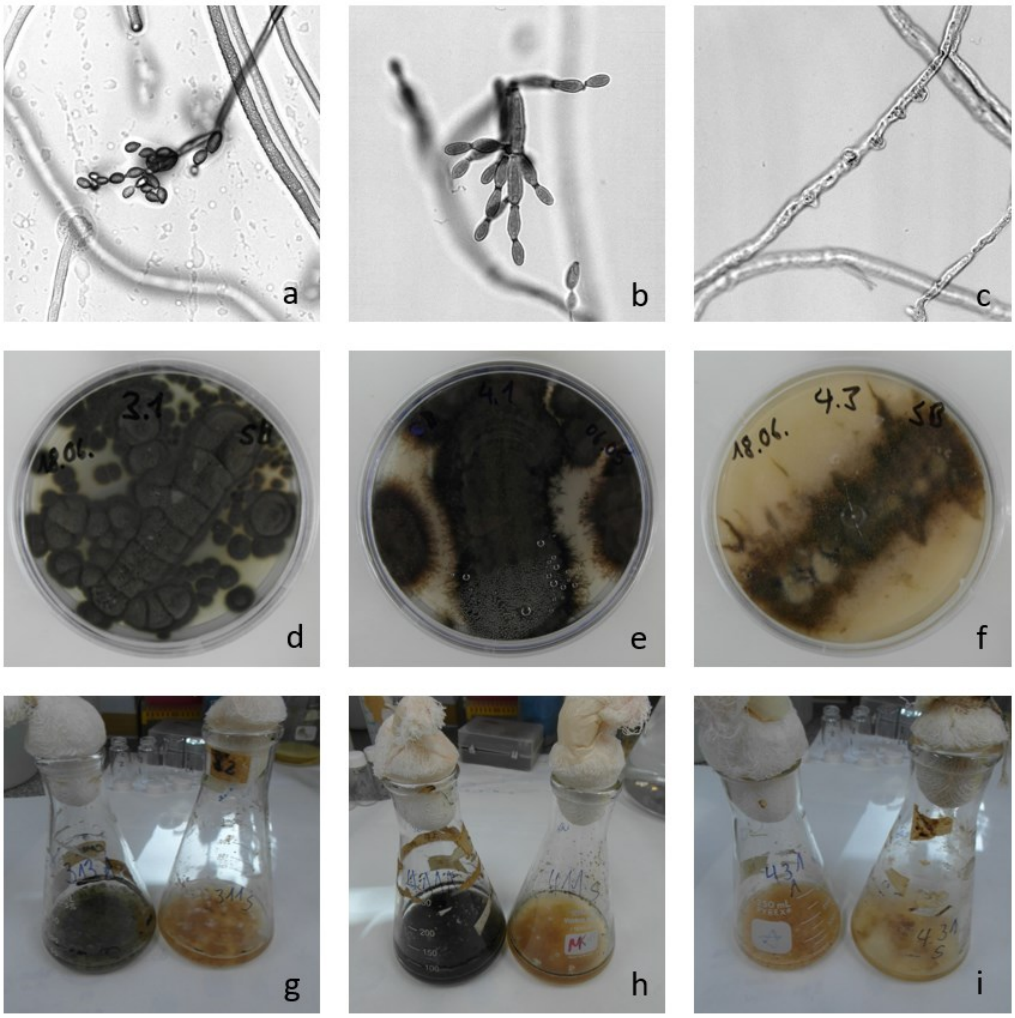

Figure 2.6 Filamentous fungi cultivation

Selected and identified fungi, from left to right *Cladosporium michoacanense* (a, d, g)*, Cladosporium* sp. (*cladosporioides* species complex)(b, e, h)*, Didymella* sp. (c, f, i)*;* top microscopy of sporangium and micelia (a-c), middle row cultures on Potato Dextrose Agar (d-f) and bottom row comparison of shaken culture versus static culture (g-i).

2.3.4 Enzymatic Characterization

The following section shows the incubation time-dependent enzyme secretion results from 24 to 120 h under agitation and static condition for each isolated fungal strain to characterize the hydrolyzation capacities at 30 °C.

2.3.4.1 Enzymatic Production of *Cladosporium michoacanense*

Cladosporium michoacanense 1.1 showed the most potent activation under agitation with a relatively late onset of enzyme secretion compared to studies analyzing the same enzymes [40] (Table 2.4). The most significant activity was detected at 72 h for the hydrolyzation of CMC, xylan, and *p*np-phosphate in an alkaline medium; 96 h for *p*np-β-D-glycopyranoside; 120 h for *p*np-β-D-cellobiose, *p*np-β-D-xylanopyranoside, and *p*np-phosphate in acidic medium, indicating statistically significant differences to measurements

under static conditions for all enzymes except for exoglucanase and β-glucosidase. Interestingly, under static incubation conditions, the most potent enzyme activity was measured early between 24 to 48 h for endoglucanase, xylanase, β-xylosidase, and alkaline phosphatase and late response at 120 h for exoglucanase, β-glucosidase, and acid phosphatase. Overall, the most efficient enzyme activity for endoglucanase and xylanase could be observed at levels well above 2000 mU/mL under agitated cultivation.

Table 2.4 *Cladosporium michoacanense* 1.1 enzymes produced overtime under agitation and static conditions

	Agitation					Static				
Enzyme	**24h**	**48h**	**72h**	**96h**	**120h**	**24h**	**48h**	**72h**	**96h**	**120h**
Endoglucanase	932.2±20.7	1514.4±100.5	**2503.7±207.1***	394.5±51.8	385.2±170.0	887.4±84.8	**1061.0±23.3**	917.6±17.1	791.4±70.4	730.6±26.9
Exoglucanase	ND	ND	ND	1.4±0.7	**1.4±0.3**	ND	ND	ND	ND	**0.2±0.1**
β-glycosidase	ND	ND	ND	**1.7±0.0**	ND	ND	ND	ND	ND	**0.2±0.0**
Xylanase	360.2±105.7	969.4±120.1	**2430.1±2.1***	274.6±81.3	145.2±34.7	**737.8±88.3**	435.5±111.7	412.2±53.9	353.0±119.5	384.3±70.6
β-xylosidase	ND	ND	0.7±0.	1.1±0.3	**1.4±0.3***	**0.5±0.1**	ND	ND	ND	ND
acid phosphatase	1.4±0.6	1.7±1.0	31.0±0.3	5.9	**34.9±0.1***	ND	ND	ND	ND	**0.7±0.4**
alk. phosphatase	0.3±0.1	1.4±0.3	**2.3±0.4***	0.2±0.2	ND	**1.4±0.3**	0.6±0.3	ND	ND	ND

Data are expressed as mU/mL ± standard deviation. ND = not detected; * indicates a statistically significant difference ($p < 0.05$) between the average enzyme activity of fungi cultivated under agitation vs. static conditions for each analyzed enzyme. In bold, maximum achieved activity.

2.3.4.2 Enzymatic production of *Cladosporium* sp. (*C. cladosporioides* species complex)

Cladosporium sp. 3.1 indicated the best hydrolyzation performance under agitation at 120 h for most enzymes (Table 2.5). The late onset in enzyme production is consistent with previous studies [62]. Exceptions were endoglucanase with the highest enzyme secretion at 48 h, β-xylosidase at 24 h, and xylanase at 72 h. Under static conditions, the strongest enzyme secretion was observed at 72–96 h for most enzymes with significantly lower activity values than under agitation conditions, which is coherent with the increased pellet formation observed by comparing the incubation flasks of *C. Cladosporioides* under static and agitation conditions (Figure 2.6 Filamentous fungi cultivation g,h). This phenomenon was formerly described by Raikumar et al. for this genus [61]. Xylanase was the only exception that performed better under static conditions at 72 h of incubation. Agitation leads to better aeration and distribution of heat and nutrients bearing growth benefits for many filamentous fungi [63]. Comparing both analyzed *Cladosporium* species, an advanced enzyme production upon agitation was observed, and a relative early specialization in the production of endoglucanase and xylanase indicated a focus on the breakdown of large sugar polymers such as cellulose and hemicellulose [64]. All remaining enzymes showed a rather late onset.

Table 2.5 *Cladosporium cladosporioides* sp. 3.1 enzyme activity over time und agitation and static conditions

	Agitation					Static				
Enzyme	**24h**	**48h**	**72h**	**96h**	**120h**	**24h**	**48h**	**72h**	**96h**	**120h**
Endoglucanase	393.2±97.3	**1274.0±102.0**	328.5±68.6	14.0±11.4	14.6±11.9	761.0±70.4	638.8±140.4	945.3±120.6	**1076.4±149.4**	775.0±156.2
Exoglucanase	ND	ND	3.6±1.0	6.0±0.3	**12.0±0.6***	ND	ND	0.7±0.4	**0.9±0.6**	1.0±0.0
β-glycosidase	0.2±0.2	0.8±0.2	5.7±1.0	8.7±2.9	**11.1±0.8***	ND	ND	**0.7±0.4**	ND	ND
Xylanase	156.0±8.3	861.0±11.9	**958.9±15.5**	481.0±57.0	ND	522.1±87.6	660.0±56.1	**1113.0±865**	937.3±40.4	898.0±62.1
β-xylosidase	**1.2±0.3**	0.4±0.1	ND	ND	ND	**1.0±0.1**	ND	ND	ND	ND
acid phosphatase	0.7±0.4	1.9±0.7	3.4±0.7	6.8±0.3	**13.9±0.5***	ND	ND	0.3±0.2	**1.0±0.7**	0.9±0.1
alk. phosphatase	ND	ND	1.2±0.8	1.9±1.6	**8.0±1.5***	ND	ND	ND	ND	1.0±0.3

Data are expressed as mU/mL ± standard deviation. ND = not detected; * indicates a statistically significant difference ($p < 0.05$) between the average enzyme activity of fungi cultivated under agitation vs. static conditions for each analyzed enzyme. In bold, maximum achieved activity.

2.3.4.3 Enzymatic Production of *Didymella* sp.

The *Didymella* strain 3.3 showed a rather heterogeneous behavior (Table 4). Meanwhile, CMC and *p*np-β-D-xylanopyranoside were most effectively hydrolyzed under agitation at 24 h and 48 h, respectively. However, the best xylan hydrolyzation occurred at 72 h and for *p*np-β-D-glycopyranoside, *p*np-β-D-cellobiose, and *p*np-phosphate in alkaline medium at 96 h and 120 h in acid medium. Interestingly, while β-glucosidase, β-xylosidase, acid, and alkaline phosphatase showed low but detectable activity under agitation conditions, no activity could be detected under static conditions. On the other hand, endoglucanase and xylanase, which generally showed much higher activity, performed considerably stronger under static conditions at 96 h. These results confirm the previously described strong influence that culture conditions can exert over enzyme production [40,65].

Table 2.6 *Didymella* sp. strain 3.3 enzyme activity over time und agitation and static conditions

	Agitation					Static				
Enzyme	**24h**	**48h**	**72h**	**96h**	**120h**	**24h**	**48h**	**72h**	**96h**	**120h**
Endoglucanase	**1077.4±6.7**	1037.4±99.0	354.5±6.7	334.4±10.9	119.0±39.4	870.1±99.8	1243.0±108.1	1151.6±189.5	**1413.0±165.7***	926.7±15.0
Exoglucanase	0.4±0.2	0.7±0.2	1.0±0.3	**1.7±0.4**	1.7±0.4	0.7±0.2	**1.7±0.1**	0.6±0.2	ND	ND
β-glycosidase	ND	ND	ND	**1.6±0.7**	0.5±0.1	ND	ND	ND	ND	ND
Xylanase	202.3±15.0	233.0±98.2	**383.0±103.2**	289.2±62.1	ND	873.2±93.7	893.3±125.9	906.0±186.4	**1623.5±196.4***	624.7±141.4
β-xylosidase	**1.0±0.0**	0.5±0.1	0.4±0.1	0.1±0.0	ND	ND	ND	ND	ND	ND
acid phosphatase	ND	2.7±0.6	5.7±1.1	7.3±1.1	**7.5±1.5**	ND	ND	ND	ND	**0.3±0.1**
alk. Phosphatase	0.4±0.3	0.4±0.1	1.8±0.1	**2.1±0.5**	ND	ND	ND	ND	ND	ND

Data are expressed as mU/mL ± standard deviation. ND = not detected; * indicates a statistically significant difference ($p < 0.05$) between the average enzyme activity of fungi cultivated under agitation vs. static conditions for each analyzed enzyme. In bold, maximum achieved activity.

2.3.4.4 Comparison of Relative Enzyme Activity between Acid and Alkaline Phosphatases

Analysis of differential enzyme production between acid and alkaline phosphatase activities generally indicated more substantial secretion of enzymes upon agitation than under static conditions and stronger and prolonged acid phosphatase activity over time. Meanwhile, alkaline phosphatase showed lower and somewhat restricted activation at growth onset for strains 1.1 and 3.1; activation was strongest from 72 to 120 h for strain 3.1 (Figure 2.7).

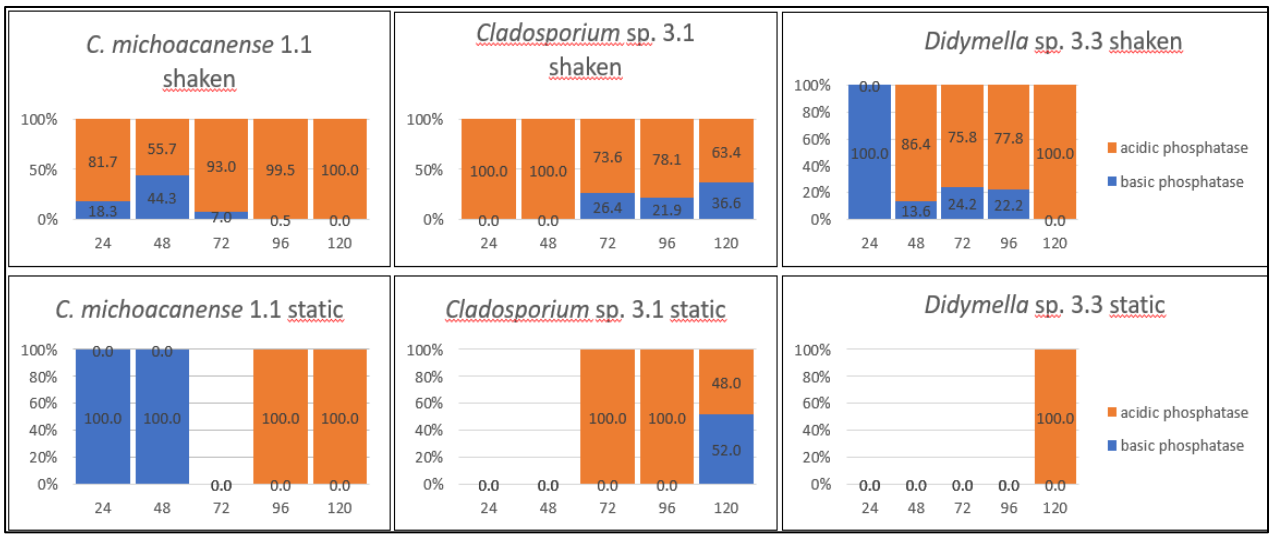

Figure 2.7 Relative phosphate activity over time comparing acidic phosphatase versus alkaline phosphatase

This behavior matches with the environmental conditions of their habitat, where slightly acidic soil pH was observed (Table 2.2.), which is also the preferred growth condition for most fungi [66]. It further coincides with the tendency that within strain 1.1 and 3.1, measured pH values of crude extract used to drop stronger over time than in strain 3.3 (Figure 2.8).

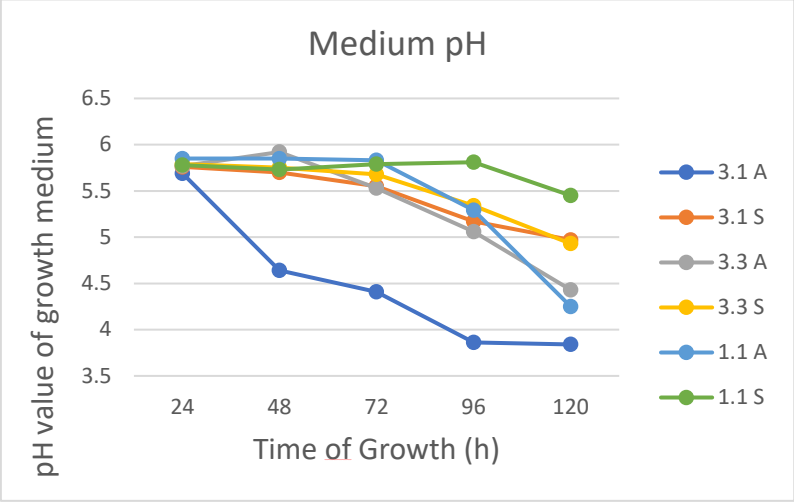

Figure 2.8 Development of growth medium pH
Measurement over time in cultures under agitation (A) and static (S) conditions for strain 1.1, 3.1 and 3.3

2.3.4.5 Temperature-Dependent Enzyme Activity

After analyzing the best growth time for differential enzyme production, results were used to determine optimal enzyme secretion under different incubation temperatures ranging from 4 to 32 °C under agitation to optimize enzyme production further. The results indicated statistically significant differences among strains (Figure 3). Meanwhile, strain 1.1 showed the best performance at temperatures ranging from 20 to 24 °C for all enzymes related to the carbon cycle and 8–12 °C for phosphatases; strain 3.1 showed somewhat differential activity indicating main enzyme activity for β-glucosidase and exoglucanase from 4 to 8 °C and for endoglucanase, β-xylosidase, and xylanase from 20 to 24 °C. Phosphatases showed opposite behavior with the highest acid phosphatase activity at 12 °C; meanwhile, alkaline phosphatase performed best at 28 °C. This controversial behavior might best be explained by the adaptation capacity of different *Cladosporium* species to varying ecological niches giving rise to its worldwide abundance [53]. It is typical for fungal strains adapted to changing environmental conditions within a single habitat [67,68]. Strain 3.3 finally showed maximum activity for β-glucosidase, endoglucanase, and xylanase at 8 °C and for exoglucanase and β-xylosidase at 20–24 °C. Phosphatase activity remained low, with the highest activity at 16 °C for both acid and alkaline phosphatase.

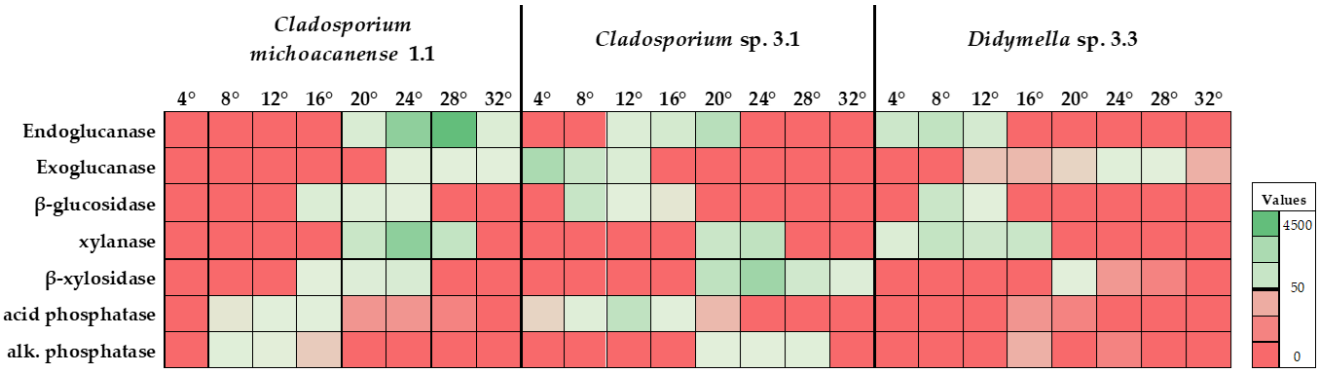

Figure 2.9 Heatmap analysis of incubation temperature dependent enzyme performance
Values showed in °C for each isolated strain. Maximum values ± SD (in mU/mL) are summarized in Table 2.7

The combination of optimal incubation time, agitation, and optimal substrate incubation temperature led to several enzymes' considerably higher activity (Table 5). *Cladosporium* strain 1.1 specialized in producing endoglucanase and xylanase with 4.56 and 3.03 U/mL activities, respectively, both showing significantly higher performances than the other two strains. Comparing these values with formerly described enzymatic activities, even in the mesophilic fungi screenings, especially endoglucanase values, they are quite competitive. For instance, Grujic et al. (2019) [69] described maximum values of 1.1 U/mL for endoglucanase in *Trichoderma guizhouense*, Ghazali et al. (2019) [70] reported the highest values of 3.93 U/mL for *Trichoderma asperellum* and 5.6 U/mL for *Aspergillus niger.* Unfortunately, most studies for psychrotrophic fungi do not apply optimization assays, so comparability is limited. However, considering the advantage of growing under extreme conditions, the *Cladosporium michoacanense* strain is an interesting candidate for potential industrial application under harsh conditions. Moreover, the relatively early onset of enzyme secretion, indicating efficient substrate hydrolyzation at 72 h, represents an important advantage confirming previous results from studies with *Cladosporium* strains [64,71].

Table 2.7 Maximum enzyme activity yield at optimal assay temperature and incubation time for each isolated strain

	Cladosporium sp. 1.1			*Cladosporium* Cladosporioides complex 3.1			*Didymella* sp. 3.3		
Enzyme	**max. yield ± SD**	**T opt °C**	**IT (h)**	**max. yield ± SD**	**T opt °C**	**IT (h)**	**max. yield ± SD**	**T opt °C**	**IT**
Endoglucanase	4563±209 a	28	72	1553±330 b	20	48	1247±21 b	8	72
Exoglucanase	107±26 a	24	96	2037±254 b	4	120	127±5 a	24	96
β-glucosidase	167±39 a	16	96	1013±151 b	8	96	917±12 b	8	120
xylanase	3036±634 a	24	72	1290±122 ab	24	72	1150±121 b	8	96
β-xylosidase	430±29 ab	24	120	2457±336 a	24	120	71±5 b	20	48
acid phosphatase	997±12 ab	12	120	1273±360 a	12	120	17±5 b	16	120
alk. phosphatase	127±21 a	8	72	137±37 b	28	120	26±7 a	16	96

Data expressed are as mU/mL ± standard deviation. IT = optimal incubation time; ND = not detected; the letters [a] and [b] indicate statistically significant differences among enzyme activities comparing the three different fungi ($p < 0.05$) if the letters are not shared between activities of the same enzyme.

On the other hand, *Cladosporium* sp. 3.1 did not reach values as high as strain 1.1 but managed to perform well for all selected enzymes with values above 1 U/mL except alkaline phosphatase. However, the onset of enzyme production appeared relatively late. Interestingly, strain 3.1 showed the significantly highest activation of 2.04 U/mL for exoglucanase at low temperatures, although former studies indicated a relatively poor performance of paramo-derived fungi for these enzymes [11]. Comparing the mesophilic fungi, results matched with reported highest activities of 1.08 U/mL and 2.37 U/mL in *Trichoderma asperellum* and *Aspergillus niger*, respectively. It is also important to mention that this high activity was reached under conditions of only 4 °C. Furthermore, β-glucosidase, which works synergistically with exoglucanase, also performed well at low temperatures (8 °C). Given that *Cladosporium cladosporioides* had formerly been described to exhibit laccase activity [64,72,73], further studies are needed to determine whether the strain could exhibit lignocellulolytic activity for industrial applications under cold conditions. Moreover, strain 3.1 showed the strongest activation for acid phosphatase, reaching 1.27 U/mL. This result further highlights the importance of applying optimization assays for psychrotolerant enzyme activity given incubation time as well as incubation temperature strongly influenced activity. Therefore, maximum acid phosphatase activity in psychrotrophic fungi of 0.03 U/mL, such as described in a screening study by Gawas-Sakhalkar et al. [74], indicates only a limited comparability to the present results.

Finally, *Didymella* 3.3 performed well only for endoglucanase, β-glucosidase, and xylanase, indicating poor performance for the rest of the enzymes, especially phosphatases, which could be related to the phytopathological behavior of many *Didymella* species allowing for the absorption of nutrients from hosts [55]. Nevertheless, all enzymes that performed better showed the highest values at low temperatures of 8 °C, indicating its potential in producing cold-adapted enzymes [9].

Wide-ranging comparison of psychrotrophic fungi enzyme activity is difficult, given that most screening studies indicate qualitative and semi-quantitative data [7,68,75–77] or activity data at a single temperature and incubation time [67], which is not directly comparable to the presented data. This strongly indicates the importance of performing studies with a more profound analysis of maximum achievable enzyme activities under optimized conditions for psychrotrophic and psychrophilic fungi isolated from habitats with extreme conditions.

2.4 Conclusions

The present study directly isolated cold-adapted fungal strains from high Andean Paramo soil, of which three strains were chosen to identify the genus and characterize their enzymatic capacity. Selecting for optimal conditions concerning growth period, incubation conditions, and optimal temperature for enzyme performance, maximum enzyme activities were determined for each strain. *Cladosporium* sp. strain 1.1 showed the most competitive enzyme activity of all analyzed strains for endoglucanase and xylanase at 72 h, and agitation and assay temperatures between 24 and 28 °C, indicating an interesting potential for the industrial application processes where reducing sugars are used such as feed animal, food industry, and fuel production. *Cladosporium* strain 3.1 of the *cladosporioides* complex indicated average performance for a broad spectrum of different enzymes except for exoglucanase, which showed the highest activity. Its good performance of acid phosphatase at 12 °C could be applied in the industry of biofertilization to improve the crop yield of plants grown under cold conditions and in the eutrophication of phosphorus from animal feces due to the consumption of phytate in grains [78]. Finally, the *Didymella* strain 3.3 showed high endoglucanase, β-glucosidase, and xylanase activities at temperatures as low as 8 °C, where most enzymes are inactivated. This strain responded closest to a psychrotrophic profile, which could be specifically interesting in industrial processes such as wastewater management and bioremediation in cold conditions, an aspect that might become increasingly important in an industrialized world tending towards energy reduction.

2.5 Chapter References

1. Jiménez-Rivillas, C.; García, J.J.; Quijano-Abril, M.A.; Daza, J.M.; Morrone, J.J. A new biogeographical regionalisation of the Páramo biogeographic province. *Aust. Syst. Bot.* **2018**, *31*, 296–310.
2. Buytaert, W.; Deckers, J.; Wyseure, G. Regional variability of volcanic ash soils in south Ecuador: The relation with parent material, climate and land use. *Catena* **2007**, *70*, 143–154.
3. Bader, M.Y.; van Geloof, I.; Rietkerk, M. High solar radiation hinders tree regeneration above the alpine treeline in northern Ecuador. *Plant Ecol*. **2007**, *191*, 33–45.
4. Paucar, B.; Carpio, M.; Alvarado Ochoa, S.P.; Valverde, F.; Parra, R. Análisis de Solubilizadores de Fósforo en Los Suelos Andisoles de Sierra Norte y Centro de Ecuador. Simposio "El Suelo y la Nutrición de Cultivos en el Ecuador". 2015. Available online: http://repositorio.iniap.gob.ec/handle/41000/2501 (accessed on 9 September 2021).
5. Hassan, N.; Rafiq, M.; Hayat, M.; Shah, A.A.; Hasan, F. Psychrophilic and psychrotrophic fungi: A comprehensive review. *Rev. Environ. Sci. Biotechnol.* **2016**, *15*, 147–172.
6. Rafiq, M.; Hassan, N.; Rehman, M.; Hasan, F. Adaptation mechanisms and applications of psychrophilic fungi. In *Fungi in Extreme Environments: Ecological Role and Biotechnological Significance*; Tiquia-Arashiro, S.M., Grube, M., Eds.; Springer International Publishing: Cham, Switzerland, 2019; pp. 157–174. https://doi.org/10.1007/978-3-030-19030-9_9.
7. Duarte, A.W.F.; Barato, M.B.; Nobre, F.S.; Polezel, D.A.; de Oliveira, T.B.; dos Santos, J.A.; Rodrigues, A.; Sette, L.D. Production of cold-adapted enzymes by filamentous fungi from King George Island, Antarctica. *Polar Biol*. **2018**, *41*, 2511–2521.
8. Duarte, A.W.F.; dos Santos, J.A.; Vianna, M.V.; Vieira, J.M.F.; Mallagutti, V.H.; Inforsato, F.J.; Wentzel, L.C.P.; Lario, L.D.; Rodrigues, A.; Pagnocca, F.C.; et al. Cold-adapted enzymes produced by fungi from terrestrial and marine Antarctic environments. *Crit. Rev. Biotechnol*. **2018**, *38*, 600–619.
9. Wang, M.; Jiang, X.; Wu, W.; Hao, Y.; Su, Y.; Cai, L.; Xiang, M.; Liu, X. Psychrophilic fungi from the world's roof. *Pers. Mol. Phylogeny Evol. Fungi* **2015**, *34*, 100–112.
10. Cortes, A.J.; Garzon, L.N.; Valencia, J.B.; Madrinan, S. On the causes of rapid diversification in the paramos: Isolation by ecology and genomic divergence in espeletia. *Front. Plant Sci.* **2018**, *9*, 1700.
11. Avellaneda-Torres, L.M.; Pulido, C.P.G.; Rojas, E.T. Assessment of cellulolytic microorganisms in soils of Nevados Park, Colombia. *Braz. J. Microbiol.* **2014**, *45*, 1211–1220.
12. Landinez-Torres, A.Y.; Becerra Abril, J.L.; Tosi, S.; Nicola, L. Soil microfungi of the colombian natural regions. *Int. J. Environ. Res. Public Health* **2020**, *17*, 8311.
13. Gualdrón-Arenas, C.; Suárez-Navarro, A.L.; Valencia-Zapata, H. Hongos del suelo aislados de zonas de vegetacion natural del paramo de chisaca, colombia. *Caldasia* **1997**, *19*, 235–245.
14. Pinos León, A.J. Exploring the Microbiome Composition of the Rhizosphere Associated with the Wild Andean Blueberry (*Vaccinium Floribundum*, Kunth) in the Highlands of Ecuador. Master's Thesis, Universidad San Francisco de Quito, Quito, Ecuador, 2020. Available online: https://repositorio.usfq.edu.ec/bitstream/23000/9113/1/141011.pdf (accessed on 5 december 2021).
15. Kuddus, M.; Roohi Arif, J.; Ramteke, P. An overview of cold-active microbial α-amylase: Adaptation strategies and biotechnological potentials. *Biotechnology* **2011**, *10*, 246–258.
16. Santiago, M.; Ramírez-Sarmiento, C.A.; Zamora, R.A.; Parra, L.P. Discovery, Molecular Mechanisms, and Industrial Applications of Cold-Active Enzymes. *Front Microbiol.* **2016**, *7*, 1408.
17. Kumar, A.; Mukhia, S.; Kumar, R. Industrial applications of cold-adapted enzymes: Challenges, innovations and future perspective. *3 Biotech* **2021**, *11*, 426.

18. de Oliveira, T.B.; de Lucas, R.C.; de Almeida Scarcella, A.S.; Pasin, T.M.; Contato, A.G.; Polizeli, M.L.T.M. Cold-active lytic enzymes and their applicability in the biocontrol of postharvest fungal pathogens. *J. Agric. Food Chem*. **2020**, *68*, 6461–6463.
19. Gerday, C.; Aittaleb, M.; Bentahir, M.; Chessa, J.-P.; Claverie, P.; Collins, T.; D'Amico, S.; Dumont, J.; Garsoux, G.; Georlette, D.; et al. Cold-adapted enzymes: From fundamentals to biotechnology. *Trends Biotechnol*. **2000**, *18*, 103–107.
20. Niñerola, A.; Ferrer-Rullan, R.; Vidal-Suñé, A. Climate change mitigation: Application of management production philosophies for energy saving in industrial processes. *Sustainability* **2020**, *12*, 717.
21. Andlar, M.; Rezić, T.; Marđetko, N.; Kracher, D.; Ludwig, R.; Šantek, B. Lignocellulose degradation: An overview of fungi and fungal enzymes involved in lignocellulose degradation. *Eng. Life Sci*. **2018**, *18*, 768–778.
22. Pasin, T.M.; Scarcella, A.S.A.; de Oliveira, T.B.; Lucas, R.C.; Cereia, M.; Betini, J.H.A.; Polizeli, M.L. Paper industry wastes as carbon sources for Aspergillus species cultivation and production of an enzymatic cocktail for biotechnological applications. *Ind. Biotechnol*. **2020**, *16*, 56–60.
23. Duncan, S.M.; Farrell, R.L.; Thwaites, J.M.; Held, B.W.; Arenz, B.E.; Jurgens, J.A.; Blanchette, R.A. Endoglucanase-producing fungi isolated from *Cape Evans* historic expedition hut on Ross Island, Antarctica. *Environ. Microbiol*. **2006**, *8*, 1212–1219.
24. Polizeli, M.L.T.M.; Rizzatti, A.C.S.; Monti, R.; Terenzi, H.F.; Jorge, J.A.; Amorim, D.S. Xylanases from fungi: Properties and industrial applications. *Appl. Microbiol. Biotechnol*. **2005**, *67*, 577–591.
25. Miri, S.; Naghdi, M.; Rouissi, T.; Kaur Brar, S.; Martel, R. Recent biotechnological advances in petroleum hydrocarbons degradation under cold climate conditions: A review. *Crit. Rev. Environ. Sci. Technol*. **2019**, *49*, 553–586.
26. Jiang, G.; Chen, P.; Bao, Y.; Wang, X.; Yang, T.; Mei, X.; Banerjee, S.; Wei, Z.; Xu, Y.; Shen, Q. Isolation of a novel psychrotrophic fungus for efficient low-temperature composting. *Bioresour. Technol*. **2021**, *331*, 125049.
27. Adhikari, P.; Jain, R.; Sharma, A.; Pandey, A. Plant Growth Promotion at Low Temperature by Phosphate-Solubilizing Pseudomonas spp. Isolated from High-Altitude Himalayan Soil. *Microb. Ecol.* **2021**. https://doi.org/10.1007/s00248-021-01702-1.
28. White, T.J.; Bruns, T.; Lee, S.; Taylor, J.W. *Amplification and Direct Sequencing of Fungal Ribosomal RNA Genes for Phylogenetics*; Academic Press, Inc.: New York, NY, USA, 1990; pp. 315–322.
29. Hall, T. BioEdit : A user-friendly biological sequence alignment editor and analysis program for Windows 95/98/NT. *Nucleic Acids Symp. Ser.* **1999**, *41*, 95–98.
30. Thompson, J.D.; Higgins, D.G.; Gibson, T.J. CLUSTAL W: Improving the sensitivity of progressive multiple sequence alignment through sequence weighting, position-specific gap penalties and weight matrix choice. *Nucleic Acids Res*. **1994**, *22*, 4673–4680.
31. Kumar, S.; Stecher, G.; Tamura, K. MEGA7: Molecular Evolutionary Genetics Analysis Version 7.0 for Bigger Datasets. *Mol. Biol. Evol*. **2016**, *33*, 1870–1874.
32. Miller, G.L. Use of dinitrosalicylic acid reagent for determination of reducing sugar. *Anal. Chem*. **1959**, *31*, 426–428.
33. Contato, A.G.; de Oliveira, T.B.; Aranha, G.M.; de Freitas, E.N.; Vici, A.C.; Nogueira, K.M.V.; de Lucas, R.C.; de Almeida Scarcella, A.S.; Buckeridge, M.S.; Silva, R.N.; et al. Prospection of fungal lignocellulolytic enzymes produced from jatoba (*Hymenaea courbaril*) and tamarind (*Tamarindus indica*) seeds: Scaling for bioreactor and saccharification profile of sugarcane bagasse. *Microorganisms* **2021**, *9*, 533.
34. Garen, A.; Siddiqi, O. Suppression of mutations in the alkaline phosphatase structural cistron of *E. coli*. *Proc. Natl. Acad. Sci. USA* **1962**, *48*, 1121–1127.
35. Kersters-Hilderson, H.; Claeyssens, M.; Van Doorslaer, E.; Saman, E.; De Bruyne, C.K. [60] β-D-xylosidase from *Baccilus pumilus*. In *Methods in Enzymology*; Complex Carbohydrates Part D; Academic Press: Cambridge, MA, USA, 1982; Volume 83, pp. 631–639. Available online:

https://www.sciencedirect.com/science/article/pii/0076687982830620 (accessed on 19 August 2021).
36. Hribljan, J.A.; Suarez, E.; Heckman, K.A.; Lilleskov, E.A.; Chimner, R.A. Peatland carbon stocks and accumulation rates in the Ecuadorian paramo. *Wetl. Ecol. Manag*. **2016**, *24*, 113–127.
37. Roa García, C.; Brown, S.; Krzic, M.; Lavkulich, L.; Roa-García, M.C. Relationship of soil water retention characteristics and soil properties: A case study from the Colombian Andes. *Can. J. Soil Sci*. **2021**, *101*, 147–156.
38. Zúñiga-Silgado, D.; Rivera-Leyva, J.C.; Coleman, J.J.; Sánchez-Reyez, A.; Valencia-Díaz, S.; Serrano, M.; de-Bashan, L.E.; Folch-Mallol, J.L. Soil type affects organic acid production and phosphorus solubilization efficiency mediated by several native fungal strains from Mexico. *Microorganisms* **2020**, *8*, 1337.
39. Rowley, M.C.; Grand, S.; Verrecchia, E.P. Calcium-mediated stabilisation of soil organic carbon. *Biogeochemistry* **2018**, *137*, 27–49.
40. Opfergelt, S.; Georg, R.B.; Delvaux, B.; Cabidoche, Y.-M.; Burton, K.W.; Halliday, A.N. Mechanisms of magnesium isotope fractionation in volcanic soil weathering sequences, Guadeloupe. *Earth Planet Sci. Lett*. **2012**, *341*, 176–185.
41. Rahimi, H.; Pazira, E.; Tajik, F. Effect of soil organic matter, electrical conductivity and sodium adsorption ratio on tensile strength of aggregates. *Soil Tillage Res*. **2000**, *54*, 145–153.
42. Ishiguro, M.; Makino, T. Sulfate adsorption on a volcanic ash soil (allophanic Andisol) under low pH conditions. *Colloids Surf.-Physicochem. Eng. Asp*. **2011**, *384*, 121–125.
43. Hazelton, P.; Murphy, B. *Interpreting Soil Test Results: What Do All the Numbers Mean?* Csiro Publishing: Clayton, Australia, 2016; p. 201.
44. Motsara, M.R.; Roy, R.N. *Guide to Laboratory Establishment for Plant Nutrient Analysis. FAO Fertilizer and Plant Nutrition Bulletin*; Food and Agriculture Organization of the United Nations: Rome, Italy, 2008; p. 219.
45. Sembiring, M. Bacterial and fungi phosphate solubilization effect to increase nutrient uptake and potatoes (*Solanum tuberosum* L.) production on Andisol Sinabung area. *J. Agron*. **2017**, *16*, 131–137.
46. Geoportal Ecuador—Infraestructura de Datos Espaciales. Available online: http://www.geoportaligm.gob.ec/portal/ (accessed on 19 October 2021).
47. Bensch, K.; Braun, U.; Groenewald, J.Z.; Crous, P.W. The genus Cladosporium. *Stud. Mycol*. **2012**, *72*, 1–401.
48. Del-Cid, A.; Ubilla, P.; Ravanal, M.-C.; Medina, E.; Vaca, I.; Levicán, G.; Eyzaguirre, J.; Chávez, R. Cold-active xylanase produced by fungi associated with Antarctic marine sponges. *Appl. Biochem. Biotechnol*. **2014**, *172*, 524–532.
49. Wang, X.; Wu, X.; Jiang, S.; Yin, Q.; Li, D.; Wang, Y.; Wang, D.; Chen, Z. Whole genome sequence and gene annotation resource for *Didymella bellidis* associated with tea leaf spot. *Plant Dis*. **2021**, *105*, 1168–1170.
50. Zhang, J.; Bruton, B.D.; Biles, C.L. Cell wall-degrading enzymes of *Didymella bryoniae* in relation to fungal growth and virulence in cantaloupe fruit. *Eur. J. Plant Pathol*. **2014**, *139*, 749–761.
51. Rafiq, M.; Nadeem, S.; Hassan, N.; Hayat, M.; Sajjad, W.; Zada, S.; Sajjad, W.; Hasan, F. Fungal recovery and characterization from Hindu Kush mountain range, Tirich Mir glacier, and their potential for biotechnological applications. *J. Basic Microbiol*. **2020**, *60*, 444–457.
52. Hassan, N.; Hasan, F.; Nadeem, S.; Hayat, M.; All, P.; Khan, M.; Sajjad, W.; Zada, S.; Rafiq, M. Community analysis and characterization of fungi from Batura Glacier, Karakoram Mountain Range, Pakistan. *Appl. Ecol. Environ. Res*. **2018**, *16*, 5323–5341.
53. Pacelli, C.; Bryan, R.A.; Onofri, S.; Selbmann, L.; Shuryak, I.; Dadachova, E. Melanin is effective in protecting fast and slow growing fungi from various types of ionizing radiation. *Environ. Microbiol*. **2017**, *19*, 1612–1624.

54. Dadachova, E.; Casadevall, A. Ionizing radiation: How fungi cope, adapt, and exploit with the help of melanin. *Curr. Opin. Microbiol*. **2008**, *11*, 525–531.
55. Ravikumar, R. Effect of transport phenomena of *Cladosporium cladosporioides* on decolorization and chemical oxygen demand of distillery spent wash. *Int. J. Environ. Sci. Technol*. **2015**, *12*, 1581–1590.
56. Mohan Kumar, N.S.; Ramasamy, R.; Manonmani, H.K. Production and optimization of l-asparaginase from Cladosporium sp. using agricultural residues in solid state fermentation. *Ind. Crops Prod*. **2013**, *43*, 150–158.
57. Quintanilla, D.; Hagemann, T.; Hansen, K.; Gernaey, K.V. Fungal morphology in industrial enzyme production-modelling and monitoring. In *Filaments in Bioprocesses*; Krull, R., Bley, T., Eds.; Springer: Berlin/Heidelberg, Germany, 2015; pp. 29–54. Available online: https://www.webofscience.com/wos/woscc/full-record/WOS:000365169300003 (accessed on 19 October 2021).
58. Abrha, B.; Gashe, B.A. Cellulase production and activity in a species of Cladosporium. *World J. Microbiol. Biotechnol*. **1992**, *8*, 164–166.
59. Maya-Yescas, M.E.; Revah, S.; Le Borgne, S.; Valenzuela, J.; Palacios-González, E.; Terrés-Rojas, E.; Vigueras-Ramírez, G. Growth of *Leucoagaricus gongylophorus* Möller (Singer) and production of key enzymes in submerged and solid-state cultures with lignocellulosic substrates. *Biotechnol. Lett*. **2021**, *43*, 845–854.
60. Peñalva, M.A.; Arst, H.N. Regulation of gene expression by ambient ph in filamentous fungi and yeasts. *Microbiol. Mol. Biol. Rev.* **2002**, *66*, 426–446.
61. Zucconi, L.; Canini, F.; Temporiti, M.E.; Tosi, S. Extracellular enzymes and bioactive compounds from Antarctic terrestrial fungi for bioprospecting. *Int. J. Environ. Res. Public Health* **2020**, *17*, 6459.
62. Hassan, N.; Rafiq, M.; Hayat, M.; Nadeem, S.; Shah, A.A.; Hasan, F. Potential of psychrotrophic fungi isolated from siachen glacier, Pakistan, to produce antimicrobial metabolites. *Appl. Ecol. Environ. Res*. **2017**, *15*, 1157–1171.
63. Grujic, M.; Dojnov, B.; Potocnik, I.; Atanasova, L.; Duduk, B.; Srebotnik, E.; Druzhinina, I.S.; Kubicek, C.P.; Vujčić, Z. Superior cellulolytic activity of *Trichoderma guizhouense* on raw wheat straw. *World J. Microbiol. Biotechnol*. **2019**, *35*, 194.
64. Ghazali, M.F.S.M.; Zainudin, N.A.I.M.; Abd Aziz, N.A.; Mustafa, M. Screening of lignocellulolytic fungi for hydrolyzation of lignocellulosic materials in paddy straw for bioethanol production. *Malays. J. Microbiol*. **2019**, *15*, 379–386.
65. Ji, L.; Yang, J.; Fan, H.; Yang, Y.; Li, B.; Yu, X.; Zhu, N.; Yuan, H. Synergy of crude enzyme cocktail from cold-adapted *Cladosporium cladosporioides* Ch2-2 with commercial xylanase achieving high sugars yield at low cost. *Biotechnol. Biofuels* **2014**, *7*, 130.
66. Aslam, M.S.; Aishy, A.; Samra, Z.Q.; Gull, I.; Athar, M.A. Identification, Purification and characterization of a novel extracellular laccase from *Cladosporium cladosporioides*. *Biotechnol. Biotechnol. Equip*. **2012**, *26*, 3345–3350.
67. Halaburgi, V.M.; Sharma, S.; Sinha, M.; Singh, T.P.; Karegoudar, T.B. Purification and characterization of a thermostable laccase from the ascomycetes *Cladosporium cladosporioides* and its applications. *Process Biochem*. **2011**, *46*, 1146–1152.
68. Gawas-Sakhalkar, P.; Singh, S.M.; Naik, S.; Ravindra, R. High-temperature optima phosphatases from the cold-tolerant Arctic fungus *Penicillium citrinum*. *Polar Res*. **2012**, *31*, 11105.
69. Krishnan, A.; Convey, P.; Gonzalez-Rocha, G.; Alias, S.A. Production of extracellular hydrolase enzymes by fungi from King George Island. *Polar Biol*. **2016**, *39*, 65–76.
70. Fenice, M.; Selbmann, L.; Zucconi, L.; Onofri, S. Production of extracellular enzymes by Antarctic fungal strains. *Polar Biol*. **1997**, *17*, 275–280.
71. Wang, N.; Zang, J.; Ming, K.; Liu, Y.; Wu, Z.; Ding, H. Production of cold-adapted cellulase by Verticillium sp. isolated from Antarctic soils. *Electron. J. Biotechnol.* **2013**, *16*, 10. Available online: http://www.ejbiotechnology.info/index.php/ejbiotechnology/article/view/1302 (accessed on 9 December 2021).

72. Salunke, M.; Sondge, D.B.; Yadav, S.; Warkhade, R.; Rathod, S.; Kate, S. Alkaline phosphatase production by *Enterobacter hormaechei* isolated from birds fecal waste and its optimization. *Int. J. Adv. Sci. Technol*. **2020**, *29*, 9.

Chapter 3

Potential impacts of seasonal and altitudinal changes on enzymatic peat decomposition in the High Andean Paramo region of Ecuador

This chapter is based on the article with the same name currently under revision in the journal Science of the Total Environment

Abstract: The Andean Paramo is a vast ecosystem, characterized by distinct vegetational zones at several altitudinal levels with huge water storage and carbon fixation capacity within its peat-like andosols, due to a slow decomposition rate of organic matter. These characteristics become mutually related as enzymatic activities increase with temperature and are associated with oxygen penetration, restricting the activity of many hydrolytic enzymes according to the enzyme Latch Theory. This study describes the changing activity of sulfatase (Sulf), phosphatase (Phos), n-acetyl-glucosaminidase (N-Ac), cellobiohydrolase (Cellobio), β-glucosidase (β-Glu), and peroxidase (POX) on an altitudinal scale from 3600-4200 m, in rainy and dry seasons at 10 and 30 cm sampling depth, related to physical and chemical soil characteristics, like metals and organic elements. Linear fixed-effect models were established to analyze these environmental factors to determine distinct decomposition patterns. The data suggests a strong tendency toward decreasing enzyme activities at higher altitudes and in the dry season up to two-fold stronger activation for Sulf, Phos, Cellobio, and β-Glu. Especially the lowest altitude showed considerably stronger N-Ac, β-Glu, and POX activity. Although sampling depth revealed significant differences for all hydrolases but Cellobio, it had minor effects on model outcomes. Further organic rather than physical or metal components of the soil explain the enzyme activity variations. Although the levels of phenols coincided mostly with the soil organic carbon content, there was no direct relation between hydrolases, POX activity, and phenolic substances. The outcome suggests that slight environmental changes with global warming might cause important changes in enzyme activities leading to increased organic matter decomposition at the borderline between the paramo region and downslope ecosystems. Expected extremer dry seasons could cause critical changes as aeration increases peat decomposition leading to a constant liberation of carbon stocks, which puts the paramo region and its ecosystem services in great danger.

Keywords: extracellular enzyme activity, soil, enzyme latch, climate change

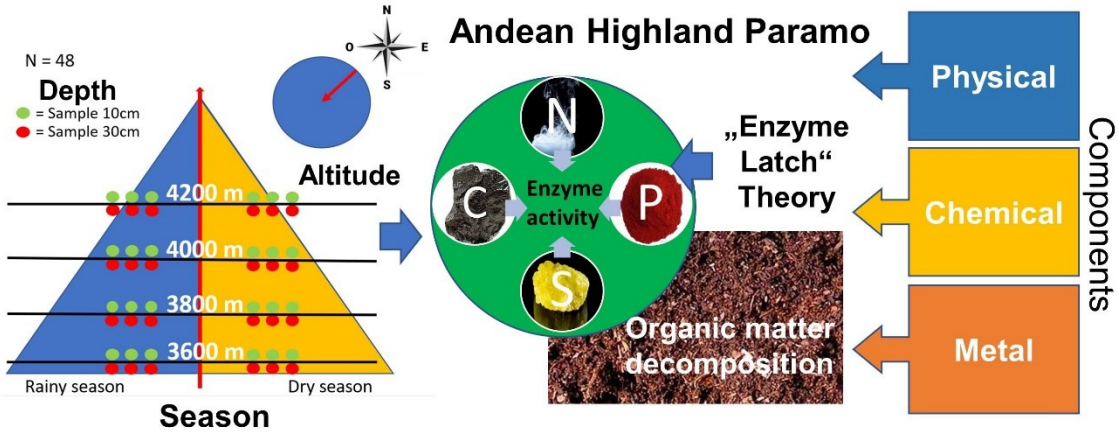

Figure 3.1 Graphical Abstract

3.1 Introduction

3.1.1 Climate change

Climate change is without any doubt one of the biggest threats humanity is currently facing [1,2]. It is common sense among the scientific community that the increasing temperatures have the potential to further fuel the existing global warming processes leading to probably irreversible effects [3–5]. Although 192 countries have recognized the danger climate change can unleash especially upon future generations, as can be seen by the signing of the treaty of the Kyoto Protocol ratified in 2005 [6], efforts have been too few and the global community lies well behind the fulfilling of its aims towards CO_2 emission reduction [7].

The greatest dangers lie in the positive feedback mechanisms of climate change, which means those mechanisms which once unchained by rising temperatures can cause a further elevation of temperature by themselves, making climate change a self-accelerating process. The melting of the white protective shields of the Arctic and Antarctic region and Greenland that reflect solar energy back to space [8], the liberation of huge cristalized methane-hydrate reservoirs deep in the ocean that have a higher greenhouse gas potential than CO2 in the atmosphere and can change their agregation state upon small temperature changes [9], irreversible desertifications that critically limit carbon fixation in continantal climates [10] but most of all the fact that more than three times the amount of carbon already circulating in the atmosphere lies fixed below ground and is greatly threatened to be released with rising temperatures and subsequent rising degradation rates [11] force us to double our present mitigation efforts.

3.1.1.1 Climate change in the paramo ecosystem

The South American high Andean paramo ecosystem is a particularly vulnerable area to climatic changes due to its extreme climatic and geographic conditions [12,13]. It covers altitudes from 3400 to 5000 m [14,15] which gives rise to the formerly mentioned extreme temperature fluctuations throughout the day and night times and extreme radiation rates [16] with highly adapted flora and fauna. These characteristics make the ecosystem an especially interesting study site for global warming effects similar to those frequently reported for high latitude peatland regions [17,18] meanwhile, studies in the paramo remain very scarce. Changes in climatic conditions on different altitudinal levels can be seen as models for future environmental changes, upon temperature increase [19].

The loss of this unique environment means not only the loss of many endemic species [20] but also the loss of its ecosystem services [21]. As described in Chapter 1, the paramo region has a vast water storage capacity important for the water supply in many South American cities as well as for the existence of the downslope tropical cloud forests, lying on both sides of the Andean Mountain chain with substantial environmental and economic importance [22,23].

3.1.2 Organic matter decomposition

The degradation of organic matter is driven by the soil microbiome responsible to produce a series of degrading enzymes which constitutes an important factor against the fixating process. As the composition of microorganisms changes over altitudinal gradients [19,24], global warming could increase the decomposition rate [25] up to the point where the carbon sink could turn into a carbon source due to the massive liberation of CO_2 instead of fixing it [11]. This effect is of great concern to the scientific community. It has extensively been studied for the thawing permafrost soils in the northern hemisphere and [26–28] is therefore considered one of the major irreversible effects if the temperature rises more than 1.5°C in the future [7]. Nevertheless, the same effect is hardly studied in mountain peatlands, especially considering those of Southern America.

Although the temperature is apparently the key driving factor in enzyme activity changes [29] for northern peatlands and its effect is commonly known, several other factors are involved. As organic matter decomposition is mainly driven by secretion of enzymes from microorganisms, their composition plays a key role in degrading processes. Many studies have shown the direct relation of microbiome diversity and its interaction with the present vegetation [30,31]. The upslope shift of vegetational zones therefore can directly influence microbiome composition [32] and subsequently might influence degrading capacities among vegetational zones which will be described in more detail in Chapter 4.

3.1.2.1 Extracelular enzymes

3.1.2.1.1 The Enzyme Latch Theory

Extensive retention of water leads to waterlogging in andisols which can replace oxygen between soil aggregates [33]. Although most of the degrading enzymes belong to the family of hydrolases, which are not oxygen dependent, their action can be considerably impaired due to direct inhibition of hydrolases by phenolic substances. Although there are enzymes able to degrade these phenols, such as the Phenol oxidases (POX), these are oxygen dependent. Thus, increased aeration of soil could increase POX activity and thereby eliminate inhibitory substances for hydrolase activity leading to increased organic matter degradation (Figure 3.2). This effect was first observed by Friedman and colleagues [34,35] and is known as the “Enzyme Latch Theory”. Although the literature is inconsistent about the magnitude of the effect and the exact mechanism remains elusive [36], several studies observe significantly higher degradation rates in peatland regions during droughts and upon artificial aeration of peat [37,38].

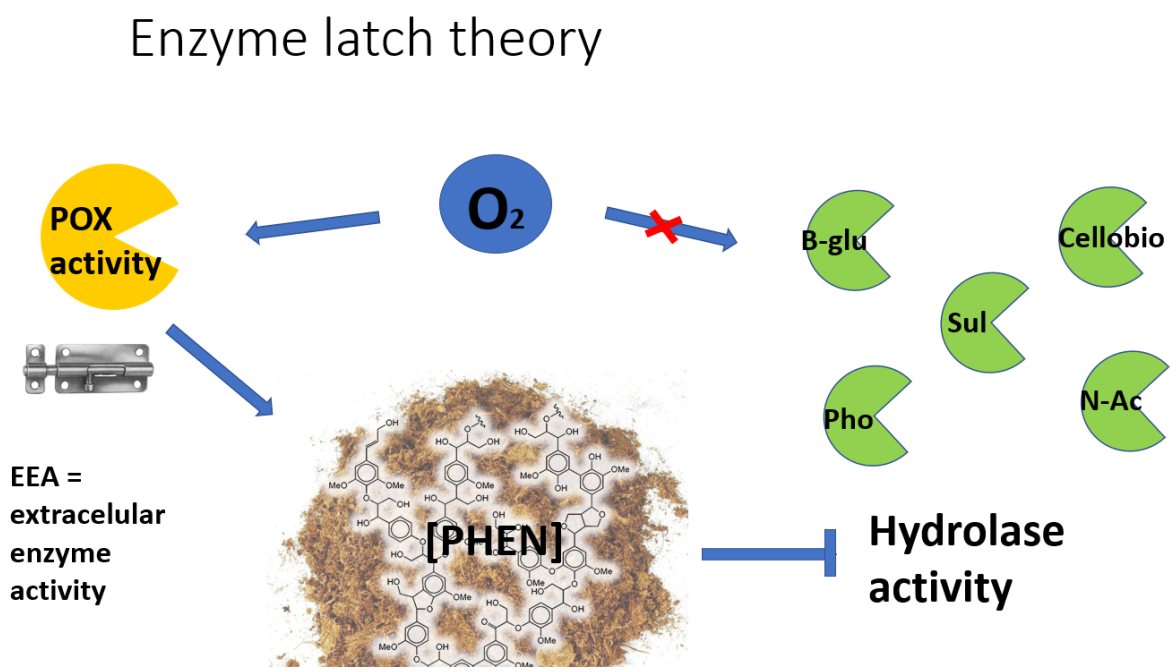

Figure 3.2 The Enzyme Latch Theory
Although oxygen does not exert an effect on hydrolase activity it is necessary for POX activity, which in turn degrades phenolic substances (PHEN). These substances are able to inhibit hydrolase activity. Therefore, the absence of oxygen can indirectly inhibit also the activity of hydrolases

The Ecuadorian paramo is a particularly interesting site to study the mentioned effects, as it lies in the center of the Andean paramo belt. Its thick peat deposits area exposed to seasonal changes between dry and rainy climates and vegetational zones within conserved areas, which are clearly distinguishable.

The present chapter aims to analyze the enzyme activity involved in the degradation of organic matter over a spectrum of different elements (C, N, S, P) in forming organic molecules as an approximation to the overall degrading process within paramo soil. Measurements across an altitudinal gradient at the rainy and dry seasons, and across two different depths, were used to estimate whether these effects are further influenced by abiotic factors under constant temperature conditions.

To the best of our knowledge, this is the first study that relates the concepts of enzyme-driven decomposition of organic matter and soil characteristics to the Enzyme Latch Theory in a global warming scenario within the paramo region. Most former enzymatic studies of Andean ecosystems are either related to the agrological importance and fertility of paramo soil [39] or were performed at considerably lower elevations in strongly differing environments [40].

3.2 Material and Methods

3.2.1 Sample Sites

The sampling site of the National Reserve “Los Ilinizas” in Northern Ecuador lies 60 km Southeast of the capital Quito (Figure 3.3 a) [41]. It was chosen due to the conserved paramo landscape at the center of the eastern Andean Paramo belt with thick layers of peat-like mollic andosol. Its slowly rising slopes present plains where samples were collected at four different heights, each 200 meters of altitude, following a linear transect towards the volcano peak (Figure 3.3 a) to avoid climatic bias such as changes in radiation, wind, and precipitation on different mountainsides. These sampling sites represent the frontier between high mountain forest and the paramo region (3600 m), shrub paramo (3800 m), grass paramo (4000 m) and superparamo at the frontier to the rocky zone of the volcano (4200 m) (Table 3.1and Figure 3.3 1 b). The mean temperature lies between 9° and 11°C presenting extremes from 0° to 22°C and means of annual precipitation from 500 up to 3000 mm [42]. Samples were taken from one square meter plots presenting open conserved vegetation with three replication sites, at least 20 m apart, at each altitude. They were isolated at depths of 10 and 30 cm (Figure 1 a).

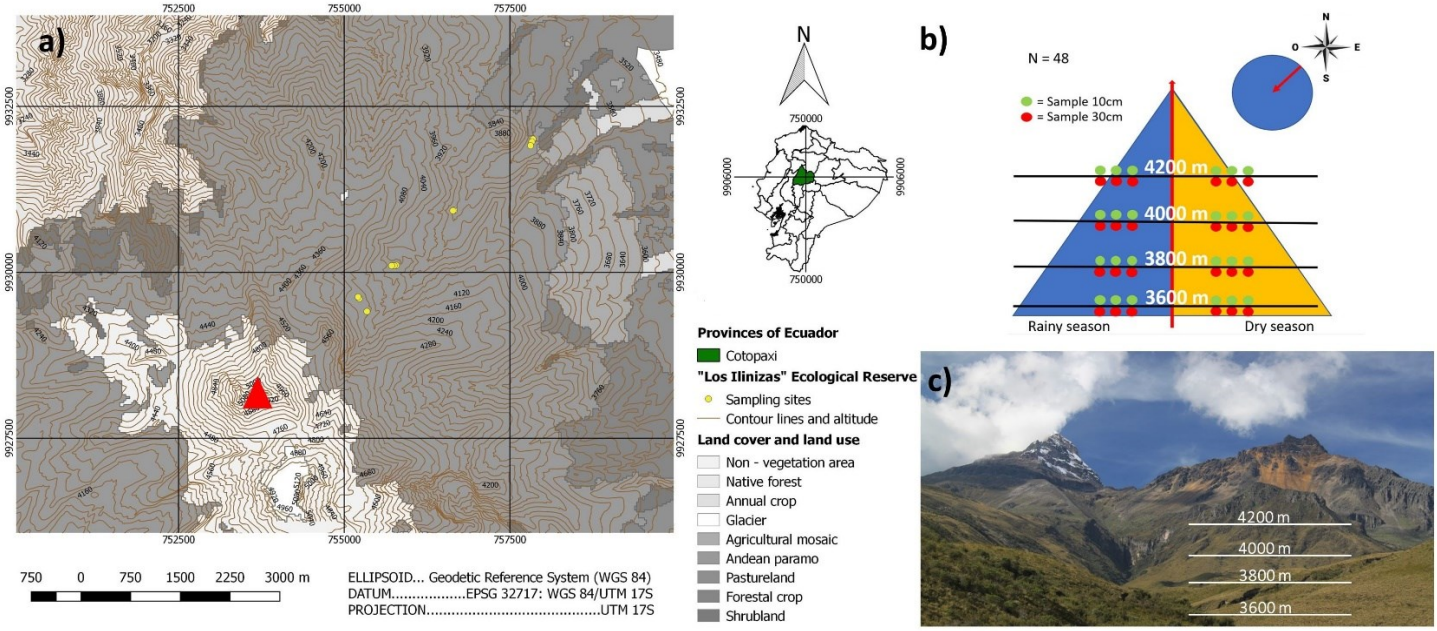

Figure 3.3 Sampling sites
a) Map of geo-localized sampling sites (yellow dots) on a linear transect towards the volcano peak (red triangle) (Open access shape files taken form the Geographical Military Institute of Ecuador [44] visualized with QGIS), b) Graphical figure of sampling for Enzyme Activity Assays (green and red dots), c) Picture of the volcano “Los Ilinizas” and the paramo landscape indicating estimates of the four different vegetational zones (Photograph by Stefan Brück 2020)

Samples were collected in early February 2019, following several weeks of the dry season, and in April 2020 within rainy season confirmed by open access precipitation data

from the National Institute of Meteorology of Ecuador (INAMHI) [43] resulting in a total of 48 analyzed samples. Dataloggers HOBO Pro V2 (ONSET, MA, USA) were installed at each height to collect soil temperature data at 10 cm depth. Samples were kept in a cooler within sterile falcon tubes at 4°C for enzyme activity and directly transferred to the laboratory.

Table 3.1 Sampling site characteristics

Sampling point	Altitude	vegetational zone	Georeference	Type of soil	Dominant vegetation families	average temperature C°		
						rainy	dry	anual
1	3600	subparamo	-78.68329,-0.61507	mollic andisole	Melastomataceae, Poaceae, Asteraceae, Erycaceae	11.54	12.87	11.33
2	3800	shrub paramo	-78.69400,-0.62446	mollic andisole	Rosaceae, Poaceae, Asteraceae, Gentianaceae, Verbenaceae	11.90	10.20	10.83
3	4000	grass paramo	-78.70200,-0.63199	mollic andisole	Poaceae, Asteraceae, Verbenaceae	10.85	10.34	9.97
4	4200	superparamo	-78.70671,-0.63654	mollic andisole	Poaceae, Apiaceae, Rosaceae, Asteraceae	10.60	7.96	9.55

3.2.2 Soil characteristics

Soil type was confirmed with the colorimetric key according to Munsell [44], soil texture estimates were performed as described by Sponagel et al. [45,46], and the detection of amorphous allophanes as described by Fieldes and Perrott [47]. Soil pH and conductivity were determined by creating 1:5 and 1:2.5 slurries respectively with deionized water, which was measured on a Potentiometer S500 (Mettler Toledo, Switzerland) after one hour of stirring, following protocols by Rayment and Higginson [48]. To determine density and humidity, soil samples were collected with volumetric cylinders (50 mL) whose water content was measured gravimetrically before and after oven-drying at 110°C following standard procedures [49]. Soil organic carbon (SOC), total Nitrogen (Nt), as well as S, P, Ca, Mg, Zn, K, Cu, Fe and Mn were analysed in the Ecuadorian National Institute of Agricultural Research (INIAP) according to international standards.

Soil Phenolic substances (Phen) content was determined using Folin-Ciocalteu's phenol reagent and Na_2CO_3 according to the protocol of Pinsonneault et al. [29], with absorbance measured after 1.5 hours incubation on a Synergy H1 Hybrid Reader (Bio Tek Instruments, CA, USA) at 750 nm. Results were calculated using Phenol Standard curves, and dry weight correction was applied.

3.2.3 Measurement of hydrolytic enzyme activities

Samples were stored at 4°C and measured for a maximum of three weeks after sampling following recommendations by DeForest et al. [50]. Organic material, stones, and larger particles (>2 mm) were manually removed from the soil samples, and one gram of soil was used to produce a suspension in 50 mL of sterile distilled water, which was further homogenized in a low-energy ultrasonic bath SK3300B (VWR, USA) for six minutes to break apart soil particles [51]. Enzyme substrates were prepared using 4-Methylumbelliferyl (MUF)-phosphate (for EC 3.1.3.1 y 2) , -Sulfate (for EC 3.1.6) , -ß-D-glucoside (for EC 3.2.1.21), -ß-D-cellobiose (for EC 3.2.1.91), and -N-acetyl-ß-D-glucosamine (for EC 3.2.1.52) (Sigma-Aldrich, Germany) at a final concentration of 1 mmol/L. Except for the well-soluble MUF-phosphate, and -Sulfate, 0.03 vol% Dimethyl-sulfoxide (DMSO) (Merck, Germany) was used to assure complete dissolution of the substrates in stock solutions. Substrates were chosen as representatives involved in Carbon, Nitrogen, Phosphorus, and Sulfur cycles [29,52] as an approximation for overall organic matter decomposition.

The fluorescence of released MUF for each different substrate was measured spectrophotometrically following recommendations by Marx et al. [53] and German et al. [54]. A volume of 50 µL of soil sample suspension, 50 µL of 0.1 molar MES buffer (Sigma-Aldrich, Germany), pH 6.1, and 100 µL of each analyzed respective enzyme substrate, were transferred to a black 96-well plate. Plates were then incubated at 10°C as the representative mean temperature and pH of sampling sites [54]. Fluorescence was analyzed over 5 hours using 7-time points with at least four repeated measurements per sample on a Synergy H1 Hybrid Reader with software Gen5 (Bio Tek Instruments, CA, USA) at 360 nm excitation and 460 nm emission wavelength (APPX 3.1). Sample-specific standard curves were generated using MUF concentrations as a reference to avoid quenching effects (APPX 3.2). Dry weight conversion was applied to the soil sample, and activity was calculated as $nmol*g_{soil}^{-1}*h^{-1}$ presented with standard errors.

3.2.4 Measurement of phenol oxidase activity

Soil samples for phenol oxidase measurement were prepared according to the above-mentioned procedure with the difference that 1 g of soil was diluted in 125 mL of 10 mM phosphate buffer, pH 6.1. Substrate. 3,4-Dihydroxy-L-phenylalanine (L-DOPA) (Sigma-Aldrich, Germany) at 25 mM and 2,2'-azino-bis-3-ethylbenzothiazoline-6-sulfonic acid (ABTS) (Fisher Scientific, SL, USA) at 10 mM final concentration were prepared as substrates.

Absorbance was measured at 419 nm spectrophotometrically on a Synergy H1 Hybrid Reader with software Gen5. 200 µL of soil suspension, 50 µL of the substrate, and in case of peroxidase measurement 10 µL of 0.03% H_2O_2 were transferred to transparent 96-well plates with 6 replicates for each sample. Samples were measured overtime for six hours.

L-DOPA showed more consistent results than ABTS, and the addition of peroxide lead to ineffective results, probably due to its optimal performance at ph below 4 [55], which is why the presented data only accounts for L-DOPA measurement without peroxide addition. Final enzyme activity was calculated as nmol*g_{soil}^{-1}*h^{-1} presented with standard errors according to German et al. [54] based on the extinction factor from the literature.

3.2.5 Statistical analysis

All data analysis was performed using Microsoft EXCEL 365 and the licensed version of STATA 16.0. The Shapiro Wilk test was performed to analyze the Normal distribution of data and Levene's Test for homoscedasticity. ANOVA was performed for altitude, independent t-test for depth, and paired t-test for each season. In case data did not fulfill assumptions for parametric analysis after natural log transformation (APPX 3.3), non-parametric tests such as Wilcoxon ranked sum and Wilcoxon signed-rank tests were applied. The same way Pearson and Spearman linear regression analysis was performed. Anyhow there was no observed difference in significance outcomes between parametric and non-parametric tests applied for the same data.

To reduce the number of variables applicable to statistic modeling, three distinct principal component analyses (PCA) were performed over subsets of variables creating new variables for "components of organic matter" (organic), including SOC, Nt, P, S, and Phen, "physical and chemical properties of the soil" (physical), including pH, Hum, Cond, Dens, and "metals", including K, Ca, Mg, Zn, Cu, Fe, and Mn. Kaiser-Meyer-Olkin Test was used to check for the pertinency of chosen variables. Diagnostic outcomes considerably improved removing the variables Nt, PHEN, Mg, and Zn from the final PCA (APPX 3.4).

To perform multivariate analysis, linear fixed-effect models were applied using each enzyme activity as the dependent variable, altitude, depth, and season as categorical predictor variables and, "organic" and "physical" as continuous predictor variables. The normal distribution of residuals was tested using Shapiro Wilk, and collinearity was checked with the variance inflation factor (threshold < 9). The Akaike's information criterion and the Bayesian information criterion were used as diagnostic parameters to fit models. It is worthy of mentioning that the continuous variable "metals" was removed from all models as it consistently worsened diagnostic outcomes and, in no case resulted in significant model estimates for the particular variable. Beta-estimates were used to demonstrate normalized differences between predictor variables (APPX 3.5).

3.3 Results

Exploratory statistical analysis was performed to study the change of physical and chemical factors within soil samples due to altitude season and depth. Tables 1, 2,and 3 show the results of the different variables that were analyzed according to the grouping

that was used for later PCA analysis. As expected for mollic andosol, levels of SOC and Nt were elevated across all analyzed altitudes [56] with similar levels (Table 3.2). Mean data did not change over the seasons but there was a significant reduction with depth. Phosphorus, as well as Sulfur levels, decreased with altitude but due to environmental variation, only Sulfur showed significant difference from other levels in the superparamo region. In the case of phenolic substances, highest levels coincided with SOC and Nt at the grass-paramo but there was no significance pattern observable.

Table 3.2 Components of organic matter in different scenarios

Variables		SOC	Nt	P	S	Phen
		%	%	ppm	ppm	ppm
Altitude n=48	3600 m	4.03 ± 0.59 a	0.23 ± 0.03 a	**13.7** ± 1.0 a	**10.3** ± 2.0 a	1.08 ± 0.17 a
	3800 m	3.78 ± 0.27 a	0.22 ± 0.02 a	10.8 ± 1.3 a	6.5 ± 0.8 ab	1.10 ± 0.18 a
	4000 m	**4.79** ± 0.33 a	**0.30** ± 0.03 a	12.4 ± 1.9 a	7.4 ± 0.6 a	**1.58** ± 0.46 a
	4200 m	3.93 ± 0.26 a	0.23 ± 0.02 a	9.2 ± 1.1 a	4.6 ± 0.6 b	0.69 ± 0.10 a
Season n=48	dry	**4.48** ± 0.26 a	**0.25** ± 0.02 a	9.9 ± 0.7 a	**8.3** ± 1.1 a	0.93 ± 0.10 a
	rainy	3.79 ± 0.28 a	0.23 ± 0.02 a	**13.2** ± 1.1 b	6.1 ± 0.5 a	**1.30** ± 0.25 a
Depth n=48	10 cm	**4.73** ± 0.27 a	**0.29** ± 0.02 a	**14.5** ± 1.0 a	**8.2** ± 1.1 a	**1.21** ± 0.20 a
	30 cm	3.53 ± 0.23 b	0.20 ± 0.01 b	8.6 ± 0.6 b	6.2 ± 0.7 a	1.02 ± 0.19 a

SOC = Soil organic carbon, Nt = total Nitrogen, Phen = Phenolic substances, bold = highest value of each category

The physical characteristics of conductivity, bulk density, and humidity were relatively constant over different altitudes (Table 3.3). There was a slight decrease in mean values with rising altitude observable in measured pH values, but differences are so small that they are not statistically significant. As could be expected, there was a significant difference in density and humidity with the seasons, as well as a considerable difference in conductivity, which was also the only variable that presented notable changes with depth.

Table 3.3 Physical and chemical properties of soil in different scenarios

Variables		pH	Cond	Dens	Hum
			µS	g/L	%
Altitude n=48	3600 m	**6.43** ± 0.10 a	**22.75** ± 4.13 a	1208 ± 48 a	26.39 ± 2.66 a
	3800 m	6.39 ± 0.13 a	17.62 ± 2.60 a	**1250** ± 49 a	27.26 ± 1.79 a
	4000 m	6.08 ± 0.10 a	17.61 ± 2.31 a	1164 ± 69 a	**31.02** ± 3.00 a
	4200 m	5.96 ± 0.04 a	16.73 ± 2.45 a	1313 ± 79 a	29.53 ± 1.86 a
Season n=48	dry	**6.44** ± 0.08 a	**23.17** ± 2.29 a	1092 ± 26 a	22.09 ± 0.98 a
	rainy	5.99 ± 0.05 a	14.18 ± 1.38 b	**1376** ± 40 b	**35.01** ± 1.07 b
Depth n=48	10 cm	6.18 ± 0.08 a	**21.50** ± 2.28 a	1218 ± 43 a	**29.91** ± 1.85 a
	30 cm	**6.24** ± 0.08 a	15.85 ± 1.73 b	**1249** ± 46 a	27.19 ± 1.47 a

Cond = Conductivity, Dens = Bulk density, Hum = Humidity

Concerning the metal content of soil samples (Table 3.4), these elements showed a pretty heterogenous distribution across different altitudes with no clearly distinguishable

pattern. There were no statistically significant changes with seasons, except for Mg whose concentration was higher in rainy season. Generally, values indicated a mineral-rich soil, typical for volcano-derived mollic soils [15,57] with Mg and Ca reaching especially high levels. These were also the only metals whose contend significantly reduced with depth which fits to the decrease in conductivity.

Table 3.4 Metal components of soil samples in different scenarios

Variables		K meq/100g	Ca meq/100g	Mg meq/100g	Zn ppm	Cu ppm	Fe ppm	Mn ppm
Altitude n=48	3600 m	0.15 ± 0.05 a	**6.3** ± 1.0 a	**1.5** ± 0.3 a	**5.52** ± 0.62 a	4.72 ± 0.33 a	336 ± 44 a	5.06 ± 0.73 a
	3800 m	0.22 ± 0.03 a	4.7 ± 0.6 a	0.9 ± 0.2 a	4.96 ± 0.56 a	6.17 ± 0.24 a	300 ± 34 a	5.19 ± 0.85 a
	4000 m	**0.31** ± 0.04 a	5.5 ± 0.7 a	1.0 ± 0.1 a	5.47 ± 0.53 a	5.98 ± 0.15 a	**386** ± 38 a	**6.33** ± 0.56 a
	4200 m	0.28 ± 0.03 a	4.8 ± 0.6 a	0.8 ± 0.1 a	3.48 ± 0.59 a	**6.29** ± 0.25 a	356 ± 33 a	6.13 ± 0.65 a
Season n=48	dry	**0.26** ± 0.03 a	**5.5** ± 0.5 a	0.8 ± 0.1 a	**5.75** ± 0.38 a	5.53 ± 0.23 a	324 ± 27 a	4.91 ± 0.32 a
	rainy	0.21 ± 0.03 a	5.2 ± 0.6 a	**1.3** ± 0.2 b	5.20 ± 0.41 a	**6.05** ± 0.19 a	**366** ± 26 a	**6.45** ± 0.59 a
Depth n=48	10 cm	0.23 ± 0.03 a	**6.6** ± 0.5 a	**1.3** ± 0.2 a	**5.52** ± 0.40 a	5.65 ± 0.18 a	**352** ± 22 a	**5.93** ± 0.47 a
	30 cm	**0.25** ± 0.03 a	4.1 ± 0.4 b	0.8 ± 0.1 b	5.43 ± 0.40 a	**5.92** ± 0.24 a	338 ± 31 a	5.43 ± 0.53 a

bold = highest value of each category

Seven different substrates were used to measure the activity of enzyme families involved in the nutrient cycles of organic matter (Table 3.5). All analyzed enzyme activities except for Cellobiohydrolase showed the highest values at the lowest altitude. In the case of Peroxidase, there was more than two-fold decrease which was statistically significant. Furthermore, the minor level of enzyme activity for all hydrolases, except Sulfatase, was measured at the highest altitude. Although most statistical analyses of the data failed to show significant differences with exception of β-Glu and POX, there is a clear pattern of decreasing activity with rising altitude observable across all analyzed enzymes. Moreover, all hydrolase activities were significantly higher in the dry compared to the rainy season. Close to two-fold differences were observed for Phos, Sulf, Cellobio, and β-Glu, being POX the only exception. Additionally, sampling depth had a notable impact on enzyme activity with a significant decrease for all enzymes except Cellobio.

Table 3.5 Mean enzyme activity of soil samples

Variables		Phos	Sulf	N-Ac	Cellobio	β-Glu	POX
Altitude n=48	3600 m	**4764** ± 868 a	**333** ± 73 a	**345** ± 73 a	82 ± 14 a	**690** ± 172 a	**859** ± 134 a
	3800 m	4257 ± 623 a	195 ± 34 a	223 ± 25 a	**84** ± 11 a	509 ± 68 a	333 ± 59 b
	4000 m	4259 ± 426 a	226 ± 31 a	226 ± 24 a	79 ± 7 a	455 ± 51 ab	252 ± 44 b
	4200 m	3531 ± 737 a	217 ± 41 a	184 ± 39 a	52 ± 7 a	284 ± 46 b	393 ± 62 b
Season n=48	dry	**5740** ± 414 a	**329** ± 39 a	**295** ± 40 a	**97** ± 7 a	**625** ± 89 a	408 ± 58 a
	rainy	2665 ± 294 b	157 ± 17 b	194 ± 21 b	51 ± 4 b	344 ± 38 b	**511** ± 88 a
Depth n=48	10 cm	**5089** ± 515 a	**314** ± 40 a	**316** ± 38 a	**81** ± 8 a	**612** ± 88 a	**542** ± 94 a
	30 cm	3316 ± 360 b	171 ± 20 b	174 ± 19 b	67 ± 7 a	358 ± 44 b	377 ± 44 b

Phos = Phosphatase, Sulf = Sulfatase, N-Ac = N-Acetil-glucosidase, Cellobio = Cellobiohydrolase, β-Glu = β-glucosidase, POX = Peroxidase, Mean values in nmol/g*h

The observed significant differences due to sampling depth and seasonal changes, account for more significance variation at altitudinal levels which is possibly causing the lack of significance. Two-way anova confirmed this pattern of altitude contrasted to the season for all enzymes, but Phosphatase and Sulfatase (Table 3.6).

Table 3.6 Two-way ANOVA analysis of enzyme activity over Altitude Season and their interaction

	Altitude		Season		season#altitude	
Enzyme	**F**	**p-value**	**F**	**p-value**	**F**	**p-value**
Phosphatase	1.08	NS	39.73	**0**	2.17	NS
Sulfatase	2.52	0.0713	19.78	**0.0001**	2.25	0.0972
N-Ac	3.14	**0.0357**	6.55	**0.0143**	3.57	**0.0223**
Cellobio	4.47	**0.0085**	42.26	**0**	3.09	**0.0155**
ß-Glu	3.76	**0.0182**	10.58	**0.0023**	2.3	0.0917
POX	10.53	**0**	1.52	NS	0.29	NS

There is also a clear pattern toward the synergistic behavior of analyzed enzymes in their degradation activity. This relationship was further confirmed by simple regression analysis, revealing highly significant correlation between all hydrolases with r^2 values from 0,66 up to 0,86, again with POX as the only exception (Table 3.7). This analysis further revealed a strong correlation between SOC, Nt, and Sulfur compared to hydrolase activities, as well as the significant correlation of humidity, and density with Sulfatase, Phosphatase, and Cellobio, which further demonstrates the importance of seasonal aspects.

Table 3.7 Correlation among enzyme activity and important physical and chemical soil characteristics

	Sulf	Phos	N-Ac	Cellobio	ß-glu	POX	pH	Hum	Dens	SOC	Nt	P	S
Sulf	1.00												
Phos	0.77 ***	1.00											
N-Ac	0.75 ***	0.66 ***	1.00										
Cellobio	0.66 ***	0.77 ***	0.68 ***	1.00									
ß-glu	0.76 ***	0.67 ***	0.86 ***	0.79 ***	1.00								
POX	0.20	0.05	0.13	-0	0.15	1.00							
pH	0.28	0.34 *	0.33 *	0.58 ***	0.43 **	-0.01	1.00						
Hum	-0.32 *	-0.46 **	-0.12	-0.41 **	-0.14	0.03	-0.52 ***	1.00					
Dens	-0.41 **	-0.48 ***	-0.27	-0.49 ***	-0.35 *	0.05	-0.40 **	0.50 ***	1.00				
SOC	0.43 **	0.55 ***	0.52 ***	0.47 ***	0.55 ***	0.02	0.01	0.09	-0.36 *	1.00			
Nt	0.38 **	0.50 ***	0.46 **	0.40 **	0.44 **	0.01	-0.10	0.23	-0.19	0.87 ***	1.00		
P	0.26	0.12	0.32 *	0.06	0.29 *	0.33 *	-0.23	0.44 **	0.05	0.46 ***	0.59 ***	1.00	
S	0.66 ***	0.38 **	0.69 ***	0.58 ***	0.72 ***	0.13	0.51 ***	-0.04	-0.27	0.37 **	0.28 *	0.29 *	1.00

statistically significant correlation: * p<0.05; ** p<0.01; *** p<0.001

Information from the exploratory analysis was used to create linear fixed-effect models for each enzyme family. Figure 2 shows the relationship of the “organic” and “physical”

components, as well as different altitudes, seasons, and depths to reveal which factors significantly account for the greatest variance of enzyme activity as the dependent variable. To determine significance levels, altitude 1, dry season, and 10 cm depth were used as references to compare with the remaining categories following the concept of dummy variables.

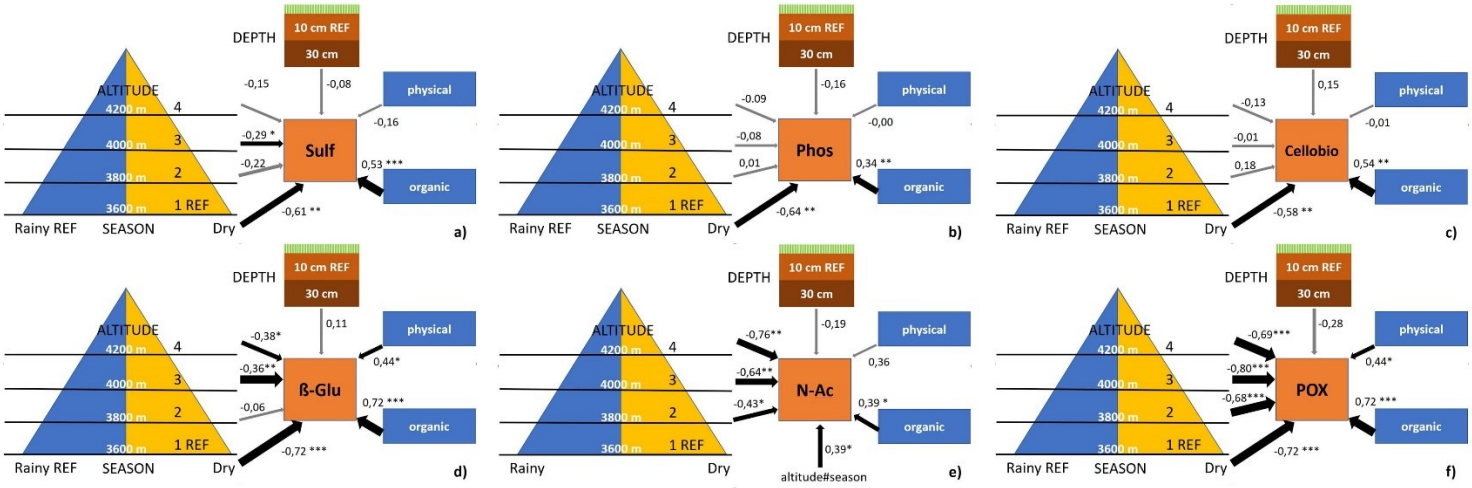

Figure 3.4 Linear fixed-effect models with enzyme activity as dependent
a) Sulf = Sulfatase, b) Phos = Phosphatase, c) Cellobio = Cellobiohydrolase, d) ß-Glu = ß-Glucosidase, e) N-Ac = N-Acetyl-Glucosaminidase, f) POX = Phenol-oxidase. REF = Reference categories for comparison with remaining categories of the same categorical variable. "physical" and "organic" indicate principal components of physical and chemical variables as described in methods. Values on arrows indicate beta-estimates, black arrows indicate significant model estimates, * p<0,05, ** p<0,01, ***p<0,001. All models were designed equally with exception of N-Ac where Season was replaced by the interaction term altitude#season

The "organic" component showed significance for all analyzed enzymes including POX, meanwhile "physical" components played a significant role only for β-Glu and POX. Interestingly in all model's depth lost its importance as a driving factor of enzyme activity meanwhile season showed significance with beta-estimates up to -0,72. Altitude had highly significant impact on N-Ac and POX levels as well as to lesser extents on β-Glu and Sulf. Only for Cellobio and Phos no altitudinal impact was measurable in model estimates and their significance.

To remain comparability all chosen model parameters were similar among enzymes, with a slight modification for N-Ac where Season was replaced by the interaction term of the season with altitude which led to improved model diagnostic parameters.

3.4 Discussion

3.4.1 Soil characteristics

Soil shows a complex interplay between a multitude of biological, chemical, and physical factors mutually influencing each other. Drastic altitudinal changes within the paramo highlands cause the appearance of different vegetational zones [58]. It is well described how vegetation can shape the soil microbiome through interaction at the rhizosphere and nutrient intake [30,59,60] and the microbial community is further influenced by physical and chemical characteristics of soil [61]. The present study analysis a part of this complex interplay by the measurement of soil derived enzyme activity as an approximation for organic matter degradation within different vegetational zones of the paramo region in Northern Ecuador.

To avoid soil type derived bias in chemical, physical and microbiome parameters, sampling sites were chosen within the area of mollic andosol on a linear transect towards the volcano peak as described above. Soil analysis therefore showed relatively little variation in physical aspects and those observed were mainly given by seasonal changes rather than altitudinal differences as to be expected for humidity and density which are directly related to precipitation. Interestingly pH was relatively high for peatland and did not change significantly neither with altitude nor with season or depth consistent with former observations [15]. Furthermore, the physical component did not show significant estimates for most of the linear fixed effect models that were implemented. This is an important observation as pH is commonly known as one of the most important factors influencing enzyme activity apart from temperature [54,62]. Given that differences were marginal, it is unlikely that pH could have act as a driving factor of enzyme activity in the present analysis and it highlights to a certain extent comparability among chosen sampling sites.

Minerals were distributed in a heterogenous way on different levels of altitude mostly not showing significant differences. Only for Mg and Ca sampling depth had a significant influence which can be explained by the frequent association of these elements with organic matter [63]. This finding therefore coincides with soil parameters involved in organic matter composition where SOC as well as Nt and P decreased with depth but not with altitude.

Interestingly pH was strongly correlated with sulfur content although one might rather expect an inverse correlation as sulfur tends to acidify soils forming inorganic acids [64]. Another important observation is, that the organic component showed strong correlation with enzyme activities in fixed effect models for all analyzed enzymes indicating that biochemical rather than physical factors were drivers in the analyzed area. In this context it was rather surprising that phenolic substances failed to show any correlation neither with hydrolase nor with POX activity against all expectations due to the “Enzyme Latch” theory, even though former studies equally failed to show this correlation [38,65].

3.4.2 Altitudinal dependence of enzyme activity

Initial analysis of enzyme activity did not suggest a direct linear relation to altitude considering statistically outcomes, where only β-Glu and POX showed significant differences for few altitudes. Nevertheless, there is a visible tendency towards reduced enzyme activity with rising altitude supported by several findings. First, the mean values of all analyzed enzyme family activities decreased with five out of six maximum values at the lowest altitude and four out of six minimum values at the highest altitude. This tendency was further underlined by the synergistic behavior of enzymes showing high correlation values among each other which was similarly observed in former studies [29]. The fact that Cellobio did not show the strongest activation at the lowest level might be explained by the fact that Zn, Ca and Mg levels were highest at the lowest altitude, where Zn tends to inhibit Cellobiohydrolase activity but not those of other hydrolases, and on the other hand the opposite effect that Ca and Mg levels which tend to increase most enzyme activity do not show an activating effect on that enzyme [66].

Second, the separation by season considerably increased significance outcome indicating that variation due to seasonal changes exhibited an annihilating effect on the altitudinal tendency. Finally, the linear fixed effect models showed negative estimates for almost all different altitudes in all measured enzymes using the lowest altitude as the baseline reference. These estimates were significant principally for β-Glu N-Ac and POX. Taken together these results indicate a strong influence of altitude on organic matter degrading processes although these changes do not necessarily follow a straight linear decrease with altitude, a phenomena that had formerly been observed for mountain ecosystems [67]. One especially notable outcome is the pronounced cleft between enzyme activity at the lowest elevation indicating the borderline between paramo and high Andean Mountain forests at 3600 m and the shrub paramo at 3800 m. Especially POX showed a two-fold difference due to only 200 m difference of altitude but also hydrolases indicated similar behavior. This is consistent with the “Enzyme Latch” theory where higher POX activity leads to a decrease in inhibiting phenolic substances which negatively affects hydrolase activity. However, although the levels of phenolic substances at the lowest elevation present the second lowest value after the super-paramo there is almost no observed mean difference to shrub paramo, indicating that the underlying mechanism apparently depends on additional factors.

Mean values tended to show stronger variation at the lowest altitude which is probably due to the observed increasing vegetational diversity and less homogeneity among different sampling sites compared to the very uniform appearance of grass paramo where differences in vegetation among sampling sites are marginal. Although a strong effort was made to find comparable sampling sites with open vegetation to avoid species dependent root associated microbiome bias [68], at lower elevations vegetation becomes denser, complicating the task. These same finding might further explain the drastic changes in enzyme activity between subparamo and shrub paramo. Apart from low

temperatures, strong winds and radiation hinder the growth of vegetation that is not completely adapted to the environmental circumstances in the paramo region [16]. The appearance of new plant families at lower elevations might mutually influence the growth of others, offering wind shelter and shadow [69]. This coincides with field observations where remnants of Mountain forest reach higher elevations within protected valleys [70]. Vegetation knowingly affects microbiome composition indicating highest diversity indices for bacteria and fungi in this area (unpublished data). A deeper analysis of altitude related microbial changes of bacteria, archaebacteria and fungi within the studied paramo site is currently underway which therefore might explain the observed changes in enzyme activity [71]. More studies are necessary to explain the intrinsic relation with the unique vegetation of the paramo region.

Interestingly, the enzyme activities of phosphatases and sulfatases strongly increased at the lowest elevations coinciding with higher levels of sulfur and phosphate which might facilitate the nutrient uptake at lower elevations by root systems [72]. Although the paramo region is extremely rich in organic matter, it is not considered the most fertile region for crop planting because it bears dramatic climatic changes not suitable for many crops. More interestingly its lack in decomposition capacity decreases the liberation of nutrients to the point where they become available for plants [12,73]. Frequently, paramo soil is transported to lower regions and sold as “nutrient rich black soil” on South American markets. If temperature rises and soil nutrients will be liberated in a constant manner, it is most probably that the observed upslope shift of agriculturally used land [74] will further rise and put an additional threat to the paramo region due to invasion of conserved sites. Moreover, the lowest elevation at 3600 m presents the borderline between the paramo and downslope mountainous ecosystems and the observed changes might present evidence for the existence of a critical turning point. Considering that minor changes in altitude can lead to extreme effects on organic matter decomposition in a scenario of future global warming it is possible that even slight changes in temperature could have severe effects on ecosystem alterations within the paramo region.

The opposite effect to the lowest elevation was visible at the grass paramo region at 4000 m elevation, where the weakest POX activity was found. This coincides with highest levels of phenolic substances and the greatest SOC and Nt content. These findings support the theory that the “Enzyme Latch” impairs efficient organic matter degradation at this elevation [65] and identifies the grass paramo as the most promising carbon sink within the paramo region. Nevertheless, the study failed to show a direct relation to the hydrolase activities that might have been expected.

3.4.3 Enzyme activity depending on seasonal changes

Although Ecuador lacks four seasons due to its ubication at the equator line, there are pronounced rainy and dry seasons. Mean temperatures are similar between both seasons and although fluctuation is greater in dry season, the most important difference lies in

precipitation [43]. The enzyme activity of all analyzed hydrolases increased remarkably about 2-fold in dry season with especially high levels at the lowest elevation. POX was the only exception, which is surprising because according to the "Enzyme Latch" theory dry climate increases aeration of peat which leads to increased oxidase activity [52]. One possible explanation might be that POX depends on copper which exhibits a strong activating effect [66] and levels of the metal where higher in rainy season, nevertheless differences were not significant.

The present results are consistent with former reports about increasing organic matter decomposition due to seasonal [29] as well as drought induced [37,75] effects but fail to confirm the effect driven by oxidases [35].

Increasing surface evaporation due to rising temperatures allowing oxygen to further penetrate the upper layers of soil [33] and tendencies towards extreme climate phenomena with prolonged droughts and flooding events instead of consistent rainfall [76] could further accelerate degrading processes of paramo peat leading to a probable drastic reduction of this unique ecosystem within the future [76]. Finally, the great water retention capacity of peatland is given by its large amounts of organic matter [23]. If decomposition rates increase, these retention capacities may drop leading not only to the loss of ecosystem services [22] but even more importantly to increased aeration releasing a vicious circle of peat decomposition. These drought events can already be observed in the paramo due to increasing incidences of wildfires adding dramatically to the release of greenhouse gases and the destruction of peat [77,78]. Taken together seasonal changes are expected to accelerate peat decomposition processes within the paramo region under global warming conditions. Nevertheless, the present study presents only two transversal timepoints to study the phenomena which is why time dependent studies crossed with climatic analysis should be performed to understand the underlying dynamics of this complex ecosystem.

3.4.4 The role of depth in enzyme activity variation

Decreasing enzyme activity with sampling depth is a commonly known phenomena [79], as it is the surface area where greatest microbiome diversification and nutrition intake are taking place [30], meaning that statistically significant differences between depths is not a surprising outcome. Therefore, it is rather remarkable that in the developed models, the variable depth totally lost its importance as a driver of change. None of the observed models resulted in significant estimates for depth using topsoil (10 cm) as reference. On one hand depth was chosen although its effect is well described, because most soil types present drastic structural changes already within the first 30 cm of depth [56], which is not the case for mollic andosol. The relatively young, volcanic ash derived soil presents hardly matured thick A horizons whose structure and color barely changes with profundity [15], which might account for lesser changes with sampling depth as can be observed in other soil types. On the other hand, the observed differences, although

statistically significant, might have lost importance in direct comparison to other driving factors whose importance has been discussed above. This finding therefore further underlines the importance of altitudinal and seasonal influences on organic matter decomposition.

3.5 Conclusion

The present study is most relevant for the climate change-related research in the paramo region given that several new research perspectives arose by the presented results in a region where research is still very scarce, considering its environmental but also socio-economic importance. The observation that enzyme activity consistently decreases with altitude even under constant temperature conditions and without apparent pH changes implies that changes of vegetational zones with altitude play a key role in its degradation processes most probably due to microbiome changes. It is therefore necessary to further study the direct relation of the specific interaction between the vegetation and the microbiome. Given that the degradation of organic matter is directly related to its carbon fixation capacity, shown by its significant correlation with the organic component, it would further be interesting to address greenhouse gas liberation and study functional diversity of bacteria and fungi related to it as well as levels of soil oxygenation as a key factor in decomposition processes. The second important finding is, that seasonal changes induce drastic changes in enzyme activity showing considerably stronger activation in dry season, especially at lower elevations. This might indicate the existence of a tipping point between high Andean downslope ecosystems and the paramo region due to marginal changes in elevation and therefore most importantly the temperature. Future global warming thus puts a serious threat to this unique ecosystem whose importance is consequently underestimated in environmental policies [22].

3.6 Chapter References

1. Pachauri RK, Mayer L, Intergovernmental Panel on Climate Change, editors. Climate change 2014: synthesis report. Geneva, Switzerland: Intergovernmental Panel on Climate Change; 2015. 151 p.

2. Patz JA, Gibbs HK, Foley JA, Rogers JV, Smith KR. Climate change and global health: Quantifying a growing ethical crisis. Ecohealth. 2007 Dec;4(4):397–405.

3. Zhang F, Zhang H, Pei S, Zhan L, Ye W. Effects of Arctic Warming on Microbes and Methane in Different Land Types in Svalbard. Water. 2021 Nov;13(22):3296.

4. Hansen J, Kharecha P, Sato M, Masson-Delmotte V, Ackerman F, Beerling DJ, et al. Assessing "Dangerous Climate Change": Required Reduction of Carbon Emissions to Protect Young People, Future Generations and Nature. Plos One. 2013 Dec 3;8(12):e81648.

5. Gruber N. Warming up, turning sour, losing breath: ocean biogeochemistry under global change. Philos Trans R Soc -Math Phys Eng Sci. 2011 May 28;369(1943):1980–96.

6. ¿Qué es el Protocolo de Kyoto? | CMNUCC [Internet]. [cited 2022 Aug 8]. Available from: https://unfccc.int/es/kyoto_protocol

7. IPCC. IPCC international panel on climate change - report 2014 [Internet]. 2014 [cited 2022 Jan 10]. Available from: https://archive.ipcc.ch/pdf/assessment-report/ar5/syr/AR5_SYR_FINAL_SPM_es.pdf

8. Zarnetske PL, Gurevitch J, Franklin J, Groffman PM, Harrison CS, Hellmann JJ, et al. Potential ecological impacts of climate intervention by reflecting sunlight to cool Earth. Proc Natl Acad Sci U S A. 2021 Apr 13;118(15):e1921854118.

9. Chen W, Pinho B, Hartman RL. Flash crystallization kinetics of methane (sI) hydrate in a thermoelectrically-cooled microreactor. Lab Chip. 2017 Sep 12;17(18):3051–60.

10. Msangi JP. Drought hazard and desertification management in the drylands of Southern Africa. Environ Monit Assess. 2004 Dec;99(1–3):75–87.

11. Jin H, Ma Q. Impacts of Permafrost Degradation on Carbon Stocks and Emissions under a Warming Climate: A Review. Atmosphere. 2021 Nov;12(11):1425.

12. Buytaert W, Cuesta-Camacho F, Tobon C. Potential impacts of climate change on the environmental services of humid tropical alpine regions. Glob Ecol Biogeogr. 2011 Jan;20(1):19–33.

13. Pepin N, Bradley RS, Diaz HF, Baraer M, Caceres EB, Forsythe N, et al. Elevation-dependent warming in mountain regions of the world. Nat Clim Change. 2015 May;5(5):424–30.

14. Jiménez-Rivillas C, García JJ, Quijano-Abril MA, Daza JM, Morrone JJ. A new biogeographical regionalisation of the Páramo biogeographic province. Aust Syst Bot. 2018;31(4):296.

15. Buytaert W, Deckers J, Wyseure G. Regional variability of volcanic ash soils in south Ecuador: The relation with parent material, climate and land use. CATENA. 2007 Jul 15;70(2):143–54.

16. Bader MY, van Geloof I, Rietkerk M. High solar radiation hinders tree regeneration above the alpine treeline in northern Ecuador. Plant Ecol. 2007 Jul 1;191(1):33–45.

17. Li L, Xue B. Methane emissions from northern lakes under climate change: a review. SN Appl Sci. 2021 Nov 24;3(12):883.

18. Peatlands and climate change | IUCN [Internet]. 2018 [cited 2018 Sep 21]. Available from: https://www.iucn.org/resources/issues-briefs/peatlands-and-climate-change

19. Siles JA, Margesin R. Abundance and Diversity of Bacterial, Archaeal, and Fungal Communities Along an Altitudinal Gradient in Alpine Forest Soils: What Are the Driving Factors? Microb Ecol. 2016;72:207–20.

20. Hermes C, Segelbacher G, Schaefer HM. A framework for prioritizing areas for conservation in tropical montane cloud forests. Écoscience. 2018 Jan 2;25(1):97–108.

21. Bremer LL, Farley KA, DeMaagd N, Suárez E, Cárate Tandalla D, Vasco Tapia S, et al. Biodiversity outcomes of payment for ecosystem services: lessons from páramo grasslands. Biodivers Conserv. 2019 Mar 1;28(4):885–908.

22. Viviroli D, Archer DR, Buytaert W, Fowler HJ, Greenwood GB, Hamlet AF, et al. Climate change and mountain water resources: overview and recommendations for research, management and policy. Hydrol Earth Syst Sci. 2011 Feb 4;15(2):471–504.

23. Aparecido LMT, Teodoro GS, Mosquera G, Brum M, Barros F de V, Pompeu PV, et al. Ecohydrological drivers of Neotropical vegetation in montane ecosystems. Ecohydrology. 2018 Apr;11(3):e1932.

24. Nottingham AT, Fierer N, Turner BL, Whitaker J, Ostle NJ, McNamara NP, et al. Microbes follow Humboldt: temperature drives plant and soil microbial diversity patterns from the Amazon to the Andes. Ecology. 2018 Nov;99(11):2455–66.

25. Blagodatskaya E, Blagodatsky S, Khomyakov N, Myachina O, Kuzyakov Y. Temperature sensitivity and enzymatic mechanisms of soil organic matter decomposition along an altitudinal gradient on Mount Kilimanjaro. Sci Rep [Internet]. 2016 Apr [cited 2020 May 17];6(1). Available from: http://www.nature.com/articles/srep22240

26. Hodgkins SB, Tfaily MM, McCalley CK, Logan TA, Crill PM, Saleska SR, et al. Changes in peat chemistry associated with permafrost thaw increase greenhouse gas production. Proc Natl Acad Sci U S A. 2014 Apr 22;111(16):5819–24.

27. Anisimov O, Reneva S. Permafrost and changing climate: the Russian perspective. Ambio. 2006 Jun;35(4):169–75.

28. Voigt C, Marushchak ME, Mastepanov M, Lamprecht RE, Christensen TR, Dorodnikov M, et al. Ecosystem carbon response of an Arctic peatland to simulated permafrost thaw. Glob Change Biol. 2019 May;25(5):1746–64.

29. Pinsonneault AJ, Moore TR, Roulet NT. Temperature the dominant control on the enzyme-latch across a range of temperate peatland types. Soil Biol Biochem. 2016 Jun;97:121–30.

30. Chen M, He S, Li J, Hu W, Ma Y, Wu L, et al. Co-occurrence patterns between bacterial and fungal communities in response to a vegetation gradient in a freshwater wetland. Can J Microbiol. 2019 Oct;65(10):722–37.

31. Zheng Y, Chen L, Ji NN, Wang YL, Gao C, Jin SS, et al. Assembly processes lead to divergent soil fungal communities within and among 12 forest ecosystems along a latitudinal gradient. New Phytol. 2021 Aug;231(3):1183–94.

32. Collins CG, Stajich JE, Weber SE, Pombubpa N, Diez JM. Shrub range expansion alters diversity and distribution of soil fungal communities across an alpine elevation gradient. Mol Ecol. 2018 May;27(10):2461–76.

33. Górecki K, Rastogi A, Stróżecki M, Gąbka M, Lamentowicz M, Łuców D, et al. Water table depth, experimental warming, and reduced precipitation impact on litter decomposition in a temperate Sphagnum-peatland. Sci Total Environ. 2021 Jun 1;771:145452.

34. Freeman C, Ostle N, Kang H. An enzymic "latch" on a global carbon store. Nature. 2001 Jan;409(6817):149–149.

35. Freeman C, Ostle NJ, Fenner N, Kang H. A regulatory role for phenol oxidase during decomposition in peatlands. Soil Biol Biochem. 2004 Oct;36(10):1663–7.

36. Bragazza L, Buttler A, Robroek BJM, Albrecht R, Zaccone C, Jassey VEJ, et al. Persistent high temperature and low precipitation reduce peat carbon accumulation. Glob Change Biol. 2016 Dec;22(12):4114–23.

37. Estop-Aragonés C, Zając K, Blodau C. Effects of extreme experimental drought and rewetting on CO2 and CH4 exchange in mesocosms of 14 European peatlands with different nitrogen and sulfur deposition. Glob Change Biol. 2016 Jun;22(6):2285–300.

38. Brouns K, Verhoeven JTA, Hefting MM. Short period of oxygenation releases latch on peat decomposition. Sci Total Environ. 2014 May;481:61–8.

39. Avellaneda-Torres LM, León Sicard TE, Torres Rojas E. Impact of potato cultivation and cattle farming on physicochemical parameters and enzymatic activities of Neotropical high Andean Páramo ecosystem soils. Sci Total Environ. 2018 Aug;631–632:1600–10.

40. Nottingham AT, Turner BL, Whitaker J, Ostle N, Bardgett RD, McNamara NP, et al. Temperature sensitivity of soil enzymes along an elevation gradient in the Peruvian Andes. Biogeochemistry. 2016 Feb;127(2–3):217–30.

41. Instituto Geográfico Militar Ecuador [Internet]. [cited 2022 May 24]. Available from: http://www.geograficomilitar.gob.ec/productos-y-servicios/

42. Altamirano LL, Hermida IP, de Biodiversidad L, Gutiérrez DI, Leiton B, Iza C, et al. MINISTERIO DEL AMBIENTE (MAE) DIRECION NACIONAL DE BIODIVERSIDAD (DNB). 2008;195.

43. Instituto Nacional de Meteorología e Hidrología – INAMHI [Internet]. [cited 2022 Feb 14]. Available from: http://www.inamhi.gob.ec/

44. Cochrane S. The Munsell Color System: A scientific compromise from the world of art. Stud Hist Philos Sci Part A. 2014 Sep 1;47:26–41.

45. Eckelmann W, Sponagel H, Grottenthaler W, Hartmann KJ u a. Bodenkundliche Kartieranleitung. - 5. verbesserte und erweiterte - Auflage. Schweizerbart'sche Verlagsbuchhandlung; 2005.

46. Vos C, Don A, Prietz R, Heidkamp A, Freibauer A. Field-based soil-texture estimates could replace laboratory analysis. Geoderma. 2016 Apr 1;267:215–9.

47. Fieldes M, Perrott KW, New Zealand, Soil Bureau, New Zealand, Department of Scientific and Industrial Research. The nature of allophane in soils. part 3, part 3,. Wellington, N.Z.: Govt. Printer; 1966.

48. Rayment GE, Higginson FR. Australian laboratory handbook of soil and water chemical methods. Inkata Press; 1992.

49. Frogbrook ZL, Bell J, Bradley RI, Evans C, Lark RM, Reynolds B, et al. Quantifying terrestrial carbon stocks: examining the spatial variation in two upland areas in the UK and a comparison to mapped estimates of soil carbon. Soil Use Manag. 2009 Sep;25(3):320–32.

50. DeForest JL. The influence of time, storage temperature, and substrate age on potential soil enzyme activity in acidic forest soils using MUB-linked substrates and l-DOPA. Soil Biol Biochem. 2009 Jun 1;41(6):1180–6.

51. Stemmer M, Gerzabek MH, Kandeler E. Organic matter and enzyme activity in particle-size fractions of soils obtained after low-energy sonication. Soil Biol Biochem. 1998 Jan 1;30(1):9–17.

52. Dunn C, Jones TG, Girard A, Freeman C. Methodologies for Extracellular Enzyme Assays from Wetland Soils. Wetlands. 2014 Feb;34(1):9–17.

53. Marx MC, Wood M, Jarvis SC. A microplate fluorimetric assay for the study of enzyme diversity in soils. Soil Biol Biochem. 2001 Oct 1;33(12):1633–40.

54. German DP, Weintraub MN, Grandy AS, Lauber CL, Rinkes ZL, Allison SD. Optimization of hydrolytic and oxidative enzyme methods for ecosystem studies. Soil Biol Biochem. 2011 Jul;43(7):1387–97.

55. Bach CE, Warnock DD, Van Horn DJ, Weintraub MN, Sinsabaugh RL, Allison SD, et al. Measuring phenol oxidase and peroxidase activities with pyrogallol, l-DOPA, and ABTS: Effect of assay conditions and soil type. Soil Biol Biochem. 2013 Dec;67:183–91.

56. Food and Agriculture Organization of the United Nations, editor. World reference base for soil resources. Rome: Food and Agriculture Organization of the United Nations; 1998. 88 p. (World soil resources reports).

57. ALLABY MA. mollic horizon. In: ALLABY M, editor. A Dictionary of Earth Sciences. Oxford University Press; 2008.

58. Keating PL. Changes in Paramo Vegetation Along an Elevation Gradient in Southern Ecuador. J Torrey Bot Soc. 1999;126(2):159–75.

59. Bahram M, Netherway T, Hildebrand F, Pritsch K, Drenkhan R, Loit K, et al. Plant nutrient-acquisition strategies drive topsoil microbiome structure and function. New Phytol. 2020 Aug;227(4):1189–99.

60. Ward SE, Orwin KH, Ostle NJ, Briones JI, Thomson BC, Griffiths RI, et al. Vegetation exerts a greater control on litter decomposition than climate warming in peatlands. Ecology. 2015 Jan;96(1):113–23.

61. Wan W, Tan J, Wang Y, Qin Y, He H, Wu H, et al. Responses of the rhizosphere bacterial community in acidic crop soil to pH: Changes in diversity, composition, interaction, and function. Sci Total Environ. 2020 Jan 15;700:134418.

62. Li X, Wang Y, Zhang Y, Wang Y, Pei C. Response of soil chemical properties and enzyme activity of four species in the Three Gorges Reservoir area to simulated acid rain. Ecotoxicol Environ Saf. 2021 Jan 15;208:111457.

63. Johnson DW, Todd DE, Trettin CC, Mulholland PJ. Decadal changes in potassium, calcium, and magnesium in a deciduous forest soil. Soil Sci Soc Am J 72 1795 – 1805. 2009;72(6):1795–805.

64. Rengel Z. Handbook of Soil Acidity. CRC Press; 2003. 511 p.

65. Romanowicz KJ, Kane ES, Potvin LR, Daniels AL, Kolka RK, Lilleskov EA. Understanding drivers of peatland extracellular enzyme activity in the PEATcosm experiment: mixed evidence for enzymic latch hypothesis. Plant Soil. 2015 Dec;397(1–2):371–86.

66. Chang A, Jeske L, Ulbrich S, Hofmann J, Koblitz J, Schomburg I, et al. BRENDA, the ELIXIR core data resource in 2021: new developments and updates. Nucleic Acids Res. 2021 Jan 8;49(D1):D498–508.

67. Huang HL, Zong N, He NP, Tian J. [Characteristics of soil enzyme stoichiometry along an altitude gradient on Qinghai-Tibet Pla-teau alpine meadow, China]. Ying Yong Sheng Tai Xue Bao J Appl Ecol. 2019 Nov;30(11):3689–96.

68. Bulgarelli D, Schlaeppi K, Spaepen S, Ver Loren van Themaat E, Schulze-Lefert P. Structure and functions of the bacterial microbiota of plants. Annu Rev Plant Biol. 2013;64:807–38.

69. Calderón-Loor M, Cuesta F, Pinto E, Gosling WD. Carbon sequestration rates indicate ecosystem recovery following human disturbance in the equatorial Andes. PloS One. 2020;15(3):e0230612.

70. Wille M, Hooghiemstra H, Hofstede R, Fehse J, Sevink J. Upper forest line reconstruction in a deforested area in northern Ecuador based on pollen and vegetation analysis. J Trop Ecol. 2002 May;18(3):409–40.

71. Adamczyk M, Hagedorn F, Wipf S, Donhauser J, Vittoz P, Rixen C, et al. The Soil Microbiome of GLORIA Mountain Summits in the Swiss Alps. Front Microbiol. 2019;10:1080.

72. de Oliveira LB, Marques ACR, de Quadros FLF, Farias JG, Piccin R, Brunetto G, et al. Phosphorus allocation and phosphatase activity in grasses with different growth rates. Oecologia. 2018 Mar;186(3):633–43.

73. Hofstede R, Calles J, López V, Polanco R, Torres F, Ulloa J, et al. Hofstede - Impacto cambio climático en el páramo 2014-025.pdf [Internet]. [cited 2020 Jun 12]. Available from: https://portals.iucn.org/library/sites/library/files/documents/2014-025.pdf

74. Morueta-Holme N, Engemann K, Sandoval-Acuña P, Jonas JD, Segnitz RM, Svenning JC. Strong upslope shifts in Chimborazo's vegetation over two centuries since Humboldt. Proc Natl Acad Sci. 2015 Oct 13;112(41):12741–5.

75. Fenner N, Freeman C. Drought-induced carbon loss in peatlands. Nat Geosci. 2011 Dec;4(12):895–900.

76. Carrillo-Rojas G, Schulz HM, Orellana-Alvear J, Ochoa-Sánchez A, Trachte K, Célleri R, et al. Atmosphere-surface fluxes modeling for the high Andes: The case of páramo catchments of Ecuador. Sci Total Environ. 2020 Feb 20;704:135372.

77. Holloway JE, Lewkowicz AG, Douglas TA, Li X, Turetsky MR, Baltzer JL, et al. Impact of wildfire on permafrost landscapes: A review of recent advances and future prospects. Permafr Periglac Process. 2020 Jul;31(3):371–82.

78. Román-Cuesta RM, Carmona-Moreno C, Lizcano G, New M, Silman M, Knoke T, et al. Synchronous fire activity in the tropical high Andes: an indication of regional climate forcing. Glob Change Biol. 2014 Jun;20(6):1929–42.

79. Jian S, Li J, Chen J, Wang G, Mayes MA, Dzantor KE, et al. Soil extracellular enzyme activities, soil carbon and nitrogen storage under nitrogen fertilization: A meta-analysis. Soil Biol Biochem. 2016 Oct;101:32–43.

Chapter 4

Microbiota composition in an altitudinal gradient of paramo soils.

This chapter is based on information collected to be considered for publication during the accrual period of the doctorate´s scholarship.

Abstract: The Andean paramo region is characterized by astonishing biodiversity with extremely high levels of endemism, its accumulation of thick peat-like organic matter deposits, and its related capacity to retain great amounts of water. The low decomposing activity is directly linked to its microbial composition which has not yet been studied in detail. The present study aimed to amplify 16S- for archaea and bacteria and ITS-sequences for fungi, for differential analysis on 4 distinct altitudes marking vegetational zones in the dry and rainy season of the Iliniza national reserve in Ecuador. Samples were taken in triplicate and pooled (n=24).
Taxonomical data of richness and abundance revealed that bacterial communities tended to variate stronger with the season than with altitudinal effects. The most abundant phyla were Acidobacteriota, Actinobacteriota and Bacteriodota. Proteobacteriota which are commonly described as the leading soil phylum only showed little abundance. Fungi on the other hand showed greater variation in diversity either for altitudinal as well as seasonal effects. Ascomycota, Basidiomycota and Mortierellomycota were most abundant. In comparison to enzyme activity levels measured in chapter 3, the overall pattern of fungal diversity could explain to a greater extent the observed differences in the decomposition of organic matter. Furthermore, the distribution of fungal classes indicates unique patterns for the paramo environment which invites for further investigation. To our knowledge the present study presents the first taxonomical analysis considering both bacteria and fungi community structures in High Andean paramo soils

Key words: Bacteria, Fungi, 16S, ITS, taxonomical analysis, paramo, soil

4.1 Introduction

4.1.1 The microbial community of soil

For many decades the whole microbiota composition of virtually any biological community within an ecosystem presented a large gap of knowledge for scientists. Less than 1% of microorganisms present within a simple soil sample is effectively cultivatable under laboratory conditions and cultivation, isolation, and subsequent identification used to be the medium of choice [1]. With the development of second-generation sequencing in 2005 known as pyrosequencing and Illumina platforms in 2007, a revolution started in the field of microbiota

analysis which made it not only technically possible but also affordable for investigation in lower-income countries [2]. Nevertheless, microbiota analysis is still vastly unexplored in Ecuador. The only internationally published articles concerning paramo microbiota are either of bacterial species directly related to *Espeletia* species [3] or performed at the Sumaco volcano in Ecuador with lower altitudes and without taking seasonal aspect into account [4].

Mountain ecosystems like the Andean Paramo Highland are particularly interesting for the analysis of microbiota changes given that they are characterized by dramatic changes in climatic and biotic characteristics within a small geographical area [5,6]. It is known that these changes can greatly influence the composition of microbes. These shifts in microbial community structures over altitudinal gradients are also crucial for understanding climate change effects on ecosystems [7]. Studies analyzing the outcomes of experimental soil warming [8], vegetational changes [9], or water availability [10] have gained important insights into short-time effects that can be expected, but communities on an altitudinal gradient had a long time to establish their structure and can gain important additional information about the long-time effects [6].

Meta-analysis-based studies revealed that ecological niches will shift to higher elevations at an average rate of 12,2 meters each decade, which is at least twice as fast as previously estimated [11]. In how far this prediction will be correct depends on the velocity with which climate change keeps taking place and the still fairly understood intrinsic response of ecosystems to the change. Considering the complexity of microbial composition and the diversity of communities within defined ecosystems, research still requires many more studies to predict future outcomes of climate change scenarios.

Individual fungi species might have a bigger intrinsic tolerance to changing environments than isolated bacterial species, due to the larger regulatory potential of eucaryotic cells [12]. On the other hand, the faster reproductive cycles and greater genome flexibility causes bacteria to rapidly adapt to changes due to microevolutional processes, leading to their extensive diversity [13]. It can therefore be expected that changes could be reflected rapidly within microbiota communities of both kingdoms.

The interplay between local soil characteristics, vegetation, and soil-derived microorganisms is very complex to study [1]. At first sight, local conditions such as soil characteristics but also microclimates determine which vegetation will be able to grow and which associated microorganisms will appear within the ecosystem [14]. Nevertheless, many

studies have shown, that plants can considerably influence microclimates and microbial activity in the decomposition of organic matter are a major driver of change in the cycling of soil nutrients, pH, but also physical factors [15]. Therefore, it is not possible to establish simple causal connections but rather necessary to analyze mutual effects.

4.1.2 Function of microorganisms in soil

4.1.2.1 The role of bacteria

Edaphic bacteria are the most abundant and diverse group of organisms in soil and therefore have a multitude of different functions. They are the main drivers of organic matter decomposition and the recycling of nutrients. They are involved in the cycling of all major elements such as carbon, nitrogen, phosphorus, and sulfur, in both directions, fixation within organic matter as well as liberation in form of gases, some of which are mainly causing the greenhouse effect [16], and inorganic compounds which are easily assimilated by plant roots [14]. The interplay of bacteria involved in nitrogen cycling is of particular interest given their dominant function in the bacterial kingdom. Nitrifying bacteria are crucial for the availability of nitrogen for plant roots and therefore soil fertility, and denitrifying bacteria which liberate soils from excess nitrates but also liberate the potent greenhouse gas nitrous oxide (N_2O) are of central importance in the role of antropogenic access use of fertilizers and the destruction of the ozone layer [17].

Bacteria can further degrade many kinds of contaminants and pesticides and are therefore critical for conservation as well as restauration of ecosystems [18]. They greatly interfere with soil characteristics and structure and are therefore involved in filtration and retention of water which strongly shapes the type of vegetation growing on it. Bacteria can then in turn establish close relationships with the vegetation, mainly by root interaction which is crucial for plant development, growth, and the resistance to biotic and abiotic factors [15]. Taken together edaphic bacteria are essential for the development, maintenance, and restoration of the ecological and structural function of soil which shapes the landscapes on earth.

4.1.2.2 The role of fungi

At first sight there appears to be a great functional redundance between edaphic fungi and bacteria since both have a great potential to adapt to virtually every known environment prone to life and participate in similar ecological processes [19,20]. The alteration of fungal

communities has therefore the potential to affect the whole function of ecosystems similar to the case of bacteria [12,21].

Fungi can be classified into three main functional groups, namely biological controllers, ecosystem regulators and decomposing and matter transforming fungi [19]. They can secrete a wide array of enzymes useful in the breakdown of organic matter and the availability of soil nutrients or establish antagonistic or symbiotic interactions with other organisms mainly plants. Taking a closer look certain patterns of differential behavior of fungi compared to bacteria become noticeable. First as described in chapter 1, fungi are specialized on the breakdown of plant cell wall compounds such as polyphenols which is crucial to further enzymatic breakdown of sequestered organic material [22]. Fungi hyphae have the potential to infiltrate into compact organic matter and mechanically burst structures allowing the infiltration of specialized enzymes greatly accelerating the decomposition process especially of recalcitrant woody matter [12]. These same hyphae are further recognized as an essential network for efficient nutrient and water uptake favoring plant growth and stress and pathogen resistance in form of mycorrhiza [19,23]. They are also used to transmit signals to orchestrate an array of different ecological functions, including antagonistic as well as symbiotic interactions [24].

Moreover, fungi have 40-55% carbon use efficiency (CUE). They therefore store and recycle considerably more carbon compared to bacteria. Decrease in fungi abundance can hence negatively influence overall CUE in soil [25] which might be important in a climate change scenario.

4.1.2.3 Abiotic factors that influence microorganism growth

There are many different physical and chemical factors that affect microbiota composition. Microbial richness and abundance is most evidently correlated with temperature as many microorganisms are closely adapted to their local environment [22,26], pH [7] and humidity [10] but also the availability of nutrients, soil structure [27], salinity [28] the presence of heavy metals among other factors can considerably influence the establishment of the local soil microorganism community.

4.1.3 The taxonomical identification of microorganisms

4.1.3.1 Marker Genes and Barcodes

Marker genes in compositional analysis are specific regions within a genome, amplified to identify species based on only few gene sequences derived from a single gene [1]. In general terms these so-called barcodes must fulfill certain criteria in order to be reliable. First, they

should be present in all cells that form part of the community one wants to analyze. Second, sequences should be derived from a region within the gene which is sufficiently variable to discriminate between different species but also sufficiently conserved to allow for identification [29] (Figure 4.1 Marker gene selection criteria). Furthermore, this variable region should be flanked by highly conserved regions to allow for efficient priming in PCR amplification. Third, they should be reasonably well described as genes by the scientific community. The larger the available reference bases are, the more reliable identification will be and less sequences will drop out of analysis due to unknown origin [30,31].

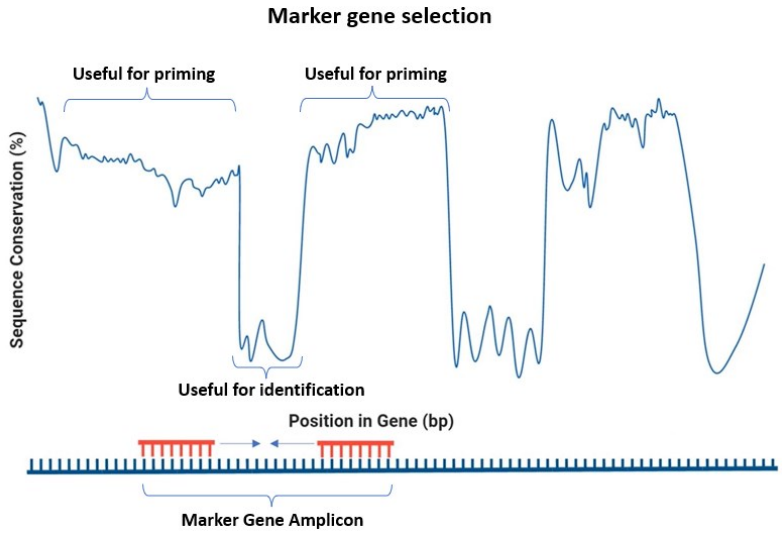

Figure 4.1 Marker gene selection criteria

A marker gene fragment should consist of a variable region that allows for identification, flanked by conserved regions that allow stable primer interaction. Image adapted from www.Zymogene.com

4.1.3.1.1 16S

The gene that encodes 16S ribosomal RNA in Archaea as well as Bacteria is by far the most commonly used marker gene to analyze bacterial community structure in ecological and evolutional studies [1]. It bears unique properties such as its presence in virtually every known bacterial and archaea species and extreme sequence conservation due to its vital importance for cells on one hand and an evolutionary variable domain structure on the other hand [32]. The frequent usage of the marker gene, in turn, led to the development of large genomic libraries where sequences can be aligned for taxonomic identification. This is important given that marker gene studies can only consider sequences from previously described species being one of the major drawbacks for their application. Recently, marker gene studies have been replaced by metagenomic high throughput shotgun sequencing due to the advances in technology. Nevertheless, the improvement of sequence specificity and open access informatic analyzing

tools such as QIIME made competitive marker gene studies available to a greater audience which gives the opportunity to investigate ecosystems in the whole world that would otherwise not be possible to analyze [30].

4.1.3.1.2 ITS

The most commonly used barcodes for fungi identification are called internal transcribed spacer (ITS) regions. Although the 18S gene for the eucaryotic small subunit of ribosomal RNA is also present in fungi it presents a low resolution for fungal identification. Several other marker genes like Cytochrome C, commonly used for animals, protein-coding marker regions and large ribosomal subunits (LSU) have been proposed in contrast but the single most universally applicable region remains ITS [29]. Today there is a vast collection of ITS sequences assigned to taxonomically identified species in the Unite v8.0 [33,34] data base, which was used for assignation in the present study.

4.1.3.1.3 OTUs vs ASVs

To estimate the microbial composition of a sample based on marker gene sequences it is necessary to taxonomically align sequences with international reference bases such as GreenGenes for bacteria [35] and Unite v8.0 for fungi [33]. Traditionally the way to organize these sequences was to cluster similar sequences up to a determined threshold (97% or 99% respectively) into operational taxonomic units (OTUs) [36,37]. The danger of this approach is that, if the threshold is to low, different species with high sequence similarity within the marker gene region can be falsely clustered together within a single OTU. On the other hand, when the chosen threshold is too high, PCR and sequence errors can lead to new sequences that can erroneously be considered as new OTUs [36].

A newer approach is the computation of amplicon sequence variants (ASVs) also called denoising methods. In this approach first all similar sequence reads are counted to identify rare sequences probably due to sequence errors. Algorithms of error modeling are then applied to identify the probability that a given sequence represents an exact copy of its origin. Therefore, ASVs represent exact sequences with a defined probability rather than artificially created consensus sequences within an OTU [36,37].

Species identification with ASVs is more reliable and data is easier to compare among different studies. In the present study the ASV approach was selected due to the probability to

find sequence variants due to the high endemism in the paramo ecosystem (see Chapter 1.4) and to their higher reliability with fungal sequences [38].

4.1.3.2 Bias of sequence counts

The study of microorganism abundance based on sequence counts is widely used approach to get more information about diversity. Nevertheless, its application bears several drawbacks compared to shotgun-sequencing that need to be discussed to handle information with care. First, many cells bear several copies of a gene and for many microorganisms this number is unknown. The program PICRUSt2 includes an algorithm to correct for the error, based on information about copy numbers from whole genome sequencing approaches. Present data is intended to be analyzed by this algorithm prior to publication [39]. Second, during PCR polymerase amplification new artificial sequences can be created due to reading and writing errors. Proof-read polymerases can reduce the number of errors but can also create chimera sequences, UCHIME as an implement of DADA2 removes sequences using an algorithm that can predict where sequence joining may appear due matching subregions of one or more ASVs and DADA2 assigns low reliability to unique sequences such as those appearing due to polymerase errors which leads to sequence filtering [40].

Another issue is the initial sampling load. Given the very small amount of DNA used for Illumina sequencing, minor pipetting errors can lead to considerable misinterpretation of abundance especially when compared to other samples. The use of relative abundance can help to mitigate the effect but has its own drawbacks, as discussed in section 97.

4.1.4 Diversity indices

4.1.4.1 Alpha diversity

Alpha diversity is considered as the species diversity within a defined population [41], in the present case the pooled soil samples as described in 4.2.1.

4.1.4.1.1 Richness

The count of the number of species found within a defined area seems to be a trivial indicator but still remains one of the most important aspects of diversity [42]. In microbial composition studies it becomes far more complex due to the problems arising with the widely discussed ecological concept of species in microorganisms (especially bacteria) but also due to

the complex estimation of real species counts based on marker gene sequences, as previously discussed. Unassigned sequences of species which have not yet been described or due to artifacts in the sequencing process further complicate the task. Still, the most important drawback of richness to estimate diversity or even community structure is its vulnerability to rare species which can greatly enhance apparent diversity without major ecological significance. Therefore, it is useful only together with more advanced indices which consider abundance as well.

4.1.4.1.2 Shannon index

The Shannon index or Shannon-Wiener index is the most widely used diversity index since its development in 1948 when it was initially used as a measurement of entropy [43] and was adapted to ecology as a measure of uncertainty to predict a certain species picked out of a random population. Therefore, the lower the number, the higher the predictive uncertainty and hence the biodiversity. The advantage of the index is, that it considers both, species richness and abundance for the calculation but when there is one very dominant species even in the presence of several rare species, it tends to underestimate diversity because the index tends towards 0 [44].

The index is calculated according to the following formula:

$$H' = -\sum_{i=1}^{R} p_i \ln p_i$$

where p_i is the proportional abundance of each species respective to the total of species and R is the specific richness

4.1.4.1.3 Pielou index

The Pielou index is a measure of evenness, meaning how equally distributed are species in the analyzed population. The calculation is based on the Shannon index but deals with the problem that Shannon tends to overweight rare species and singletons. Its values vary from 0 to 1. The closer the value is to 1 the more equally distributed are all analyzed species in the given area.

The index is calculated according to the following formula:

$$J' = \frac{H'}{H'_{\max}}$$

With "H'_{max} = ln S" and S is the number of species for each taxonomical level [45].

4.1.4.2 Beta diversity

Beta diversity measures represent the differential analysis of diversity between different populations to discriminate local from regional effects [41].

4.1.4.2.1 Jaccard index

The Jaccard index is a measurement for the similarity between two data sets. It is a qualitative measurement that takes only richness into account.

It is calculated using the following formula:

I_J = c / (a + b + c)

Where:
a is the number of species present in site A
b is the number of species present in site B
c is the number of species present in both sites

its values range from 0 to 1. If both sites share all species the value is 0, if both sides do not share a single species the value is 1 [46].
Given values of Jaccard can be used in a distance matrix to determine how similar a set of sampling sites are in terms of richness.

4.1.4.2.2 Bray-Curtis dissimilarity

The Bray-Curtis dissimilarity compares the abundance of species between two samples It ranges from 0 to 1.
If the calculated value is 0, then both sites have the same composition.
If the calculated value is 1, then both sides do not share a single species.

It is calculated using the following formula:

$$BC_{ij} = 1 - \frac{2C_{ij}}{S_i + S_j}$$

Where:

BC$_{ij}$ is the sum of the least abundant commonly shared species among both samples

Si is the sum of all individuals counted in site i

Sj is the sum of all individuals counted in site j

4.1.5 Objective

The present chapter aims to describe the bacterial and fungal composition on an altitudinal gradient in the northern paramo region of Ecuador in the dry and rainy seasons, in contrast to the enzyme activity measurement described in chapter 3.

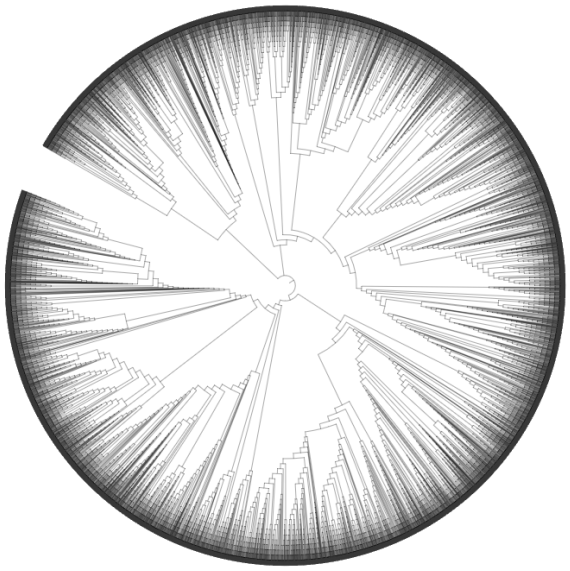

Figure 4.2. Cladogram of representative ASVs found in the analyzed soil samples. Image extracted from Qiime2 fasttree2

4.2 Materials and Methods

4.2.1 Sample collection and genomic DNA extraction

Samples were collected at four different altitudes (3600-4200 m) and as described in Chapter 3.2.1at two different seasons. Soil samples at 10 cm depth from the formerly described three replication sites (Figure 2.2 Sampling sites) and from each altitude were taken with sterilized collection tubes and transported at 4°C to the laboratory. Samples from all three replication sites were mixed under sterile conditions to create a pool. Three different soil samples from each pool, giving a total of 24 samples, were used to isolate genomic DNA applying the standard protocol of the SurePrep genomic DNA Kit (Fisher BioReagents, SL, USA). DNA was quantified on a NanoDrop 2000 (Thermo Fisher Scientific, SL, USA).

4.2.2 Amplification and Sequencing to get raw data

The MACROGEN (South Korea) 16S and ITS amplification and sequencing service was used to receive sequencing raw data, applying primer pairs for the regions targeting 16S (V3-V4) (Bakt_341F:CCTACGGGNGGCWGCAG and Bakt_805R: GACTACHVGGGTATCTAATCC) for bacteria and archaebacteria and targeting ITS2 region (ITS3 : GCATCGATGAAGAACGCAGC and ITS4 : TCCTCCGCTTATTGATATGC) for fungi, on an Illumina platform : Sequencing on Miseq 300bp paired-end, 100K reads per library using the Herculase II Fusion DNA Polymerase Nextera XT Index Kit V2 (Illumina, CA, USA) (Figure 4.3 Workflow Macrogen).

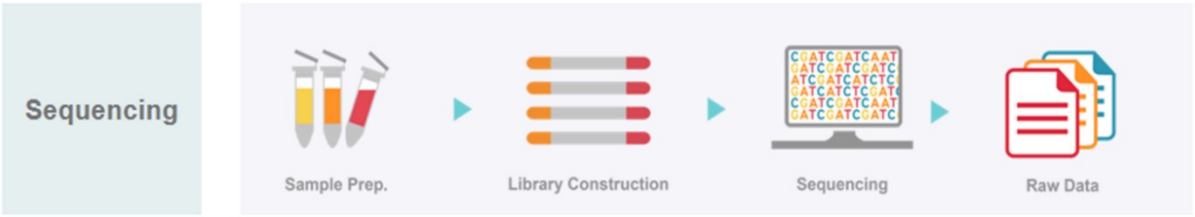

Figure 4.3 Workflow Macrogen
Steps performed to obtain Raw Data from prepared gDNA samples

4.2.3 Raw data preparation

The raw data was processed applying QIIME 2 (2021.8) software packages [31] as follows: The plugin cutadapt [47] was used to remove adapter sequences from multiplexed paired-end reads. Sequences were than quality filtered, dereplicated, amplicon errors were

corrected, reads were checked for chimera sequences and paired-end reads were merged, applying the Divisive Amplicon Denoising Algorithm 2 (DADA2) [40]. Resulting amplicon sequence versions were taxonomically classified using the q2-feature-classifier plugin [30] by comparison with annotated reference sequence databases Greengenes 13_8 99% for bacteria and archaebacteria [35] and UNITE v8.0 99% for fungi [33], aligned with MAFFT [48] and applied to phylogenetic analysis using q2-fasttree2 [49] (APPX 4.1)

4.2.4 Analysis of processed data

Taxonomic information was then reduced to the phylum, family and genus level using the plugin q2-taxacolapse [50]. Information on species level was not processed due to higher reliability of results on genus level based on a single marker gene. Richness, Shannon index [43] for diversity, Pielou index for evenness, Bray-Courtis- and Jaccard-distance matrices were obtained from the alpha-diversity metrics package q2-diversity separated by altitude and season. The Qiime2-emperor package was used to visualize PCoA results [51]. Heatmaps were established with the Qiime2-heatmap plugin [52]. (APPX 4.2)

4.2.5 Statistical analysis and graphical visualization

All data analysis was performed using Microsoft EXCEL 365 and the licensed version of STATA 16.0. The Shapiro Wilk Test was performed to analyze Normal distribution of data and Levene's Test for homoscedasticity. ANOVA was performed for altitude, independent t-test for depth and paired t-test for season. In case data did not fulfill assumptions for parametric analysis after natural log transformation, non-parametric test such as Kruskal-Wallis, Wilcoxon ranked sum and Wilcoxon signed rank test were applied.

4.3 Results

The sequencing of samples with paired-end 100k reads illumina sequencing (301 read length) resulted in 48 samples divided into 24 16S amplicons and 24 ITS amplicons each with 12 amplicons for rainy and dry season. Raw data statistics indicate an average of 50-60 million Total read bases (bp) and total reads between 175,000 and 220,000 with a phred Quality score around 94% of bases with 99% base call accuracy and 86-88% with 99.9% base call accuracy (APPX 4.3). These statistics indicate a high comparability of raw data outcomes between the two sampling periods and high sample and library quality.

After quality filtering and database cleanup a total of 13,245 amplicon sequence variants (ASVs) for 24 16S samples within a total of 1,183,725 valid reads and 5973 ASVs for 24 ITS samples within a total of 2,165,524 reads were found.

Taxonomical classification revealed that Archaea were present at an abundance of only 0.03% in a single phylum in the analyzed samples meanwhile alpha diversity analysis for bacteria indicated an average of 34 Phyla, 263 families and 378 genera of bacteria and an average of 14 phyla, 123 families and 154 genera of fungi.

To avoid bias by sequencing effort which often correlates with observed richness, rarefaction curves were established to analyze whether the used sampling depth was sufficient to comprehensively represent the true microbial community. Rarefaction for both 16S and ITS samples was based on either observed ASVs (Figure 4.4 Rarefaction curves for 16S samples a and Figure 4.5 Rarefaction curves for ITS samples a) or the Shannon index (Figure 4.4 Rarefaction curves for 16S samples b and Figure 4.5 Rarefaction curves for ITS samplesb) of the random subsample. All analyzed samples considering both 16S and ITS showed the tendency to level off early before reaching the final sequencing depth, indicating that further sampling effort or sampling depth would not have resulted in greater richness.

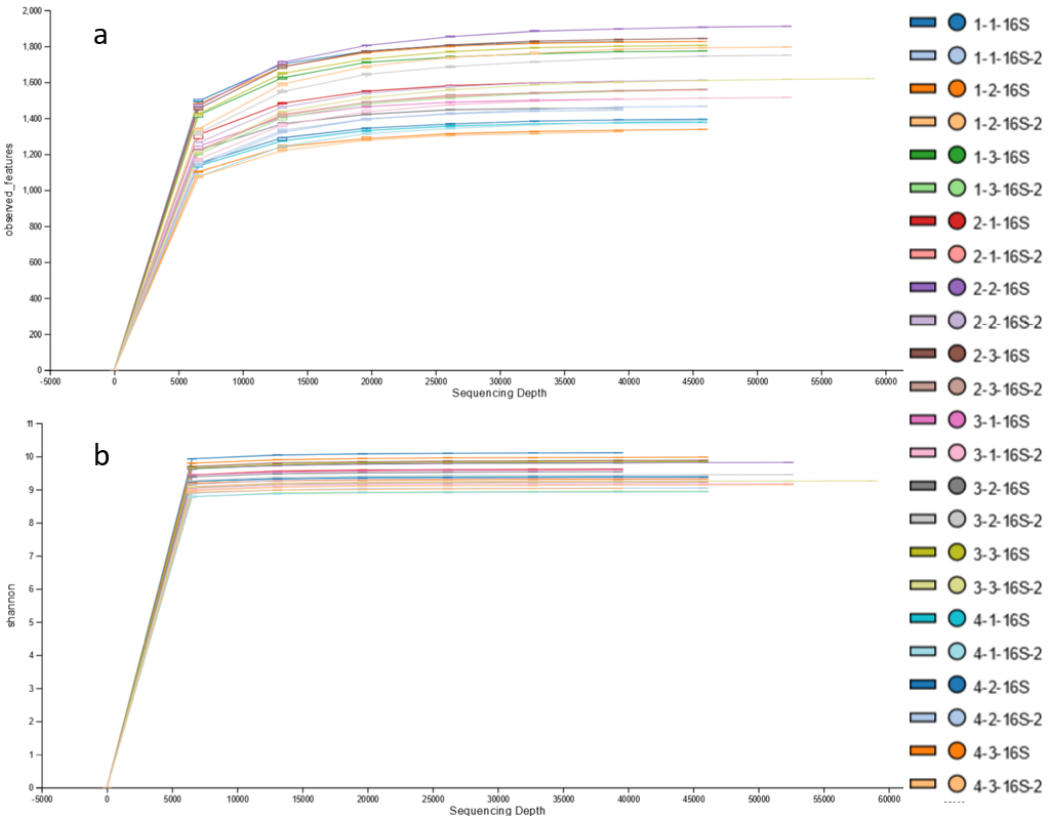

Figure 4.4 Rarefaction curves for 16S samples

Sequencing depth in the x-axis is contrasted to a) observed ASVs and b) Shannon indices on the y-axis

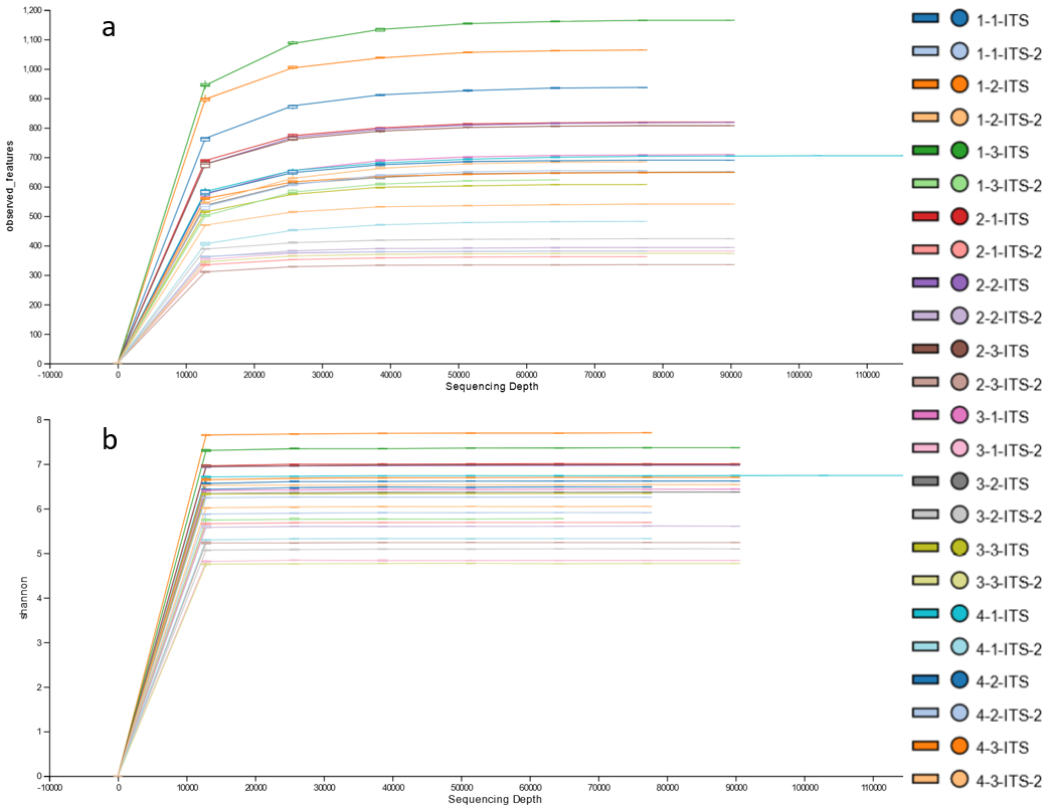

Figure 4.5 Rarefaction curves for ITS samples
Sequencing depth in the x-axis is contrasted to a) observed ASVs and b) Shannon indices on the y-axis

Then differential analysis by altitude and season was applied to compare the microbiota composition at the taxonomical level phylum, family and genus. The results in Table 4.1 Altitudinal and seasonal changes of bacterial diversity indices for bacterial sequences indicated that species richness represented by observed ASVs gradually declined with rising altitude giving the most significant results especially between altitude 1 and altitude 4. Although there is a consistent decline in diversity indicated by Shannon index with rising altitude results only revealed statistical significance at the phylum level. Apparently, the evenness of bacteria species distribution is not affected by altitude as there were no observable differences in the Pielou-Index.

Interestingly for 16S bacterial sequences there were no statistically significant changes among the dry and the rainy season at phylum level and differences in richness stayed insignificant at family and genus level. Nevertheless, the Shannon and Pielou index behaved differently at family and genus level, indicating significant higher diversity in rainy season compared to dry season (smaller Shannon value) and the Pielou index for evenness is

significantly going down, showing less evenly distributed bacterial communities in rainy season.

Table 4.1 Altitudinal and seasonal changes of bacterial diversity indices

		level 2 = Phylum						level 5 = Family						level 6 = Genus					
16S = bacteria		OTUs		Shannon		Pielou		OTUs		Shannon		Pielou		OTUs		Shannon		Pielou	
		Mean	SD	Mean	SD	Mean	SD	Mean	SD	Mean	SD	Mean	SD	Mean	SD	Mean	SD	Mean	SD
Altitude n = 24	1	36 ± 2	a	3.00 ± 0.06	a	0.58 ± 0.02	a	285 ± 20	a	6.12 ± 0.25	a	0.75 ± 0.03	a	418 ± 31	a	6.72 ± 0.22	a	0.77 ±	0.03 a
	2	34 ± 1	ab	2.96 ± 0.04	ab	0.58 ± 0.01	a	272 ± 17	a	6.03 ± 0.22	a	0.75 ± 0.02	a	393 ± 24	ab	6.59 ± 0.16	a	0.76 ±	0.01 a
	3	34 ± 2	a	2.96 ± 0.06	a	0.58 ± 0.02	a	256 ± 14	ab	6.00 ± 0.18	a	0.75 ± 0.02	a	361 ± 22	bc	6.51 ± 0.09	a	0.77 ±	0.01 a
	4	31 ± 1	b	2.83 ± 0.07	b	0.57 ± 0.02	a	238 ± 9	b	5.89 ± 0.07	a	0.75 ± 0.01	a	340 ± 12	c	6.48 ± 0.04	a	0.77 ±	0.01 a
Season n= 24	dry	34 ± 2	a	2.94 ± 0.09	a	0.58 ± 0.01	a	266 ± 19	a	6.16 ± 0.15	a	0.77 ± 0.01	a	374 ± 34	a	6.66 ± 0.19	a	0.78 ±	0.01 a
	rainy	34 ± 2	a	2.94 ± 0.08	a	0.58 ± 0.01	a	259 ± 27	a	5.85 ± 0.07	b	0.73 ± 0.01	b	382 ± 41	a	6.49 ± 0.08	b	0.76 ±	0.01 b

Results are presented as mean +/- standard deviation. Values that do not share the same assigned letter, indicate statistically significant results between groups ($p<0.05$)

Results for the differential analysis of fungal indices revealed a similar tendency as in bacteria (Table 4.2 Altitudinal and seasonal changes of fungi diversity indices) with declining species richness towards higher elevations. Nevertheless, there is a rather sudden decrease between altitude 1 (3600m) and altitude 2 (3800 m) and to a lesser degree between altitude 2 and altitude 3 (4000 m) leading to statistically significant differences at family and genus level. The Shannon index is also highest for the first altitude but fails to show statistically significant differences except for the phylum level. Again, evenness seems to be quite homogenous among altitudes.

Analyzing seasonal effects revealed that fungal communities apparently tend to react stronger to these changes. Although on phylum level only the Shannon index showed significantly greater diversity in rainy season, on family and genus level all indices indicated significant differences between seasons. Meanwhile the diversity increased with rainy season, the evenness tended to decrease as indicated by lower Pielou indices.

Table 4.2 Altitudinal and seasonal changes of fungi diversity indices

		level 2 = Phylum						level 5 = Family						level 6 = Genus					
ITS = fungi		OTUs		Shannon		Pielou		OTUs		Shannon		Pielou		OTUs		Shannon		Pielou	
		Mean	SD	Mean	SD	Mean	SD	Mean	SD	Mean	SD	Mean	SD	Mean	SD	Mean	SD	Mean	SD
Altitude n = 24	1	15 ± 1	ab	2.31 ± 0.17	a	0.60 ± 0.04	a	157 ± 15	a	4.42 ± 0.37	a	0.61 ± 0.04	a	198 ± 24	a	4.76 ± 0.36	a	0.62 ±	0.04 a
	2	14 ± 2	ab	1.96 ± 0.16	ab	0.52 ± 0.04	ab	116 ± 28	b	4.20 ± 0.48	a	0.61 ± 0.04	a	145 ± 39	ab	4.48 ± 0.51	a	0.63 ±	0.04 a
	3	13 ± 1	a	1.88 ± 0.28	b	0.50 ± 0.07	ab	110 ± 10	b	3.87 ± 0.38	a	0.57 ± 0.05	a	139 ± 12	b	4.23 ± 0.27	a	0.59 ±	0.03 a
	4	15 ± 1	b	1.75 ± 0.20	b	0.44 ± 0.05	b	110 ± 15	b	4.23 ± 0.29	a	0.63 ± 0.04	a	135 ± 18	b	4.55 ± 0.29	a	0.64 ±	0.04 a
Season n= 24	dry (1)	15 ± 1	a	2.09 ± 0.19	a	0.54 ± 0.06	a	137 ± 22	a	4.47 ± 0.25	a	0.63 ± 0.02	a	173 ± 31	a	4.77 ± 0.28	a	0.64 ±	0.02 a
	rainy (2)	14 ± 2	a	1.86 ± 0.33	b	0.49 ± 0.08	a	110 ± 24	b	3.89 ± 0.33	b	0.58 ± 0.04	b	135 ± 29	b	4.24 ± 0.31	b	0.60 ±	0.04 b

Results are presented as mean +/- standard deviation. Values that do not share the same assigned letter, indicate statistically significant results between groups ($p<0.05$)

Taken together, meanwhile rising altitude tends to significantly decrease bacterial as well as fungal richness, the overall effect on diversity and evenness is less important. Interestingly the seasonal effect appears to be the opposite for bacteria were richness stayed

almost the same but indices for diversity and evenness changed. At this point fungal communities revealed differences to bacterial communities where all three analyzed indices were significantly affected by season.

To visualize compositional differences of microbiota between different altitudes at two seasons, PCoA analysis for 16S and ITS data was performed and visualized with biplots (Figure 4.6 PCoA analysis for 16S) The Jaccard distance matrix was chosen to show differences between species richness and the Bray-Curtis dissimilarity to also consider the abundance of species.

Again, the plots for 16S bacterial sequences indicate that sequence repetitions are grouping clearly together as a result of the pool that was established. The differences between altitudes are gradual and the observed Jaccard distances are almost equidistant considering species richness. Furthermore, there is a clear separation between samples of the dry compared to samples of the rainy season showing the greatest difference among samples from the same site at altitude 1. The greatest similarity can be observed for samples of the dry season between altitude 2 and 3. This finding is supported by the Bray-Curtis dissimilarity which indicates a very similar behavior. Again, the greatest difference between seasons can be seen for samples of altitude 1 and again altitude 2 and 3 are grouping closer together.

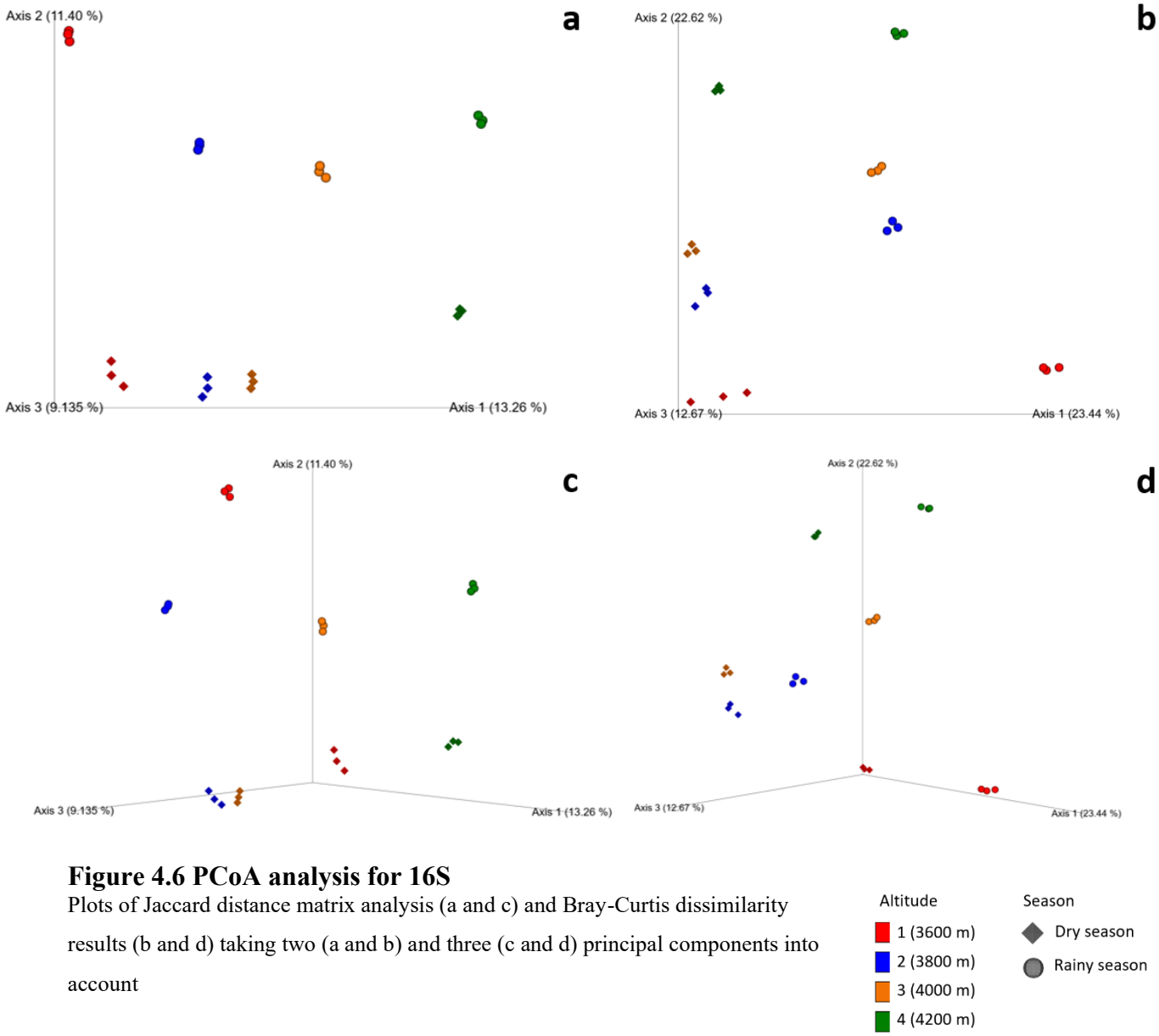

Figure 4.6 PCoA analysis for 16S

Plots of Jaccard distance matrix analysis (a and c) and Bray-Curtis dissimilarity results (b and d) taking two (a and b) and three (c and d) principal components into account

Beta-diversity biplots for ITS reveal a slightly different picture. Although there is also a clearly gradual difference for altitudes 2, 3 and 4, altitude 1 falls out of line and shows stronger differences to the rest, considering the Jaccard distance matrix for species richness in the 2D plot. Like in bacteria there is a notable difference between seasons, but it is less pronounced for fungi compared to bacteria.

The biggest difference can be observed in the Bray-Curtis three dimensional plot were the gradual difference is lost due to the sample of altitude one grouping suddenly between samples of altitude 2 and 3. Samples of altitude 4 seem to present the greatest distance to the rest of samples.

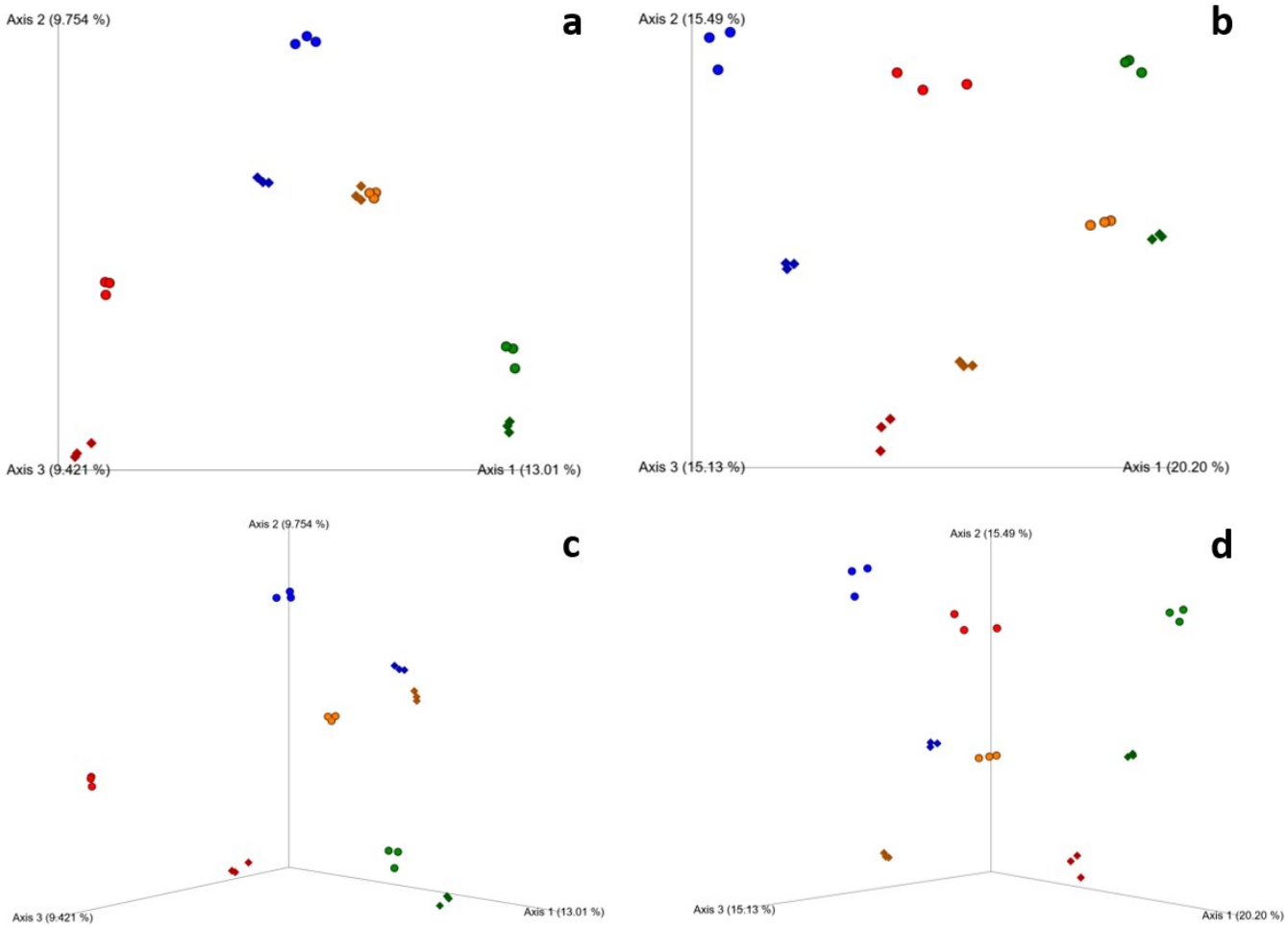

Figure 4.7 PCoA analysis for ITS
Plots of Jaccard distance matrix analysis (a and c) and Bray-Curtis dissimilarity results (b and d) taking two (a and b) and three components into account (c and d)

Out of 46 detected bacterial phyla, 13 phyla showed relative abundance of more than 1% at different altitudes and seasons (Figure 4.8 Relative abundance of bacteria phyla). In all analyzed samples the most abundant phylum was Acidobacteriota with over 30% of total abundance and Actinobacteriota around 20% of total abundance leading to the fact that half of the total abundance of observed bacterial phyla are represented by only two phyla. These were followed by Bacteroidota and Bdellovibrionota as third and fourth most abundant phyla, being the first altitude in rainy season the only exception were numbers of Bacteroidota were superior to Actinobacteriota. There were relatively minor changes among the mentioned phyla with altitude and season. The most prominent changes among samples were visible at the less prominent phyla. Chloroflexi, for instance, is more abundant in dry season at higher elevations

meanwhile in rainy season it is generally less abundant with exception of altitude 2. Firmicutes were heterogeneously distributed among altitudes but almost twice as abundant in rainy season. Similarly, Latescibacterota were less abundant in dry season, close to the 1% threshold at each altitude but populations increased considerably with rainy season up to 10.8% at altitude 3 being 10 times mora abundant than in dry season. It is also worthy to mention that this population growth was most prominent at altitude 1 and 3 being altitude 2 rather like altitude 4, indicating that microbial composition is not always gradual on altitudinal levels.

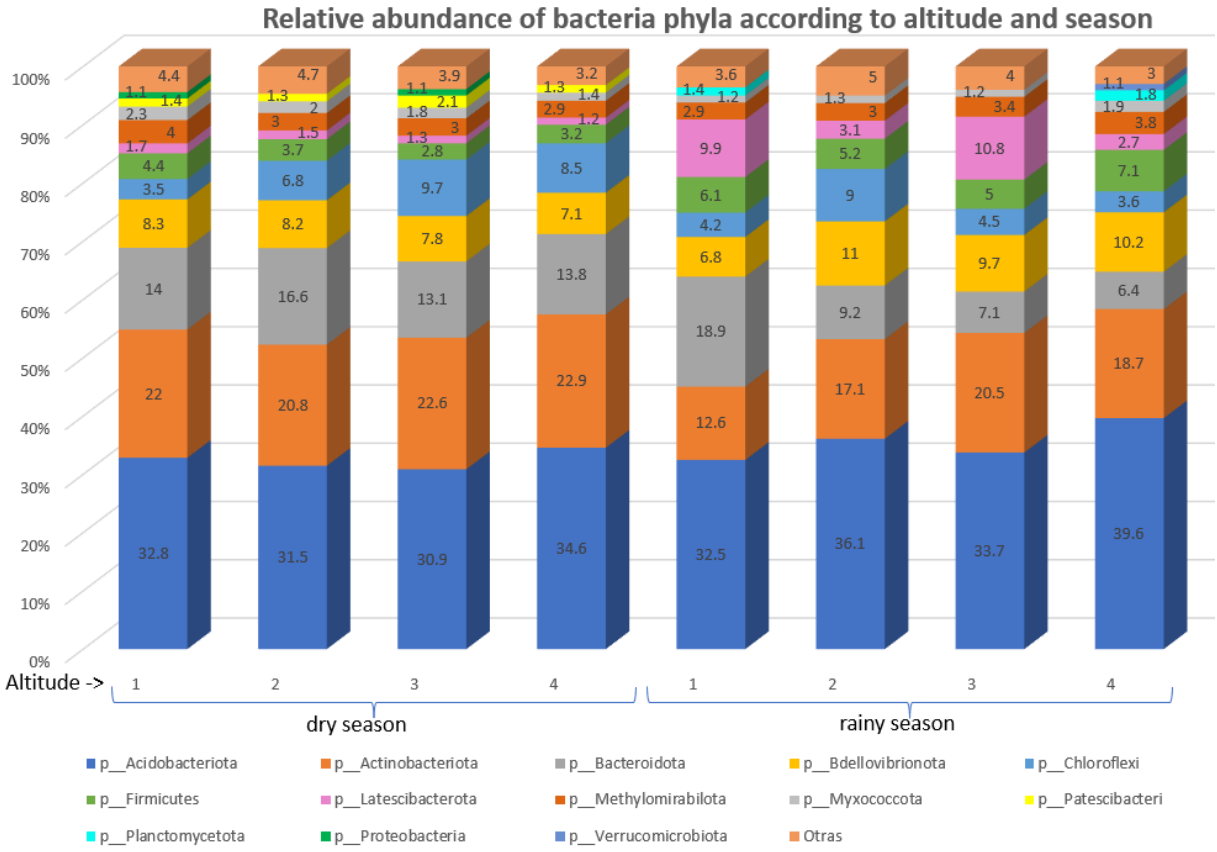

Figure 4.8 Relative abundance of bacteria phyla
Only phyla with at least 1% relative abundance are represented

Finally, several phyla appeared or disappeared according to season. Patescibacteri for example were present in all dry season samples but did not play a role in rainy season. Similarly, proteobacteriota were only present in abundance above 1% on altitude 1 and 3 in dry season but absent in rainy season. On the other hand, planctomycetota were only detected at higher levels in rainy season at altitudes 1 and 4. Verrucomicrobiota at last was only abundant in rainy season at altitude 4. It is important to mention that the established threshold of 1% causes phyla close to 1% of abundance to drop out if they are only slightly different in abundance which is for example the case for Planctomycetota in rainy season. Nevertheless, raw data indicates that

the observed differences in phyla between rainy and dry season were meaningful. Furthermore, the remaining phyla below 1% (including those which were not assignable) together represented an abundance of only 3-4.7 % which supports the present findings.

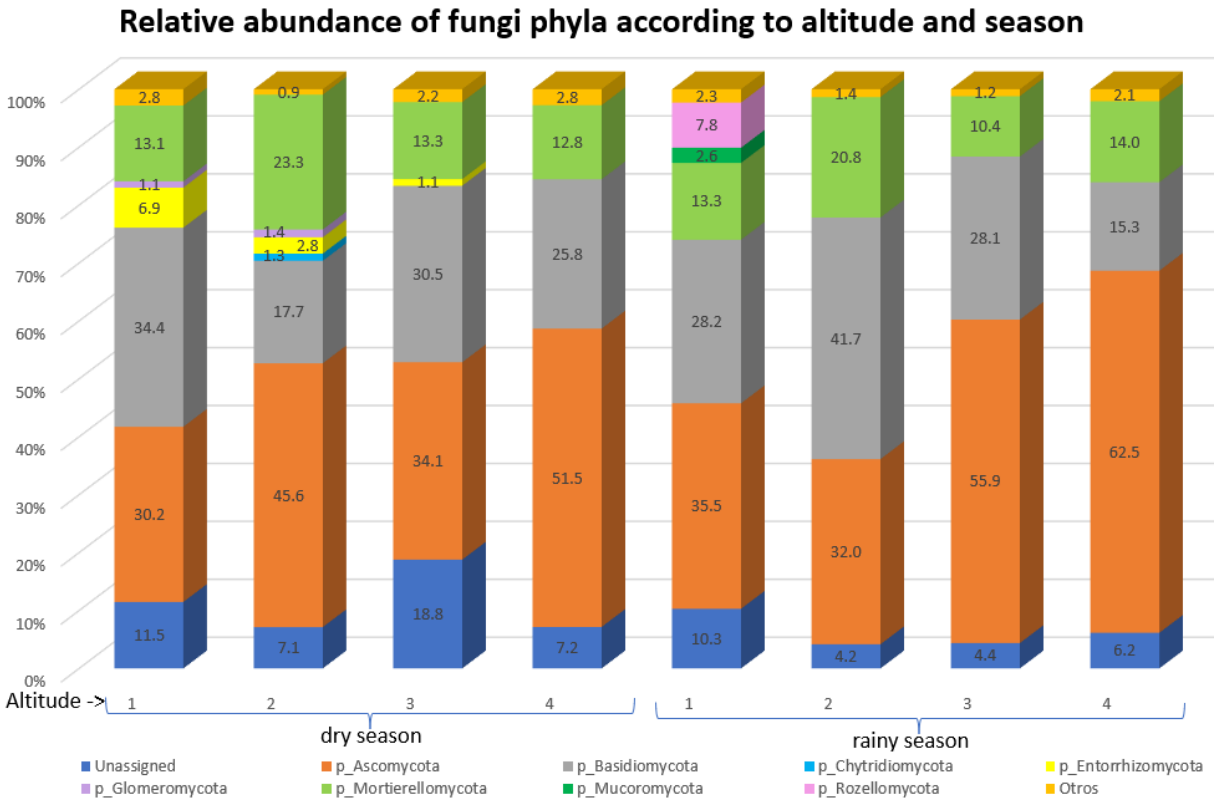

Figure 4.9 Relative abundance of fungi phyla
Only phyla with at least 1% relative abundance are represented

Out of 18 detected fungal phyla, only 8 phyla showed relative abundance of more than 1% at different altitudes and seasons (Figure 4.9 Relative abundance of fungi phyla). At simple sight it is notable that phyla were more diverse at the altitudes 1 and 2 compared to altitudes 3 and 4 where the total abundance over 1% was represented by only 3 phyla indicating their considerable dominance in the paramo ecosystem and their capability to adapt to harsh environmental conditions. In all analyzed samples the most abundant phylum was Ascomycota followed by Basidiomycota which are generally the most prominent phyla in fungal analysis. Interesting is only the fact that in direct relation Basidiomycota were more abundant only at altitude 1 in dry season and even stronger in rainy season at altitude 2. It is further noteworthy that Ascomycota constitute over 50 % of all found fungi in dry season at altitude 4 and in rainy season at altitude 3 and 4 being by far the most dominant phylum. Again, for Basidiomycota, altitude 2 showed differential behavior compared to altitude 1 and 3 which were more

comparable, a similar effect as observed with Latescibacterota in bacteria. The third most abundant phylum and the last one which was present in all analyzed samples is Mortierellomycota which tended to be most present at altitude 2 with more than 20% of abundance independent of seasonal effects.

Just like in bacteria the appearance of some phyla greatly depended on the season and also similar, these changes were more prominent in altitude 1 and 2. Therefore, the phylum Entorrhizomycota showed abundance over 1% only in dry season from altitude 1 to 3, identical to Glomeromycota at altitude 1 and 2. Chytridiomycota was only present in dry season at altitude 2 where raw data indicated its presence also at altitude one well below the 1% threshold indicating generally greater diversity of phyla in dry season. However, in rainy season there were other phyla more prominent than in dry season. Rocellomycota only appears in the lowest elevation and only in rainy season with a surprisingly high value. Very similar behavior shows Mucoromycota which is also shows meaningful abundance only in rainy season at altitude 1.

Finally, it is important to mention that in fungal classification a considerable amount of sequences failed to be clearly assigned to their taxonomical unit, which shows the greater interest in bacterial studies were data availability is better.

Given that there were very view fungi phyla within the threshold abundance, analysis was amplified to the next taxonomical level of classes. On this level appearance of dominant classes is more difficult to assign. Constantly high levels of abundance, around 10%, are only shown by Lecanoromycetes and Mortierellomycetes, followed by Agaricomycetes which are the most abundant fungal class at altitude 1 and 3 in dry season and especially at altitude 2 in rainy season but play a minor role in altitudes 3 and 4 in rainy season. Also quite abundant are Dothideomycetes although their presence is more abundant in dry season and Saccharomycetes which interestingly shows greatest abundance in rainy season at altitude 4.

It is notable that some fungal classes appear to be sensitive to altitudinal and seasonal changes, like Entorrhizomycetes that are only abundant in dry season and clearly decline with altitude or Ascomycota which show the opposite effect being abundant only in altitude 3 and 4. Orbiliomycetes only appears in rainy season at elevation 1 but in greater abundance. In contrast some classes of fungi seem to specialize on certain altitudinal levels such as Geminibasidiomycetes which are only present in altitude 3 with greater abundance in rainy season. Other fungal classes finally are difficult to discriminate by altitudinal or seasonal effects. Tremellomycetes for instance show a general considerable abundance at each altitude and in both seasons but without presenting a logical pattern in their distribution.

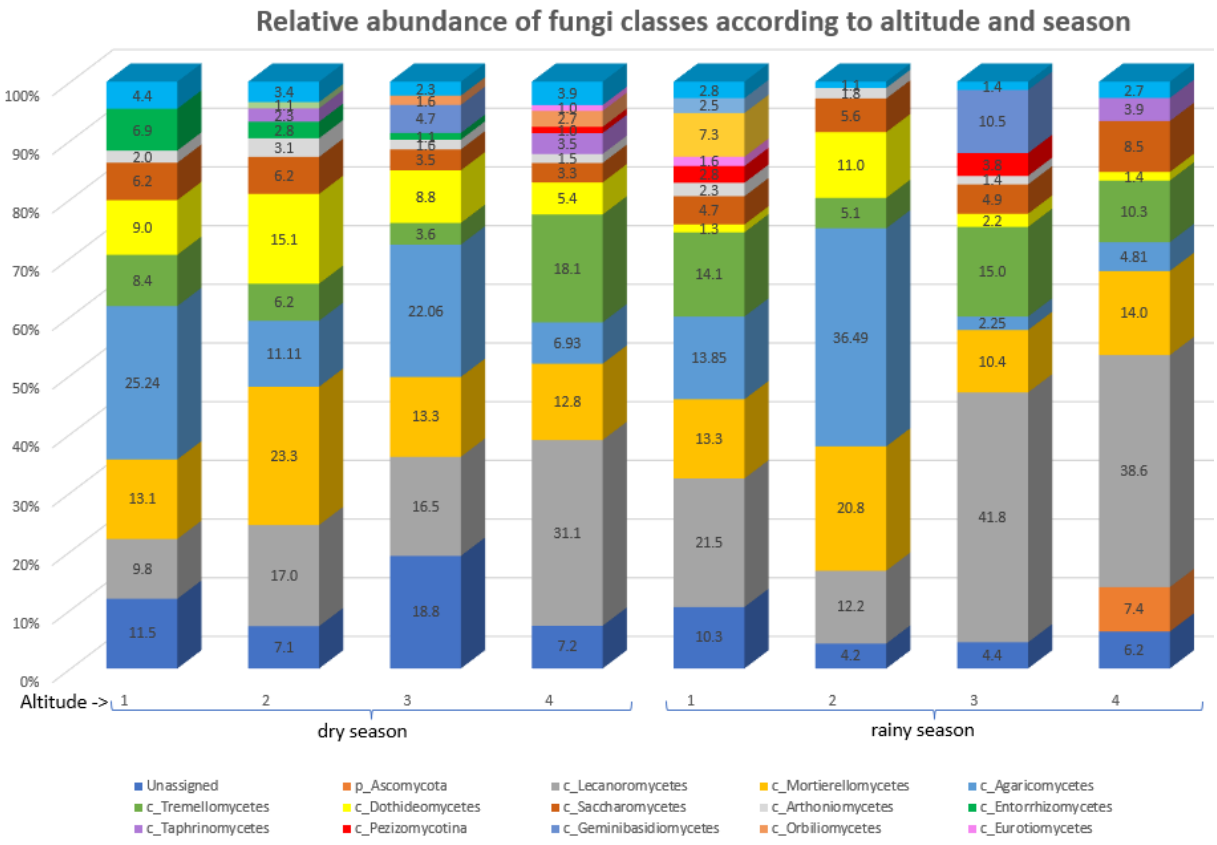

Figure 4.10 Relative abundance of fungi classes
Only phyla with at least 1% relative abundance are represented

Taken together observable patterns on higher taxonomical levels become difficult to interpret on lower levels when microbiota composition becomes increasingly complex. It is also worthy to mention that the interpretation of relative abundancies have to be interpreted with care given that, if a certain abundance of one taxonomical level goes down, all other fractions relative to it tend to go up. For example in Figure 4.10 Relative abundance of fungi classes the sudden appearance of 10.5% Geminibasidiomycetes which was not present in other samples of rainy season causes a relative downshift of all other related classes. This effect can lead to misinterpretations of data.

To compare the real abundance among all samples, show the absence of certain phyla in samples and also reveal phylogenetic relation among different phyla a heatmap analysis will be performed. (APPX 4.4)

4.4 Discussion

Initial alpha-diversity analysis revealed a trend of decreasing diversity with altitude. Although statistically significant differences for richness and diversity indices of bacteria as

well as fungi where most noticeable between the lowest and highest elevation and rather on higher taxonomical levels it follows a trend of previously reported studies were diversity indices tend to decrease, although the relationship is not always linear [4,26].

Especially in the case of fungal richness and diversity there is a drastic statistically significant decrease ($p<0,001$) between altitude 1 and 2, ~8-times bigger than those between the following altitudes. The difference becomes most recognizable at family and genus level. This fact is particularly interesting in direct comparison to enzyme activities, analyzed in chapter 3 where the same trend is clearly observed. For bacteria the decrease of indices on the same level are not significant. Here the most prominent difference is observed between elevation 3 and 4. Again, this was the second biggest difference observed for enzyme activity. Or from a different point of view, the marginal differences between elevation 2 and 3 in contrast to the elevations 1 and 4, for fungi as well as bacteria, reflect the same behavior of enzyme activity in organic matter decomposition for most analyzed enzymes indicating a direct relationship. Further statistical analysis is necessary to deeper analyze this association. Worthy to mention, that compositional diversity does not necessarily reflect functional diversity. It would be most interesting to see whether predicted functional diversity of the main decomposing species shows the same relationship with enzyme activity.

Furthermore, altitude does not reflect the only connection between microbial biodiversity and enzyme activity. Looking at the differential results for season related diversity, although in case of bacteria there is no statistically significant difference, the picture for fungi is quite the opposite. At family and genus level all diversity indices were statistically significant indicating a notably greater diversity and a more homogenous distribution in dry season compared to rainy season. On one hand, this is quite surprising considering that fungal diversity is usually positively correlated to humidity [53]. On the other hand, the water retention capacity of paramo soils causes that even in dry season soils remain humid but the sinking water table depth allows for greater oxygen penetration [9] which favors aerobic microbes which are more frequent among fungi than bacteria [12]. Furthermore, this penetration activates phenol-oxidases commonly expressed among several fungi species [22,54] which play a key role in the breakdown of phenolic substances, responsible for the concept of the enzyme latch released on hydrolase activity [55]. Again, the same pattern appears, that with greater fungal diversity the activity of enzymes increases.

Taken together the present results lead to the suggestion that the observed threshold at the frontier between the paramo and downslope ecosystems is rather dependent on fungal than bacterial diversity as fungal diversity shows the same trends as enzyme activity on an altitudinal

scale as well as upon seasonal differentiation. Bacterial diversity in turn might play a bigger role in the decrease at the superparamo which reflects the highest analyzed elevation of the paramo ecosystem.

The beforementioned observations are mostly supported by the PCoA analysis of beta-diversity indices. Samples of altitude 2 and 3 are clearly grouping together both, in case of bacteria and fungi, when considering the Jaccard distance matrix which only considers richness. The only exception is the ITS Bray-Curtis analysis where samples of altitude 1 almost locate between altitude 2 and 3. Again, the most distant group of samples reflects altitude 1, followed by altitude 4 which is coherent with diversity index analysis.

Nevertheless, considering seasonal effects in PCoA analysis differences for bacterial composition seem to be bigger for bacteria rather than fungi which is contradictive to the diversity index results. The difference might be explained when we recognize that PCoA analysis considers both, separation by altitude and season at a time. The overall mean for all analyzed altitudes at once compared between the dry and rainy season might mask the differences taken for each altitude. Another interesting fact is that now it becomes visible at which altitude seasonal differences are biggest. In both bacteria and fungi these can be observed for altitude 1 which is again coherent with the enzyme activity results and supports the idea of an existing tipping point between paramo ecosystem and downslope ecosystems.

Taxa-Barplot analysis revealed that Acidobacteriota and Actinobacteriota together represent around 50% of total bacterial abundance. Both phyla have been frequently reported to be among the most prominent in soil sample analysis. As the name tells, they are tolerant to low pH like those found in wetland soils due to the abundance of humic acids and other organic acids of anaerobic metabolism and together with Verrucomicrobia are a marker phylum for oligotrophic metabolism [9,56,57].

Interestingly a study performed in the permafrost region of Canada showed a similar tendency in analyzed wetland probes where Acidobacteriota and Actinobacteriota were also the most abundant bacterial phyla. This finding could further underline the relative comparability of the high Andean Paramo peatland with high northerly located peatlands.

The meaning of Acidobacteriota abundance to infer ecological function is difficult given that most species belonging to the phylum constantly fail to be cultivated for further studies [57]. The most abundant phylum in the studied samples happens to be the least understood among the highly abundant soil phyla [58]. What is known is that they belong to the “keystone bacterial taxa” for carbon turnover in the decomposition of organic matter [59]. Nevertheless,

the fact that abundance levels barely vary among different altitudinal levels and even between seasons leads to the suggestion that they are not the driving factor of differential decomposition due to changing environmental conditions in the present study.

Another interesting aspect is that Acidobacteria seem to be more abundant in natural wetlands than those with high intervention or artificial origin [60] which fits to the good conservational state of the chosen study site and the forementioned comparable site in Canada [61].

Actinobacteriota have also been described to play an important role in organic matter decomposition [60]. Again, there is little variation with altitudinal levels but apparently, they are relatively less abundant in rainy season at lower elevations which might account to some degree for the lower enzyme activity in the rainy season as described in chapter 3. This finding is also consistent with the phylum of bacteroidota also frequently described as abundant in soil samples and known for the secretion of polyglucan decomposing enzymes [62]. Functional analysis could further reveal to which degree these observations might explain the observed variation.

Another remarkable finding is, that most studies report Proteobacteriota to be the most abundant bacterial soil phyla including mountain ecosystems [4,7] as well as wetlands [60] whose members are surprisingly almost absent in the analyzed samples of the paramo. Its presence above 1% of total abundance could only be detected in dry season for altitude 1 and 3. The ecological meaning of this observation is difficult to interpret on that taxonomical level, given the astonishing diversity of Proteobacteriota as the largest detected phylum in meta-analysis studies [60,63]. Furthermore, its absence in almost all analyzed samples does not add information to the interpretation of altitudinal effects.

Taken together, the most frequent bacterial phyla were apparently rather dependent on seasonal than altitudinal changes given that their levels remained relatively constant. This is consistent with the observation of environmental modelling were the most frequent taxa were usually not those who explained community structure dependent on drivers of change but rather less abundant indicator taxa [58,59]

We also found that less abundant phyla are more prone to these changes. In part this might be due to the implemented threshold, but most taxa that dropped out due to slightly minor levels than 1% did not change the tendency observed in the taxa-bar-plot.

One of the most remarkable tendencies was that the usually underrepresented phylum Bdellovibrionota showed levels between 6.8 and 11% relative abundance. Being more abundant in the rainy season than in dry season. The fact that this phylum is consistently underrepresented

in former studies is clearly due to the fact that Bdellovibrionota was just recently supposed as a new phylum [64]. Its former belonging to Proteobacteriota further explains the relative underrepresentation of this phylum in the present study. Frequent reorganization of the bacterial tree of life makes comparation among bacterial studies difficult to interpret [58,65].

Finally, different phyla showed distinctive abundance due to seasonal effects being either present in the dry or rainy season but either less frequent or almost absent in the opposite one. Firmicutes and Latescibacterota relatively more abundant in rainy season, Planctomycetota only in rainy season which is consistent to their tendency to humid environments [60] and Patescibacteri are restricted to the dry season.

Particularly wetland taxonomical analysis have revealed many sequences which have not yet been assigned to taxonomic units, either for bacteria [60] and to greater extent as well for fungi [10]. Considering the lack of studies and the unique environment in terms of abiotic factors as well as its abundance of endemic plant species, the paramo region is most certainly a hotspot to encounter new microbial species. On one hand this limits the implication of the present data as especially adapted species with potentially important ecological functions might be overseen, but on the other hand it underlines the importance to further investigate this unique environment for which the present study could be seen as a first important baseline. Moreover, the percentages of unassigned species considered in each taxa-barplot in case of bacteria did not pass the 1% threshold. In case of fungi, the percentage was considerably higher leading ot a greater level of uncertainty as can be observed in Figure 4.9 (dark blue = not assigned).

Fungi phyla were greatly dominated by Ascomycota as well as Basidiomycota as commonly observed in fungal soil composition studies [7,66,67] followed only by a third phylum Mortierellomycota present in all analyzed studies.

In most soil types, ascomycetes are the dominant phylum [68] which is congruent with the present data. Interestingly in the lowest elevation in dry season and altitude 2 in rainy season basidiomycetes levels were superior to ascomycetes. It was formerly reported that in grassland dominated landscapes basidiomycetes can become the principle decomposers of organic matter [67] but the question remains why these changes do not apply to the grass species dominated higher elevations. The greater capability of adaptation for ascomycetes compared to basidiomycetes might explain this phenomena considering more difficult conditions at higher elevations [69]. Given that among basidiomycetes are many species such as white and brown rot fungi, specialized on phenolic substance breakdown their presence might explain in part

why at lower elevations enzyme activity as a proxy for organic matter decomposition is stronger activated, due to the absence of the enzyme latch, even at the same temperature conditions (see discussion chapter 3). Nevertheless, basidiomycetes distribution does not follow a clearly linear trend which makes interpretation more difficult.

Moreover, considering the great taxonomical and functional diversity within the two main phyla interpretation of the ecological meaning is difficult. Historically only eight distinctive fungi phyla were used [70] until in 2018 a new categorization was suggested by Tedersoo and collegues [71] introducing a total of 18 phyla to bear more information on taxonomically higher levels. Nevertheless, this number is still considerably lower than the amount of bacterial phyla where in the reference database are 89 established phyla [35], which is why statistical analysis on this level for fungi are less informative. Although we amplified the compositional analysis to class level, deeper analysis on the family or genus level might still reveal new insights.

Still, there are some interesting aspects that remain to be discussed. For example, Rocellomycota was abundant to a surprisingly high percentage only in altitude 1 of rainy season. What appears to be a data error becomes more explainable when we consider that the value shows a low deviation in the three repetitions and the same fungi phylum drops out at dry season, altitude 1, just below the 1% threshold with 0,89%, indicating that it is also only appearing in the lowest elevation. Therefore, it seems to be reasonable to discuss that fungi species belonging to the phylum Rocellomycota as well as Mucoromycota, which shows the same tendency, are highly sensitive to altitudinal and seasonal effects but show considerable abundance under the right conditions. That might be interesting in the context of climate change indicating that minor changes might have an important impact on the fungi composition.

Entorrhizomycota, a recently described phylum [72], instead were only present in dry season and mostly at altitude 1. A greater abundance of this phylum, to our knowledge, has not been reported for soil samples before, as known species are specialized in endoparasitism [73]. They are known for a relative recent evolutional diversification [74] which fits to the speciation pattern in paramo landscapes as described in chapter 1. Further analysis of the phylum might therefore reveal newly described species.

Interestingly, this finding directly coincides with the highest enzyme activity observed in chapter 3 although these fungi are categorized among the pathogenic rather than decomposing agents [73]. Whether there is a functional connectivity between the two observed aspects remains to be studied. Still it has been reported that fungal endoparasitism could reduce the abundance of certain grass species, changing vegetational composition towards herbal

plants which might cause more drastic environmental changes [19]similar to those observed at the frontier of the paramo to downslope ecosystems [75].

Analysis of fungal abundance surprisingly showed quite an opposite image to the analysis on phylum level. Apparently on class level there is quite heterogenous distribution of frequent fungal taxa upon altitudinal changes. In dry season there are 12 fungal classes abundant for altitude 4 compared to only 9 in altitude 1 indicating apparent less diverse fungal communities at lower elevations. The opposite appears in rainy season where altitude 1 and 3 showed the greatest number of abundant classes (10 and 12 respectivly). The observed tendency in dry season stands in sharp contrast to the analysis of diversity indices with a clear tendency towards decrease in diversity with rising altitude which also became visible only upon analysis of higher taxonomical levels like family and genus. This indicates that lower taxonomical levels can confound interpretations.

Nevertheless, there are some observations that call the attention. First the clear dominance of Lecanoromycetes at higher elevations in the dry season but more dominantly in the rainy season where the class reaches almost 42% of total relative abundance and a consistent reduction of Geminibasidiomycetes and to a lesser extent Dothideomycetes at higher elevations demonstrates the replacement of sensitive species towards more resistant species. Lecanoromycetes are often associated to algae forming lichenicolous symbionts which are none for their capacity of resistance in oligotrophic environmentos [76]. At simple sight the lichenicolous diversity especially in the rocky zone of the superparamo es easily noticeable. The disappearance on the other hand might be due to several sexually reproducting Geminibasidiomycetes [77] whose fruiting bodies might be difficult to develop under extreme conditions which diminishes their distribution. Meanwhile Dothideomycetes which compromises the largest fungal class in the kingdom are frequently associated with pathogenic lifestyle which largely depends on host species whose abundance might decrease with altitude [78].

Others like Tremellomycetes and show a rather heterogenous distribution over altitudes which suggests rather a dependence on biotic factors and soil characteristics rather than climatic change to explain variation which might depend on their mostly single celled form of yeasts[79]. Among Pezizomycotina there are again many pathogenic fungi, which indicates that their abundance might rather depent on vegetational zones than climatic changes due to altitudinal effects.

Again, there is evidence that not only most frequent taxa play the most important role in decomposing effects. Deacon et al. (2005)[67] reported that less abundant taxa frequently showed higher degradation activity and also a broader substrate spectrum. This is consistent with the formerly discussed observation for bacteria.

4.5 Conclusion

The bacterial composition within the paramo ecosystem on altitudinal gradients does not follow most formerly described distribution patterns in soil. The considerable predominance of Acidobacteriota and the underrepresentation of Proteobacteriota but also the presence of relatively rare taxon like Latescibacteriota in surprisingly great abundance indicates a pretty unique pattern for the paramo ecosystem. Nevertheless, the distribution of analyzed different bacterial taxa over different altitudinal levels with different vegetational zones stays surprisingly constant. Changes are mostly observable in minor taxa which still might explain for ecological changes as these minor taxa can serve as indicators of change.

The distribution of fungal phyla but mostly considering the closer look at the taxonomical level of classes reveals again pretty unique patterns for the paramo environment which invite researchers to investigate this pattern most probably related to a variation of new species.

Moreover, greater variation due to altitudinal changes were observed for the fungal composition. Here some distribution patterns in phylum abundance closely reflect findings to the observed enzyme activities in chapter 3 which might be related to the capability of basidiomycetes to break up hard woody structures abundant in paramo plants which further facilitates organic matter breakdown by bacteria and other fungi. This supports the idea of an existing tipping point for environmental changes at the frontier of the paramo region and the vulnerability of the unique ecosystem for draught induced increase in decomposition upon future extreme climatic phenomena which are already increasing in number.

Interpretation of fungal composition is difficult due to the lack of representative comparable studies in the field and considerable gaps in the taxonomical assignment. Nevertheless, the present study might add to the knowledge useful for the interpretation of future studies, given that it represents the first fungi composition study in paramo soils.

4.6 Chapter References

1. Bálint M, Bahram M, Eren AM, Faust K, Fuhrman JA, Lindahl B, et al. Millions of reads, thousands of taxa: microbial community structure and associations analyzed via marker genes. FEMS Microbiol Rev. 2016 Sep 1;40(5):686–700.

2. Heather JM, Chain B. The sequence of sequencers: The history of sequencing DNA. Genomics. 2016 Jan;107(1):1–8.

3. Ruiz-Pérez CA, Restrepo S, Zambrano MM. Microbial and Functional Diversity within the Phyllosphere of Espeletia Species in an Andean High-Mountain Ecosystem. Appl Environ Microbiol. 2016 Jan 8;82(6):1807–17.

4. Díaz M, Quiroz-Moreno C, Jarrín-V P, Piquer-Esteban S, Monfort-Lanzas P, Rivadeneira E, et al. Soil Bacterial Community Along an Altitudinal Gradient in the Sumaco, a Stratovolcano in the Amazon Region. Front For Glob Change [Internet]. 2022 [cited 2022 Mar 24];5. Available from: https://www.frontiersin.org/article/10.3389/ffgc.2022.738568

5. Siles JA, Cajthaml T, Filipova A, Minerbi S, Margesin R. Altitudinal, seasonal and interannual shifts in microbial communities and chemical composition of soil organic matter in Alpine forest soils. Soil Biol Biochem. 2017 Sep;112:1–13.

6. Rustad LE. The response of terrestrial ecosystems to global climate change: Towards an integrated approach. Sci Total Environ. 2008 Oct 15;404(2):222–35.

7. R SJ and M. Abundance and Diversity of Bacterial, Archaeal, and Fungal Communities Along an Altitudinal Gradient in Alpine Forest Soils: What Are the Driving F... - PubMed - NCBI [Internet]. 2018 [cited 2018 Sep 10]. Available from: https://www.ncbi.nlm.nih.gov/pubmed/26961712

8. Delarue F, Buttler A, Bragazza L, Grasset L, Jassey VEJ, Gogo S, et al. Experimental warming differentially affects microbial structure and activity in two contrasted moisture sites in a Sphagnum-dominated peatland. Sci Total Environ. 2015 Apr 1;511:576–83.

9. Elliott DR, Caporn SJM, Nwaishi F, Nilsson RH, Sen R. Bacterial and fungal communities in a degraded ombrotrophic peatland undergoing natural and managed re-vegetation. PloS One. 2015;10(5):e0124726.

10. Kitson E, Bell NGA. The Response of Microbial Communities to Peatland Drainage and Rewetting. A Review. Front Microbiol. 2020 Oct 29;11:582812.

11. Chen IC, Hill JK, Ohlemüller R, Roy DB, Thomas CD. Rapid Range Shifts of Species Associated with High Levels of Climate Warming. Science. 2011 Aug 19;333(6045):1024–6.

12. Boer W de, Folman LB, Summerbell RC, Boddy L. Living in a fungal world: impact of fungi on soil bacterial niche development⋆. FEMS Microbiol Rev. 2005 Sep 1;29(4):795–811.

13. Shi A, Fan F, Broach JR. Microbial adaptive evolution. J Ind Microbiol Biotechnol. 2022 Apr 14;49(2):kuab076.

14. Zhang C, Liu G, Xue S, Wang G. Soil bacterial community dynamics reflect changes in plant community and soil properties during the secondary succession of abandoned farmland in the Loess Plateau. Soil Biol Biochem. 2016 Jun 1;97:40–9.

15. Bahram M, Netherway T, Hildebrand F, Pritsch K, Drenkhan R, Loit K, et al. Plant nutrient-acquisition strategies drive topsoil microbiome structure and function. New Phytol. 2020 Aug;227(4):1189–99.

16. You X, Wang S, Du L, Wu H, Wei Y. Effects of organic fertilization on functional microbial communities associated with greenhouse gas emissions in paddy soils. Environ Res. 2022 Oct 1;213:113706.

17. Bru D, Ramette A, Saby NPA, Dequiedt S, Ranjard L, Jolivet C, et al. Determinants of the distribution of nitrogen-cycling microbial communities at the landscape scale. ISME J. 2011 Mar;5(3):532–42.

18. Javaid MK, Ashiq M, Tahir M. Potential of Biological Agents in Decontamination of Agricultural Soil. Scientifica. 2016 May 3;2016:e1598325.

19. Frąc M, Hannula SE, Bełka M, Jędryczka M. Fungal Biodiversity and Their Role in Soil Health. Front Microbiol. 2018;9:707.

20. Tamotsu H, Naoyuki M. Cryophilic fungi to denote fungi in cryosphere. 2012 Nov 27 [cited 2021 Aug 17]; Available from: https://nipr.repo.nii.ac.jp/index.php?active_action=repository_view_main_item_detail&page_id=13&block_id=104&item_id=12953&item_no=1

21. Escalas A, Hale L, Voordeckers JW, Yang Y, Firestone MK, Alvarez-Cohen L, et al. Microbial functional diversity: From concepts to applications. Ecol Evol. 2019;9(20):12000–16.

22. Brück SA, Contato AG, Gamboa-Trujillo P, de Oliveira TB, Cereia M, de Moraes Polizeli M de LT. Prospection of Psychrotrophic Filamentous Fungi Isolated from the High Andean Paramo Region of Northern Ecuador: Enzymatic Activity and Molecular Identification. Microorganisms. 2022 Feb;10(2):282.

23. Frey SD. Mycorrhizal Fungi as Mediators of Soil Organic Matter Dynamics. Annu Rev Ecol Evol Syst [Internet]. 2019 Nov [cited 2022 Sep 25];50(1). Available from: https://par.nsf.gov/biblio/10128087-mycorrhizal-fungi-mediators-soil-organic-matter-dynamics

24. Venturi V, Keel C. Signaling in the Rhizosphere. Trends Plant Sci. 2016 Mar 1;21(3):187–98.

25. Ullah MR, Carrillo Y, Dijkstra FA. Drought-induced and seasonal variation in carbon use efficiency is associated with fungi:bacteria ratio and enzyme production in a grassland ecosystem. Soil Biol Biochem. 2021 Apr 1;155:108159.

26. Kumar S, Suyal DC, Yadav A, Shouche Y, Goel R. Microbial diversity and soil physiochemical characteristic of higher altitude. PLOS ONE. 2019 Mar 15;14(3):e0213844.

27. Liao H, Hao X, Zhang Y, Qin F, Xu M, Cai P, et al. Soil aggregate modulates microbial ecological adaptations and community assemblies in agricultural soils. Soil Biol Biochem. 2022 Sep 1;172:108769.

28. Zhang W wen, Wang C, Xue R, Wang L jie. Effects of salinity on the soil microbial community and soil fertility. J Integr Agric. 2019 Jun 1;18(6):1360–8.

29. Schoch CL, Seifert KA, Huhndorf S, Robert V, Spouge JL, Levesque CA, et al. Nuclear ribosomal internal transcribed spacer (ITS) region as a universal DNA barcode marker for Fungi. Proc Natl Acad Sci. 2012 Apr 17;109(16):6241–6.

30. Bokulich NA, Kaehler BD, Rideout JR, Dillon M, Bolyen E, Knight R, et al. Optimizing taxonomic classification of marker-gene amplicon sequences with QIIME 2's q2-feature-classifier plugin. Microbiome. 2018 May 17;6:90.

31. Bolyen E, Rideout JR, Dillon MR, Bokulich NA, Abnet CC, Al-Ghalith GA, et al. Reproducible, interactive, scalable and extensible microbiome data science using QIIME 2. Nat Biotechnol. 2019;37(8):852–7.

32. Tringe SG, Hugenholtz P. A renaissance for the pioneering 16S rRNA gene. Curr Opin Microbiol. 2008 Oct 1;11(5):442–6.

33. Abarenkov K, Zirk A, Piirmann T, Pöhönen R, Ivanov F, Nilsson RH, et al. UNITE QIIME release for Fungi [Internet]. UNITE Community; 2021 [cited 2022 Feb 18]. Available from: https://plutof.ut.ee/#/doi/10.15156/BIO/1264708

34. Nilsson RH, Larsson KH, Taylor AFS, Bengtsson-Palme J, Jeppesen TS, Schigel D, et al. The UNITE database for molecular identification of fungi: handling dark taxa and parallel taxonomic classifications. Nucleic Acids Res. 2019 Jan 8;47(D1):D259–64.

35. McDonald D, Clemente JC, Kuczynski J, Rideout JR, Stombaugh J, Wendel D, et al. The Biological Observation Matrix (BIOM) format or: how I learned to stop worrying and love the ome-ome. GigaScience. 2012;1(1):7.

36. Chiarello M, McCauley M, Villéger S, Jackson CR. Ranking the biases: The choice of OTUs vs. ASVs in 16S rRNA amplicon data analysis has stronger effects on diversity measures than rarefaction and OTU identity threshold. PLOS ONE. 2022 Feb 24;17(2):e0264443.

37. Jeske JT, Gallert C. Microbiome Analysis via OTU and ASV-Based Pipelines—A Comparative Interpretation of Ecological Data in WWTP Systems. Bioengineering. 2022 Apr;9(4):146.

38. Joos L, Beirinckx S, Haegeman A, Debode J, Vandecasteele B, Baeyen S, et al. Daring to be differential: metabarcoding analysis of soil and plant-related microbial communities using amplicon sequence variants and operational taxonomical units. BMC Genomics. 2020 Oct 22;21(1):733.

39. Douglas GM, Maffei VJ, Zaneveld JR, Yurgel SN, Brown JR, Taylor CM, et al. PICRUSt2 for prediction of metagenome functions. Nat Biotechnol. 2020 Jun;38(6):685–8.

40. Callahan BJ, McMurdie PJ, Rosen MJ, Han AW, Johnson AJA, Holmes SP. DADA2: high-resolution sample inference from Illumina amplicon data. Nat Methods. 2016;13(7):581.

41. Whittaker RH. Evolution and Measurement of Species Diversity. TAXON. 1972;21(2–3):213–51.

42. Alcolado PM. Conceptos e indices relacionados con Ia diversidad. :16.

43. Shannon CE. A mathematical theory of communication. Bell Syst Tech J. 1948 Jul;27(3):379–423.

44. Moreno CE, Barragán F, Pineda E, Pavón NP. Reanálisis de la diversidad alfa: alternativas para interpretar y comparar información sobre comunidades ecológicas. Rev Mex Biodivers. 2011 Dec;82(4):1249–61.

45. Pielou EC. The measurement of diversity in different types of biological collections. J Theor Biol. 1966 Dec 1;13:131–44.

46. Jaccard P. The Distribution of the Flora in the Alpine Zone.1. New Phytol. 1912;11(2):37–50.

47. Martin M. Cutadapt removes adapter sequences from high-throughput sequencing reads. EMBnet J. 2011;17(1):pp-10.

48. Katoh K, Standley DM. MAFFT multiple sequence alignment software version 7: improvements in performance and usability. Mol Biol Evol. 2013;30(4):772–80.

49. Price MN, Dehal PS, Arkin AP. FastTree 2–approximately maximum-likelihood trees for large alignments. PloS One. 2010;5(3):e9490.

50. Weiss S, Xu ZZ, Peddada S, Amir A, Bittinger K, Gonzalez A, et al. Normalization and microbial differential abundance strategies depend upon data characteristics. Microbiome. 2017 Mar;5(1):27.

51. Vázquez-Baeza Y, Pirrung M, Gonzalez A, Knight R. EMPeror: a tool for visualizing high-throughput microbial community data. Gigascience. 2013;2(1):16.

52. Hunter JD. Matplotlib: A 2D Graphics Environment. Comput Sci Eng. 2007;9(3):90–5.

53. Coleine C, Selbmann L, Guirado E, Singh BK, Delgado-Baquerizo M. Humidity and low pH boost occurrence of Onygenales fungi in soil at global scale. Soil Biol Biochem. 2022 Apr 1;167:108617.

54. Brouns K, Verhoeven JTA, Hefting MM. Short period of oxygenation releases latch on peat decomposition. Sci Total Environ. 2014 May;481:61–8.

55. Freeman C, Ostle NJ, Fenner N, Kang H. A regulatory role for phenol oxidase during decomposition in peatlands. Soil Biol Biochem. 2004 Oct;36(10):1663–7.

56. Van Trump JI, Wrighton KC, Thrash JC, Weber KA, Andersen GL, Coates JD. Humic acid-oxidizing, nitrate-reducing bacteria in agricultural soils. mBio. 2011;2(4):e00044-00011.

57. Kalam S, Basu A, Ahmad I, Sayyed RZ, El-Enshasy HA, Dailin DJ, et al. Recent Understanding of Soil Acidobacteria and Their Ecological Significance: A Critical Review. Front Microbiol [Internet]. 2020 [cited 2022 Sep 26];11. Available from: https://www.frontiersin.org/articles/10.3389/fmicb.2020.580024

58. Ramirez KS, Knight CG, de Hollander M, Brearley FQ, Constantinides B, Cotton A, et al. Detecting macroecological patterns in bacterial communities across independent studies of global soils. Nat Microbiol. 2018 Feb;3(2):189–96.

59. Banerjee S, Schlaeppi K, van der Heijden MGA. Keystone taxa as drivers of microbiome structure and functioning. Nat Rev Microbiol. 2018 Sep;16(9):567–76.

60. Lv X, Yu J, Fu Y, Ma B, Qu F, Ning K, et al. A meta-analysis of the bacterial and archaeal diversity observed in wetland soils. ScientificWorldJournal. 2014;2014:437684.

61. Wilhelm RC, Niederberger TD, Greer C, Whyte LG. Microbial diversity of active layer and permafrost in an acidic wetland from the Canadian High Arctic. Can J Microbiol. 2011 Apr;57(4):303–15.

62. Larsbrink J, McKee LS. Bacteroidetes bacteria in the soil: Glycan acquisition, enzyme secretion, and gliding motility. Adv Appl Microbiol. 2020;110:63–98.

63. Jiao S, Wang J, Wei G, Chen W, Lu Y. Dominant role of abundant rather than rare bacterial taxa in maintaining agro-soil microbiomes under environmental disturbances. Chemosphere. 2019 Nov;235:248–59.

64. Waite DW, Chuvochina M, Pelikan C, Parks DH, Yilmaz P, Wagner M, et al. Proposal to reclassify the proteobacterial classes Deltaproteobacteria and Oligoflexia, and the phylum Thermodesulfobacteria into four phyla reflecting major functional capabilities. Int J Syst Evol Microbiol. 2020 Nov;70(11):5972–6016.

65. Zhou Z, Wang C, Luo Y. Meta-analysis of the impacts of global change factors on soil microbial diversity and functionality. Nat Commun. 2020 Jun 17;11(1):3072.

66. Bayranvand M, Akbarinia M, Salehi Jouzani G, Gharechahi J, Kooch Y, Baldrian P. Composition of soil bacterial and fungal communities in relation to vegetation composition and soil characteristics along an altitudinal gradient. FEMS Microbiol Ecol. 2021 Jan 5;97(1):fiaa201.

67. Deacon LJ, Janie Pryce-Miller E, Frankland JC, Bainbridge BW, Moore PD, Robinson CH. Diversity and function of decomposer fungi from a grassland soil. Soil Biol Biochem. 2006 Jan 1;38(1):7–20.

68. Egidi E, Delgado-Baquerizo M, Plett JM, Wang J, Eldridge DJ, Bardgett RD, et al. A few Ascomycota taxa dominate soil fungal communities worldwide. Nat Commun. 2019 May 30;10(1):2369.

69. Pandey A, Dhakar K, Jain R, Pandey N, Gupta VK, Kooliyottil R, et al. Cold Adapted Fungi from Indian Himalaya: Untapped Source for Bioprospecting. Proc Natl Acad Sci India Sect B Biol Sci. 2019 Dec 1;89(4):1125–32.

70. Spatafora JW, Aime MC, Grigoriev IV, Martin F, Stajich JE, Blackwell M. The Fungal Tree of Life: From Molecular Systematics to Genome-Scale Phylogenies. In: The Fungal Kingdom [Internet]. John Wiley & Sons, Ltd; 2017 [cited 2022 Sep 17]. p. 1–34. Available from: https://onlinelibrary.wiley.com/doi/abs/10.1128/9781555819583.ch1

71. Tedersoo L, Sánchez-Ramírez S, Kõljalg U, Bahram M, Döring M, Schigel D, et al. High-level classification of the Fungi and a tool for evolutionary ecological analyses. Fungal Divers. 2018 May 1;90(1):135–59.

72. Bauer R, Garnica S, Oberwinkler F, Riess K, Weiß M, Begerow D. Entorrhizomycota: A New Fungal Phylum Reveals New Perspectives on the Evolution of Fungi. PloS One. 2015;10(7):e0128183.

73. Riess K, Bauer R, Kellner R, Kemler M, Piątek M, Vánky K, et al. Identification of a new order of root-colonising fungi in the Entorrhizomycota: Talbotiomycetales ord. nov. on eudicotyledons. IMA Fungus. 2015 Jun;6(1):129–33.

74. Riess K, Schön ME, Ziegler R, Lutz M, Shivas RG, Piątek M, et al. The origin and diversification of the Entorrhizales: deep evolutionary roots but recent speciation with a

phylogenetic and phenotypic split between associates of the Cyperaceae and Juncaceae. Org Divers Evol. 2019 Mar 1;19(1):13–30.

75. Cortes AJ, Garzon LN, Valencia JB, Madrinan S. On the Causes of Rapid Diversification in the Paramos: Isolation by Ecology and Genomic Divergence in Espeletia. Front Plant Sci. 2018 Dec 3;9:1700.

76. Pino-Bodas R, Zhurbenko MP, Stenroos S. Phylogenetic placement within Lecanoromycetes of lichenicolous fungi associated with Cladonia and some other genera. Persoonia. 2017 Dec;39:91–117.

77. Nguyen HDT, Chabot D, Hirooka Y, Roberson RW, Seifert KA. Basidioascus undulatus: genome, origins, and sexuality. IMA Fungus. 2015 Jun;6(1):215–31.

78. Haridas S, Albert R, Binder M, Bloem J, LaButti K, Salamov A, et al. 101 Dothideomycetes genomes: A test case for predicting lifestyles and emergence of pathogens. Stud Mycol. 2020 Jun;96:141–53.

79. Xz L, Qm W, M G, M G, Av K, Ht L, et al. Towards an integrated phylogenetic classification of the Tremellomycetes. Stud Mycol [Internet]. 2015 Jun [cited 2022 Sep 29];81. Available from: https://pubmed.ncbi.nlm.nih.gov/26955199/

5 Outlook

The present work is considered to open a new research area within the Faculty of Biological Science at the Central University of Ecuador. Together with my colleagues Paulina Guarderas (ecologist) and Byron Medina (botany), we want to analyze the "Ecosystem services of the paramo region of Ecuador and (the threat of) climate change".

The first objective is to finish the analysis of the microbial composition study and publish the work. Given that the initial phase of raw data processing and feature table analysis are basically finished, the intention is to deepen analysis to higher taxonomical levels and focus on the estimated functional diversity by applying the predictive tool PiCRUST. Furthermore, it is necessary to analyze in more detail the relationship between the analyzed microbiota community structure and the measurement of enzyme activity in contrast to the abiotic soil characteristics. Moreover, in the future, the possibility of applying real-time PCR analysis should be considered to normalize abundance data and avoid errors in their analysis.

The results presented in this doctoral thesis indicate a strong influence of seasonal effects on enzyme activities and microbial composition, as discussed in Chapters 3 and 4. To give continuity to the present work and start the accrual period of the doctorate scholarship, a new project was initiated in the paramo region of the Antisana volcano national park. It is one of the biggest paramo highland planes, ideal to analyze seasonal effects on a uniform and flat area at an altitude of 4000 m. To determine the effect of seasonal droughts, in August 2022, nine random experimental cells were established to be compared to nine random control cells. To simulate seasonal drying, small transparent roofs with open sides were installed, and drainage channels were dug to avoid lateral water filtration (Figure 5.1). The aim is to analyze changes in enzyme activity and microbiota community structure over a period of six months using 5-time points. The work is connected to two pre-grade thesis projects as mentioned in the next section.

Figure 5.1 Installation of experimental cells

6 Undergraduate thesis related to the doctorate

The following is a list of theses that were accompanied by the author as a tutor during the establishment of the doctoral thesis and are directly related to the present work.

Name	Title	State
Wendy Pacheco	Optimización de parámetros en la cuantificación de fenol-oxidasas (POX) y peroxidasas de suelo andisol representativo para ecosistemas alto andinos del páramo de la Reserva Ecológica "Los Ilinizas"	Finished. http://www.dspace.uce.edu.ec/handle/25000/25085
Kevin Toapanta	Relación entre la actividad enzimática de hidrolasas (fosfatasa y sulfatasa) y la concentración de sulfatos y fosfatos con la fertilidad de suelos conservados e intervenidos de la reserva ecológica "Los Ilinizas"	Finished. http://www.dspace.uce.edu.ec/handle/25000/24856
Paola Buitrón	Actividad de hidrolasas en la descomposición de materia orgánica y su relación con carbono y nitrógeno orgánico en zonas conservadas e intervenidas de la Reserva Ecológica "Los Ilinizas"	Finished. http://www.dspace.uce.edu.ec/handle/25000/24519
Sandy Arguello	Diversidad microbiana en relación a un gradiente altitudinal en el páramo del Volcán Ilinizas.	Finished. http://www.dspace.uce.edu.ec/handle/25000/27676
Liliana Rojas	Influencia de los microclimas y la entomofauna en la descomposición de materia orgánica en un gradiente altitudinal de la Reserva Ecológica "Los Ilinizas".	Finished. Under the revision of the committee Access link
Thesis of the project for the accrual period of the doctorate´s scholarship		
Andrii Caisabanda	Determinación del efecto sobre la composición bacteriana de sequía inducida sobre el tiempo, en el páramo del Volcán Antisana.	Currently in progress
Jordan Álvarez	Cambios en la enzimática del suelo y la descomposición de materia orgánica en suelo altoandino en las faldas del Volcán Antisana bajo los efectos de estacionalidad climática inducida	Currently in progress

7 Appendices

3.7 APPX 2.1

Temperature data collected from dataloggers

Dataloggers were left for 18 months in the field at altitudes of 3600, 3800, 4000, and 4200 m above sea level, in direct proximity to the sampling sites. The temperature was measured with a sensor at 10 cm soil depth in an interval of one measurement every 15 minutes. Dataloggers were made to collect relative humidity data but paramo field conditions led to erroneous measurements probably due to the extreme climatic conditions.

The figure shows a representative data collection at sampling site 1 (3600 m) from march 2020 to march 2021.

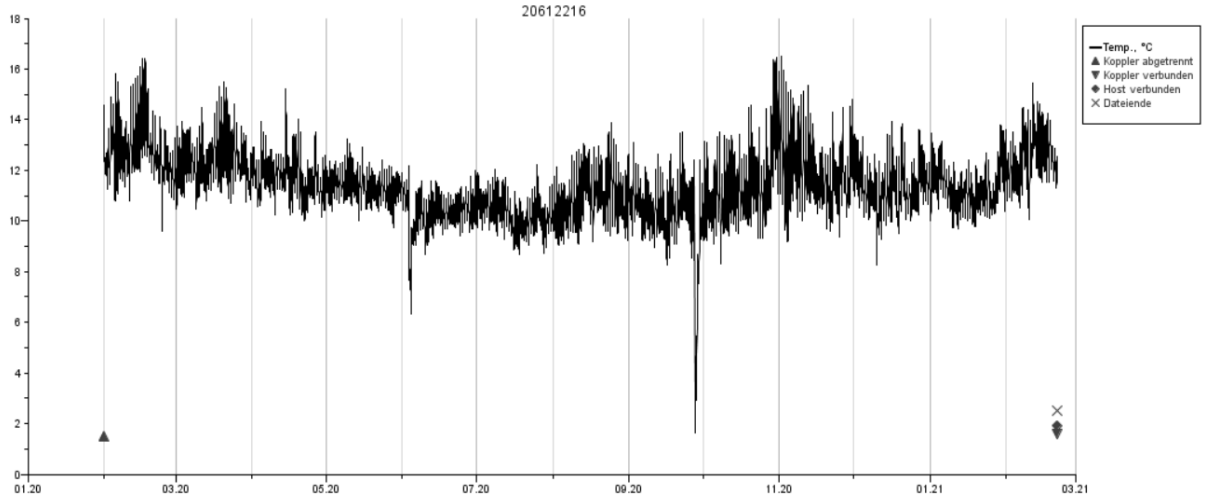

Example of one of four data recording curves of a HOBO (altitude 1 shown).

The black line represents consecutive measurements during 18 months

Appx table 2.1: Temperature and Humidity recordings at 4 different altitudes

	HOBO1		HOBO2		HOBO3		HOBO4	
Average	Temperature	Humidity	Temperature	Humidity	Temperature	Humidity	Temperature	Humidity
Janurary Feburary	12.871	32.698	10.198	N/A*	10.339	N/A*	7.955	54.246
April May	11.538	46.02	11.904	N/A*	10.854	N/A*	10.595	N/A*
Average whole year	11.334	57.195	10.831	N/A*	9.966	N/A*	9.552	N/A*

* due to paramo climatic conditions humidity recording failed at higher altitudes

3.8 APPX 2.2

INIAP soil characteristics

The measurement of total nitrogen (Nt) and Sulfur is based on the Dumas dry combustion method. It is considered the sum of ammonia, nitrogen in organic compounds, and inorganic nitrogen within a measured sample to estimate the available nitrogen from the natural decomposition of organic matter. Alternatively, Nitrogen can be determined by the Kjeldahl applying reducing agents previous to the digestion.

Information is taken from The Food and Agricultural Organization of the United Nations (FAO) GLOSOLAN-SOP-13 global standard operating procedure for soil total nitrogen, 2021

Soil organic carbon (SOC) is measured by applying the Walkley-Black method using Titration and colorimetric measurement. Soil organic carbon is used as an estimator for soil organic matter, affecting all other soil characteristics. It is composed of decomposed, partly decomposed, and yet undecomposed organic materials derived from organisms within the present ecosystem.

Information is taken from The Food and Agricultural Organization of the United Nations (FAO) GLOSOLAN global standard operating procedure for soil organic carbon, 2019

Soil available phosphorus (P) measured in Olsen (0.5 M $NaHCO_3$ at pH 8.5)

Measurement based on the solubilization of metal-fixed phosphates with sodium hydrogen carbonate and subsequent spectrophotometric measurement of absorbance at 882 nm using Phosphomolybdic heteropolyacid yellow for colorimetry. Organic matter is previously filtered with activated carbon under agitation to avoid interference in the colorimetry.

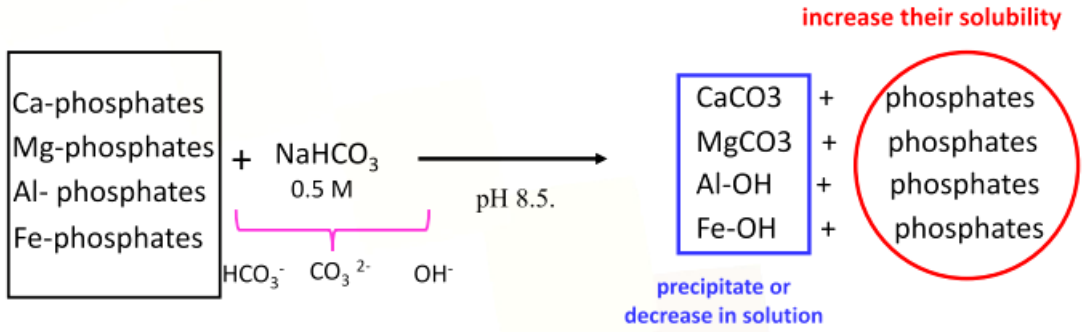

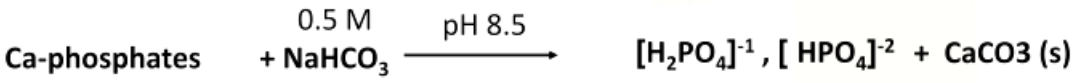

Measurement of relative bioavailability of inorganic ortho-phosphate. Phosphate is extracted from soil using 0,5 N bicarbonate at pH 8.5. It is based on the competitive desorption of phosphate by hydroxide as well as bicarbonate ions from soil particles. Liberated phosphate forms complexes with ammonium molybdate and antimony potassium. If these complexes are reduced with ascorbic acid they form a blue color detectable at 880 nm [1].

The method is mostly useful for neutral and alkaline soils but gives reasonable results for slightly acid soils as well [2] which is why it is suitable for the tested paramo soils.

Reaction equation:

Ca-phosphates + $NaHCO_3$ - $^{pH\ 8.5}\rightarrow$ $[H_2PO_4]^{-1}$ / $[HPO_4]^{-2}$ + $CaCO_3$ (s)

Protocol:

- Prepare a NaHCO3 solution at 0.5 N and adjust pH to 8.5
- Prepare a mixed reagent containing:
    - 200 mL deionized water
    - 50 mL 4 M H_2SO_4
    - 15 mL of 4% NH_4-molybdate solution
    - 30 mL of 1.75% ascorbic acid
    - 5 mL of 0.0275 KSb-tartrate solution
- Prepare soil samples (oven dried at 35°C) and mill and sift it (Mesh 10 < 2 mm)
- Mix 5 g of soil with 0,5 g phosphate free charcoal and add 100 mL of the $NaHCO_3$ solution
- Shake for 30 min at 180 rpm horizontally
- Filter on a Whatman No. 42 filter
- Aliquot 3 mL of solution and add 3 mL of the prepared mixed solution
- Vortex and stand for 30 min
- Measure and compare absorbance at 882 nm
- Contrast results to a standard curve of KH2PO4 at concentrations of 0, 0.4, 0.8, 1.2, 1.6 and 2.0 mg P L^{-1}

The protocol is based on the international standard procedure of the Food and Agriculture Organization of the United Nation (FAO).

Information is taken from Etchevers et al. The Food and Agricultural Organization of the United Nations (FAO) GLOSOLAN - SOP training sessions 2021

3.9 APPX 2.3

Protocol Adam's medium with wheat bran

	For each 50 mL:	**Example for 750 mL:**
KH_2PO_4	0,05 g	0,75
$MgSO_4$* 7 H_2O	0,025 g	0,375
Yeast extract	0,1 g	1,5
Glucose	1 g	15

	+ 50 mL H_2O dest.	
1% Wheat Bran (Farelo de trigo) → 10 g/L		7,5

Adjust pH to 6,0 with HCl (5N)

3.10 APPX 2.4

Method Activity measurement for natural (DNS method) and synthetic substrates (p-nitrophenol)

1) All substrates were diluted in water:
   - Synthetic substrates: 2 mM;
   - Natural substrates: 0.5%

2) Reaction:
   - 25 µL substrate
   - 10 µL sodium-acetate buffer 50 mM pH 5.0
   - 15 µL crude extract

3) 20 min incubation at 50 °C ;
4) Synthetic substrates: 50 µL of Na_2CO_3 0,2 M lecture at 410 nm;
   Natural substrates: 50 µL DNS lecture at 540 nm.

   BLANC: after adding Na_2CO_3 or DNS, add the crude extract to the respective blanc.

   - Enzymes used with natural substrates:
     - Xylanase (beechwood xylan 0,5%);
     - Endoglucanase (carboximetilcelulose 0,5%);

   - Enzymes with synthetic substrates:
     - Cellobiohydrolase (para-nitrophenol-β-D-cellobiose);
     - β-glycosidase (para-nitrophenol-β-D-glycopyranoside);
     - β-xylosidase (para-nitrophenol-β-D-xylanopyranosíde);

5) Calculation of enzyme activity:

Enzyme activity (EA) = Abs – Abs (blanc) x (1/slope) / time (min) / volume of crude extract (mL)

3.11 APPX 2.5

Statistical Analysis of enzyme activities

Differences between incubation types

Table Appendix: Statistical analysis applied to measured enzyme activities in Table 2.4, 2.5 and 2.6

Fungal strain	Enzyme	Applied test	p value	
fungi 1.1	endoglucanase	T-test	0.0006	*
	exoglucanase	U Mann Whitney	0.0749	
	xilanase	T-test	0.0000	*
	beta-xylosidase	T-test	0.0194	*
	beta-glucosidase	U Mann Whitney	0.0161	*
	acid phosphatase	T-test	0.0000	*
	alkaline phosphatase	T-test	0.0466	*
fungi 3.1	endoglucanase	T-test	0.3001	
	exoglucanase	T-test	0.0000	*
	xilanase	T-test	0.0678	
	beta-xylosidase	T-test	0.7223	
	beta-glucosidase	T-test	0.0001	*
	acid phosphatase	T-test	0.0000	*
	alkaline phosphatase	T-test	0.0033	*
fungi 3.3	endoglucanase	U Mann Whitney	0.0223	*
	exoglucanase	U Mann Whitney	0.2302	
	xilanase	T-test	0.005	*
	beta-xylosidase	U Mann Whitney	0.0161	*
	beta-glucosidase	U Mann Whitney	0.1012	
	acid phosphatase	U Mann Whitney	0.1187	
	alkaline phosphatase	U Mann Whitney	0.0776	

Differences between the maximum yield of each analyzed fungi

One-way-ANOVA and Kruskal-Wallis test with Sidak-Bonferroni or Dunn post-hoc test

Table Appendix: Statistical analysis applied to measured enzyme activities in Table 2.7

Enzyme	Applied test	post-hoc	p value	differences among groups (post-hoc)
endoglucanase	anova	sidak-bonferroni	0.0000	1 to 2 and 1 to 3
exoglucanase	anova	sidak-bonferroni	0.0000	1 to 2 and 2 to 3
xilanase	kkw	Dunn test	0.0509	1 to 3
beta-xylosidase	kkw	Dunn test	0.0273	2 to 3
beta-glucosidase	anova	sidak-bonferroni	0.0004	1 to 2 and 1 to 3
acid phosphatase	kkw	Dunn test	0.0273	2 to 3
alkaline phosphatase	anova	sidak-bonferroni	0.0075	1 to 2 and 2 to 3

3.12 APPX 3.1

Fluorescence analysis

Example of fluorescence measurement of β-glucosidase activity with 4-methylumbelliferyl-β-D-glucoside. The following reflects an example of the procedure applied to all different substrates and measurements:

	Measured Fluorescence			
Minutes	A1	A2	A3	A4
0	1883	1753	1817	1752
30	2479	2203	2119	2129
60	2933	2437	2470	2812
120	3813	3008	3067	3374
180	4694	3695	3742	3980
240	5643	4257	4243	4874

The four graphical lines indicate four replications of the same soil sample (A1-A4). The slope from each line was used to calculate a total average for further activity calculation.

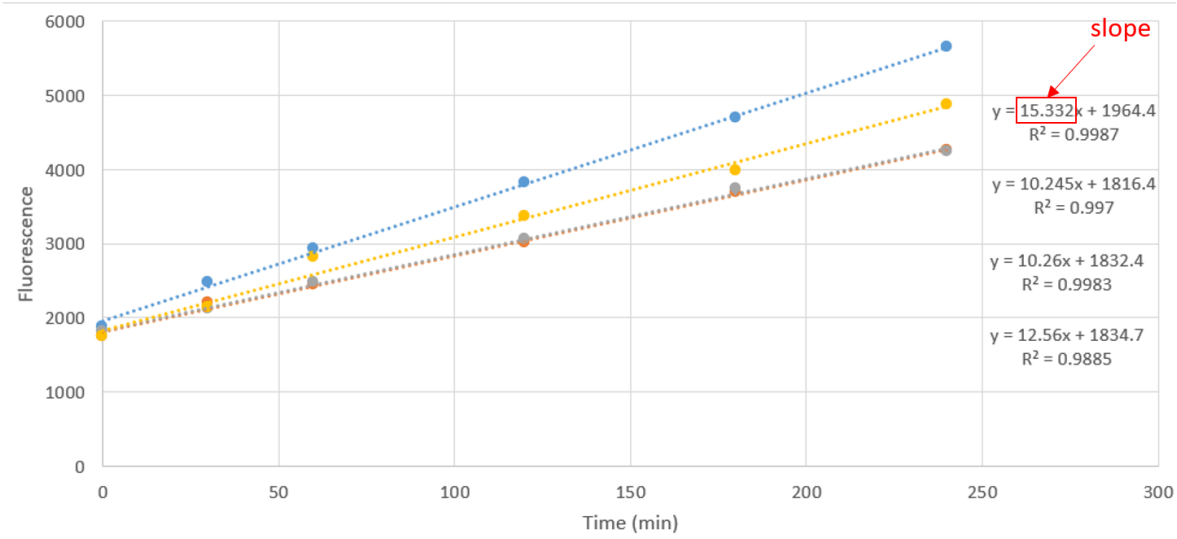

Slope	
A1	15.332
A2	10.245
A3	10.26
A4	12.56
Average	12.10
SD	2.09

From the slope average of the measurement, the slope of the negative control was subtracted to correct for autofluorescence effects from buffer and substrate in absence of enzyme. To correlate fluorescence values with MUF concentration, the average corrected slope was divided by the slope of the standard curve (see APPX 3.2)

$$pmol * well^{-1} * \min^{-1} = \frac{Slope\_SoilSample}{Slope\_Std.-curve}$$

These results led to the measured enzyme activity for each well. To calculate general activity in nmol per gram of soil for each hour, dilutions, initial weights, and volumes were taken into account, according to the following equation:

Calculate the fluorescence into nmol/g TB*h:

$$nmol * g^{-1}TB * h^{-1} = \frac{x * 60 * ExV * 100}{1000 * A * IW * DM}$$

x = Activity in pmol*well^{-1}*min^{-1}

60 = Conversion to h^{-1}

ExV = Extractions volume in µl (usually 50ml or 50000µl)

1000 = Conversion from pmol to nmol

A = Aliquot from the Extraction solution in µl (usually 50µl)

Furthermore, the calculated value was corrected for soil dry weight given that fresh soil was used for enzyme activity measurement and the amount of moisture between different soil types can vary greatly:

IW = Initial weight in g

100/DM = Conversion to g dry matter soil (DM)

3.13 APPX 3.2

Sample specific standard curves with MUF

The following figure is an example of a standard curve performed with known concentrations of 4-methylumbelyferyl. The value excluded for further calculation is the slope within the linear function (see APPX 3.1)

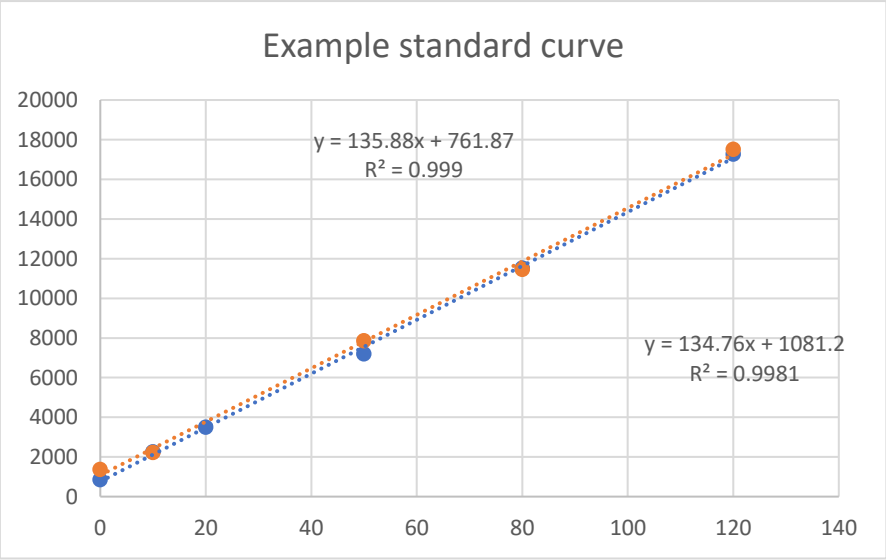

Slopes Average slopes

135.88 135.32

134.76

3.14 APPX 3.3

In case of non-normality of data, natural logarithmic transformation was applied to complete assumptions for PCA analysis. Most of the variables showed normal distribution afterwards. Those who did not, were transformed with square root transformation (root_x) or multiplicative inverse (1/x here named div_x). All variables fulfilled assumptions after transformation except for environmental temperature due to repetitive data. Therefore, this variable was eliminated for further analysis. Worthy to mention that temperature was meant to be kept constant to analyze the degrading process independent from temperature.

3.15 APPX 3.4

Principal Component Análysis (PCA)

PCA 1 physical with transformed data

Due to the violation of normality for pH, conductivity and density transformed data was used to run PCA analysis.

```
. pwcorr div_ph ln_conductividad ln_densidad humedad, sig
```

	div_ph	ln_con~d	ln_den~d	humedad
div_ph	1.0000			
ln_conduct~d	-0.3228 0.0252	1.0000		
ln_densidad	0.3961 0.0053	-0.2974 0.0401	1.0000	
humedad	0.5288 0.0001	-0.3120 0.0308	0.5008 0.0003	1.0000

In the STATA output, the first value No collinearity was observed among chosen variables (threshold 0.8 r^2)

```
. factortest div_ph ln_conductividad ln_densidad humedad

Determinant of the correlation matrix
Det                =     0.444


Bartlett test of sphericity

Chi-square         =            36.356
Degrees of freedom =                 6
p-value            =             0.000
H0: variables are not intercorrelated


Kaiser-Meyer-Olkin Measure of Sampling Adequacy
KMO                =     0.732
```

```
. estat kmo

Kaiser-Meyer-Olkin measure of sampling adequacy
```

Variable	kmo
div_ph	**0.7281**
ln_conduct~d	**0.8242**
ln_densidad	**0.7490**
humedad	**0.6864**
Overall	**0.7317**

The here presented index is basically identical to the one achieved with non-transformed data (see next section). Kaiser-Meyer-Olkin index indicates high applicability of PCA to the given set of variables.

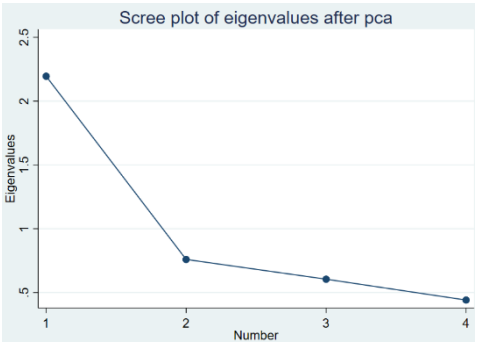


```
. pca div_ph ln_conductividad ln_densidad humedad
```

Principal components/correlation — Number of obs = 48; Number of comp. = 4; Trace = 4; Rho = 1.0000

Rotation: (unrotated = principal)

Component	Eigenvalue	Difference	Proportion	Cumulative
Comp1	2.19497	1.43555	0.5487	0.5487
Comp2	.759427	.154843	0.1899	0.7386
Comp3	.604584	.163568	0.1511	0.8897
Comp4	.441016	.	0.1103	1.0000

Principal components (eigenvectors)

Variable	Comp1	Comp2	Comp3	Comp4	Unexplained
div_ph	0.5221	0.1610	0.6660	0.5078	0
ln_conduct~d	-0.4106	0.9081	0.0616	0.0534	0
ln_densidad	0.5059	0.2573	-0.7377	0.3656	0
humedad	0.5503	0.2883	0.0922	-0.7782	0

Sum of eigenvalues indicates that PC1 explains for most of the given variance, so we stay with only one factor (value >1)

Eigenvalues show that PC1 is explained to a certain degree by all used variables

→ PC1 can be used as a new variable describing physical parameters of soil

PCA 1 physical without transformation of data

```
. pwcorr ph conductividad densidad humedad, sig
```

	ph	conduc~d	densidad	humedad
ph	1.0000			
conductivi~d	0.3366 0.0193	1.0000		
densidad	-0.3995 0.0049	-0.2767 0.0569	1.0000	
humedad	-0.5159 0.0002	-0.2662 0.0674	0.4970 0.0003	1.0000

No collinearity was observed among chosen variables (threshold 0.8 r^2)

```
. factortest ph conductividad densidad humedad

Determinant of the correlation matrix
Det               =     0.457


Bartlett test of sphericity

Chi-square        =           35.068
Degrees of freedom =              6
p-value           =          0.000
H0: variables are not intercorrelated


Kaiser-Meyer-Olkin Measure of Sampling Adequacy
KMO               =     0.720
```

```
. estat kmo

Kaiser-Meyer-Olkin measure of sampling adequacy
```

Variable	kmo
ph	0.7169
conductivi~d	0.7947
densidad	0.7384
humedad	0.6808
Overall	0.7203

Kaiser index indicates the applicability of the given PCA for the given variables (threshold >0.6) due to the absence of collinearity.

```
. pca ph conductividad densidad humedad

Principal components/correlation                  Number of obs    =         48
                                                  Number of comp.  =          4
                                                  Trace            =          4
    Rotation: (unrotated = principal)             Rho              =     1.0000
```

Component	Eigenvalue	Difference	Proportion	Cumulative
Comp1	2.16431	1.3723	0.5411	0.5411
Comp2	.792009	.196143	0.1980	0.7391
Comp3	.595866	.148051	0.1490	0.8880
Comp4	.447815	.	0.1120	1.0000

Principal components (eigenvectors)

Variable	Comp1	Comp2	Comp3	Comp4	Unexplained
ph	-0.5320	-0.0443	0.6658	0.5212	0
conductivi~d	-0.3997	0.8933	-0.1498	-0.1407	0
densidad	0.5102	0.2900	0.7188	-0.3728	0
humedad	0.5449	0.3404	-0.1327	0.7547	0

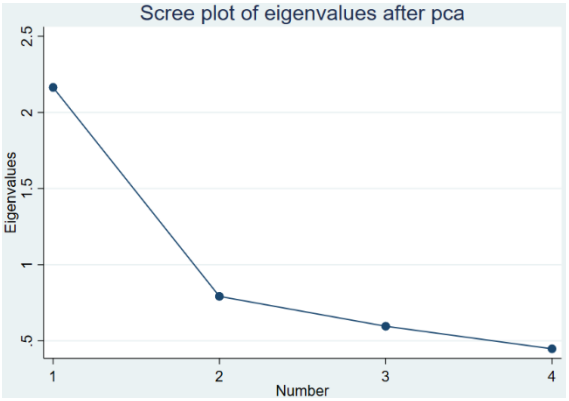

Sum of eigenvalues indicates that PC1 explains for most of the given variance, so we stay with only one factor (value >1)

Eigenvalues show that PC1 is explained to a certain degree by all used variables

→ PC1 can be used as new variable describing physical parameters of soil

Factor loadings (pattern matrix) and unique variances

Variable	Factor1	Uniqueness
ph	-0.7827	0.3874
conductivi~d	-0.5880	0.6543
densidad	0.7505	0.4367
humedad	0.8017	0.3573

Given that results of Eigenvalues, kmo and screeplots are highly similar between transformed and non-transformed data we can consider non-transformed data due to simple interpretation in the discussion of the work. The violation of normality assumption in this case is acceptable especially given that the output variable again shows normality and homoscedasticity for all given scenarios (altitude, depth, and season).

PCA 2 organic elements with transformed data

Due to the violation of normality for sulphur and phenolic-substance measurements transformed data was used to run PCA analysis. Natural logarithmic transformation fulfilled the assumptions.

Worthy to mention that SOC and Nt showed high colinearity in the análisis which is why they were replaced by the ratio SOC/Nt which is often applied in soil science and the variable "organic matter" OM because to its important relation to the global topic. SOC and OM are transformations of each other applying a coefficient which is why they behave identically.

```
. pwcorr soc_nt ln_azufre fosforo mo ln_fenoles_corr, sig
```

	soc_nt	ln_azu~e	fosforo	mo	ln_fen~r
soc_nt	1.0000				
ln_azufre	-0.0445 0.7641	1.0000			
fosforo	-0.2320 0.1126	0.3052 0.0349	1.0000		
mo	-0.0361 0.8076	0.2955 0.0414	0.5183 0.0002	1.0000	
ln_fenoles~r	0.0436 0.7684	-0.0316 0.8311	0.1235 0.4030	0.0088 0.9524	1.0000

No collinearity observed among chosen variables (threshold r=0.8)

Ln_fenoles_corr shows very low correlation with any other variable which is why its usage is discussable.

```
Determinant of the correlation matrix
Det                 =     0.585


Bartlett test of sphericity

Chi-square          =            23.837
Degrees of freedom  =                10
p-value             =             0.008
H0: variables are not intercorrelated


Kaiser-Meyer-Olkin Measure of Sampling Adequacy
KMO                 =     0.560
```

```
. pca soc_nt ln_azufre fosforo mo ln_fenoles_corr

Principal components/correlation                  Number of obs    =         48
                                                  Number of comp.  =          5
                                                  Trace            =          5
    Rotation: (unrotated = principal)             Rho              =     1.0000
```

Component	Eigenvalue	Difference	Proportion	Cumulative
Comp1	1.80561	.764864	0.3611	0.3611
Comp2	1.04074	.049303	0.2081	0.5693
Comp3	.99144	.256918	0.1983	0.7676
Comp4	.734523	.306836	0.1469	0.9145
Comp5	.427687	.	0.0855	1.0000

Principal components (eigenvectors)

Variable	Comp1	Comp2	Comp3	Comp4	Comp5	Unexplained
soc_nt	-0.2278	0.5079	0.7702	-0.1642	0.2646	0
ln_azufre	0.4605	-0.0828	0.3821	0.7944	-0.0636	0
fosforo	0.6258	0.0743	-0.1606	-0.2195	0.7273	0
mo	0.5825	0.0793	0.2247	-0.4860	-0.6064	0
ln_fenoles~r	0.0719	0.8505	-0.4296	0.2399	-0.1713	0

Kmo indicates applicability of PCA to the given set of variables (Threshold > 0,5). Nevertheless, Eigenvalues indicate two PCs that could be applied of which phenolic substances account for 85% of its variation. We therefore analyzed the possibility to drop out phenolic substances in order to improve results (shown below).

```
. pwcorr soc_nt ln_azufre fosforo mo, sig
```

	soc_nt	ln_azu~e	fosforo	mo
soc_nt	1.0000			
ln_azufre	-0.0445 0.7641	1.0000		
fosforo	-0.2320 0.1126	0.3052 0.0349	1.0000	
mo	-0.0361 0.8076	0.2955 0.0414	0.5183 0.0002	1.0000

```
. factortest soc_nt ln_azufre fosforo mo

Determinant of the correlation matrix
Det                 =     0.603


Bartlett test of sphericity

Chi-square          =            22.646
Degrees of freedom  =                 6
p-value             =             0.001
H0: variables are not intercorrelated


Kaiser-Meyer-Olkin Measure of Sampling Adequacy
KMO                 =     0.584
```

Variable	kmo
soc_nt	0.4460
ln_azufre	0.7480
fosforo	0.5625
mo	0.5734
Overall	0.5839

Kaiser-Meyer-Olkin measure of sampling adequacy

Variable	kmo
mo	0.5876
ln_azufre	0.7410
fosforo	0.5856
Overall	0.6122

Dropping out soc_nt leads to improved kmo measure and a single principal component

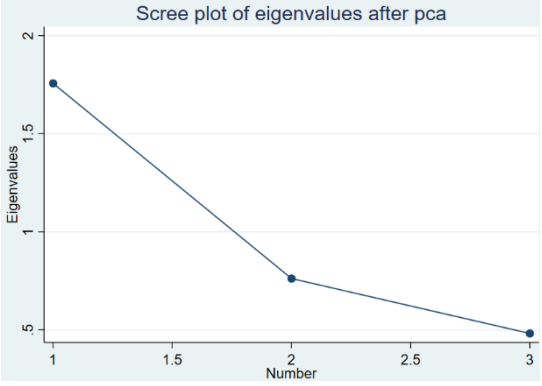

(threshold 0,6)

```
. pca mo ln_azufre fosforo

Principal components/correlation                  Number of obs    =         48
                                                  Number of comp.  =          3
                                                  Trace            =          3
    Rotation: (unrotated = principal)             Rho              =     1.0000
```

Component	Eigenvalue	Difference	Proportion	Cumulative
Comp1	1.7567	.995008	0.5856	0.5856
Comp2	.761694	.280091	0.2539	0.8395
Comp3	.481603	.	0.1605	1.0000

Principal components (eigenvectors)

Variable	Comp1	Comp2	Comp3	Unexplained
mo	0.6147	-0.3612	0.7012	0
ln_azufre	0.4895	0.8718	0.0199	0
fosforo	0.6185	-0.3310	-0.7127	0

Results show one single PC which accounts for all three chosen variables to a considerable degree.

PCA 2 organic elements with transformed data

Applying lessons from PCA realized with transformed data, non-transformed data was used for the PCA to be able to compare. Results again were almost identical to those achieved with transformed data.

Kaiser-Meyer-Olkin measure of sampling adequacy

Variable	kmo
azufre	0.7238
fosforo	0.6006
mo	0.5853
Overall	0.6168

(Threshold is 0,6)

```
. pca azufre fosforo mo
```

Principal components/correlation — Number of obs = 48; Number of comp. = 3; Trace = 3; Rho = 1.0000

Rotation: (unrotated = principal)

Component	Eigenvalue	Difference	Proportion	Cumulative
Comp1	1.78089	1.03698	0.5936	0.5936
Comp2	.743914	.268718	0.2480	0.8416
Comp3	.475196	.	0.1584	1.0000

Principal components (eigenvectors)

Variable	Comp1	Comp2	Comp3	Unexplained
azufre	0.5020	0.8536	0.1395	0
fosforo	0.5988	-0.4594	0.6561	0
mo	0.6241	-0.2458	-0.7417	0

Factor analysis/correlation — Number of obs = 48

Method: principal-component factors — Retained factors = 1

Rotation: orthogonal varimax (Kaiser off) — Number of params = 3

Factor	Variance	Difference	Proportion	Cumulative
Factor1	1.78089	.	0.5936	0.5936

Rotated factor loadings (pattern matrix) and unique variances

Variable	Factor1	Uniqueness
azufre	0.6699	0.5512
fosforo	0.7990	0.3615
mo	0.8329	0.3064

Scoring coefficients (method = regression; based on varimax rotated factors)

Variable	Factor1
azufre	0.37617
fosforo	0.44867
mo	0.46766

PCA 3 metals with transformed data

```
. pwcorr ln_ca ln_mg ln_zn root_fe ln_mn root_k, sig
```

	ln_ca	ln_mg	ln_zn	root_fe	ln_mn	root_k
ln_ca	**1.0000**					
ln_mg	**0.7954**	**1.0000**				
	0.0000					
ln_zn	**0.6096**	**0.3299**	**1.0000**			
	0.0000	**0.0220**				
root_fe	**0.5584**	**0.6730**	**0.4512**	**1.0000**		
	0.0000	**0.0000**	**0.0013**			
ln_mn	**0.5106**	**0.4727**	**0.5909**	**0.5241**	**1.0000**	
	0.0002	**0.0007**	**0.0000**	**0.0001**		
root_k	**0.4309**	**0.2222**	**0.6463**	**0.4826**	**0.5821**	**1.0000**
	0.0022	**0.1291**	**0.0000**	**0.0005**	**0.0000**	

Ln_ca and ln_mg show pretty high collinearity which is why ln_mg could drop out of the model.

```
. factortest ln_ca ln_mg ln_zn root_fe ln_mn root_k
```

Determinant of the correlation matrix
Det = **0.024**

Bartlett test of sphericity

Chi-square = **165.589**
Degrees of freedom = **15**
p-value = **0.000**
H0: variables are not intercorrelated

Kaiser-Meyer-Olkin Measure of Sampling Adequacy
KMO = **0.692**

Kaiser-Meyer-Olkin measure of sampling adequacy

Variable	kmo
ln_ca	**0.6484**
ln_mg	**0.5512**
ln_zn	**0.7206**
root_fe	**0.7442**
ln_mn	**0.8415**
root_k	**0.7380**
Overall	**0.6921**

```
. factortest ln_ca ln_zn root_fe ln_mn root_k

Determinant of the correlation matrix
Det                 =     0.118


Bartlett test of sphericity

Chi-square          =            95.261
Degrees of freedom  =                10
p-value             =             0.000
H0: variables are not intercorrelated


Kaiser-Meyer-Olkin Measure of Sampling Adequacy
KMO                 =     0.806
```

Variable	kmo
ln_ca	0.7833
ln_zn	0.7718
root_fe	0.8200
ln_mn	0.8697
root_k	0.7960
Overall	0.8060

```
. pca ln_ca ln_zn root_fe ln_mn root_k

Principal components/correlation                  Number of obs    =         48
                                                  Number of comp.  =          5
                                                  Trace            =          5
    Rotation: (unrotated = principal)             Rho              =     1.0000
```

Component	Eigenvalue	Difference	Proportion	Cumulative
Comp1	3.15811	2.52392	0.6316	0.6316
Comp2	.634191	.113662	0.1268	0.7585
Comp3	.520529	.104317	0.1041	0.8626
Comp4	.416212	.145252	0.0832	0.9458
Comp5	.27096	.	0.0542	1.0000

Principal components (eigenvectors)

Variable	Comp1	Comp2	Comp3	Comp4	Comp5	Unexplained
ln_ca	0.4393	0.4939	-0.5775	-0.0273	0.4784	0
ln_zn	0.4708	-0.3002	-0.4640	0.1315	-0.6750	0
root_fe	0.4225	0.5828	0.5616	0.2809	-0.2958	0
ln_mn	0.4558	-0.1736	0.2748	-0.8274	0.0451	0
root_k	0.4461	-0.5442	0.2457	0.4674	0.4754	0

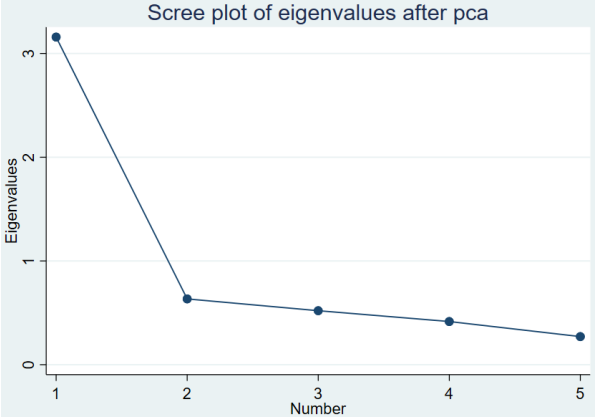

PCA 3 metals with untransformed data

```
. factortest ca zn fe mn k

Determinant of the correlation matrix
Det                 =     0.128


Bartlett test of sphericity

Chi-square          =           91.514
Degrees of freedom  =               10
p-value             =            0.000
H0: variables are not intercorrelated


Kaiser-Meyer-Olkin Measure of Sampling Adequacy
KMO                 =     0.729


Kaiser-Meyer-Olkin measure of sampling adequacy
```

Variable	kmo
ca	0.6933
zn	0.6852
fe	0.7500
mn	0.8654
k	0.7087
Overall	0.7289

Factortest shows differences to the results with transformed-data (kmo=0,806)

Nevertheless, it lies within the threshold of acceptance (r>0,6).

Furthermore, looking at the PCs and their eigenvectors, values are almost identical with and without log-transformation

```
. pca ca zn fe mn k

Principal components/correlation                  Number of obs    =         48
                                                  Number of comp.  =          5
                                                  Trace            =          5
    Rotation: (unrotated = principal)             Rho              =     1.0000
```

Component	Eigenvalue	Difference	Proportion	Cumulative
Comp1	3.01367	2.29049	0.6027	0.6027
Comp2	.72318	.167809	0.1446	0.7474
Comp3	.55537	.061587	0.1111	0.8584
Comp4	.493783	.279784	0.0988	0.9572
Comp5	.214	.	0.0428	1.0000

Principal components (eigenvectors)

Variable	Comp1	Comp2	Comp3	Comp4	Comp5	Unexplained
ca	0.4346	0.5835	-0.1837	-0.5083	0.4224	0
zn	0.4975	-0.2548	-0.2744	-0.3496	-0.7000	0
fe	0.4301	0.5095	0.1241	0.6836	-0.2698	0
mn	0.4230	-0.2869	0.8339	-0.1443	0.1502	0
k	0.4469	-0.5026	-0.4244	0.3624	0.4860	0

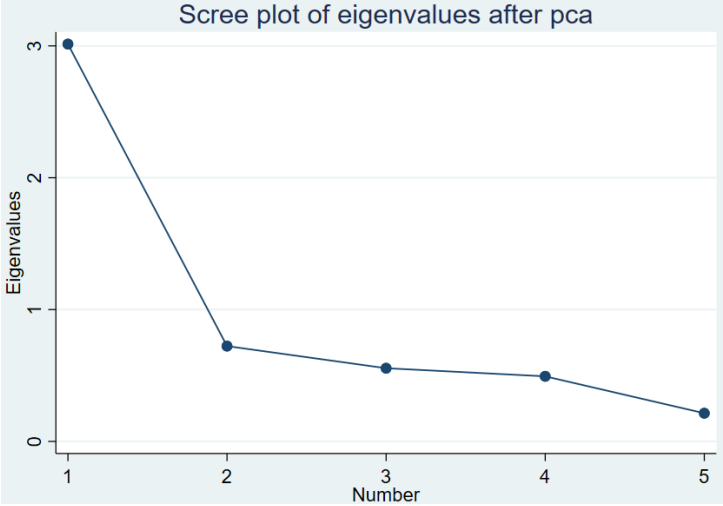

Again there is only one PC accounting for most of the variation observed for the chosen variables

```
. factor ca zn fe mn k, pcf
(obs=48)

Factor analysis/correlation                    Number of obs    =         48
    Method: principal-component factors        Retained factors =          1
    Rotation: (unrotated)                      Number of params =          5
```

Factor	Eigenvalue	Difference	Proportion	Cumulative
Factor1	**3.01367**	**2.29049**	**0.6027**	**0.6027**
Factor2	**0.72318**	**0.16781**	**0.1446**	**0.7474**
Factor3	**0.55537**	**0.06159**	**0.1111**	**0.8584**
Factor4	**0.49378**	**0.27978**	**0.0988**	**0.9572**
Factor5	**0.21400**	.	**0.0428**	**1.0000**

LR test: independent vs. saturated: chi2(**10**) = **93.57** Prob>chi2 = **0.0000**

Factor loadings (pattern matrix) and unique variances

Variable	Factor1	Uniqueness
ca	**0.7545**	**0.4308**
zn	**0.8637**	**0.2540**
fe	**0.7466**	**0.4426**
mn	**0.7343**	**0.4608**
k	**0.7758**	**0.3981**

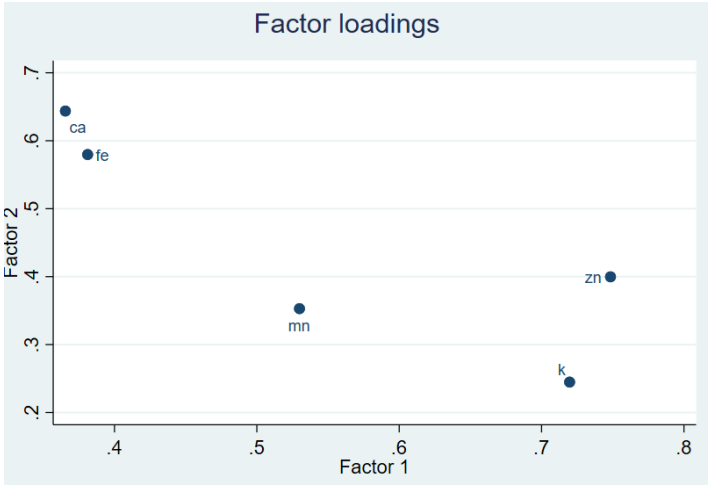


```
. predict f1
(option regression assumed; regression scoring)

Scoring coefficients (method = regression; based on varimax rotated factors)
```

Variable	Factor1	Factor2	Factor3
ca	-0.11340	0.45829	-0.02441
zn	0.49574	0.02259	-0.06072
fe	-0.00144	0.33613	0.04598
mn	0.12923	0.06816	0.03460
k	0.35882	-0.12624	0.04352

Summary:

In all three PCA analysis Eigenvalues of variables and resulting factors were insignificantly different among transformed and untransformed data. In physic and organic data even the kmo resulted very similar and only in metals differed slightly. In each case one single principal component accounted for variance of all included variables which results in a total of three new variables.

F1_physic: All initially considered variables were kept due to an acceptable kmo measure and the absence of collinearity among variables.

F1_organic: soc_nt and fenoles_corr were removed from the dataset given that their elimination considerably improved the kmo index. SOC and Nt showed high levels of collinearity which is

why MO was used as a proxy for both of them (MO is an estimation of organic matter based on SOC using coefficient multiplication and therefore somehow represents also the nitrogen content).

F1_metals: Magnesium was removed from the inicial set of variables due to its high value of collinearity with Calcium.

3.16 APPX 3.5

Linear fixed-effect models

Models were chosen due to three principal characcteristics. First the linear combination of chosen variables should make sense in biological terms of what we wanted to show and how results can be logically interpreted. Second, chosen model parameters among different analyzed enzymes should be similar in order to be able to compare the outcomes. Finally, and importantly, all possible parameter combinations were chequed for the model's meaningfullness (r2>0,6), significance (p-value <0,05), Akaike's information criterion and Bayesian information criterion (AIC/BIC, biggest value), the absence of colinearity (varian inflation factor VIF < 10) and the normal distribution of residuals as a requisite for the application of linear fixed effect models (Shapiro Wilk of residuals). The image below shows the outcomes of the six final chosen models for the different enzymes, as produced by STATA 16.0:

```
. regress sulphatase i.altitude i.depth i.season c.f1_physic c.f1_organic, beta
```

Source	SS	df	MS	Number of obs	=	48
				F(7, 40)	=	12.07
Model	903987.394	7	129141.056	Prob > F	=	0.0000
Residual	428081.52	40	10702.038	R-squared	=	0.6786
				Adj R-squared	=	0.6224
Total	1332068.91	47	28341.8918	Root MSE	=	103.45

sulphatase	Coef.	Std. Err.	t	P>|t|	Beta
altitude					
2	-83.58662	46.66979	-1.79	0.081	-.2172674
3	-112.9232	48.14833	-2.35	0.024	-.2935224
4	-55.65203	59.88893	-0.93	0.358	-.1446568
2.depth	-27.13654	42.43038	-0.64	0.526	-.0814482
2.season	-204.5325	71.33711	-2.87	0.007	-.6138887
f1_physic	26.4474	38.23884	0.69	0.493	.1570973
f1_organic	89.98052	23.39086	3.85	0.000	.5344832
_cons	421.4757	68.79301	6.13	0.000	.

```
.
. regress phosphatase i.altitude i.depth i.season c.f1_physic c.f1_organic, beta
```

Source	SS	df	MS	Number of obs	=	48
				F(7, 40)	=	11.97
Model	173044892	7	24720698.8	Prob > F	=	0.0000
Residual	82580962.4	40	2064524.06	R-squared	=	0.6769
				Adj R-squared	=	0.6204
Total	255625854	47	5438847.96	Root MSE	=	1436.8

phosphatase	Coef.	Std. Err.	t	P>|t|	Beta
altitude					
2	39.05056	648.2053	0.06	0.952	.0073273
3	-415.8424	668.741	-0.62	0.538	-.0780275
4	-486.0884	831.8083	-0.58	0.562	-.0912082
2.depth	-747.0616	589.3233	-1.27	0.212	-.1618619
2.season	-2963.732	990.8142	-2.99	0.005	-.6421363
f1_physic	-2.21221	531.1063	-0.00	0.997	-.0009486
f1_organic	798.3342	324.8799	2.46	0.018	.3423192
_cons	6273.85	955.4788	6.57	0.000	.

```
.
. regress nac i.altitude i.depth i.season c.f1_physic c.f1_organic, beta
```

Source	SS	df	MS	Number of obs	=	48
				F(7, 40)	=	8.87
Model	755720.863	7	107960.123	Prob > F	=	0.0000
Residual	487066.435	40	12176.6609	R-squared	=	0.6081
				Adj R-squared	=	0.5395
Total	1242787.3	47	26442.2829	Root MSE	=	110.35

nac	Coef.	Std. Err.	t	P>|t|	Beta
altitude					
2	-63.97983	49.78136	-1.29	0.206	-.1721733
3	-131.238	51.35847	-2.56	0.015	-.3531689
4	-102.1364	63.88184	-1.60	0.118	-.274855
2.depth	-14.00304	45.25929	-0.31	0.759	-.0435126
2.season	-151.2677	76.09329	-1.99	0.054	-.4700438
f1_physic	37.92072	40.7883	0.93	0.358	.2331992
f1_organic	100.1759	24.95037	4.02	0.000	.616047
_cons	401.4854	73.37957	5.47	0.000	.

```
. regress cellobio i.altitude i.depth i.season c.f1_physic c.f1_organic, beta

      Source |       SS           df       MS      Number of obs   =        48
-------------+----------------------------------   F(7, 40)        =     12.38
       Model |  43921.9469         7  6274.56384   Prob > F        =    0.0000
    Residual |  20272.3281        40  506.808202   R-squared       =    0.6842
-------------+----------------------------------   Adj R-squared   =    0.6289
       Total |  64194.2749        47  1365.83564   Root MSE        =    22.512

------------------------------------------------------------------------------
    cellobio |      Coef.   Std. Err.      t    P>|t|                     Beta
-------------+----------------------------------------------------------------
    altitude |
           2 |    15.35519   10.15604     1.51   0.138                .1818144
           3 |   -1.081401   10.47779    -0.10   0.918               -.0128044
           4 |   -11.07016   13.03272    -0.85   0.401               -.1310772
             |
     2.depth |    11.36563   9.233481     1.23   0.226                .1553946
    2.season |   -42.63347   15.52402    -2.75   0.009               -.5828987
  f1_physic |   -.3077713   8.321341    -0.04   0.971               -.0083278
 f1_organic |    20.24523   5.090199     3.98   0.000                .5478019
       _cons |    88.99876   14.97038     5.94   0.000                      .
------------------------------------------------------------------------------

.
. regress bglu i.altitude i.depth i.season c.f1_physic c.f1_organic, beta

      Source |       SS           df       MS      Number of obs   =        48
-------------+----------------------------------   F(7, 40)        =     13.47
       Model |  4317952.5         7  616850.358   Prob > F        =    0.0000
    Residual |  1831326.87        40  45783.1718   R-squared       =    0.7022
-------------+----------------------------------   Adj R-squared   =    0.6501
       Total |  6149279.38        47  130835.731   Root MSE        =    213.97

------------------------------------------------------------------------------
        bglu |      Coef.   Std. Err.      t    P>|t|                     Beta
-------------+----------------------------------------------------------------
    altitude |
           2 |   -48.09503    96.5285    -0.50   0.621               -.0581848
           3 |   -301.4529   99.5866    -3.03   0.004                -.364694
           4 |   -309.5928    123.87    -2.50   0.017               -.3745415
             |
     2.depth |    74.80797     87.76     0.85   0.399                .1045024
    2.season |   -515.0831   147.5486    -3.49   0.001               -.7195414
  f1_physic |    159.7427   79.09052     2.02   0.050                .4416292
 f1_organic |    258.5117     48.38     5.34   0.000                .7146888
       _cons |    869.7103   142.2866     6.11   0.000                      .
------------------------------------------------------------------------------

.
. regress phenolox i.altitude i.depth i.season c.f1_physic c.f1_organic, beta

      Source |       SS           df       MS      Number of obs   =        48
-------------+----------------------------------   F(7, 40)        =      5.99
       Model |  321.193126         7  45.8847323   Prob > F        =    0.0001
    Residual |  306.417519        40  7.66043797   R-squared       =    0.5118
-------------+----------------------------------   Adj R-squared   =    0.4263
       Total |  627.610645        47   13.353418   Root MSE        =    2.7677

------------------------------------------------------------------------------
    phenolox |      Coef.   Std. Err.      t    P>|t|                     Beta
-------------+----------------------------------------------------------------
    altitude |
           2 |   -5.704077   1.248617    -4.57   0.000               -.6830641
           3 |   -6.657493   1.288175    -5.17   0.000               -.7972358
           4 |   -5.768006   1.602286    -3.60   0.001               -.6907196
             |
     2.depth |   -2.031367   1.135195    -1.79   0.081               -.2808885
    2.season |   -.5694804   1.908574    -0.30   0.767               -.0787452
  f1_physic |    .9307832   1.023053     0.91   0.368                .2547137
 f1_organic |   -.2760245    .625806    -0.44   0.662               -.0755356
       _cons |    10.42662   1.840509     5.67   0.000                      .
------------------------------------------------------------------------------
```

3.17 APPX 4.1

QIIME2 code for Raw data preparation

import of FASTAQ files into QIIME2

manifest file in home folder

```
qiime tools import \
  --type 'SampleData[PairedEndSequencesWithQuality]' \
  --input-path manifest-file-16S.txt \
  --output-path paired-end-demux-16S.qza \
  --input-format PairedEndFastqManifestPhred33V2
```

```
qiime tools import \
  --type 'SampleData[PairedEndSequencesWithQuality]' \
  --input-path manifest-file-ITS.txt \
  --output-path paired-end-demux-ITS.qza \
  --input-format PairedEndFastqManifestPhred33V2
```

Trimming primer sequences from demultiplexed artifacts

*adapter sequences

Nextera Forward: CTGTCTCTTATACACATCTCCGAGCCCACGAGAC

Nextera Reverse: CTGTCTCTTATACACATCTGACGCTGCCGACGA

primer sequences Bacterias 16S v3/v4 Bakt_341F y Bakt_805R

Forward: CCTACGGGNGGCWGCAG

Reverse: GACTACHVGGGTATCTAATCC

primer sequences ITS

3F: GCATCGATGAAGAACGCAGC

4R: TCCTCCGCTTATTGATATGC

```
qiime cutadapt trim-paired \
--i-demultiplexed-sequences paired-end-demux-16S.qza \
--p-front-f 'CCTACGGGNGGCWGCAG' \
--p-front-r 'GACTACHVGGGTATCTAATCC' \
--p-cores 2 \
--p-match-adapter-wildcards \
--p-match-read-wildcards \
--p-discard-untrimmed \
--o-trimmed-sequences paired-end-trimprimer-16S.qza \
--verbose
```

```
qiime cutadapt trim-paired \
--i-demultiplexed-sequences paired-end-trimprimer-16S.qza \
--p-front-f 'CTGTCTCTTATACACATCTCCGAGCCCACGAGAC' \
--p-front-r 'CTGTCTCTTATACACATCTGACGCTGCCGACGA' \
--p-cores 2 \
--p-match-adapter-wildcards \
--p-match-read-wildcards \
--o-trimmed-sequences paired-end-trimfinal-16S.qza \
```

--verbose

Cut adapter sequences

qiime cutadapt trim-paired \

--i-demultiplexed-sequences trimmed_sequencesprimers.qza \

--p-front-f 'CTGTCTCTTATACACATCTCCGAGCCCACGAGAC' \

--p-front-r 'CTGTCTCTTATACACATCTGACGCTGCCGACGA' \

--p-match-read-wildcards \

--p-match-adapter-wildcards \

--p-cores 2 \

--output-dir paired-end-trimadapters.qza \

--verbose \

Visualization for process control

qiime demux summarize \

--i-data paired-end-demux-16S.qza \

--o-visualization demux-16S.qzv

DADA 2 – data filtering

trunc parameter were chosen, visualizing denosing-stats and remove those below a threshold for the qualitiy index Q < 30.

16S refers to dry season and 16S-2 to rainy season which were later merged to final-16S, accordingly with ITS

qiime dada2 denoise-paired \

```
--i-demultiplexed-seqs trimmed_sequencesadapters.qza \
--p-trim-left-f 0 \
--p-trim-left-r 0 \
--p-trunc-len-f 277 \
--p-trunc-len-r 230 \
--o-table table.qza \
--o-representative-sequences rep-seqs-16S.qza \
--o-denoising-stats denoising-stats-16S.qza \
--verbose \

qiime dada2 denoise-paired \
  --i-demultiplexed-seqs paired-end-trimfinal-ITS.qza \
  --p-trim-left-f 0 \
  --p-trim-left-r 0 \
  --p-trunc-len-f 280 \
  --p-trunc-len-r 220 \
  --o-table table-ITS.qza \
  --o-representative-sequences rep-seqs-ITS.qza \
  --o-denoising-stats denoising-stats-ITS.qza \
--verbose

qiime dada2 denoise-paired \
  --i-demultiplexed-seqs paired-end-trimfinal-16S-2.qza \
  --p-trim-left-f 0 \
  --p-trim-left-r 0 \
  --p-trunc-len-f 251 \
```

```
  --p-trunc-len-r 193 \
  --o-table table-16S-2.qza \
  --o-representative-sequences rep-seqs-16S-2.qza \
  --o-denoising-stats denoising-stats-16S-2.qza \
--verbose

qiime dada2 denoise-paired \
  --i-demultiplexed-seqs paired-end-trimfinal-ITS-2.qza \
  --p-trim-left-f 0 \
  --p-trim-left-r 0 \
  --p-trunc-len-f 258 \
  --p-trunc-len-r 201 \
  --o-table table-ITS-2.qza \
  --o-representative-sequences rep-seqs-ITS-2.qza \
  --o-denoising-stats denoising-stats-ITS-2.qza \
--verbose

qiime feature-table merge \
 --i-tables table-16S.qza \
 --i-tables table-16S-2.qza \
 --o-merged-table final-table-16S.qza

qiime feature-table merge-seqs \
 --i-data rep-seqs-16S.qza \
 --i-data rep-seqs-16S-2.qza\
 --o-merged-data final-rep-seqs-16S.qza
```

```
qiime feature-table merge \
 --i-tables table-ITS.qza \
 --i-tables table-ITS-2.qza \
 --o-merged-table final-table-ITS.qza

qiime feature-table merge-seqs \
 --i-data rep-seqs-ITS.qza \
 --i-data rep-seqs-ITS-2.qza\
 --o-merged-data final-rep-seqs-ITS.qza
```

3.18 APPX 4.2

QIIME2 code for analysis of processed data

Phylogenetic tree modeling

16S

```
qiime phylogeny align-to-tree-mafft-fasttree \
  --i-sequences final-rep-seqs-16S.qza \
  --o-alignment final-aligned-rep-seqs-16S.qza \
  --o-masked-alignment final-masked-aligned-rep-seqs-16S.qza \
  --o-tree final-unrooted-tree-16S.qza \
  --o-rooted-tree final-rooted-tree-16S.qza
```

ITS

```
qiime phylogeny align-to-tree-mafft-fasttree \
```

```
  --i-sequences final-rep-seqs-ITS.qza \
  --o-alignment final-aligned-rep-seqs-ITS.qza \
  --o-masked-alignment final-masked-aligned-rep-seqs-ITS.qza \
  --o-tree final-unrooted-tree-ITS.qza \
  --o-rooted-tree final-rooted-tree-ITS.qza
```

*Exportation of phylogenetic tree. See figure 4.1 as a result *

```
qiime tools export \
  --input-path unrooted-tree.qza \
  --output-path exported-tree
```

****Calculation of alfa beta diversity****

Sampling depth values were chosen visualizing results of rarefaction curves. Given that even the lowest count-level was reasonably high with only a small difference to the maximum count, the sample value with the lowest count was used as sampling depth in both 16S as well as ITS.

```
qiime diversity core-metrics-phylogenetic \
  --i-phylogeny final-rooted-tree-16S.qza \
  --i-table table-final-16S.qza \
  --p-sampling-depth 39731 \
  --m-metadata-file final-metadata-16S.tsv \
  --output-dir final-core-metrics-results-16S
```

```
qiime diversity core-metrics-phylogenetic \
  --i-phylogeny final-rooted-tree-ITS.qza \
  --i-table final-table-ITS.qza \
```

```
  --p-sampling-depth 70198 \
  --m-metadata-file final-metadata-ITS.tsv \
  --output-dir final-core-metrics-results-ITS
```

****Taxonomical alignment to generate reference-sequences****

16S

```
qiime tools import \
  --type 'FeatureData[Sequence]' \
  --input-path sh_refs_qiime_ver8_dynamic_10.05.2021.fasta \
  --output-path final-ref-seqs-16S.qza

qiime tools import \
  --type 'FeatureData[Taxonomy]' \
  --input-format HeaderlessTSVTaxonomyFormat \
  --input-path sh_taxonomy_qiime_ver8_dynamic_10.05.2021.txt \
  --output-path final-ref-taxonomy-16S.qza

qiime feature-classifier fit-classifier-naive-bayes \
  --i-reference-reads ref-seqs.qza \
  --i-reference-taxonomy ref-taxonomy.qza \
  --o-classifier classifier.qza
```

extract-reads only applied to 16S sequences, used to extract “sequencing-like” reads from a reference base to train the classifier. It is not recommended for ITS sequences as can be seen in: https://docs.qiime2.org/2018.4/tutorials/feature-classifier/#extract-reference-reads

```
qiime feature-classifier extract-reads \
  --i-sequences silva-138-99-seqs.qza \
  --p-f-primer CCTACGGGNGGCWGCAG \
  --p-r-primer GACTACHVGGGTATCTAATCC \
  --p-trunc-len 416 \
  --p-min-length 374 \
  --p-max-length 466 \
  --o-reads ref-seqs-16S.qza

qiime taxa barplot \
  --i-table final-table-16S.qza \
  --i-taxonomy final-taxonomy-16S.qza \
  --m-metadata-file final-metadata.txt \
  --o-visualization final-taxa-bar-plots-16S.qzv

qiime taxa barplot \
  --i-table final-table-ITS.qza \
  --i-taxonomy final-taxonomy-ITS.qza \
  --m-metadata-file final-metadata.txt \
  --o-visualization final-taxa-bar-plots-ITS.qzv
```

taxa colapse, to summarize results on different taxonomical levles – Phylum, Family and Genus

the value of level 2 can be replaced by level 5 and 6

16S

qiime taxa collapse \

--i-table final-table-16S.qza \

--i-taxonomy final-taxonomy-16S.qza \

--p-level 2 \

--o-collapsed-table final-taxa-collapsed-16S.qza

qiime feature-table summarize \

--i-table taxa-collapsed.qza \

--o-visualization taxa-collapsed-16S.qzv

ITS

qiime taxa collapse \

--i-table final-table-ITS.qza \

--i-taxonomy taxonomy-final-ITS.qza \

--p-level 2 \

--o-collapsed-table final-taxa-collapsed-ITS.qza

3.19 APPX 4.3

Raw data quality statistics

		Dry Season Samples				Rainy Season Samples			
		Total read bases	Total reads	Q20%	Q30%	Total read bases	Total reads	Q20%	Q30%
16S	min	46,786,236	155,436	93.08	85.41	43,684,732	145,132	93.59	85.74
	max	65,521,078	217,678	93.62	86.24	57,995,476	192,676	94.06	86.67
	average	59,042,384	179,134	93.45	86.01	52,865,583	175,633	93.75	86.17
ITS	min	62,969,802	209,202	93.92	86.94	51,375,884	170,684	94.58	87.47
	max	72,625,280	241,280	94.91	88.54	63,022,176	209,376	95.03	88.52
	average	66,727,035	221,685	94.36	87.68	58,774,991	195,266	94.79	88.17

3.20 APPX 4.4

Heatmap creation

16S

```
qiime feature-table heatmap \
--i-table final-taxa-collapsed-16S.qza \
--m-sample-metadata-file metadata-final-16S.txt \
--m-sample-metadata-column altura \
--p-cluster features \
--p-color-scheme winter \
--o-visualization final-heatmap-16S.qzv \
--verbose

qiime feature-table heatmap \
--i-table final-taxa-collapsed-16S.qza \
--m-sample-metadata-file metadata-final-16S.txt \
--m-sample-metadata-column altura \
--p-cluster features \
--p-color-scheme coolwarm \
--o-visualization final-heatmap-16S-coolwarm.qzv \
--verbose
```

ITS

```
qiime feature-table heatmap \
--i-table final-taxa-collapsed-ITS.qza \
--m-sample-metadata-file metadata-final-ITS.txt \
--m-sample-metadata-column altura \
--p-cluster features \
--p-color-scheme magma \
--o-visualization final-heatmap-ITS-magma.qzv \
--verbose
```

Heatmap for 16S bacteria:

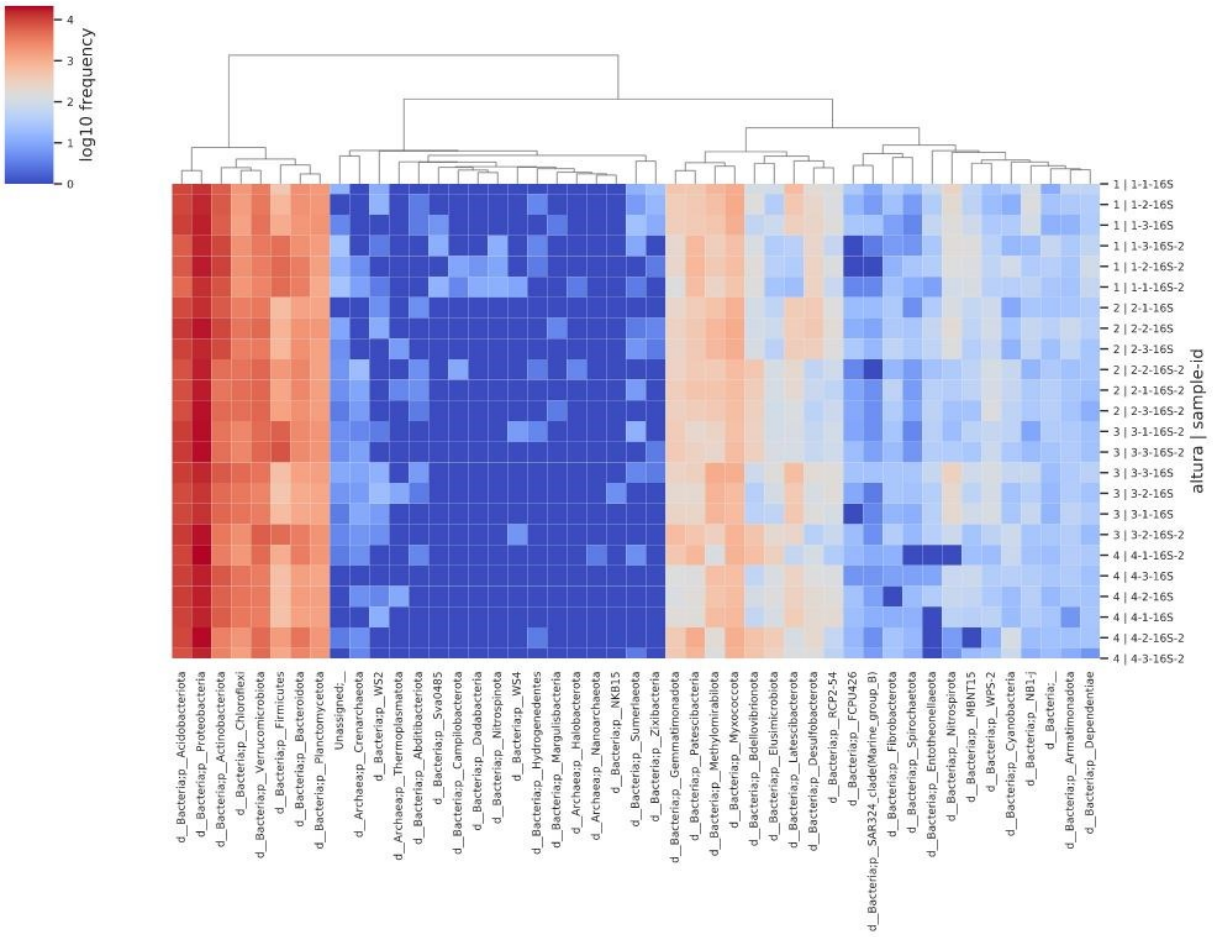

Heatmap for ITS fungi:

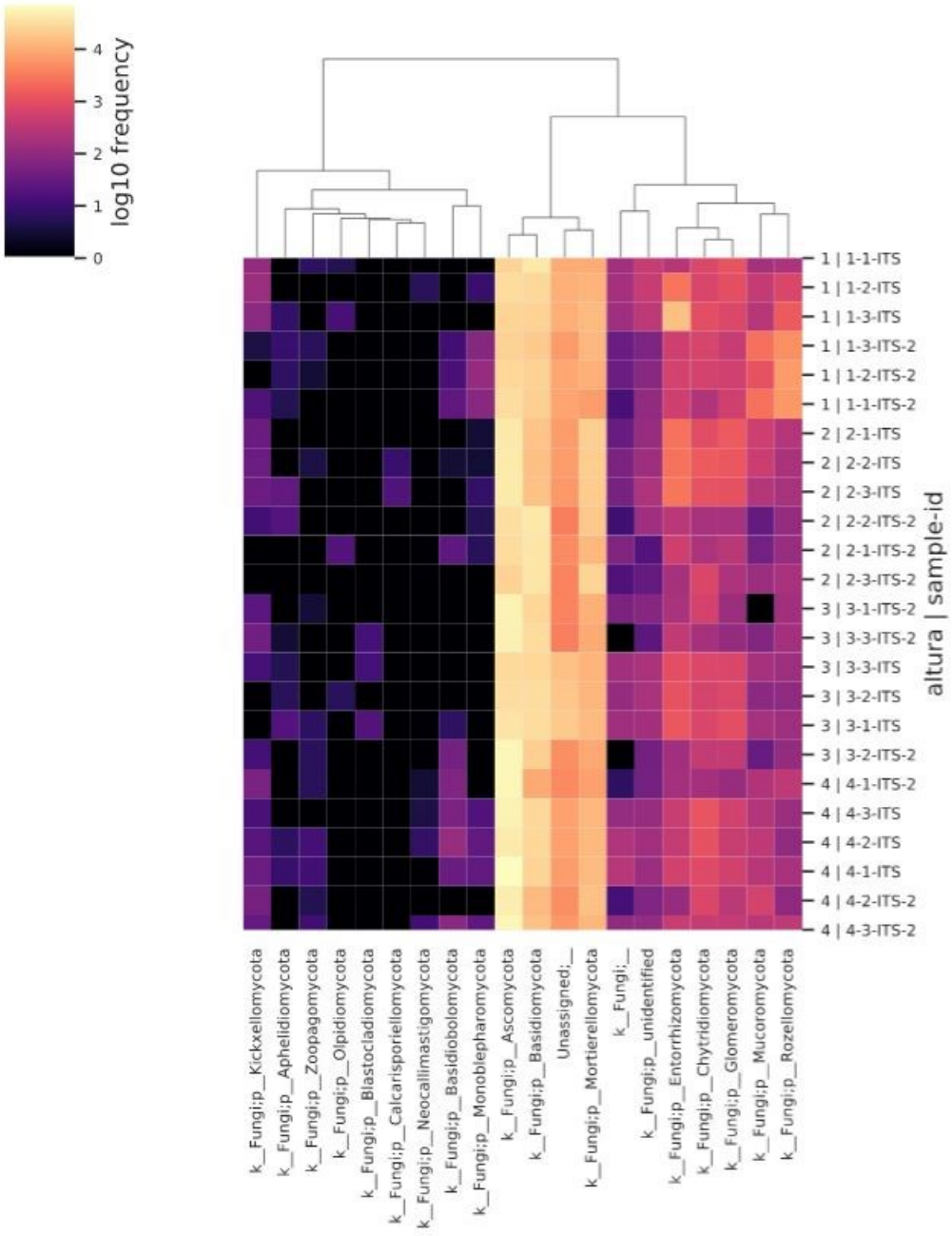

7.15 APPX 5 Publication

microorganisms MDPI

Article

Prospection of Psychrotrophic Filamentous Fungi Isolated from the High Andean Paramo Region of Northern Ecuador: Enzymatic Activity and Molecular Identification

Stefan Alexander Brück [1,2,3], Alex Graça Contato [2], Paul Gamboa-Trujillo [1,3], Tássio Brito de Oliveira [4], Mariana Cereia [4] and Maria de Lourdes Teixeira de Moraes Polizeli [2,4,*]

[1] Facultad de Ciencias Biológicas, Universidad Central del Ecuador, Quito 170403, Ecuador; brueck.stefan@gmail.com (S.A.B.); jpgamboa@uce.edu.ec (P.G.-T.)
[2] Departamento de Bioquímica e Imunologia, Faculdade de Medicina de Ribeirão Preto, Universidade de São Paulo, Ribeirão Preto 14049-900, Brazil; alexgraca.contato@gmail.com
[3] Facultad de Ingeniería Química, Universidad Central del Ecuador, Quito 170521, Ecuador
[4] Departamento de Biologia, Faculdade de Filosofia, Ciências e Letras de Ribeirão Preto, Universidade de São Paulo, Ribeirão Preto 14050-901, Brazil; oliveiratb@yahoo.com.br (T.B.d.O.); macereia@ffclrp.usp.br (M.C.)
* Correspondence: polizeli@ffclrp.usp.br; Tel.: +55-16-3315-4680

Abstract: The isolation of filamentous fungal strains from remote habitats with extreme climatic conditions has led to the discovery of a series of enzymes with attractive properties that can be useful in various industrial applications. Among these, cold-adapted enzymes from fungi with psychrotrophic lifestyles are valuable agents in industrial processes aiming towards energy reduction. Out of eight strains isolated from soil of the paramo highlands of Ecuador, three were selected for further experimentation and identified as *Cladosporium michoacanense*, *Cladosporium* sp. (cladosporioides complex), and *Didymella* sp., this last being reported for the first time in this area. The secretion of seven enzymes, namely, endoglucanase, exoglucanase, β-D-glucosidase, endo-1,4-β-xylanase, β-D-xylosidase, acid, and alkaline phosphatases, were analyzed under agitation and static conditions optimized for the growth period and incubation temperature. *Cladosporium* strains under agitation as well as incubation for 72 h mostly showed the substantial activation for endoglucanase reaching up to 4563 mU/mL and xylanase up to 3036 mU/mL. Meanwhile, other enzymatic levels varied enormously depending on growth and temperature. *Didymella* sp. showed the most robust activation at 8 °C for endoglucanase, β-D-glucosidase, and xylanase, indicating an interesting profile for applications such as bioremediation and wastewater treatment processes under cold climatic conditions.

Keywords: psychrotrophic fungi; high Andean Paramo; cold-adapted enzymes; bioprospecting

check for updates

Citation: Brück, S.A.; Contato, A.G.; Gamboa-Trujillo, P.; de Oliveira, T.B.; Cereia, M.; de Moraes Polizeli, M.d.L.T. Prospection of Psychrotrophic Filamentous Fungi Isolated from the High Andean Paramo Region of Northern Ecuador: Enzymatic Activity and Molecular Identification. *Microorganisms* **2022**, *10*, 282. https://doi.org/10.3390/microorganisms10020282

Academic Editor: Carlos A. Jerez

Received: 29 October 2021
Accepted: 14 January 2022
Published: 26 January 2022

Publisher's Note: MDPI stays neutral with regard to jurisdictional claims in published maps and institutional affiliations.

1. Introduction

The High Andean mountain region is marked by the paramo ecosystem, neotropical grassland covering mountainsides from 3500 up to 5000 m of altitude from Southern Venezuela, Colombia, Ecuador, and Northern Peru [1]. It is considered a hotspot of biodiversity mainly due to the fact of its high degree of endemic species adapted to extreme environmental conditions [2] such as intense radiation close to the equator line [3], nighttime temperatures close to the freezing point, and low availability of nutrients [4]. Fungi growing under these conditions tend to develop a psychrophilic or psychrotrophic profile, developing at 0 °C with optimum growth conditions of ≤15 and 15–20 °C, respectively [5,6]. This restricted ecological group has been found in terrestrial and marine environments from Polar Regions, deep water and marine sediments of the oceans, and high mountains [7–9].

The Paramo Region of South America is a vastly unexplored area in terms of soil-derived microorganisms. Geospatial separation by Andean mountain chains creates a series of unique habitats, forcing microbes to adapt to a variety of given conditions, increasing

the biological diversity with unique species within different paramo regions [10]. Most surveys of soil-borne fungi were conducted in the Colombian Paramo Region [11–13]. Information about fungi composition in Ecuadorian paramo soils is very scarce [14], and screenings for active enzymatic fungi with possible industrial applications have not been performed yet. Fungi isolated from the paramo can secrete cold-adapted enzymes [15], which are interesting in industrial procedures requiring low temperatures and employing energy to cool down the process. Nowadays, cold-active enzymes are mostly used in meat tenderization, food processing, flavoring, baking, brewing, cheese production, and animal feed [16,17]. They require low activation energies while showing during the meantime the highest activities, at low temperatures, of up to a 10-fold increase compared to mesophilic homologues [18], allowing for energy reduction [19], which might become increasingly important due to the tendency towards neutral carbon dioxide balances in times of global warming [20].

Enzymes can break down plant cell wall components, such as those of the cellulolytic system (endoglucanases, exoglucanases, and β-glucosidase), for efficient cellulose cleavage and of the xylanolytic system (mainly endoxylanase and β-xylosidase) for xylan breakdown to the level of reducing sugars. They are widely applied to biotechnological processes in areas such as the food industry, production of fuels, detergents, and biopulping [21–24]. Especially interesting for these cold-adapted enzymes are the treatment of wastewater and environmental bioremediation in countries with shallow temperatures due to the necessity of stable in situ applications without the need for heating [25,26].

Fungi further gain increasing importance as biofertilizers to improve crop yield. Given the broad range of climatic zones where crops are planted, biofertilizers must be equally adapted to these conditions including cold regions with generally lower productivity [6]. Cold adapted phosphatases can hydrolyze organic phosphate sources, which become assimilable by plant roots, improving their economic and ecologic growth, eliminating the need for chemical fertilizers [9,27].

The present study, therefore, aimed to investigate filamentous fungi from paramo soil and optimize incubation conditions for optimal enzyme activity yield to analyze whether their extreme living conditions led to adapted enzymes of the carbon and phosphate cycle with possible interesting applications in the industry comparable to reported enzyme activities for mesophilic fungi. Unfortunately, soil-associated fungi of this region are poorly described and have never been analyzed for their enzymatic hydrolyzation capacities to the best of our knowledge.

2. Materials and Methods

2.1. Sample Collection and Preparation

Two sampling sites were established, each at two different altitudes within the grassland paramo (4000 m asl) and at the frontier between grassland paramo and superparamo (4150 m asl), lying on a lineal transect towards the peak of the volcano Northern Iliniza to guarantee similar climatic conditions and soil characteristics (Figure 1). Each sampling site was carefully selected for level ground, open vegetation in a good conservation state, and the absence of animal signs or human interference. Georeferencing with a GPS (Garmin, Olathe, KS, USA) was applied at each sampling site (Table S1). Then, 10 cm of topsoil was removed together with vegetation, and three soil samples were taken with sterile instruments, giving 12 samples. Data dataloggers (HOBO, Lakeville, MN, USA) were established at different altitudes to collect temperature data. Soil samples were analyzed by the Ecuadorian National Institute for Agricultural Research (INIAP) for organic matter (OM), total nitrogen (Nt), phosphorus, potassium, calcium magnesium (Olsen modified), and sulfur (calcium phosphate standard protocols). Conductivity was measured with water-saturated paste and pH in a soil-to-water ratio of 1:2.5.

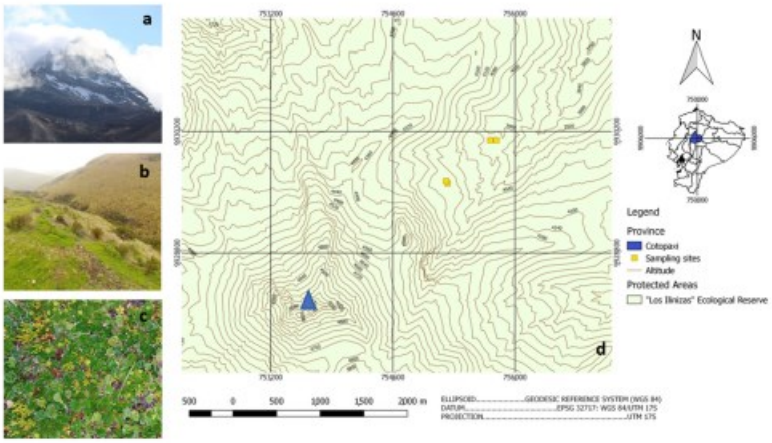

Figure 1. Sampling sites with a vision of the Illiniza north volcano (**a**); typical Andean grass paramo landscape (**b**); typical conserved paramo vegetation (**c**); the georeferenced linear transect of sampling towards the volcano peak (blue triangular) at the bottom left (**d**) (Source: (**a**–**c**) Author 2020; (**d**) modified from [28]).

Soil samples were diluted with sterile water at dilutions of 0.1 g in 10, 100, and 1000 mL with three replicates each, and 50 µL of each dilution were distributed with a sterilized spreading rod on 10 cm Petri dish containing 12 mL of potato dextrose agar (PDA) (Sigma–Aldrich, Saint Louis, MO, USA) with streptomycin at 1 mg/mL (GM, London, UK). Then, Petri dishes were incubated for 48 h at 20 °C. After incubation, eight samples of clearly isolated and visibly round-shaped fungal colonies were picked with sterile toothpicks and transferred to a fresh PDA petri dish for cultivation.

For the growth assay, each fungus was picked with a sterile toothpick and inoculated at the center of a PDA Petri dish. Then dishes were incubated at 4, 30, and 40 °C, respectively, for a total of 35 days. Growth was measured weekly in cm growth-diameter of the halo through the inoculation point.

2.2. *Fungal Strain Identification*

2.2.1. DNA Extraction

To obtain genomic DNA of three fungal strains, the mycelia were macerated with a mortar and pestle in TES lysis buffer (Tris 100 mM; EDTA 10 mM; 2% SDS). First, lysed tissue was incubated at 65 °C for 15 min. Then, 140 µL of 5 M NaCl were added, and the mixture was incubated on ice for 30 min. Afterward, 600 µL of chloroform/isoamyl alcohol (24:1) were added and centrifuged at 10,000× *g* for 10 min at 4 °C. The supernatant was isolated and mixed with 50 µL sodium acetate 3 M (pH 5.2) and 300 µL isopropanol. After the second centrifugation under the same conditions, the supernatant was discarded, and the mixture was washed twice with 600 µL of 70% ethanol following centrifugation steps. After discarding the final supernatant, the resulting pellet was diluted in 50 µL TE buffer (Tris 10 mM; EDTA 1 mM) and 5 µL RNAse (10 mg/mL).

2.2.2. Polymerase Chain Reaction

Genomic DNA was used to amplify the fungal ITS region (ITS1-5.8S-ITS2) applying the primer pairs ITS4 and ITS5 [29]. For amplification reactions, a PCR Master Mix Kit was used (Promega, Madison, WI, USA), following the manufacturer's instructions. To visualize the amplification, product electrophoresis was performed on a 1% agarose gel stained with Nancy dye (Sigma–Aldrich, Saint Louis, MO, USA). Next, the amplification products were purified using the Wizard® SV Gel kit and PCR Clean-Up System (Promega) following the kit's instructions. Finally, the PCR product was quantified on a NanoDrop® (Thermo Scientific, Waltham, MA, USA).

2.2.3. DNA Sequencing

Sequencing reactions were performed with the BigDye® Terminator Cycle Sequencing Kit (Life Technologies, Carlsbad, CA, USA) following the manufacturer's instructions and analyzed with ABI 3500 XL sequencer system (Life Technologies). Resulting forward and reverse sequences were quality checked and merged into a consensus sequence with BioEdit v.7.0.5.3 [30]. The BLASTn tool of the public NCBI-GenBank (www.ncbi.nlm.nih.gov) and the Trichokey database (http://isth.info/) were used to compare contigs with homologous sequences (both accessed on 12 April 2019). After a second, quality control sequences were aligned with homologous sequences from culture collections applying the ClustalW tool [31]. Then, the sequences were subjected to phylogenetic analysis. The phylogeny was assembled using the neighbor-joining method, calculating the evolutionary distance using the 2-parameter Kimura model, and are expressed as the units of the number of base substitutions per site. The rate variation among sites was modeled with a gamma distribution (shape parameter = 1). The analysis involved 58 nucleotide sequences. All positions containing gaps and missing data were eliminated. There was a total of 430 positions in the final data set. Tree support was calculated with bootstrap analysis with 1000 pseudo-replications, and the tree was inferred using MEGA v.7.0 [32].

2.3. Preparation of Crude Enzyme Extract

Isolated fungi were pre-cultured at 20 °C on inclined agar PDA medium in test tubes until sporulation. Concentrations of 10^6–10^7 spores per mL were established in sterile water using a Neubauer chamber for counting. These spores were then used to inoculate 50 mL of sterile Adam's medium (pH = 6) with 1% wheat bran in 125 mL Erlenmeyer flasks (Adam's medium for 50 mL: 0.05 g KH_2PO_4, 0.025 g $MgSO_4 \cdot 7H_2O$, 0.1 g yeast extract, and 1 g glucose + 50 mL H_2O distilled). Triplicates were incubated at 20 °C under static and shaking conditions (120 rpm), respectively, for 120 h harvesting each 24 h. Each crude extract sample from flasks was filtered over Whatman paper using a vacuum pump and applied on the same day for enzyme assays.

2.4. Enzyme Activity Assay

2.4.1. Enzyme Determination with Natural Substrates

To measure enzyme activity, the crude enzyme extract was mixed with respective water-diluted substrates to obtain activity over time according to the Miller method [33]. Reducing sugars were quantified using 3,5-dinitrosalicylic acid (DNS) combined with 0.5% carboxymethylcellulose (CMC) (endoglucanase measurement) (Sigma–Aldrich®) and 0.5% xylan beechwood (endoxylanase measurement) in the following relation: 25 µL substrate, 10 µL buffer sodium acetate 50 mM pH 5.0, and 15 µL crude extract. Mixes were incubated in a thermocycler (Eppendorf®, Hamburg, Germany) for 20 min at 30 °C. In the assay to determine optimal incubation temperatures, a range was established from 4 to 32 °C. Then, 50 µL DNS was added to interrupt enzyme activity, and sample-absorbance was measured at 540 nm on a spectrophotometer (Shimadzu, Kyoto, Japan) compared to glucose and xylose standard curves (0–1 mg/mL). Blancs were established adding enzyme extract after incubation, directly interrupting the reaction with DNS. The results were expressed as

milliunits per mL (mU/mL), defined as the enzyme quantity that releases one µmol of reducing sugars per minute per mL.

2.4.2. Enzyme Determination with Synthetic Substrates

To measure enzyme activity, the crude enzyme extract was mixed with respective water-diluted substrates to obtain activity over time. The amount of released *p*-nitrophenol as a result of enzyme cleavage was measured for the following substrates: *p*-nitrophenol-β-D-glycopyranoside (β-D-glucosidase measurement), *p*-nitrophenol-β-D-xylanopyranoside (β-D-xylosidase measurement), and *p*-nitrophenol-β-D-cellobiose (exoglucanase measurement) (all substrates obtained from Sigma—Aldrich®) used in the following relation: 25 µL substrate, 10 µL sodium acetate buffer 50 mM pH 5.0, and 15 µL crude extract [34].

For the measurement of phosphatases with *p*-nitrophenyl phosphate (acid and alkaline phosphatase), the assay mix was prepared accordingly using 10 µL crude extract, 40 µL substrate, and 100 µL buffer, where acid phosphatase was measured with acetate buffer 100 mM, pH 4.5 and alkaline phosphatase with Tris-HCl 100 mM, pH 8.0 (modified according to [35]). Mixes were incubated in a thermocycler (Eppendorf®) for 20 min at 30 °C. In the assay to determine optimal incubation temperatures, a range was established from 4 to 32 °C in steps of 4 °C. Then, 50 µL (100 µL for phosphatases) of 0.2 M Na_2CO_3 solution was added to interrupt enzyme activity and sample-absorbance was measured at 410 nm compared to a *p*-nitrophenol–standard curve (0–1 mg/mL) [36]. Blancs were established by adding enzyme extract after incubation, directly interrupting the reaction with Na_2CO_3 solution. The results are expressed as milliunits per mL (mU/mL), defined as the enzyme quantity that releases one µmol of *p*-nitrophenol per minute per mL.

2.5. Statistical Analysis

Measured enzyme activity is expressed as the mean ± standard deviation using Microsoft EXCEL. The Shapiro–Wilk test was used to prove the normal distribution of data and the Levene's test for homoscedasticity. To test for statistical difference between incubation types (i.e., agitation and static), averages of the maximum enzyme activities were compared using the *t*-test for independent variables or Mann–Whitney U test, respectively. To analyze maximum yields among the three studied fungi, one-way ANOVA or Kruskal–Wallis's test were applied following Sidak–Bonferroni or Dunn post-hoc tests. All statistical analyses were performed using licensed STATA 16.0.

3. Results and Discussion

3.1. Sample Site Conditions and Soil Characteristics

This sampling sites in the Iliniza National Reserve were chosen due to the fact of their proximity to glacial areas of stratified volcanos in the High Andean region. At a 4000 m altitude, the vegetation zone of conserved paramo highlands is grassland, mainly characterized by herbaceous plants such as sphagnum mosses, tussock grass, and rosette plants (Figure 1b,c). At 4150 m asl, the zone of the superparamo builds the frontier between the last zone of abundant vegetation and the beginning of the rocky glacial zone with only sporadic vegetation. Close to the equator, the radiation at this altitude is very high, causing drastic daily temperature changes between day and nighttime with an average temperature of 9.6 °C (Table S1). Due to the volcanic ash deposition and slow decomposition, the slightly acidic soil (pH 5.87–6.15) has mainly a sandy–loam texture with 7.7–9% organic matter, which is very high, as expected for Andisols [37]. The stabilization of large organic particles also accounts for its vast water retention capacity [38], which, together with the related oxygen availability, directly interferes with the development of microorganisms and the solubilization of phosphorus [39]. The formation of humic acids in the breakdown of organic matter allows for the formation of metal–humus complexes retaining chelated ions like calcium [40] and magnesium [41], which might explain their abundance in analyzed soils and further account for the observed high levels of conductivity [42]. On the other hand, under the environmental conditions of the paramo region, organic matter breakdown is

slow. It might negatively interfere with nutrient availability due to the microbial activity as indicated by the observed low phosphorus, sulfur [43], and nitrogen levels (Table 1) [44–46].

Table 1. Soil characteristics at sampling sites.

Sample Site	Soil Type	Soil Texture	pH	COND (µS/cm²)	Nt %	OM %	P (ppm)	S (ppm)	K (meq/100 g)	Ca (meq/100 g)	Mg (meq/100 g)
1	Andisol	sandy loam, loamy	6.15	21.5	0.31	8.8	9.01	8.4	0.54	9.78	1.71
2			6.78	21.3	0.36	9.7	14	9.3	0.48	9.76	1.28
3	Andisol	sandy loam	5.93	15.51	0.25	7.7	6.04	4.7	0.42	7.49	1.01
4			5.87	20.8	0.27	9	12	4.1	0.37	4.87	0.73

COND = conductivity, Nt = total nitrogen, and OM = organic matter.

3.2. Screening for Cultivable Fungi

The first screening for cultivable fungal strains from soil samples showed relatively few growing colonies clearly separated from each other, allowing for easy isolation of distinct strains. Out of 12 soil samples, eight colonies were chosen for the study. These strains were further screened for their capacity to grow at different temperature conditions. Generally, all strains showed better growth at 4 °C than 30 °C, indicating their adaptation to cold environments (Figure S1). At 40 °C, no development could be detected. The results showed a potentially psychrophilic profile for the best growing behavior of strain 3.3 at 4 °C given that it was not able to grow at 30 °C and psychrotrophic profiles for the strains 1.1 and 3.1 at 30 °C [5], which were chosen for further experimentation (Figure S2).

3.3. Identification of Fungi

Phylogenetic analysis of the ITS region revealed that all three fungi were ascomycetes with strains 1.1 and 3.1 belonging to the genus *Cladosporium*: *C. michoacanense* and *Cladosporium* sp. 3.1 (*C. Cladosporioides* species complex), respectively, and 3.3 to the genus *Didymella* (Figure 2). Since the ITS region is not sufficient for species delimitation in some of these groups, other secondary barcodes would be needed for more accurate identification. The genus *Cladosporium* is a highly heterogeneous group with cosmopolitan distribution and strong capability of adaptation [47] with species formerly isolated from arctic soils [8,23] and marine sponges [48]. A third strain belonged to the genus *Didymella* which has mainly been studied due to the existence of pathological strains and plant–host interaction [49] but so far to a lesser extent due to the fact of its resistance to extreme conditions and, therefore, its arising enzymatic capacities [50]. Both *Cladosporium* and *Didymella* strains have formerly been reported in soil isolates from Himalaya mountain environments [51,52]. Still, only *Cladosporium* has formerly been described for Andean regions [12,14], and the present study is the first registry of the genus *Didymella* in the paramo ecosystem.

Images taken of the growth behavior in culture dishes of PDA indicate a dark brown colorization of mycelia, which possibly shows intense melanin pigmentation as a protective adaptation to the strong radiation in their natural habitat as formerly described [53,54] (Figure S3d–f). Furthermore, differential growth behavior was detected under static and agitation conditions (Figure S3g–i). Especially, the *Cladosporium* strains tended to grow better under agitation, developing a darker aspect apparently due to the stronger sporulation [55]. Meanwhile, its impact on *Didymella* was less evident.

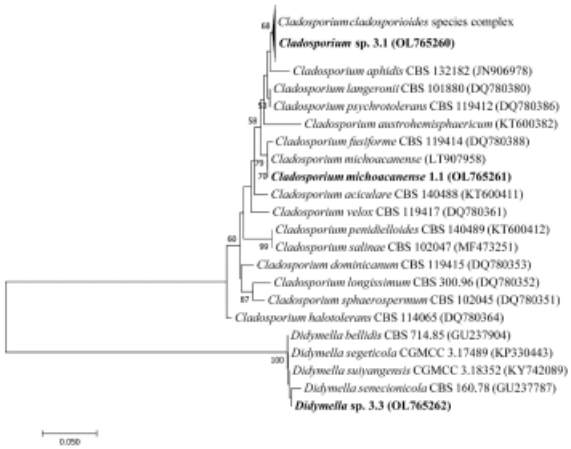

Figure 2. Phylogenetic analysis of filamentous fungi isolated from paramo soil samples (bold) and the closest related species.

3.4. Enzymatic Characterization

The following section shows the incubation time-dependent enzyme secretion results from 24 to 120 h under agitation and static condition for each isolated fungal strain to characterize the hydrolyzation capacities at 30 °C.

3.4.1. Enzymatic Production of *Cladosporium michoacanense*

Cladosporium michoacanense 1.1 showed the most potent activation under agitation with a relatively late onset of enzyme secretion compared to studies analyzing the same enzymes [34] (Table 2). The most significant activity was detected at 72 h for the hydrolyzation of CMC, xylan, and *p*np-phosphate in an alkaline medium; 96 h for *p*np-β-D-glycopyranoside; 120 h for *p*np-β-D-cellobiose, *p*np-β-D-xylanopyranoside, and *p*np-phosphate in acidic medium, indicating statistically significant differences to measurements under static conditions for all enzymes except for exoglucanase and β-glucosidase. Interestingly, under static incubation conditions, the most potent enzyme activity was measured early between 24 to 48 h for endoglucanase, xylanase, β-xylosidase, and alkaline phosphatase and late response at 120 h for exoglucanase, β-glucosidase, and acid phosphatase. Overall, the most efficient enzyme activity for endoglucanase and xylanase could be observed at levels well above 2000 mU/mL under agitated cultivation.

Table 2. *Cladosporium michoacanense* 1.1 enzymes produced overtime under agitation and static conditions.

	Agitation					Static				
Enzyme	**24 h**	**48 h**	**72 h**	**96 h**	**120 h**	**24 h**	**48 h**	**72 h**	**96 h**	**120 h**
Endoglucanase	932.2 ± 20.7	1514.4 ± 100.5	**2503.7 ± 207.1** *	394.5 ± 51.8	385.2 ± 170.0	887.4 ± 84.8	**1061.0 ± 23.3**	917.6 ± 17.1	791.4 ± 70.4	730.6 ± 26.9
Exoglucanase	ND	ND	ND	1.4 ± 0.7	**1.4 ± 0.3**	ND	ND	ND	ND	**0.2 ± 0.1**
β-Glucosidase	ND	ND	ND	**1.7 ± 0.0**	ND	ND	ND	ND	ND	**0.2 ± 0.0**
Xylanase	360.2 ± 105.7	969.4 ± 120.1	**2430.1 ± 2.1** *	274.6 ± 81.3	145.2 ± 34.7	**737.8 ± 88.5**	435.5 ± 111.7	412.2 ± 53.9	353.0 ± 119.5	384.3 ± 70.6
β-Xylosidase	ND	ND	0.7±0.	1.1 ± 0.3	**1.4 ± 0.3** *	**0.5 ± 0.1**	ND	ND	ND	ND
Acid phosphatase	1.4 ± 0.6	1.7 ± 1.0	31.0 ± 0.3	5.9	**34.9 ± 0.1** *	ND	ND	ND	ND	**0.7 ± 0.4**
Alkaline phosphatase	0.3±0.1	1.4 ± 0.3	**2.3 ± 0.4** *	0.2 ± 0.2	ND	**1.4 ± 0.3**	0.6 ± 0.3	ND	ND	ND

Data are expressed as mU/mL ± standard deviation. ND = not detected; * indicates a statistically significant difference ($p < 0.05$) between the average enzyme activity of fungi cultivated under agitation vs. static conditions for each analyzed enzyme. In bold, maximum achieved activity.

3.4.2. Enzymatic Production of *cladosporium* sp. (*C. Cladosporioides* Species Complex)

Cladosporium sp. 3.1 indicated the best hydrolyzation performance under agitation at 120 h for most enzymes (Table 3). The late onset in enzyme production is consistent with previous studies [56]. Exceptions were endoglucanase with the highest enzyme secretion at 48 h, β-xylosidase at 24 h, and xylanase at 72 h. Under static conditions, the strongest enzyme secretion was observed at 72–96 h for most enzymes with significantly lower activity values than under agitation conditions, which is coherent with the increased pellet formation observed by comparing the incubation flasks of *C. Cladosporioides* under static and agitation conditions (Figure S3g,h). This phenomenon was formerly described by Raikumar et al. for this genus [55]. Xylanase was the only exception that performed better under static conditions at 72 h of incubation. Agitation leads to better aeration and distribution of heat and nutrients bearing growth benefits for many filamentous fungi [57]. Comparing both analyzed *Cladosporium* species, an advanced enzyme production upon agitation was observed, and a relative early specialization in the production of endoglucanase and xylanase indicated a focus on the breakdown of large sugar polymers such as cellulose and hemicellulose [58]. All remaining enzymes showed a rather late onset.

Table 3. *Cladosporium cladosporioides* sp. 3.1 enzyme activity over time und agitation and static conditions.

	Agitation					Static				
Enzyme	**24 h**	**48 h**	**72 h**	**96 h**	**120 h**	**24 h**	**48 h**	**72 h**	**96 h**	**120 h**
Endoglucanase	393.2 ± 97.3	**1274.0 ± 102.0**	328.5 ± 68.6	14.0 ± 11.4	14.6 ± 11.9	761.0 ± 70.4	638.8 ± 140.4	945.3 ± 120.6	**1076.4 ± 149.4**	775.0 ± 156.2
Exoglucanase	ND	ND	3.6 ± 1.0	6.0 ± 0.3	**12.0 ± 0.6** *	ND	ND	0.7 ± 0.4	**0.9 ± 0.6**	1.0 ± 0.0
β-Glucosidase	0.2 ± 0.2	0.8 ± 0.2	5.7 ± 1.0	8.7 ± 2.9	**11.1 ± 0.8** *	ND	ND	**0.7 ± 0.4**	ND	ND
Xylanase	156.0 ± 8.3	861.0 ± 11.9	**958.9 ± 15.5**	481.0 ± 57.0	ND	522.1 ± 87.6	660.0 ± 56.1	**1113.0 ± 865**	937.5 ± 40.4	898.0 ± 62.1
β-Xylosidase	**1.2 ± 0.3**	0.4 ± 0.1	ND	ND	ND	**1.0 ± 0.1**	ND	ND	ND	ND
Acid phosphatase	0.7 ± 0.4	1.9 ± 0.7	3.4 ± 0.7	6.8 ± 0.3	**13.9 ± 0.5** *	ND	ND	0.3 ± 0.2	**1.0 ± 0.7**	0.9 ± 0.1
Alkaline phosphatase	ND	ND	1.2 ± 0.8	1.9 ± 1.6	**8.0 ± 1.5** *	ND	ND	ND	ND	**1.0 ± 0.3**

Data are expressed as mU/mL ± standard deviation. ND = not detected; * indicates a statistically significant difference ($p < 0.05$) between the average enzyme activity of fungi cultivated under agitation vs. static conditions for each analyzed enzyme. In bold, maximum achieved activity.

3.4.3. Enzymatic Production of *Didymella* sp.

The *Didymella* strain 3.3 showed a rather heterogeneous behavior (Table 4). Meanwhile, CMC and *p*np-β-D-xylanopyranoside were most effectively hydrolyzed under agitation at 24 h and 48 h, respectively. However, the best xylan hydrolyzation occurred at 72 h and for *p*np-β-D-glycopyranoside, *p*np-β-D-cellobiose, and *p*np-phosphate in alkaline medium at

96 h and 120 h in acid medium. Interestingly, while β-glucosidase, β-xylosidase, acid, and alkaline phosphatase showed low but detectable activity under agitation conditions, no activity could be detected under static conditions. On the other hand, endoglucanase, and xylanase, which generally showed much higher activity, performed considerably stronger under static conditions at 96 h. These results confirm the previously described strong influence that culture conditions can exert over enzyme production [34,59].

Table 4. *Didymella* sp. strain 3.3 enzyme activity over time und agitation and static conditions.

	Agitation					Static				
Enzyme	**24 h**	**48 h**	**72 h**	**96 h**	**120 h**	**24 h**	**48 h**	**72 h**	**96 h**	**120 h**
Endoglucanase	**1077.4 ± 6.7**	1037.4 ± 99.0	354.5 ± 6.7	334.4 ± 10.9	119.0 ± 39.4	870.1 ± 99.8	1243.0 ± 108.1	1151.6 ± 189.5	**1413.0 ± 165.7 ***	926.7 ± 15.0
Exoglucanase	0.4 ± 0.2	0.7 ± 0.2	1.0 ± 0.3	**1.7 ± 0.4**	1.7 ± 0.4	0.7 ± 0.2	**1.7 ± 0.1**	0.6 ± 0.2	ND	ND
β-Glucosidase	ND	ND	ND	**1.6 ± 0.7**	0.5 ± 0.1	ND	ND	ND	ND	ND
Xylanase	202.3 ± 15.0	233.0 ± 98.2	**383.0 ± 103.2**	289.2 ± 62.1	ND	873.2 ± 93.7	893.3 ± 125.9	906.0 ± 186.4	**1623.5 ± 196.4 ***	624.7 ± 141.4
β-Xylosidase	**1.0 ± 0.0**	0.5 ± 0.1	0.4 ± 0.1	0.3 ± 0.0	ND	ND	ND	ND	ND	ND
Acid phosphatase	ND	2.7 ± 0.6	5.7 ± 1.1	7.3 ± 1.1	**7.5 ± 1.5**	ND	ND	ND	ND	**0.3 ± 0.1**
Alkaline phosphatase	0.4 ± 0.3	0.4 ± 0.1	1.8 ± 0.1	**2.1 ± 0.5**	ND	ND	ND	ND	ND	ND

Data are expressed as mU/mL ± standard deviation. ND = not detected; * indicates a statistically significant difference ($p < 0.05$) between the average enzyme activity of fungi cultivated under agitation vs. static conditions for each analyzed enzyme. In bold, maximum achieved activity.

3.4.4. Comparison of Relative Enzyme Activity between Acid and Alkaline Phosphatases

Analysis of differential enzyme production between acid and alkaline phosphatase activities generally indicated more substantial secretion of enzymes upon agitation than under static conditions and stronger and prolonged acid phosphatase activity over time. Meanwhile, alkaline phosphatase showed lower and somewhat restricted activation at growth onset for strains 1.1 and 3.1; activation was strongest from 72 to 120 h for strain 3.1 (Figure S4). This behavior matches with the environmental conditions of their habitat, where slightly acidic soil pH was observed (Table 2), which is also the preferred growth condition for most fungi [60]. It further coincides with the tendency that within strain 1.1 and 3.1, measured pH values of crude extract used to drop stronger over time than in strain 3.3 (Figure S5).

3.4.5. Temperature-Dependent Enzyme Activity

After analyzing the best growth time for differential enzyme production, results were used to determine optimal enzyme secretion under different incubation temperatures ranging from 4 to 32 °C under agitation to optimize enzyme production further. The results indicated statistically significant differences among strains (Figure 3). Meanwhile, strain 1.1 showed the best performance at temperatures ranging from 20 to 24 °C for all enzymes related to the carbon cycle and 8–12 °C for phosphatases; strain 3.1 showed somewhat differential activity indicating main enzyme activity for β-glucosidase and exoglucanase from 4 to 8 °C and for endoglucanase, β-xylosidase, and xylanase from 20 to 24 °C. Phosphatases showed opposite behavior with the highest acid phosphatase activity at 12 °C; meanwhile, alkaline phosphatase performed best at 28 °C. This controversial behavior might best be explained by the adaptation capacity of different *Cladosporium* species to varying ecological niches giving rise to its worldwide abundance [47]. It is typical for fungal strains adapted to changing environmental conditions within a single habitat [61,62]. Strain 3.3 finally showed maximum activity for β-glucosidase, endoglucanase, and xylanase at 8 °C and for exoglucanase and β-xylosidase at 20–24 °C. Phosphatase activity remained low, with the highest activity at 16 °C for both acid and alkaline phosphatase.

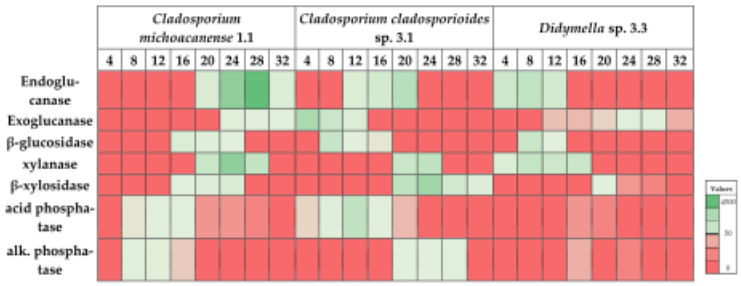

Figure 3. Heatmap analysis of incubation temperature (°C) dependent enzyme performance for each isolated strain. Maximum values ± SD (in mU/mL) are summarized in Table 5.

Table 5. Maximum enzyme activity yield at optimal assay temperature and incubation time for each isolated strain.

	Cladosporium michoacanense 1.1			*Cladosporium Cladosporioides Complex* 3.1			*Didymella* sp. 3.3		
Enzyme	**Maximum Yield ± SD**	**T opt °C**	**IT (h)**	**Maximum Yield ± SD**	**T opt °C**	**IT (h)**	**Maximum Yield ± SD**	**T opt °C**	**IT (h)**
Endoglucanase	**4563** ± 209 ^{a}	28	72	1553 ± 330 ^{b}	20	48	1247 ± 21 ^{b}	8	72
Exoglucanase	107 ± 26 ^{a}	24	96	**2037** ± 254 ^{b}	4	120	127 ± 5 ^{a}	24	96
β-Glucosidase	303 ± 39 ^{a}	16	96	**1013** ± 151 ^{b}	8	96	917 ± 12 ^{b}	8	120
Xylanase	**3036** ± 634 ^{a}	24	72	1290 ± 122 ^{ab}	24	72	1150 ± 121 ^{b}	8	96
β-Xylosidase	430 ± 29 ^{ab}	24	120	**2457** ± 336 ^{a}	24	120	71 ± 5 ^{b}	20	48
Acid phosphatase	97 ± 12 ^{ab}	12	120	**1273** ± 360 ^{a}	12	120	17 ± 5 ^{b}	16	120
Alkaline phosphatase	127 ± 21 ^{a}	8	72	**137** ± 37 ^{b}	28	120	26 ± 7 ^{c}	16	96

Data expressed are as mU/mL ± standard deviation. IT = optimal incubation time; ND = not detected; the letters ^{a} and ^{b} indicate statistically significant differences among enzyme activities comparing the three different fungi ($p < 0.05$) if the letters are not shared between activities of the same enzyme.

The combination of optimal incubation time, agitation, and optimal substrate incubation temperature led to several enzymes' considerably higher activity (Table 5). *Cladosporium* strain 1.1 specialized in producing endoglucanase and xylanase with 4.56 and 3.03 U/mL activities, respectively, both showing significantly higher performances than the other two strains. Comparing these values with formerly described enzymatic activities, even in the mesophilic fungi screenings, especially endoglucanase values, they are quite competitive. For instance, Grujic et al. (2019) [63] described maximum values of 1.1 U/mL for endoglucanase in *Trichoderma guizhouense*, Ghazali et al. (2019) [64] reported the highest values of 3.93 U/mL for *Trichoderma asperellum* and 5.6 U/mL for *Aspergillus niger*. Unfortunately, most studies for psychrotrophic fungi do not apply optimization assays, so comparability is limited. However, considering the advantage of growing under extreme conditions, the *Cladosporium michoacanense* strain is an interesting candidate for potential industrial application under harsh conditions. Moreover, the relatively early onset of enzyme secretion, indicating efficient substrate hydrolyzation at 72 h, represents an important advantage confirming previous results from studies with *Cladosporium* strains [58,65].

On the other hand, *Cladosporium* sp. 3.1 did not reach values as high as strain 1.1 but managed to perform well for all selected enzymes with values above 1 U/mL except alkaline phosphatase. However, the onset of enzyme production appeared relatively late. Interestingly, strain 3.1 showed the significantly highest activation of 2.04 U/mL for exoglucanase at low temperatures, although former studies indicated a relatively poor performance of paramo-derived fungi for these enzymes [11]. Comparing the mesophilic

fungi, results matched with reported highest activities of 1.08 U/mL and 2.37 U/mL in *Trichoderma asperellum* and *Aspergillus niger*, respectively. It is also important to mention that this high activity was reached under conditions of only 4 °C. Furthermore, β-glucosidase, which works synergistically with exoglucanase, also performed well at low temperatures (8 °C). Given that *Cladosporium cladosporioides* had formerly been described to exhibit laccase activity [58,66,67], further studies are needed to determine whether the strain could exhibit lignocellulolytic activity for industrial applications under cold conditions. Moreover, strain 3.1 showed the strongest activation for acid phosphatase, reaching 1.27 U/mL. This result further highlights the importance of applying optimization assays for psychrotolerant enzyme activity given incubation time as well as incubation temperature strongly influenced activity. Therefore, maximum acid phosphatase activity in psychrotrophic fungi of 0.03 U/mL, such as described in a screening study by Gawas-Sakhalkar et al. [68], indicates only a limited comparability to the present results.

Finally, *Didymella* 3.3 performed well only for endoglucanase, β-glucosidase, and xylanase, indicating poor performance for the rest of the enzymes, especially phosphatases, which could be related to the phytopathological behavior of many *Didymella* species allowing for the absorption of nutrients from hosts [49]. Nevertheless, all enzymes that performed better showed the highest values at low temperatures of 8 °C, indicating its potential in producing cold-adapted enzymes [9].

Wide-ranging comparison of psychrotrophic fungi enzyme activity is difficult, given that most screening studies indicate qualitative and semi-quantitative data [7,62,69–71] or activity data at a single temperature and incubation time [61], which is not directly comparable to the presented data. This strongly indicates the importance of performing studies with a more profound analysis of maximum achievable enzyme activities under optimized conditions for psychrotrophic and psychrophilic fungi isolated from habitats with extreme conditions.

4. Conclusions

The present study directly isolated cold-adapted fungal strains from high Andean Paramo soil, of which three strains were chosen to identify the genus and characterize their enzymatic capacity. Selecting for optimal conditions concerning growth period, incubation conditions, and optimal temperature for enzyme performance, maximum enzyme activities were determined for each strain. *Cladosporium* sp. strain 1.1 showed the most competitive enzyme activity of all analyzed strains for endoglucanase and xylanase at 72 h, and agitation and assay temperatures between 24 and 28 °C, indicating an interesting potential for the industrial application processes where reducing sugars are used such as feed animal, food industry, and fuel production. *Cladosporium* strain 3.1 of the *cladosporioides* complex indicated average performance for a broad spectrum of different enzymes except for exoglucanase, which showed the highest activity. Its good performance of acid phosphatase at 12 °C could be applied in the industry of biofertilization to improve the crop yield of plants grown under cold conditions and in the eutrophication of phosphorus from animal feces due to the consumption of phytate in grains [72]. Finally, the *Didymella* strain 3.3 showed high endoglucanase, β-glucosidase, and xylanase activities at temperatures as low as 8 °C, where most enzymes are inactivated. This strain responded closest to a psychrotrophic profile, which could be specifically interesting in industrial processes such as wastewater management and bioremediation in cold conditions, an aspect that might become increasingly important in an industrialized world tending towards energy reduction.

Supplementary Materials: The following are available online at https://www.mdpi.com/article/10.3390/microorganisms10020282/s1, Figure S1: Growth of 8 different isolated fungal strains; Figure S2. Growth curves of isolated fungal strains at 4 °C and 30 °C; Supplementary Figure S3: Selected and identified fungi, from left to right *Cladosporium michoacanense* (a, d, g), *Cladosporium* sp. (cladosporioides species complex)(b, e, h), *Didymella* sp. (c, f, i); Figure S4: Relative phosphate activity over time comparing acidic phosphatase versus alkaline phosphatase; Figure S5: Development of

growth medium pH over time in cultures under agitation (A) and static (S) conditions for strain 1.1, 3.1 and 3.3; Table S1: Sampling sites characteristic.

Author Contributions: Conceptualization, S.A.B., M.d.L.T.d.M.P., and P.G.-T.; methodology, A.G.C., M.C., P.G.-T. and T.B.d.O.; formal analysis, S.A.B. and A.G.C.; resources, M.d.L.T.d.M.P., T.B.d.O. and P.G.-T.; data curation, S.A.B., A.G.C. and T.B.d.O.; writing—original draft preparation, S.A.B.; essay—review and editing, A.G.C., T.B.d.O., M.d.L.T.d.M.P., M.C. and P.G.-T.; visualization, S.A.B.; supervision and funding acquisition, M.d.L.T.d.M.P. All authors have read and agreed to the published version of the manuscript.

Funding: The authors thank the PhD program agreement between the Faculty of Medicine of the Central University of Ecuador and the Faculty of Medicine of the University of São Paulo in Ribeirao Preto which granted a doctorate scholarship to S.A.B. The authors thank Fundação de Amparo à Pesquisa do Estado de São Paulo (FAPESP) for the doctorate grants awarded to A.G.C. (Process no. 2017/25862-6) and the post-doctorate grant awarded to T.B.d.O. (Process no. 2017/09000-4), as well as the financial support from Process no. FAPESP 2008/57908-6 and 2014/50884-5 and Process no. 2018/07522-6, and the Conselho Nacional de Desenvolvimento Científico (CNPq) Process no. 574002/2008-1 and 465319/2014-9. M.L.T.M.P. (Process no. 301963/2017-7) is a Research Fellow at CNPq.

Institutional Review Board Statement: Not applicable.

Informed Consent Statement: Not applicable.

Data Availability Statement: Not applicable.

Acknowledgments: We thank the whole staff at the Laboratory for Applied Microbiology and Biotechnology, especially Emanuelle Neiverth de Freitas, Guilherme Aranha, Rosymar Coutinho de Lucas, and Thiago Pasin for laboratory support; Kevin Toapanta for QGIS support; Wendy Pacheco, Liliana Rojas, Sandy Arguello, and Paola Buitron for fieldwork support in the paramo. Furthermore, we want to thank Rosa Batallas and Diego Inclán at the National Institute of Biodiversity (INABIO) and Carlos Valles at the Ecuadorian Ministry of Environment (MAAE) for the support in permissions to access genetic resources granted in "Contrato Marco No. MAE-DNB-CM-2016-0045".

Conflicts of Interest: The authors declare no conflict of interest. The funders had no role in the study's design, in the collection, analyses, or interpretation of data, in the writing of the manuscript, or in the decision to publish the results.

References

1. Jiménez-Rivillas, C.; García, J.J.; Quijano-Abril, M.A.; Daza, J.M.; Morrone, J.J. A new biogeographical regionalisation of the Páramo biogeographic province. *Aust. Syst. Bot.* **2018**, *31*, 296–310. [CrossRef]
2. Buytaert, W.; Deckers, J.; Wyseure, G. Regional variability of volcanic ash soils in south Ecuador: The relation with parent material, climate and land use. *Catena* **2007**, *70*, 143–154. [CrossRef]
3. Bader, M.Y.; van Geloof, I.; Rietkerk, M. High solar radiation hinders tree regeneration above the alpine treeline in northern Ecuador. *Plant Ecol.* **2007**, *191*, 33–45. [CrossRef]
4. Paucar, B.; Carpio, M.; Alvarado Ochoa, S.P.; Valverde, F.; Parra, R. Análisis de Solubilizadores de Fósforo en Los Suelos Andisoles de Sierra Norte y Centro de Ecuador. Simposio "El Suelo y la Nutrición de Cultivos en el Ecuador". 2015. Available online: http://repositorio.iniap.gob.ec/handle/41000/2501 (accessed on 9 September 2021).
5. Hassan, N.; Rafiq, M.; Hayat, M.; Shah, A.A.; Hasan, F. Psychrophilic and psychrotrophic fungi: A comprehensive review. *Rev. Environ. Sci. Biotechnol.* **2016**, *15*, 147–172. [CrossRef]
6. Rafiq, M.; Hassan, N.; Rehman, M.; Hasan, F. Adaptation mechanisms and applications of psychrophilic fungi. In *Fungi in Extreme Environments: Ecological Role and Biotechnological Significance*; Tiquia-Arashiro, S.M., Grube, M., Eds.; Springer International Publishing: Cham, Switzerland, 2019; pp. 157–174. [CrossRef]
7. Duarte, A.W.F.; Barato, M.B.; Nobre, F.S.; Polezel, D.A.; de Oliveira, T.B.; dos Santos, J.A.; Rodrigues, A.; Sette, L.D. Production of cold-adapted enzymes by filamentous fungi from King George Island, Antarctica. *Polar Biol.* **2018**, *41*, 2511–2521. [CrossRef]
8. Duarte, A.W.F.; dos Santos, J.A.; Vianna, M.V.; Vieira, J.M.F.; Mallagutti, V.H.; Inforsato, F.J.; Wentzel, L.C.P.; Lario, L.D.; Rodrigues, A.; Pagnocca, F.C.; et al. Cold-adapted enzymes produced by fungi from terrestrial and marine Antarctic environments. *Crit. Rev. Biotechnol.* **2018**, *38*, 600–619. [CrossRef]
9. Wang, M.; Jiang, X.; Wu, W.; Hao, Y.; Su, Y.; Cai, L.; Xiang, M.; Liu, X. Psychrophilic fungi from the world's roof. *Pers. Mol. Phylogeny Evol. Fungi* **2015**, *34*, 100–112. [CrossRef] [PubMed]
10. Cortes, A.J.; Garzon, L.N.; Valencia, J.B.; Madrinan, S. On the causes of rapid diversification in the paramos: Isolation by ecology and genomic divergence in espeletia. *Front. Plant Sci.* **2018**, *9*, 1700. [CrossRef] [PubMed]

11. Avellaneda-Torres, L.M.; Pulido, C.P.G.; Rojas, E.T. Assessment of cellulolytic microorganisms in soils of Nevados Park, Colombia. *Braz. J. Microbiol.* **2014**, *45*, 1211–1220. [CrossRef] [PubMed]
12. Landinez-Torres, A.Y.; Becerra Abril, J.L.; Tosi, S.; Nicola, L. Soil microfungi of the colombian natural regions. *Int. J. Environ. Res. Public Health* **2020**, *17*, 8311. [CrossRef] [PubMed]
13. Gualdrón-Arenas, C.; Suárez-Navarro, A.L.; Valencia-Zapata, H. Hongos del suelo aislados de zonas de vegetacion natural del paramo de chisaca, colombia. *Caldasia* **1997**, *19*, 235–245.
14. Pinos León, A.J. Exploring the Microbiome Composition of the Rhizosphere Associated with the Wild Andean Blueberry (*Vaccinium Floribundum*, Kunth) in the Highlands of Ecuador. Master's Thesis, Universidad San Francisco de Quito, Quito, Ecuador, 2020. Available online: https://repositorio.usfq.edu.ec/bitstream/23000/9113/1/141011.pdf (accessed on 5 December 2021).
15. Kuddus, M.; Roohi Arif, J.; Ramteke, P. An overview of cold-active microbial α-amylase: Adaptation strategies and biotechnological potentials. *Biotechnology* **2011**, *10*, 246–258. [CrossRef]
16. Santiago, M.; Ramírez-Sarmiento, C.A.; Zamora, R.A.; Parra, L.P. Discovery, Molecular Mechanisms, and Industrial Applications of Cold-Active Enzymes. *Front Microbiol.* **2016**, *7*, 1408. [CrossRef]
17. Kumar, A.; Mukhia, S.; Kumar, R. Industrial applications of cold-adapted enzymes: Challenges, innovations and future perspective. *3 Biotech* **2021**, *11*, 426. [CrossRef] [PubMed]
18. de Oliveira, T.B.; de Lucas, R.C.; de Almeida Scarcella, A.S.; Pasin, T.M.; Contato, A.G.; Polizeli, M.L.T.M. Cold-active lytic enzymes and their applicability in the biocontrol of postharvest fungal pathogens. *J. Agric. Food Chem.* **2020**, *68*, 6461–6463. [CrossRef]
19. Gerday, C.; Aittaleb, M.; Bentahir, M.; Chessa, J.-P.; Claverie, P.; Collins, T.; D'Amico, S.; Dumont, J.; Garsoux, G.; Georlette, D.; et al. Cold-adapted enzymes: From fundamentals to biotechnology. *Trends Biotechnol.* **2000**, *18*, 103–107. [CrossRef]
20. Niñerola, A.; Ferrer-Rullan, R.; Vidal-Suñé, A. Climate change mitigation: Application of management production philosophies for energy saving in industrial processes. *Sustainability* **2020**, *12*, 717. [CrossRef]
21. Andlar, M.; Rezić, T.; Marđetko, N.; Kracher, D.; Ludwig, R.; Šantek, B. Lignocellulose degradation: An overview of fungi and fungal enzymes involved in lignocellulose degradation. *Eng. Life Sci.* **2018**, *18*, 768–778. [CrossRef]
22. Pasin, T.M.; Scarcella, A.S.A.; de Oliveira, T.B.; Lucas, R.C.; Cereia, M.; Betini, J.H.A.; Polizeli, M.L.T.M. Paper industry wastes as carbon sources for Aspergillus species cultivation and production of an enzymatic cocktail for biotechnological applications. *Ind. Biotechnol.* **2020**, *16*, 56–60. [CrossRef]
23. Duncan, S.M.; Farrell, R.L.; Thwaites, J.M.; Held, B.W.; Arenz, B.E.; Jurgens, J.A.; Blanchette, R.A. Endoglucanase-producing fungi isolated from *Cape Evans* historic expedition hut on Ross Island, Antarctica. *Environ. Microbiol.* **2006**, *8*, 1212–1219. [CrossRef] [PubMed]
24. Polizeli, M.L.T.M.; Rizzatti, A.C.S.; Monti, R.; Terenzi, H.F.; Jorge, J.A.; Amorim, D.S. Xylanases from fungi: Properties and industrial applications. *Appl. Microbiol. Biotechnol.* **2005**, *67*, 577–591. [CrossRef] [PubMed]
25. Miri, S.; Naghdi, M.; Rouissi, T.; Kaur Brar, S.; Martel, R. Recent biotechnological advances in petroleum hydrocarbons degradation under cold climate conditions: A review. *Crit. Rev. Environ. Sci. Technol.* **2019**, *49*, 553–586. [CrossRef]
26. Jiang, G.; Chen, P.; Bao, Y.; Wang, X.; Yang, T.; Mei, X.; Banerjee, S.; Wei, Z.; Xu, Y.; Shen, Q. Isolation of a novel psychrotrophic fungus for efficient low-temperature composting. *Bioresour. Technol.* **2021**, *331*, 125049. [CrossRef]
27. Adhikari, P.; Jain, R.; Sharma, A.; Pandey, A. Plant Growth Promotion at Low Temperature by Phosphate-Solubilizing Pseudomonas spp. Isolated from High-Altitude Himalayan Soil. *Microb. Ecol.* 2021. [CrossRef]
28. Geoportal Ecuador—Infraestructura de Datos Espaciales. Available online: http://www.geoportaligm.gob.ec/portal/ (accessed on 19 October 2021).
29. White, T.J.; Bruns, T.; Lee, S.; Taylor, J.W. *Amplification and Direct Sequencing of Fungal Ribosomal RNA Genes for Phylogenetics*; Academic Press, Inc.: New York, NY, USA, 1990; pp. 315–322.
30. Hall, T. BioEdit: A user-friendly biological sequence alignment editor and analysis program for Windows 95/98/NT. *Nucleic Acids Symp. Ser.* **1999**, *41*, 95–98.
31. Thompson, J.D.; Higgins, D.G.; Gibson, T.J. CLUSTAL W: Improving the sensitivity of progressive multiple sequence alignment through sequence weighting, position-specific gap penalties and weight matrix choice. *Nucleic Acids Res.* **1994**, *22*, 4673–4680. [CrossRef] [PubMed]
32. Kumar, S.; Stecher, G.; Tamura, K. MEGA7: Molecular Evolutionary Genetics Analysis Version 7.0 for Bigger Datasets. *Mol. Biol. Evol.* **2016**, *33*, 1870–1874. [CrossRef]
33. Miller, G.L. Use of dinitrosalicylic acid reagent for determination of reducing sugar. *Anal. Chem.* **1959**, *31*, 426–428. [CrossRef]
34. Contato, A.G.; de Oliveira, T.B.; Aranha, G.M.; de Freitas, E.N.; Vici, A.C.; Nogueira, K.M.V.; de Lucas, R.C.; de Almeida Scarcella, A.S.; Buckeridge, M.S.; Silva, R.N.; et al. Prospection of fungal lignocellulolytic enzymes produced from jatoba (*Hymenaea courbaril*) and tamarind (*Tamarindus indica*) seeds: Scaling for bioreactor and saccharification profile of sugarcane bagasse. *Microorganisms* **2021**, *9*, 533. [CrossRef] [PubMed]
35. Garen, A.; Siddiqi, O. Suppression of mutations in the alkaline phosphatase structural cistron of *E. coli*. *Proc. Natl. Acad. Sci. USA* **1962**, *48*, 1121–1127. [CrossRef]

36. Kersters-Hilderson, H.; Claeyssens, M.; Van Doorslaer, E.; Saman, E.; De Bruyne, C.K. β-D-xylosidase from *Bacillus pumilus*. In *Methods in Enzymology*; Complex Carbohydrates Part D; Academic Press: Cambridge, MA, USA, 1982; Volume 83, pp. 631–639. Available online: https://www.sciencedirect.com/science/article/pii/0076687982830620 (accessed on 19 August 2021).
37. Hribljan, J.A.; Suarez, E.; Heckman, K.A.; Lilleskov, E.A.; Chimner, R.A. Peatland carbon stocks and accumulation rates in the Ecuadorian paramo. *Wetl. Ecol. Manag.* **2016**, *24*, 113–127. [CrossRef]
38. Roa García, C.; Brown, S.; Krzic, M.; Lavkulich, L.; Roa-García, M.C. Relationship of soil water retention characteristics and soil properties: A case study from the Colombian Andes. *Can. J. Soil Sci.* **2021**, *101*, 147–156. [CrossRef]
39. Zúñiga-Silgado, D.; Rivera-Leyva, J.C.; Coleman, J.J.; Sánchez-Reyez, A.; Valencia-Díaz, S.; Serrano, M.; de-Bashan, L.E.; Folch-Mallol, J.L. Soil type affects organic acid production and phosphorus solubilization efficiency mediated by several native fungal strains from Mexico. *Microorganisms* **2020**, *8*, 1337. [CrossRef] [PubMed]
40. Rowley, M.C.; Grand, S.; Verrecchia, E.P. Calcium-mediated stabilisation of soil organic carbon. *Biogeochemistry* **2018**, *137*, 27–49. [CrossRef]
41. Opfergelt, S.; Georg, R.B.; Delvaux, B.; Cabidoche, Y.-M.; Burton, K.W.; Halliday, A.N. Mechanisms of magnesium isotope fractionation in volcanic soil weathering sequences, Guadeloupe. *Earth Planet Sci. Lett.* **2012**, *341*, 176–185. [CrossRef]
42. Rahimi, H.; Pazira, E.; Tajik, F. Effect of soil organic matter, electrical conductivity and sodium adsorption ratio on tensile strength of aggregates. *Soil Tillage Res.* **2000**, *54*, 145–153. [CrossRef]
43. Ishiguro, M.; Makino, T. Sulfate adsorption on a volcanic ash soil (allophanic Andisol) under low pH conditions. *Colloids Surf.-Physicochem. Eng. Asp.* **2011**, *384*, 121–125. [CrossRef]
44. Hazelton, P.; Murphy, B. *Interpreting Soil Test Results: What Do All the Numbers Mean?* Csiro Publishing: Clayton, Australia, 2016; p. 201.
45. Motsara, M.R.; Roy, R.N. *Guide to Laboratory Establishment for Plant Nutrient Analysis. FAO Fertilizer and Plant Nutrition Bulletin*; Food and Agriculture Organization of the United Nations: Rome, Italy, 2008; p. 219.
46. Sembiring, M. Bacterial and fungi phosphate solubilization effect to increase nutrient uptake and potatoes (*Solanum tuberosum* L.) production on Andisol Sinabung area. *J. Agron.* **2017**, *16*, 131–137. [CrossRef]
47. Bensch, K.; Braun, U.; Groenewald, J.Z.; Crous, P.W. The genus Cladosporium. *Stud. Mycol.* **2012**, *72*, 1–401. [CrossRef]
48. Del-Cid, A.; Ubilla, P.; Ravanal, M.-C.; Medina, E.; Vaca, I.; Levicán, G.; Eyzaguirre, J.; Chávez, R. Cold-active xylanase produced by fungi associated with Antarctic marine sponges. *Appl. Biochem. Biotechnol.* **2014**, *172*, 524–532. [CrossRef]
49. Wang, X.; Wu, X.; Jiang, S.; Yin, Q.; Li, D.; Wang, Y.; Wang, D.; Chen, Z. Whole genome sequence and gene annotation resource for *Didymella bellidis* associated with tea leaf spot. *Plant Dis.* **2021**, *105*, 1168–1170. [CrossRef]
50. Zhang, J.; Bruton, B.D.; Biles, C.L. Cell wall-degrading enzymes of *Didymella bryoniae* in relation to fungal growth and virulence in cantaloupe fruit. *Eur. J. Plant Pathol.* **2014**, *139*, 749–761. [CrossRef]
51. Rafiq, M.; Nadeem, S.; Hassan, N.; Hayat, M.; Sajjad, W.; Zada, S.; Sajjad, W.; Hasan, F. Fungal recovery and characterization from Hindu Kush mountain range, Tirich Mir glacier, and their potential for biotechnological applications. *J. Basic Microbiol.* **2020**, *60*, 444–457. [CrossRef]
52. Hassan, N.; Hasan, F.; Nadeem, S.; Hayat, M.; Ali, P.; Khan, M.; Sajjad, W.; Zada, S.; Rafiq, M. Community analysis and characterization of fungi from Batura Glacier, Karakoram Mountain Range, Pakistan. *Appl. Ecol. Environ. Res.* **2018**, *16*, 5323–5341. [CrossRef]
53. Pacelli, C.; Bryan, R.A.; Onofri, S.; Selbmann, L.; Shuryak, I.; Dadachova, E. Melanin is effective in protecting fast and slow growing fungi from various types of ionizing radiation. *Environ. Microbiol.* **2017**, *19*, 1612–1624. [CrossRef] [PubMed]
54. Dadachova, E.; Casadevall, A. Ionizing radiation: How fungi cope, adapt, and exploit with the help of melanin. *Curr. Opin. Microbiol.* **2008**, *11*, 525–531. [CrossRef] [PubMed]
55. Ravikumar, R. Effect of transport phenomena of *Cladosporium cladosporioides* on decolorization and chemical oxygen demand of distillery spent wash. *Int. J. Environ. Sci. Technol.* **2015**, *12*, 1581–1590. [CrossRef]
56. Mohan Kumar, N.S.; Ramasamy, R.; Manonmani, H.K. Production and optimization of l-asparaginase from Cladosporium sp. using agricultural residues in solid state fermentation. *Ind. Crops Prod.* **2013**, *43*, 150–158. [CrossRef]
57. Quintanilla, D.; Hagemann, T.; Hansen, K.; Gernaey, K.V. Fungal morphology in industrial enzyme production-modelling and monitoring. In *Filaments in Bioprocesses*; Krull, R., Bley, T., Eds.; Springer: Berlin/Heidelberg, Germany, 2015; pp. 29–54. Available online: https://www.webofscience.com/wos/woscc/full-record/WOS:000365169300003 (accessed on 19 October 2021).
58. Abrha, B.; Gashe, B.A. Cellulase production and activity in a species of Cladosporium. *World J. Microbiol. Biotechnol.* **1992**, *8*, 164–166. [CrossRef] [PubMed]
59. Maya-Yescas, M.E.; Revah, S.; Le Borgne, S.; Valenzuela, J.; Palacios-González, E.; Terrés-Rojas, E.; Vigueras-Ramírez, G. Growth of *Leucoagaricus gongylophorus* Möller (Singer) and production of key enzymes in submerged and solid-state cultures with lignocellulosic substrates. *Biotechnol. Lett.* **2021**, *43*, 845–854. [CrossRef]
60. Peñalva, M.A.; Arst, H.N. Regulation of gene expression by ambient ph in filamentous fungi and yeasts. *Microbiol. Mol. Biol. Rev.* **2002**, *66*, 426–446. [CrossRef]
61. Zucconi, L.; Canini, F.; Temporiti, M.E.; Tosi, S. Extracellular enzymes and bioactive compounds from Antarctic terrestrial fungi for bioprospecting. *Int. J. Environ. Res. Public Health* **2020**, *17*, 6459. [CrossRef] [PubMed]
62. Hassan, N.; Rafiq, M.; Hayat, M.; Nadeem, S.; Shah, A.A.; Hasan, F. Potential of psychrotrophic fungi isolated from siachen glacier, Pakistan, to produce antimicrobial metabolites. *Appl. Ecol. Environ. Res.* **2017**, *15*, 1157–1171. [CrossRef]

63. Grujic, M.; Dojnov, B.; Potocnik, I.; Atanasova, L.; Duduk, B.; Srebotnik, E.; Druzhinina, I.S.; Kubicek, C.P.; Vujčić, Z. Superior cellulolytic activity of *Trichoderma guizhouense* on raw wheat straw. *World J. Microbiol. Biotechnol.* **2019**, *35*, 194. [CrossRef]
64. Ghazali, M.F.S.M.; Zainudin, N.A.I.M.; Abd Aziz, N.A.; Mustafa, M. Screening of lignocellulolytic fungi for hydrolyzation of lignocellulosic materials in paddy straw for bioethanol production. *Malays. J. Microbiol.* **2019**, *15*, 379–386.
65. Ji, L.; Yang, J.; Fan, H.; Yang, Y.; Li, B.; Yu, X.; Zhu, N.; Yuan, H. Synergy of crude enzyme cocktail from cold-adapted *Cladosporium cladosporioides* Ch2-2 with commercial xylanase achieving high sugars yield at low cost. *Biotechnol. Biofuels* **2014**, *7*, 130. [CrossRef]
66. Aslam, M.S.; Aishy, A.; Samra, Z.Q.; Gull, I.; Athar, M.A. Identification, Purification and characterization of a novel extracellular laccase from *Cladosporium cladosporioides*. *Biotechnol. Biotechnol. Equip.* **2012**, *26*, 3345–3350. [CrossRef]
67. Halaburgi, V.M.; Sharma, S.; Sinha, M.; Singh, T.P.; Karegoudar, T.B. Purification and characterization of a thermostable laccase from the ascomycetes *Cladosporium cladosporioides* and its applications. *Process Biochem.* **2011**, *46*, 1146–1152. [CrossRef]
68. Gawas-Sakhalkar, P.; Singh, S.M.; Naik, S.; Ravindra, R. High-temperature optima phosphatases from the cold-tolerant Arctic fungus *Penicillium citrinum*. *Polar Res.* **2012**, *31*, 11105. [CrossRef]
69. Krishnan, A.; Convey, P.; Gonzalez-Rocha, G.; Alias, S.A. Production of extracellular hydrolase enzymes by fungi from King George Island. *Polar Biol.* **2016**, *39*, 65–76. [CrossRef]
70. Fenice, M.; Selbmann, L.; Zucconi, L.; Onofri, S. Production of extracellular enzymes by Antarctic fungal strains. *Polar Biol.* **1997**, *17*, 275–280. [CrossRef]
71. Wang, N.; Zang, J.; Ming, K.; Liu, Y.; Wu, Z.; Ding, H. Production of cold-adapted cellulase by Verticillium sp. isolated from Antarctic soils. *Electron. J. Biotechnol.* **2013**, *16*, 10. Available online: http://www.ejbiotechnology.info/index.php/ejbiotechnology/article/view/1302 (accessed on 9 December 2021). [CrossRef]
72. Salunke, M.; Sondge, D.B.; Yadav, S.; Warkhade, R.; Rathod, S.; Kate, S. Alkaline phosphatase production by *Enterobacter hormaechei* isolated from birds fecal waste and its optimization. *Int. J. Adv. Sci. Technol.* **2020**, *29*, 9.